The Durability of Natural Sisal Fibre Reinforced Cement-based Composites

by

Marthinus David de Klerk

Thesis presented in fulfilment of the requirements for the degree of Master in Engineering in the Faculty of Engineering at Stellenbosch University

Supervisor: Prof William Peter Boshoff

March 2015

Declaration

By submitting this thesis electronically, I, the undersigned, declare that the entirety of the work contained therein is my own original work, that I am the authorship owner thereof and that I have not previously in its entirety or in part submitted it for obtaining any qualification.

Signature: ………………………….

Date: …………..............................

i

Summary

The building industry is responsible for a substantial contribution to pollution. The production of building materials, as well as the operation and maintenance of structures leads to large amounts of carbon-dioxide (CO_2) being release in the atmosphere. The use of renewable resources and construction materials is just one of the ways in which the carbon footprint of the building industry can be reduced.

Sisal fibre is one such renewable material. Sisal fibre is a natural fibre from the Agave Sisalana plant. The possibility of incorporating sisal fibre in a cement-based matrix to replace conventional steel and synthetic fibres has been brought to the attention of researchers. Sisal fibre has a high tensile strength in excess of polypropylene fibre and comparable to PVA fibre. Sisal fibre consists mainly of cellulose, hemi-cellulose and lignin. The disadvantage of incorporating sisal fibre in a cement-based matrix is the degradation of the composite. Sisal fibres tend to degrade in an alkaline environment due to changes in the morphology of the fibre. The pore water in a cement base matrix is highly alkaline which leads to the degradation of the fibres and reduced strength of the composite over time.

Sisal fibre reinforced cement-based composites (SFRCC) were investigated to evaluate the durability of the composites. Two chemical treatments, alkaline treatment and acetylation, were performed on the fibre at different concentrations to improve the resistance of the fibre to alkaline attack. Alkaline treatment was performed by using sodium hydroxide (NaOH), while acetylation was performed by using acetic acid or acetic anhydride. Single fibre pull-out (SFP) tests were performed to evaluate the influence of chemical treatment on fibre strength, to study the fibre-matrix interaction and to determine a critical fibre length. A matrix consisting of ordinary Portland cement (OPC), sand and water were used for the SFP tests. This matrix, as well as alternative matrices containing fly ash (FA) and condensed silica fume (CSF) as supplementary cementitious material, were reinforced with 1% sisal fibre (by volume) cut to a length of 20 mm. The OPC matrix was reinforced with untreated- and treated fibre while the alternative matrices were reinforced with untreated fibre. Alternative matrices containing varying fibre volumes and lengths were also produced.

Three-point bending- (indirect), direct tensile- and compression tests were performed on specimens at an age of 28 days to determine the strength of the matrix. The remainder of the specimens were subjected to ageing by extended curing in water at 24°C and 70°C respectively and by alternate cycles of wetting and drying, after which it was tested at an age of 90 days from production to evaluate the durability of the fibre.

An increase in fibre volume led to a decrease in compressive strength and peak tensile strength. The optimum fibre length at a volume of 1% was 20 mm for which the highest compression strength was recorded. The combination of alkali treatment and acetylation was the most effective treatment condition, followed by alkali treatment at low concentrations of sodium hydroxide. At higher concentrations of sodium hydroxide, a significant reduction in strength was recorded. The addition of supplementary cementitious materials also proved to be effective in mitigating degradation, especially in the cases where CSF was used. FA proved to be less effective in reducing the alkalinity of the matrix. However, the use of FA as fine filler resulted in higher strengths. Specimens manufactured by extrusion did not have superior mechanical properties to cast specimens.

The conclusion was made that the use of sisal fibre in a cement-based matrix is effective in providing ductile failure. Chemical treatment and the addition of supplementary cementitious materials did improve the durability of the specimens, although degradation still took place.

Opsomming

Die boubedryf is verantwoordelik vir 'n aansienlike bydrae tot besoedeling. Die produksie van boumateriale, sowel as die bedryf en instandhouding van strukture lei tot groot hoeveelhede koolstof dioksied (CO_2) wat in die atmosfeer vrygestel word. Die gebruik van hernubare hulpbronne en boumateriale is maar net een van die maniere waarop die koolstof voetspoor van die boubedryf verminder kan word.

Sisal vesels is 'n voorbeeld van 'n hernubare materiaal. Sisal vesel is 'n natuurlike vesel afkomstig vanaf die Agave Sisalana plant. Die moontlikheid om sisal vesels in 'n sement gebasseerde matriks te gebruik om konvensionele staal en sintetiese vesels te vervang, is tot die aandag van navorsers gebring. Sisal vesel het 'n hoër treksterkte as polipropileen vesels en die treksterkte vergelyk goed met die van PVA vesels. Sisal vesel bestaan hoofsaaklik uit sellulose, hemi-sellulose en lignien. Die nadeel verbonde aan die gebruik van sisal vesels in 'n sement gebasseerde matriks is die degradasie van die komposiet. Sisal vesels is geneig om af te breek in 'n alkaliese omgewing as gevolg van veranderinge wat in die morfologie van die vesel plaasvind. Die water in die porieë van 'n sement gebasseerde matriks is hoogs alkalies wat lei daartoe dat die vesel afgebreek word en die sterkte van die komposiet afneem oor tyd.

Sisal vesel versterkte sement gebasseerde komposiete is ondersoek om die duursaamheid van die komposiete te evalueer. Twee chemiese behandelings, alkaliese behandeling en asetilering, is uitgevoer op die vesels teen verskillende konsentrasies om die weerstand van die vesels teen alkaliese aanslag te verbeter. Alkaliese behandeling was uitgevoer met natrium-hidroksied (NaOH) terwyl asetilering met asynsuur en asynsuurhidried uitgevoer is. Enkel vesel uittrek toetse is uitgevoer om die invloed van chemiese behandeling op veselsterkte te evalueer, om die vesel/matriks interaksie te bestudeer en om die kritiese vesellengte te bepaal. 'n Matriks wat uit gewone Portland sement (OPC), sand en water bestaan, is gebruik vir die enkel vesel uittrek toetse. Dieselfde matriks, sowel as alternatiewe matrikse wat vliegas (FA) en gekondenseerde silika dampe (CSF) as aanvullende sementagtige materiaal bevat, is versterk met 1% vesel (by volume) wat 20 mm lank gesny is. Die OPC matriks was versterk met onbehandelde- en behandelde vesels, terwyl die alternatiewe matrikse met onbehandelde vesels versterk is. Matrikse wat wisselende vesel volumes en lengtes bevat het is ook vervaardig.

Drie-punt buigtoetse (indirek), direkte trek toetse en druktoetse is uitgevoer op proefstukke teen 'n ouderdom van 28 dae om die sterkte van die matriks te bepaal. Die oorblywende

proefstukke is onderwerp aan veroudering deur verlengde nabehandeling in water teen 24°C en 70°C onderskeidelik en deur afwissilende siklusse van nat- en droogmaak waarna dit op 'n ouderdom van 90 dae vanaf vervaardiging getoets is om die duursaamheid van die matriks te evalueer.

'n Toename in vesel volume het tot 'n afname in druksterkte en piek treksterkte gelei. Die optimum vesel lengte teen 'n volume van 1% was 20 mm, waarvoor die hoogste druksterkte opgeteken is. Die kombinasie van alkaliese behandeling en asetilering was die mees effektiewe behandeling, gevolg deur alkaliese behandeling by lae konsentrasies natrium-hidroksied. Vir hoë konsentrasies natrium-hidroksied is 'n aansienlike afname in sterkte opgeteken. Die toevoeging van aanvullende sementagtige materiale was ook effektief om die degradadering van die vesels te verminder, veral in die gevalle waar CSF gebruik is. FA was minder effektief om die alkaliniteit van die matriks te verminder. Die gebruik van FA as fyn vuller het nietemin hoër sterkte tot gevolg gehad. Proefstukke wat deur ekstrusie vervaardig is, het nie beter meganiese eienskappe gehad as proefstukke wat gegiet is nie.

Daar is tot die gevolgtrekking gekom dat sisal vesel in 'n sement gebasseerde matriks wel effektief is om 'n duktiele falingsmode te voorsien. Chemiese behandeling en die toevoeging van aanvullende sementagtige materiale het die duursaamheid van die proefstukke verbeter, alhoewel degradering steeds plaasgevind het.

Acknowledgements

I would like to give all the praise to God for the opportunity I had to study at Stellenbosch in such a remarkable town. Through His guidance I was able to make the right decisions, to work hard and persevere, knowing it is for His kingdom. My character was tested and built and I believe that the challenges I faced made me a better person. I was immensely blessed through the people I met during my time in Stellenbosch.

I would also like to thank the following people:

- My supervisor, Prof WP Boshoff, for his guidance and inspiration.
- The trustees of the Wilhelm Frank bursary fund for financial support.
- My parents, David and Maretha de Klerk for their support
- My sisters and brothers in law for their encouragement.
- My friends, for all their support and the prayer group on Tuesday mornings:
    - Jascha Muller
    - Conrad de Kock
    - Diederick Dippenaar
    - Wessel Smalberger
    - Rudi van Wyk
    - Ryno Barnard
    - Deon Visser
    - Charlie de la Harpe
    - Louwrens Mostert
    - Philip Piek
    - Anneke Roux
- My colleagues.
- The personnel at the Department of Civil Engineering for all their assistance:
    - Mr Charlton Ramat
    - Mr Peter Cupido
    - Mr Hershin Adonis
    - Mr Johan van der Merwe
    - Mr Dion Viljoen
    - Mr Stephan Zeranka

Table of Contents

List of Tables

List of Figures

List of Abbreviations

BGBS – Basic Granulated Blast furnace Slag

$CaCO_3$ – Calcium Carbonate

CaO – Calcium Oxide

$Ca(OH)_2$ – Calcium Hydroxide

CBD – Compacted Bulk Density

CH_3COOH – Acetic Acid

$(CH_3CO)_2O$ – Acetic Anhydride

CO_2 – Carbon dioxide

CSF – Condensed Silica Fume

CSH – Calcium Silicate Hydrate

FA – Fly Ash

FM – Fineness Modulus

FRC – Fibre Reinforced concrete

GGBS – Ground Granulated Blast furnace Slag

HBM – Hottinger Baldwin Messtechnik

H_2O – Water

KFRC – Kenaf Fibre Reinforced Concrete

LVDT – Linear Voltage Displacement Transducer

M – Molar

NaOH – Sodium Hydroxide

NFRC – Natural Fibre Reinforced Concrete

OPC – Ordinary Portland Cement

PP – Polypropylene

PPC – Pretoria Portland Cement

PVA – Polyvinyl Alcohol

PVC – Polyvinyl Chloride

RD – Relative Density

SANS – South African National Standards

SEM – Scanning Electron Microscope

SFP – Single Fibre Pull-out

SFRC – Sisal Fibre Reinforced Concrete

SFRCC – Sisal Fibre Reinforced Cement-based Composite

SiO_2 – Silicon-dioxide

SP – Super-plasticiser

VMA – Viscosity Modifying Agent

c/s – cement to sand ratio

w/b – water to binder ratio

w/c – water to cement ratio

CHAPTER 1

Introduction

1.1. Background

The use of raw materials and energy for growth and development is causing a large amount of pollution. The use of fossil fuels for energy releases carbon-dioxide (CO_2) and other gasses into the atmosphere (Spence & Mulligan, 1995). The build-up of CO_2 in the atmosphere causes what is known as the "greenhouse effect". Heat, from the radiation of the sun, enters the atmosphere through the ozone layer and heats up the earth. The heat is trapped inside the atmosphere by the CO_2 and the average temperature of the earth increases gradually. The gradual increase in temperature is known as Global Warming (World Commision on Environment and Development, 1987). Global Warming is a big concern, because as the average temperature increases, the ice in the Arctic melts and the levels of the oceans rise. It is also prone to causing more natural disasters (Anderson & Bausch, 2006). To decrease global warming, there is a need for sustainable development.

Lately the term "sustainable development" has been used often and at times even out of context. An early definition of sustainable development is to "meet the needs of the present without compromising the ability of future generations to meet their own needs" (World Commision on Environment and Development, 1987). Another and more recent definition is "development efforts which seek to address social needs while taking care to minimize potential negative environmental impacts" (Hill & Bowen, 1996). Sustainable development can thus be classified as development that improves human wellbeing in the present, without having adverse effects on the environment in the long term.

Sustainable development within the engineering environment is often referred to as "Green Engineering". Green engineering can be defined as "the design, commercialization and use of processes and products that are feasible and economical while reducing the generation of pollution at the source and minimizing the risk to human health and the environment"

1

(U.S. Environmental Protection Agency, 2014). Green engineering is thus important to reduce global warming and the detrimental effects it has on the earth.

The construction industry accounts for a large amount of the world's carbon emissions. Buildings consume materials and energy throughout their life-cycle, from the construction to the operation and maintenance of the building. Approximately 8-20% of the world's carbon emission is primarily by the manufacturing of building materials (Spence & Mulligan, 1995). The production of Portland cement for concrete, the burning of coal or wood for firing clay brick furnaces and the production of steel for use in structures is of the main contributors. Over 75% of the energy used in construction is used for the manufacture of materials (Spence & Mulligan, 1995).

The use of renewable resources and construction materials is just one of the many ways to reduce the carbon footprint of the construction industry. Another way in which the construction industry contributes to carbon emissions is by the energy used in the operation of buildings (Spence & Mulligan, 1995). By using building materials with better insulating properties, the need for heating in the colder months and cooling in the warmer months is reduced. Buildings can also be designed more efficiently to utilise natural light and air circulation. This reduces the energy consumed by the buildings which in turn reduces electricity generation which consumes fossil fuels. The construction of durable structures is also of high importance. The maintenance and restoration of structures due to the degradation of materials and poorly constructed structures leads to further unnecessary consumption of building materials.

To mitigate the pollution and environmental degradation caused by the construction industry, more sustainable structures should be constructed. According to Spence and Mulligan (1995) sustainable development is development that takes place by using less resource-intensive and environmentally damaging technologies. In order to create more sustainable structures, recycled materials and waste can thus be used in the manufacture of materials, the energy efficiency of buildings can be improved and renewable materials can be used to substitute conventional building materials.

Recently the use of renewable resources and the reduction of non-renewable resources has been a key focus in the construction industry (Pacheco-Torgal & Jalali, 2010). The possibility of using more natural and conventional building materials is being investigated in many countries. The possibility of replacing synthetic- and steel fibres in concrete with natural fibres such as sisal, hemp, jute or flax is one of the many areas of research into renewable building materials. These fibres have tensile strengths in excess of those of polypropylene (PP) fibres and comparable to Polyvinyl Acetate (PVA) fibres. Countries like Brazil and

Kenya have an abundant supply of sisal. According to Alex Odundo (TED Blog, 2012) sisal fibre is being used in Kenya for twine and carpets, but it is only used as an alternative source of income when the other crops decline due to drought. Sisal is easily cultivated and the extraction process of the fibre, which is done mechanically, leads to employment opportunities. The use of sisal fibre in building materials can lead to industrial development in developing countries. The crops can be utilised to its full potential and provide employment and income.

1.2. Problem statement

Studies have shown that the use of sisal fibre in concrete can decrease the density of concrete which leads to a lower compressive strength. The decrease in density is caused by fibres entrapping air during the concrete mixing process, less effective compaction due to the interference of the fibres and by the lower specific weight of the fibre. The durability of sisal fibre in cement-based composites is also of concern, because the fibres tend to degrade in an alkaline environment. Cement-based composites have high alkalinity which is caused by the calcium hydroxide, $Ca(OH)_2$, formed during the hydration of cement. The need for research into the use of sisal fibre in cement-based composites arises, as the durability of building materials is of significant importance. The mechanical properties of sisal fibre reinforced cement-based composites are also of high importance to quantify the interaction between the fibres and the matrix.

1.3. Objectives

Given the international trend towards green engineering and the development of sustainable building materials, the use of natural sisal fibre in cement-based composites was investigated in order to be able to develop a sustainable building material. Previous research by Coetzee (2013) studied masonry units reinforced with sisal fibre for low cost housing. In contrast, the focus of this study was not on producing a building unit for the construction of houses. The focus was rather to determine the properties of Sisal Fibre Reinforced Cement-based Composites (SFRCC) to be able to develop products in the future. The aim was to develop a material that has better mechanical properties, that is more durable, possibly cheaper and environmentally friendly.

1.4. Methodology

The viability of sisal fibre in cement-based composites, as a sustainable building material, was investigated by reinforcing different cement-based matrices with different volumes of short, randomly orientated fibres, cut in different lengths. The challenges associated with the durability of natural sisal fibre in an alkaline environment were the main focus of this investigation.

Chemical treatment of the fibres (to reduce the degradation of the fibre due to the alkalinity of the matrix) was investigated. Two different chemical treatments, Alkali treatment and Acetylation, were used. Alkali treatment was performed with sodium hydroxide, NaOH, at five different concentrations, whereas Acetylation was performed with Acetic Acid (CH_3COOH) and Acetic Anhydride (($CH_3CO)_2O$), both at two different concentrations. In addition to the chemical treatments, the cement matrix was modified by the partial replacement of cement with other cementitious materials such as fly ash (FA) and condensed silica fume (CSF). This was done to reduce the amount of calcium hydroxide in the matrix, $Ca(OH)_2$, thus reducing the alkalinity of the pore water in the matrix.

Initially, a series of single fibre pull-out (SFP) tests was performed to study the fibre-matrix interaction. The optimum or critical fibre length (which is the longest possible embedment depth at which the fibre pulls out of the matrix without rupturing) required for ductile failure was also determined by the SFP tests. The effect of chemical treatment on the strength and critical length of the fibre was also studied by the SFP tests. The modification of the fibre surface through chemical treatment was studied by the use of a Scanning Electron Microscope (SEM).

A series of specimens, consisting of an Ordinary Portland cement (OPC) matrix reinforced with sisal fibres subjected to the different chemical treatments, were produced. In addition, specimens consisting of a matrix incorporating different supplementary cementitious materials and untreated sisal fibres were produced. The specimens were cured in water for 28 days and were tested in compression, indirect tension (or flexure) and direct tension at an age of 28 days to establish references. Thereafter, the remainder of the specimens were subjected to different ageing conditions up to an age of 90 days, after which it was tested in the same manner to evaluate the degradation of the specimens, if any. Compression tests were only performed at 28 days.

CHAPTER 2

Background Study

This chapter gives an overview on different natural fibres and possible applications of natural fibres in cement-based matrices, followed by a discussion on the interaction between fibre and matrix. The issue of durability related to the incorporation of natural fibres in cement-based matrices is discussed and possible solutions are investigated.

2.1. Natural fibre

Natural fibre can be classified as vegetable, animal or mineral fibre. Vegetable fibre originates from plants and the most common examples include flax, jute, coir, cotton, hemp and sisal. Animal fibre is products from animals and consists of proteins. Examples include wool, hair and silk. Mineral fibres are composed of minerals and an example is asbestos.

Recently attention is being drawn to vegetable fibre, because it is a renewable resource and is available at a low cost across the world (Mohan & Kanny, 2012). Most vegetable fibre has a high tensile strength and holds the potential to be used in structural applications. It can be used to replace conventional steel- and synthetic fibres and potentially to partially replace steel reinforcement. It has good thermal properties and is valued for its insulating ability when used in buildings. A recent study on kenaf fibre showed that the amount of carbon dioxide absorbed by the kenaf plant during cultivation is approximately one and a half times its weight (Mohanty et al., 2005). By using natural fibre in composites, the overall carbon footprint of the product is reduced.

Vegetable fibres can be subdivided into bast-, leaf-, seed-, fruit- and grass or reed fibres according to their origin in the plant (Kicinska-Jakubowska et al., 2012). In this investigation the focus is on sisal. Sisal is a leaf fibre from the Agave Sisalana plant which belongs to the Agavaceae family (Kirby, 1963). Leaf fibres run longitudinally through the leaf of the plant and provide strength and rigidity to the leaf (Bentur & Mindess, 2007). They can be divided

5

into median bundles or ribbon fibres which are located in the centre of the leaf and are horseshoe shaped, periphery bundles or mechanical fibres which consists of irregular rows of fibres and are located on the outside or skin of the leaf and the xylem fibres between the centre and periphery of the leaf. The median fibres are the longest and run to the tip of the leaf. (Kirby, 1963)

The median fibres are extracted through a process called decortication which means husk removal. During decortication the husk or the skin of the sisal leaf is removed and the inner fibres are exposed. An example of a decorticator can be seen in Figure 2.1. The excess waste is removed from the decorticated fibres and the fibres are left to dry after which they can be washed and used for the application desired.

Figure 2.1: Mechanical decorticator. (Goodier, 2013)

2.1.1. Composition

Vegetable fibres are natural composites with a cellular structure also sometimes referred to as a lignocellulosic structure. They consist of cellulose, hemicellulose, lignin, pectin, resins, mineral matter, fats and waxes (Kirby, 1963) with cellulose being the major constituent.

Cellulose consists of three hydroxyl groups (OH^-) of which two form intra-molecular hydrogen bonds within the cellulose macromolecule, while the rest form intermolecular hydrogen bonds with other cellulose molecules. A hydrogen bond is a bond between polar molecules, where a hydrogen atom is bound to a highly negatively charged atom (Mwaikambo & Ansell, 1999). Cellulose provides strength, stiffness and structural stability to the fibre (Kabir et al., 2012).

Hemicellulose is mainly found in the primary cell wall and is considered to be amorphous. The hemicellulose molecules are the cementing material of the fibre and are hydrogen bonded with cellulose molecules.

Lignin is amorphous and has an aromatic structure (Kabir et al., 2012). Lignin and pectin act as adhesive in conjunction with the cellulose-hemicellulose network (Kabir et al., 2012). Small amounts of organic and inorganic components are also present in the fibre structure. The chemical composition of cellulose, hemicellulose and lignin can be seen in Figure 2.2.
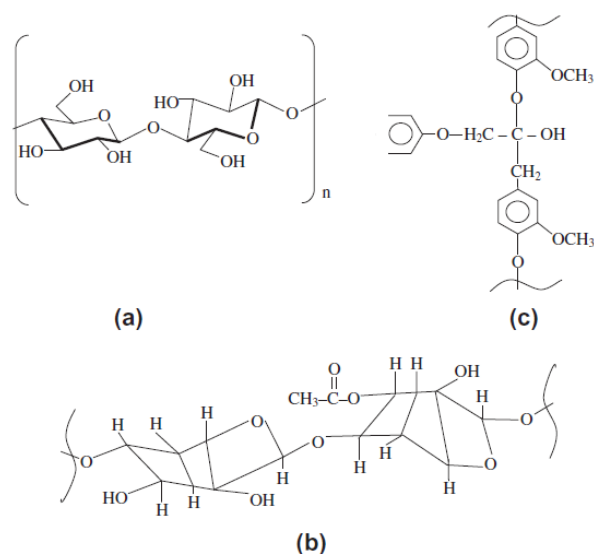
Figure 2.2: The chemical composition of (a) cellulose, (b) hemicellulose and (c) lignin (Kabir et al., 2012).

Different vegetable fibres have different compositions with regards to the amount of cellulose, hemicellulose and lignin in the plant structure (Pacheco-Torgal & Jalali, 2010). The composition of various types of vegetable fibres is presented in Table 2.1.

The properties of the fibre are determined by the cell geometry. The common structure of a fibre strand can be seen in Figure 2.3. The cell wall consists of a primary layer and secondary layers. The middle hollow canal is called the lumen. The fibre structure develops in the primary layer and is deposited to the secondary layer during the growth of the plant. The secondary layers consist of chains of helical wounded cellulose micro-fibrils. The amount of cellulose increases from the primary layer to the secondary layer, the amount of hemicellulose is similar in every layer and the amount of lignin decreases from the primary wall to the secondary walls. Fibres can be distinguished by the size of its lumen and the thickness of the cell wall. Figure 2.4 shows the cellular structure of the fibre cell wall.

Table 2.1: Composition of various vegetable fibres (Pacheco-Torgal & Jalali, 2010) (Li et al., 2007).

Fibre	Component (%)				
	Lignin	Cellulose	Hemicellulose	Extractives	Ash
Sisal	11.0	73.11	13.33	1.33	0.33
Hemp	4-13	57-77	14-22	0.9	0.8
Kenaf	15-21	31-57	18-24	-	2-5
Jute	12-26	41-72	14-22	0.2	0.5-2
Flax	2-23	43-71	19-26	2.3	5
Ramie	1	69-91	5-17	1.9	-
Banana trunk	15.07	31.48	14.98	4.46	8.65
Banana leaf	24.84	25.65	17.04	9.84	7.02
Bagasse	21.8	41.7	28.0	4.0	3.5
Coconut coir	46.48	21.46	12.36	8.77	1.05
Coconut tissue	29.7	31.05	19.22	1.74	8.39
Eucalyptus	25.4	41.57	32.56	8.2	0.22
Henequen	13	78	4-8	-	-
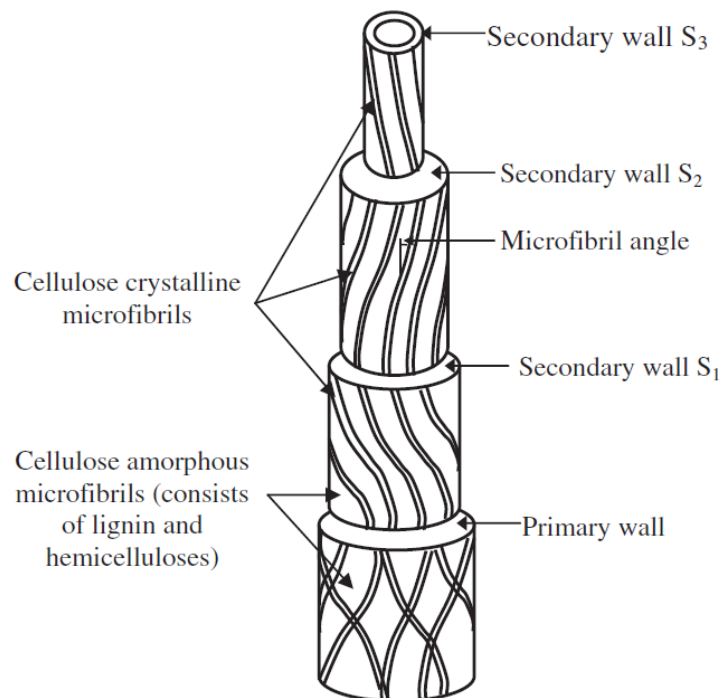
Figure 2.3: The common structure of a fibre strand (Kabir et al., 2012).

Each fibre strand consists of a bundle of fine fibre cells called ultimate fibres or fibrils. These ultimate fibre cells are in the form of tubes and have different cell geometries for different types of fibre. The ultimate fibre cells are bound together by the middle lamellae (a pectin layer binding the cell walls together) of the cells or cellular tissue. The ultimate fibres differ in length for various plants. The length of the ultimate fibres of sisal is between 0.8 and 8.0 mm (Kirby, 1963).
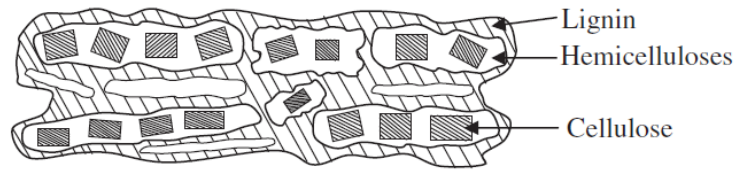
Figure 2.4: The cellular structure of the fibre cell wall (Kabir et al., 2012).

The composition of vegetable fibre allows for water absorption from the environment. The cellulose structure is divided into two regions, namely crystalline and amorphous. Water is absorbed by hemicellulose and lignin present in the amorphous region (Kabir et al., 2012). The ability of the fibre to absorb water means the fibre is of hydrophilic nature.

2.1.2. Properties

There is a significant variation in the properties of vegetable fibres, because of the difference in composition of the fibres. Factors such as climate, the origin and age of the plant and the extraction method used can also have an effect on the properties of the fibres (Mwaikambo & Ansell, 1999). This variation in the properties often leads to unpredictable behaviour of fibres in a cement matrix (Pacheco-Torgal & Jalali, 2010). The mechanical and physical properties of various vegetable fibres will be discussed in the following sections.

Mechanical properties

As mentioned previously, cellulose is the main component contributing to the strength of the fibre. However, the angle of the micro-fibrils with the axes of the fibres also determines the strength of the fibre. Fibres with a higher cellulose content and lower micro-fibrillar angle have better mechanical properties. The adhesive quality of the lignin and pectin also plays a significant role in the strength and stiffness of the fibre.

The crystallinity index of cellulose fibres is related to the amount of cellulose in the fibre structure and is usually expressed as a percentage. The crystallinity index is determined by differential scanning calorimetry or X-ray diffraction. Crystallinity also refers to the packing or order of the cellulose molecules in the fibre structure (Mwaikambo & Ansell, 1999). Fibres with a high crystallinity index and high cellulose content usually have superior mechanical properties.

Properties of natural- and synthetic fibres are presented in Table 2.2. As can be seen from Table 2.2, the tensile strength and modulus of elasticity of some of the vegetable fibres, for

9

example hemp, compare well with that of synthetic fibres such as polypropylene and PVA. Natural fibres have a low modulus of elasticity and a high tensile strength and can therefore be a suitable substitute for synthetic fibres.

The main disadvantage of natural fibres in composites is the poor compatibility between the fibre and matrix due to the high moisture absorption of the fibre and the surface impurities (Li et al., 2007). For this reason chemical treatment is necessary to modify the fibre surface.

Table 2.2: Mechanical properties of natural and synthetic fibres (Pacheco-Torgal & Jalali, 2010) (Kabir et al., 2012) (Li et al., 2007).

Properties	Specific weight (kg/m³)	Water absorption (%)	Tensile strength (MPa)	Modulus of elasticity (GPa)	Elongation at break (%)
Sisal	1370	110	347 - 378	15.2	n/a
	1450	n/a	468 - 640	9.4-22	3-7
Coconut coir	1177	93.8	95-118	2.8	n/a
Bamboo	1158	145	73-505	10-40	n/a
Hemp	1500	85-105	900	34.0	n/a
	1140	n/a	690	30-60	1.6
Jute	1300-1400	n/a	393-773	13-26.5	1.16-1.5
Flax	1500	n/a	345-1100	27.6	2.7-3.2
Ramie	1500	400-938	61.4-128	n/a	1.2-3.8
Cottton	1500-1600	287-800	5.5-12.6	n/a	7-8
Caeser weed	1409	182	300-500	10-40	n/a
Banana leaf	1031	407	384	20-51	n/a
Piassave palm	1054	34-108	143	5.6	n/a
Date palm	1300-1450	60-84	70-170	2.5-4.0	n/a
Polypropylene	913	n/a	250	2.0	n/a
PVA	1300	n/a	900	23	n/a

Physical properties

The physical properties of vegetable fibres vary according to the type of fibre and also the origin, climate, age of the plant and process of extraction used. The physical properties of various types of vegetable fibres are presented in Table 2.3.

2.2. Natural fibre reinforced cement-based composites

The use of natural fibres in cement-based composites has been studied by several authors as reported by Tolêdo Filho et al. (1999). The main function of fibres in cement-based composites is to bridge cracks in the matrix, caused by an applied load or shrinkage, allowing for ductile failure. They are used to improve the post crack performance and

toughness of the matrix. An additional function of natural fibres is to reduce the non-renewable materials consumed, thus creating a more sustainable and eco-friendly product.

Table 2.3: Physical properties of vegetable fibres (Satyanarayana et al., 2007).

Fibre	Density (kg/m^3)	Ultimate fibre length (mm)	Diameter (µm)	Crystallinity (%)	Micro-fibrillar angle (˚)
Sisal	1260-1330	3	100-300	72.2	20
Coconut coir	1390-1520	10-150	40-400	43-44	51
Jute	1450	60	18-30	n/a	7-9
Ramie	1500	120	40-50	n/a	7.5-12
Cotton	1510	35	19	n/a	33-34
Banana leaf	1500	60	150	n/a	n/a
Bagasse	450-492	n/a	n/a	47	n/a
Pineapple	1440	20-80	1.56-4.5	n/a	8-15

In a study by Awwad et al., (2012), concrete was reinforced using industrial hemp fibres. It was found that the addition of hemp fibres made it possible to reduce the coarse aggregate without affecting the flexural performance. The use of fibres also resulted in a ductile failure mode instead of brittle failure as for conventional concrete. The reduction of coarse aggregate allows for better interaction between the fibres and the cement paste. The compressive strength tend to decrease with an addition of fibres, but the flexural strength, given the correct proportion between aggregate reduction and fibre addition, were not affected. The addition of hemp fibres decreased thermal conductivity. The slump of the concrete was reduced, due to the water absorption of the fibres.

Similar results were found by Elsaid et al., (2011) who investigated kenaf fibre reinforced concrete (KFRC). The fibres were chemically treated to enhance the bond between the fibre and the cement matrix and to increase the durability of the reinforced concrete. The average compressive strength for the KFRC was lower than for the control specimens (without fibre), but the control specimens showed brittle failure by spalling of the concrete while the KFRC showed ductile failure with well distributed cracks. The kenaf fibres were clearly visible in the cracks formed. The peak flexural strength was reduced but the residual flexural strength was increased with the addition of kenaf fibres. This increase in residual strength shows that the toughness of the KFRC is higher. A toughness of approximately three times higher was measured with the addition of fibres.

Tolêdo Filho et al., (2000) found that concrete matrices reinforced with coconut and sisal fibre showed a decrease in strength and toughness after six months of exposure to open air weathering and cycles of wetting and drying. The first crack strength was however increased. This was attributed to the densening of the cement matrix around the fibre which was caused

by chemical cement hydration products transported to the fibres through capillary water. The flexibility of the fibres was reduced which influenced the deformation of the fibres and lead to a reduction in toughness.

Sedan et al., (2007) investigated hemp reinforced portland cement composites. Fibres were both untreated and treated with sodium hydroxide, NaOH (in a 6% (by weight) NaOH solution). It was found that hemp fibres causes a delay in the setting time of the cement paste. This was caused by the pectin in the fibre that fixes calcium ions on the surface of the fibre and makes it unavailable for the formation of calcium silicate hydrate (CSH). The maximum flexural strength was achieved for specimens with a 16 vol.% fibre fraction. For higher volumes, the mix was reported as non-homogenenous and poor fibre-matrix adhesion was achieved. An increase in strength of approximately 40% was achieved for NaOH treated fibres compared to untreated fibres. The peak strength was also higher, showing an improvement in the interfacial adhesion.

A recent study by Coetzee (2013) on concrete bricks and blocks reinforced with sisal fibres showed a decrease in compressive strength with the addition of fibre contents of 0.5% and 1.0% by volume. The addition of fibres decreased the density of the blocks and increased the porosity. The reduction in compressive strength can be attributed to the decrease in density. With the addition of 10% condensed silica fume (CSF), the compression strength was not affected as much. The addition of CSF decreased the porosity, especially at higher fibre volumes. The flexural strength was also reduced, but the failure mode was more ductile. With the addition of fibres, the dimensional stability of the blocks was markedly improved (Coetzee, 2013).

2.2.1. Fibre-matrix interaction

As mentioned previously, vegetable fibres consists mainly of cellulose. The cellulose consists mainly of glucose molecules (Kirby, 1963). These glucose molecules can attract molecules such as water. Water uptake takes place when the hydrophilic hydroxyl molecules in the cellulose bond with water molecules. The water molecules push the cellulose molecules apart and which leads to swelling of the fibres (Kirby, 1963). The ability of the fibre to absorb water means the fibres are of hydrophilic nature.

As can be seen from Table 2.2, vegetable fibres have high water absorption. The fibre swells when it absorbs water and as it dries, it shrinks. These dimensional changes in the fibre structure mean the fibre has poor dimensional stability which can lead to shrinkage strain in the concrete that is more than the normal shrinkage strain for concrete (Bentur & Mindess,

2007). The high water absorption causes that the fibre initially takes more space. The water in the fibre increases the water/binder ratio around the fibre, leading to a more porous matrix structure. As the water is consumed during hydration, the fibre shrinks and a gap or crack can develop between the fibre and matrix (Agopyan et al., 2005). The dimensional instability of the fibre causes a weak fibre-matrix interface and poor mechanical properties of the natural fibre reinforced concrete (NFRC). The surface impurities (ash and waxy substances) of vegetable fibre also lead to poor interfacial bonding between the fibre and matrix.

Single fibre pull-out

The desired failure mode for fibre reinforced concrete is ductile failure, which means the fibres should pull out rather than fracture. Sudden failure is caused by fibre fracture. However, a problem often associated with fibre reinforced concrete (FRC) is the premature pull-out of the fibres. The fibres pull out of the concrete matrix before the full tensile capacity of the fibre is reached. This means that the friction between the fibre and matrix interface is insufficient. To overcome premature fibre pull-out, the length of the fibre needs to be increased to increase friction. The length must however be short enough that the fibres pull out rather than fracture. With an increase in fibre length, fibres tend to form balls during the mixing process, especially at higher fibre volumes (Rieger & van Mier, 2010). Taking all these factors into account, an optimum fibre length should be found to increase strength and toughness while maintaining workability of the fresh concrete.

Single fibre pull-out tests are performed to obtain an understanding of the interaction between the fibre and matrix and to determine the critical fibre length. According to Simkins et al., (2005) most on-going research is about the behaviour of the fibre-matrix interface and interfacial failure. A single fibre is embedded at a specific depth in a concrete matrix or cement paste. The specimen is fixed at its base and a tensile force is applied to the fibre until the fibre breaks or pulls out of the matrix. The maximum pull-out force is measured and the force displacement graph is plotted.

From the force-displacement graph, the debonding energy can be measured by taking the area under the graph. In a study by Rieger & van Mier (2010), the debonding energy of steel fibres was measured as the area under the graph from the maximum pull-out force to zero force, i.e. until the fibre was pulled out completely. The debonding energy was divided by the embedded length to be able to compare different specimens. Rieger & van Mier (2010) found that more energy is needed to pull out longer embedded fibres. The maximum pull-out force stayed relatively constant, but the pull-out energy increased.

13

It was found that at shorter lengths, the matrix porosity has a bigger influence on the bond between the fibre and matrix. Singh et al., (2004) studied the effect of the embedded length on the pull-out force of polypropylene fibres and found that the maximum pull-out force increased with embedded length. The increase is due to an increase in the friction between the fibre and matrix.

At higher water/cement (w/c) ratios, matrix porosity or void formation increases. At lower w/c ratios more un-hydrated cement particles are present, but the matrix is less porous. Although the matrix is more porous at higher w/c ratios, it was found that the pull-out energy was higher. A possible explanation is the formation of cracks between the fibre-matrix interface, as well as in the matrix itself, which leads to particle interlock and higher friction. The maximum pull-out force was however lower. In a denser matrix, a clear pull-out was observed. The maximum pull-out force was higher but the pull-out energy was lower. (Rieger & van Mier, 2010)

Singh et al., (2004) also studied the effect of curing age on the bond strength of the fibre with the matrix. A w/c ratio of 0.35 and cement/sand (c/s) ratio of 0.5 was used. It was found that the maximum strength was achieved after 2 days of curing and further curing had no effect on the interfacial bond.

Morrissey et al., (1985) studied the SFP of sisal fibre. It was found that the critical length was approximately 30 mm. At shorter lengths the fibres pulled-out, while it fractured at longer lengths. The critical length was not defined as "the length for which a uniformly distributed frictional stress reaches its critical value under the maximum sustainable tensile load", but rather as the length at which there is a strong possibility for local anchorages to form.

2.2.2. Thin fibre reinforced cement members

Conventional fibre

Thin fibre cement sheets are commonly used for roofing elements and temporary walls. Recently, asbestos cement has been replaced by glass fibre cement, because of the health risks involved with mining and using asbestos.

Fibre cement sheets are classified either as flat or profiled. An extensive range of profiles are available. According to SANS 685:2006 (SANS, 2006) a broad range of dimensions exist. For flat sheets a thickness is not specified, but the thickness should agree with different length classes. For profiled sheets, the minimum thickness is 4.5 mm and the maximum thickness is 8.0 mm.

Natural fibre

Much research has been done on thin natural fibre reinforced cement members. Silva et al., (2009) studied unidirectional sisal fibres in a cement-based matrix. Flat and corrugated sheets were developed by pouring one layer of the matrix at a time, followed by a layer of sisal fibre in a steel mould. The sheets were vibrated and press formed under a compressive load.

In a study by Savastano et al., (2003) it was stated that natural fibre composites are needed to replace asbestos-cement which holds a health hazard. Waste sisal and banana fibres were used in a matrix made up of basic granulated blast furnace slag (BGBS), agricultural gypsum and hydrated lime. Gypsum and lime were added as activators. Thin members were made using this binder with varying fibre content. It was found that an addition of 4% and 8% fibre increased the flexural strength of the members and it was comparable to members where OPC were used. After exposure to tropical weather for one year, the strength reduced considerably. This was attributed to carbonation and micro-cracking of the matrix.

Another method commonly used for the production of thin fibre cement sheets is the Hatschek process. The Hatschek process was developed by Ludwig Hatschek in the 1890's for the production of asbestos cement sheets. A film of diluted fibre-cement slurry is deposited on a sieve roller as it rotates through the vat containing the slurry. The film is transferred to a felt and is transported to an accumulating roller. The film accumulates on the roller through pressure until the desired thickness of the sheet is reached. The film is cut and the sheet simply rolls of the roller (Cooke, 2002).

Thin fibre reinforced cement members can also be manufactured by extrusion. Extrusion is a possible alternative for the abovementioned processes and will be discussed in the next section.

2.3. Extrusion

There are two types of extruders, namely auger-driven extruders and piston driven extruders. In an auger driven extruder the material is forced towards the die (the desired shape to be extruded, manufactured from steel) by a rotating auger. The smaller cross section of the die causes pressure to build up and a uniform product exits the die. In a piston driven extruder, the material is forced towards the die by a piston applying a compressive force. Pressure is also built up by the decreasing cross section towards the die.

Extrusion has the advantage of producing high quality products under high shear and compressive forces. Extrusion is not limited to flat shapes, but various shapes such as hollow-, I-, and channel sections can be produced. Specimens with superior geometrical tolerances can be produced. A matrix with low porosity and high interfacial bonding is achieved, which leads to an increase in strength and toughness of the composite (Mater, 1998). Extrusion is a continuous process. The mixture used is unlike conventional concrete. It is more of a dough-like mixture containing no coarse aggregate (Aldea et al., 1998). The mixture required for extrusion is highly viscous and must be able to maintain its shape immediately after extrusion. It should also be workable enough to be extrude-able. In order to achieve this type of consistency, a low water/binder ratio must be used. A high range water reducer or super-plasticiser reduces the water requirement further and a viscosity modifying agent is added to improve the cohesion and viscosity of the mix to prevent segregation under high pressure. The mix needs to be slightly flow-able to be able to exit through the die, but cohesive enough to maintain its shape (Visser, 2007).

It has been reported that extrusion aligns the fibres in fibre reinforced concrete (De Koker, 2004). In the case of piston extrusion, the fibres are aligned in the direction of extrusion, whereas in the case of auger-driven extrusion, the fibres have a two dimensional diagonal alignment (Visser, 2007). According to De Koker (2004), fibres tend to align perpendicular to the extrusion direction in the case of auger-driven extrusion. According to Visser (2007), fibre orientation takes place in the transition zone and in the die. Visser (2007) also states that the parallel boundaries of the die, force the fibres to orientate in a two-dimensional space, but only if the fibre length is greater than the distance between the boundaries. With this two-dimensional orientation in mind, it theoretically means that the element should be able to take equal force in both directions.

Extrusion also creates the possibility for prefabrication of structural elements. During prefabrication, elements are extruded by a machine that runs on a rail. Prefabrication can be executed with superior quality control which yields elements with superior mechanical performance.

2.3.1. Addition of fly ash to improve extrusion

As mentioned, the matrix is densified through extrusion and the interfacial bond between the fibres and matrix is improved. Peled & Shah (2003) studied the effect of different production processes on the mechanical properties of FRC. PVA fibres were used and specimens were both extruded and cast. According to Peled & Shah (2003), if the same mix for extruded and cast specimens is used, where the viscosity modifying agent (VMA) is replaced by more

super-plasticiser (SP) to increase workability in the cast mix, the mode of failure is not the same. In the extruded specimen, because of low porosity (due to the high pressure at which it is formed) the fibres will fracture, whereas in the cast specimen, because of higher porosity, the fibres will pull out.

This means that for extrusion a stronger fibre is required in order to utilise the full strength of the matrix. If longer fibres are used they will fracture, leading to sudden failure. Thus, for the same type of fibre, shorter fibres should be used for an extruded mix than for a cast mix to prevent fibre fracture. However, the strength of the composite should not be limited by the strength of the fibres. The correct balance between matrix and fibre strength should be developed.

The addition of FA can however change this phenomenon. According to Peled & Shah (2003) a decrease in strength and toughness was observed for cast specimens where 70% of OPC was replaced with FA, which is known to increase the density of cast concrete. However, in the case of the extruded composite the strength and toughness increased. This was due to the change in failure mechanism. With the addition of FA, the fibres pulled out rather than fractured. It was found that the extruded specimen containing FA was more porous than the one without FA. The lower porosity is a possible explanation for the reduction in fibre-matrix bond strength. It was also found that the porosity at the fibre-matrix interface increased. Scanning Electron Microscope (SEM) images showed a layer of cementitious matrix on the fibre surface. This suggests that debonding doesn't only take place at the fibre-matrix interface, but also in the surrounding matrix. With a decrease in bond strength, the critical fibre length is increased and the failure mode changes to fibre pull-out.

2.4. Durability of fibres

Natural fibres are biodegradable and the degradation of natural fibres is mainly due to alkaline- and biological attack. The pore water in a cement-based matrix is alkaline which leads to the degradation of natural fibres in the matrix. This in turn leads to a reduction in strength and toughness of the matrix. The degradation of natural fibres in a cement-based matrix needs to be considered in order to create durable and sustainable fibre cement composites. Durability is usually measured as a loss of strength and toughness over time.

_____

2.4.1. Alkaline attack

During the process of hydration (the reaction of cement with water) calcium silicate hydrate, 3CaO.2SiO2.4H2O, further referred to as CSH, and calcium hydroxide, Ca(OH)2, are formed. Ca(OH)2 is formed due to an excess of calcium not used in the forming of CSH. The Ca(OH)2 is mainly in the form of crystals, but also in solution in the pore water in the concrete. This is a highly alkaline solution with a pH of approximately 12.5 (Owens, 2012).

When water enters the concrete matrix, it reacts with the $Ca(OH)_2$. The alkaline pore water dissolves the hemicellulose and lignin in the middle lamellae of the fibre, weakening the bond between the fibre cells. Fibres start to debond which leads to a loss of strength and stiffness. The crystallization of lime in the pores of the fibre also degrades the fibre. The fibre becomes brittle and the strength decreases (Tolêdo Filho et al., 2000). The fibres also binds $Ca(OH)_2$ crystals on the surface as was found by Agopyan et al (2005).

In a study done by Tolêdo Filho et al. (2000), sisal and coconut fibres were immersed in solutions of $Ca(OH)_2$ with a pH of 12, sodium hydroxide, NaOH, with a pH of 11, and tap water with a pH of 8.3, respectively for up to 420 days. The tensile strength of the fibres was tested and it was found that the fibres immersed in $Ca(OH)_2$ lost its strength completely after 300 days. Coconut and sisal fibres immersed in NaOH only lost 40% and 30%, respectively of their original strength after 420 days. The fibres immersed in tap water had a reduction in strength of approximately 20%. The advanced degradation of the fibres immersed in $Ca(OH)_2$ is due to the crystallization of lime in the pores of the fibres. The loss in strength for the fibres immersed in tap water was attributed to microbiological action.

2.4.2. Biological attack

In alternate cycles of wetting and drying, biological attack on the fibres is possible, leading to a reduction in the strength of the fibres (Bentur & Mindess, 2007). The biological attack is due to fungus and algae growing on the fibre. Studies have shown that fibres imbedded in a cement matrix are immune to biological attack. This is possibly due to the high alkalinity of the matrix.

2.5. Natural fibre reinforced composites with increased durability

2.5.1. Addition of supplementary cementitious materials

The alkalinity of the cement matrix can be reduced by adding supplementary cementitious materials such as fly ash (FA), condensed silica fume (CSF), ground granulated blast

furnace slag (GGBS) or metakaolin to the mix ingredients. Metakaolin is however not available in South Africa. The cement can also be partially replaced by these materials. Supplementary cementitious materials are siliceous materials meaning they consist mainly of silicon-dioxide, SiO_2, with calcium-oxide, CaO, also being a major constituent of GGBS.

FA is a by-product from the burning of pulverized coal in furnaces, which is usually found in the process of electricity generation. In South Africa FA is classified as siliceous, because it contains less than 10% CaO (Owens, 2012). FA is used extensively in concrete to improve various properties, including durability, density and later age strength. CSF is a by-product of the silicon and ferrosilicon industries. It contains high amounts of SiO_2 which speeds up the reaction with the $Ca(OH)_2$ in the concrete matrix to form additional CSH. Unlike FA, CSF reacts more effectively and exhibits higher strengths at earlier concrete age. In an earlier study by Mehta & Gjorv (1982), 30% of portland cement was replaced by CSF. Specimens showed an increase in strength at all ages and almost double the strength at 90 days.

The partial replacement of ordinary portland cement (OPC) with FA and CSF in sisal fibre reinforced concrete (SFRC) was studied by Coetzee (2013). Thermogravemetric analysis was performed to determine the reduction in $Ca(OH)_2$ for various cement pastes containing FA and CSF. No significant difference in $Ca(OH)_2$ content was recorded for cement pastes containing 30% and 40% FA, respectively. However, a replacement of 5% and 35% of the cement with CSF and FA, respectively, recorded a significant reduction in the amount of $Ca(OH)_2$. These results showed that the replacement of cement with FA does not reduce the alkalinity of the matrix sufficiently, but the addition of CSF does. Condensed silica fume is however very expensive, so from an economical viewpoint it is not recommended to use it in large volumes.

Tolêdo Filho et al., (2002) found that the replacement of 10% of OPC with undensified silica fume in SFRC lead to a reduction of almost 40% in the first crack strength of the reference specimen (10% CSF, cured for 28 days) in comparison to a control specimen with no cement replacement. Both specimens were cured for 28 days under the same conditions. An increase in flexural strength was however recorded for aged specimens in comparison with the refererence specimen. This increase can be attributed to further hydration after 28 days. As mentioned, replacement of as little as 5% of cement content with CSF can reduce the $Ca(OH)_2$ content signifficantly (Coetzee, 2013).

In the same study by Tolêde Filho et al., (2002) long sisal fibres were immersed in a CSF-slurry for 10 minutes, after which they were dried for 15 minutes before they were incorporated into the concrete matrix. The aim was to create a zone of low alkalinity around the fibres to reduce alkaline attack. At 28 days a reduction in flexural strength of 30-40%,

compared to the control specimen, was recorded. This was attributed to reduced bonding between the CSF-coated fibres and the matrix. At 180 days however, the strength increased with comparison to the 28 day reference specimen, but it still had lower strength than the control specimen. Scanning Electron Microscope (SEM) images have shown little or no damage to the fibre surface after 322 days. This confirmed that the immersion of sisal fibres in CSF prior to mixing into a concrete matrix was an effective way to reduce alkaline attack on the fibres.

GGBS is known as a hydraulic cement or latent hydraulic binder. When it is mixed with water, very little or almost no reaction takes place (Owens, 2012). When GGBS is mixed with cement, the $Ca(OH)_2$ present from the cement hydration serves as an activator for the hydration of GGBS (Pal et al., 2003). The hydration of GGBS does not produce $Ca(OH)_2$ (Owens, 2012). The addition of GGBS to concrete leads to a denser matrix. This decreases water ingress and can increase the durability. A study done by Tolêdo Filho et al., (2002) showed that the replacement of OPC with GGBS of as much as 40% did not increase the durability of sisal fibre reinforced mortar composites. The addition of GGBS did not have a significant effect on reducing the alkalinity of the matrix and showed strong deterioration over time.

2.5.2. Carbonation

Carbonation is the reaction of $Ca(OH)_2$ with carbon-dioxide (CO_2) to form calcium carbonate ($CaCO_3$). The reaction is described by the following chemical equation:

$$Ca(OH)_2 + CO_2 \rightarrow CaCO_3 + H_2O$$
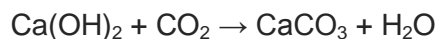
During carbonation of concrete, the $Ca(OH)_2$ combines with CO_2 from the atmosphere. The alkalinity of the concrete is reduced and the pH of the pore water can be reduced from approximately 13 to less than 9 (Tolêdo Filho et al., 2002). Carbonation is a continuous process which slows down with increasing depth. In steel reinforced concrete, carbonation is an unwanted reaction, because it causes steel corrosion and increases the rate of corrosion. However, for SFRC a lower alkalinity is sought and carbonation may be favourable to reduce fibre degradation.

Tolêdo Filho et al., (2002) conditioned sisal- and coconut fibre reinforced concrete (FRC) in a CO_2 incubator for 109 days from one day after casting. A reduction in strength, with comparison to an untreated specimen cured for 28 days in water, of approximately 10% was recorded for carbonated SFRC. In the case where specimens were exposed to 36 controlled cycles of wetting and drying after 109 days of carbonation, an increase in the flexural

strength of 108% was recorded in comparison to an untreated specimen exposed to 46 cycles. It was also found that a shorter initial curing period increases the depth of carbonation. Carbonation seems to be a promising alternative to increase the durability of SFRC.

Under carbonating conditions the strength of the fibre reinforced matrix tends to increase. This increase in strength is due to the petrification of the fibre which leads to an increase in the fibre strength and rigidity. Carbonation also leads to a denser matrix causing a better fibre-paste interface (Bentur & Mindess, 2007).

2.5.3. Chemical treatment of fibres

As mentioned previously, fibres degrade due to the high alkalinity of the pore water in a cement matrix. The alkalinity of the cement matrix can be reduced or fibres can be chemically treated in order to enhance the durability of NFRC. However, account has to be taken of the fact that chemical treatment may reduce the initial strength of the fibre.

According to Kabir et al., (2012) there are various methods of chemical treatment. The most common and simple chemical treatments are alkaline treatment and acetylation. These are also known as surface treatments. During chemical treatment, lignin, pectin, fats and waxes are removed from the surface of the fibre leading to a rough fibre surface and increase the bond strength between the fibre and the matrix. The molecular structure of the fibre is also modified. Hydrophilic hydroxyl groups are removed and the hydrophobicity of the fibre is enhanced. This reduces the migration of hydration products through the fibre which will reduce or eliminate the rate of degradation of the fibre.

The effect of chemical treatment on sisal fibre has been studied by Yang et al., (1996). The results are presented in Table 2.4. The results have been converted from units of gram/tex (g/tex), which is a standard measuring unit in the textile industry, to megapascal (MPa). One Newton/tex (N/tex) is equal to one gigapascal (GPa). Alkali treatment as well as acetylation led to an increase in the tensile strength of the fibre. An increase in elongation and stiffness of the fibre has also been recorded.

According to Martins et al., (2004), fibres submitted to less severe treatment conditions showed more significant changes than those submitted to severe conditions. It is possible to use less drastic and more economical treatment conditions. Kalia et al., (2009) studied the effect of different chemical treatments on palm fibre and found a considerable decrease in the tensile properties of the fibre. This decrease was attributed to the removal of lignin and the degradation of the cellulose chains.

Table 2.4: Effect of chemical treatment on tensile properties of sisal fibre (Yang et al., 1996).

Treatment Methods	Tensile Strength (MPa)	Tensile Modulus (MPa)	Elongation at Break (%)
Untreated	301.17	11.58	2.5
Benzol/Alcohol	380.63	9.71	3.7
Acetic Acid + Alkali	91.23	3.83	2.6
Alkali	310.98	5.20	7.5
Acetylated	325.69	3.43	8.3
Thermal	412.02	11.97	3.5
Alkali-thermal	270.76	6.87	4.7
Thermal-alkali	252.12	6.97	4.4

Alkali treatment

Alkali treatment is the most common treatment method used for natural fibres and is usually executed with a NaOH solution. Fibres are immersed in a NaOH solution of specified concentration for a specified time. The effect of alkali treatment on the properties of natural fibres depends on the concentration of the alkali solution, the temperature and the duration of the treatment.

During alkali treatment the cellulose molecules are separated and the spaces are filled with water molecules. The fibre swells and changes in the fine structure and morphology of the fibre take place (Mwaikambo & Ansell, 1999). The hydrophilic hydroxyl groups from the hemicellulose and lignin are broken down and reduced and thus also the ability of the fibre to absorb water (Kabir et al., 2012). The amount of amorphous regions is increased and the crystalline region is reduced. The crystalline packing is however improved (Mwaikambo & Ansell, 1999). Cellulose is depolymerized and the short length crystallites are exposed (Li et al., 2007). Materials such as pectin, waxy substances and natural oils are also partially removed from the surface of the fibre. This exposes the fibrils or ultimate fibres and leads to a rough fibre surface and a better fibre-matrix interaction can be achieved. In effect, the effective fibre surface area is increased. The reaction between the fibre and the NaOH during alkali treatment is described by the following chemical equation:

$$\text{Fibre-cell-OH} + \text{NaOH} \rightarrow \text{fibre-cell-O-Na}^+ + H_2O + \text{impurities.}$$

It has also been reported that alkali treatment improves the thermal behaviour of natural fibres (Kabir et al., 2012). In a study done by Mwaikambo & Ansell (1999), it was found that the correct concentration of the NaOH solution is important, because at certain concentrations fibres showed reduced thermal resistance. Kabir et al., (2012) also found that at concentrations higher than the optimum concentration, delignification takes place. During

delignification, too much of the lignin is removed, the ultimate fibres are seperated which leads to a reduction in fibre strength. This is also known as defibrillation.

In a study by Mohan & Kanny (2012), alkali treated sisal fibre were immersed in water to compare water absorption of treated- to untreated sisal fibre. Untreated fibre showed a 73% increase in weight compared to alkali treated fibre only showing a 30% increase. A 12.5% increase in tensile strength and 12.1% increase in tensile modulus was also documented. Alkaline treatment makes the fibre surface more uniform leading to a more evenly distributed shear stress along the fibre surface (Le Troëdec et al., 2009).

In a thermal analysis done by Le Troëdec et al., (2009) it was found that hemp fibres subjected to alkali treatment were more thermally stable than untreated fibres. It was also concluded through the thermal analysis that the structure of the cellulose is not affected through alkali treatment, but that is was only the fibre surface that has been modified and cleared from impurities. The stiffness of the hemp-lime composite was increased but the deformation at ultimate stress was decreased.

Alkali treatment has been studied by several authors and a summary of the concentrations used and the results obtained are presented in Table 2.5.

Table 2.5: Summary of alkaline treatment by several authors.

Author	Concentration	Results	Additional comments
(Le Troëdec et al., 2009)	6 vol% (hemp) for 48 hours (±ml/l)	Modified hemp fibres are more thermally stable. Removes amorphous compounds. Clean surface	
(Mwaikambo & Ansell, 1999)	0.8, 2, 4, 6, 8, 30, 400% NaOH. 100% = 1 M (Molar) (6% = 2.4g/litre)	Slight rise in thermal resistance between 4% and 8%. Highest crystallinity index at 6%. Rough surface	$20 \pm 2°C$ for 48 hours. Washed in distilled water containing 1% acetic acid to neutralise excess NaOH. Dried and kept in conditioning chamber.
(Martins et al., 2004)	5 and 10% NaOH (mass/volume) (50 and 100 g/l)	Removal of impurities and separation of ultimate cells. 10% for 1 hour at room temperature showed more significant changes than 5 or 10% at 50°C.	$26 \pm 2°C$ for 1 hour. Rinsed with tap water, neutralised with acetic acid
(Mohan & Kanny, 2012)	40g NaOH in 100ml distilled water	Water uptake was reduced	5 g of sisal was placed in mix. Treated at 60 °C for 1 hour.

Acetylation

Fibres can also be treated by acetylation to enhance the fibre properties and improve the durability. Acetylation of natural fibres has not been studied to the same extent as alkaline treatment. The main purpose of acetylation is to graft acetyl groups (CH_3COO^-) on the fibre cell wall and remove surface impurities. During acetylation, Acetic Acid (CH_3COOH) is generated as a by-product and should be removed before the fibre is used (Li et al., 2007).

Acetylation stabilises the cell wall, improves dimensional stability and decelerates environmental degradation. During acetylation the hydroxyl groups of the cell wall are replaced with acetyl groups (CH_3COO^-). This process is also called grafting (Kalia et al., 2009). The voids in the cell wall are filled and better fibre-matrix interaction is achieved (Kabir et al., 2012). Acetylation also reduces the hydrophilic nature of vegetable fibres by removing hemicellulose and lignin from the fibre, which means that the ability of the fibre to absorb water is reduced. In the case where water is absorbed, no additional swelling of the fibre will take place (Mwaikambo & Ansell, 1999). Martins et al., (2004) found that acetylation exposes the fibrils leading to a rougher surface texture.

Acetylation can be done with or without an acid catalyst. The strong intra-molecular bonds in the crystalline region make chemical penetration difficult. Acetic Acid is used as a catalyst to swell the fibre and accelerate the reaction, after which it is soaked in Acetic Anhydride for a period of 1-3 hours (Kabir et al., 2012). The chemical reaction is described in the following equation:

$$\text{Fibre} - \text{OH} + CH_3COOH \xrightarrow[\text{Concentrated } H_2SO_4]{(CH_3CO)_2O} \text{Fibre} - O - \overset{\displaystyle O}{\overset{\displaystyle \|}{C}} - CH_3 + H_2O$$

$$\text{Fibre} - \text{OH} + CH_3 - \overset{\displaystyle O}{\overset{\displaystyle \|}{C}} - O - \overset{\displaystyle O}{\overset{\displaystyle \|}{C}} - CH_3 \longrightarrow \text{Fibre} - O - \overset{\displaystyle O}{\overset{\displaystyle \|}{C}} - CH_3 + CH_3\overset{\displaystyle O}{\overset{\displaystyle \|}{C}} - OH$$
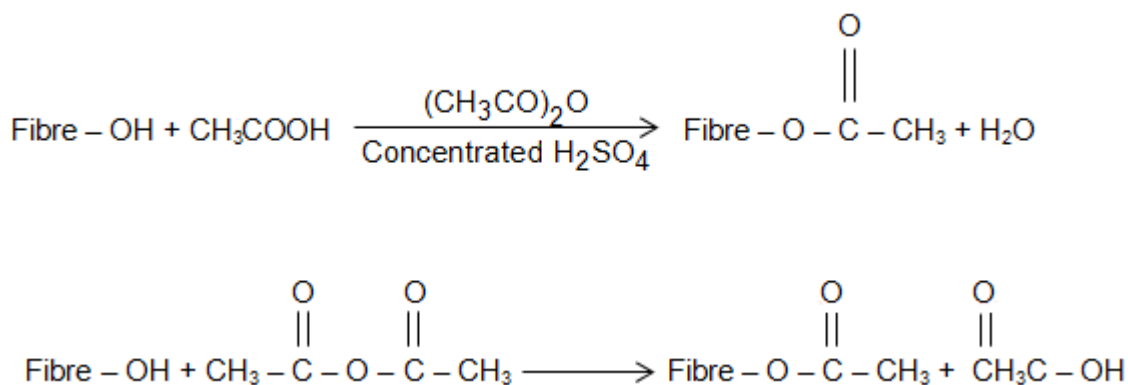
Acetylation can also be preceded by alkalisation. As mentioned previously, alkalisation separates the cellulose molecules and facilitates the penetration of other chemical compounds into the fibre. A summary of the concentrations used by different authors and the results obtained are presented in Table 2.6.

Table 2.6: Summary of acetylation by several authors.

Author	Concentration	Results	Additional comments
(Mwaikambo & Ansell, 1999)	10% Acetic Anhydride for 1 hour. 10% Acetic acid for 1 hour and then acetic anhydride containing sulphuric acid for 5 min (100% = 1 M).	Grafting was effective. Makes fibre more hygroscopic. Reduction in number of hydroxyl groups	$20 \pm 2°C$ for 1 hour. Washed in distilled water
(Martins et al., 2004)	Glacial acetic acid for 1 hour and then 500 ml of acetic anhydride containing 20 drops of H_2SO_4 for 5 min	Defibrillation at some points. Change in morphology without damaging fibre structure.	

_____

CHAPTER 3

Experimental Framework

Several initial cement-based matrices reinforced with sisal fibre were developed to determine a suitable matrix for the manufacturing of the specimens for the experimental work. SFP tests were performed to evaluate the tensile strength of the fibres and to determine the critical length for the fibres. The mechanical properties of the composites were determined by evaluating the compressive-, flexural- and direct tensile strength at 28 days. The durability was determined by testing the composite after ageing by performing flexural- and direct tensile tests and comparing the results with the 28 day un-aged results. The different ageing methods were alternate cycles of wetting and drying, extended curing in standard curing conditions (in water at $24 \pm 2°C$) and curing in lime saturated hot water.

The materials used, the fibre preparation and the specimen production are discussed in this chapter. Furthermore, the ageing methods, test methods and mix design are discussed. A brief overview of the test programme is provided at the end of the chapter.

3.1. Materials

3.1.1. Aggregate

Only fine aggregate was used in this study, as this enables the fibres to be dispersed more freely throughout the specimen and it also improves the fibre-matrix bond. The specimens produced had a thickness of only 15 mm. In these thin members the presence of coarse aggregate would have caused poor fibre distribution. Malmesbury pit sand, a local sand from the Cape Town area, usually has a relatively good grading with an even particle size distribution. Consequently, Malmesbury pit sand was used since it will enable good compaction.

A sieve analysis of the sand was performed according to SANS 201 (2002) and the results are presented in Table 3.1. The relative density (RD) and fineness modulus (FM) of the sand

were determined according to SANS 5844 (1994) and SANS 5845 (1994). Figure 3.1 presents the grading curve of the sand. The relative density (RD) of the sand was 2.6, the fineness modulus (FM) 1.51 and the dust content 3.68%. From the sieve analysis it is evident that the sand is relatively fine. Most of the particles lie between the 150 and 1180 µm sieves.

Table 3.1: Sieve analysis of Malmesbury pit sand

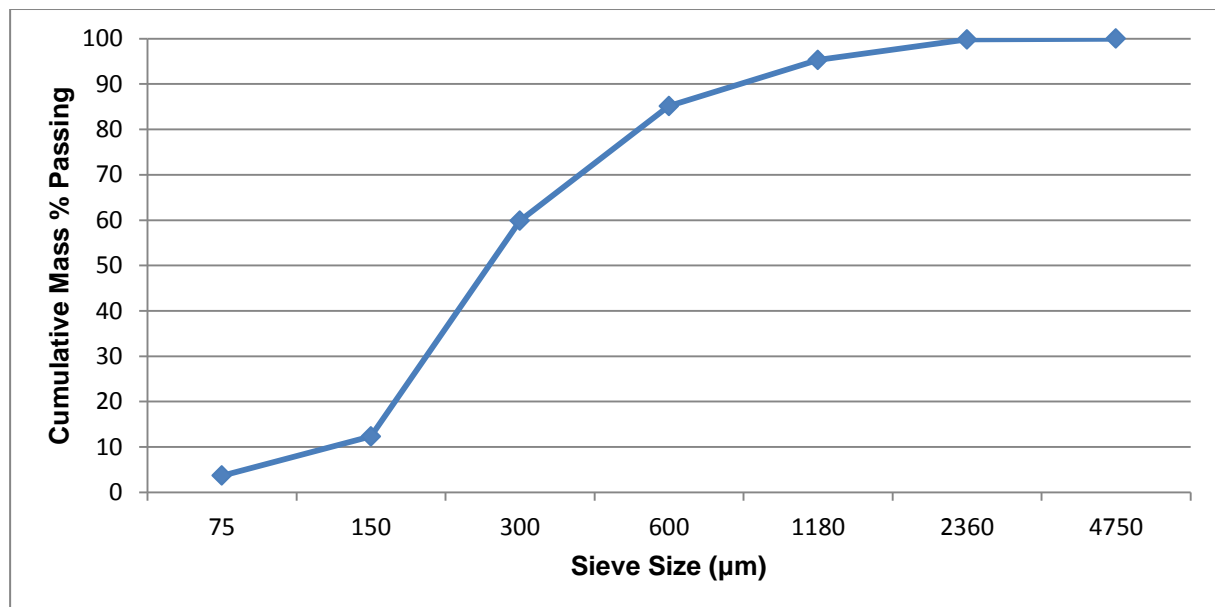| Specimen weight before washing | | | 500 g | |
| Specimen weight after washing | | | 490.20 g | |
Sieve Size (µm)	Sand Mass (g)	Cumulative Mass Retained (g)	Cumulative % Retained	Cumulative % Passing
4750	0	0	0	100
2360	1	1	0.20	99.80
1180	22.6	23.6	4.72	95.28
600	50.8	74.4	14.88	85.12
300	126.2	200.6	40.12	59.88
150	237.7	438.3	87.66	12.34
75	43.3	481.6	96.32	3.68
Pan	8.6	490.2	100	0
Washed fines	9.8	500		

Figure 3.1: Sieve analysis of Malmesbury pit sand.

27

3.1.2. Cement

The cement used for the manufacturing of the specimens was Ordinary Portland Cement (OPC) manufactured by PPC. OPC is identified as Portland Cement CEM I 52.5 N. It conforms to the 52.5 N strength class of SANS 50197-1 (2000). The relative density of the cement was 3.14. The typical chemical composition of South African CEM I cement is presented in Table 3.2.

Table 3.2: Typical chemical composition of South African CEM I cement (Owens, 2009).

Compound	Formula	Abbreviation	% by mass
Tricalcium silicate	$3CaO.SiO_2$	C_3S	60 – 73
Dicalcium silicate	$2CaO.SiO_2$	C_2S	8 – 30
Tricalcium aluminate	$3CaO.Al_2O_3$	C_3A	5 – 12
Tetracalcium aluminoferrite	$4CaO.Al_2O_3.Fe_2O_3$	C_4AF	8 – 16
Magnesia	MgO	M	1.9 – 3.2
Gypsum	Raw material	-	4.4 – 6.7
Free lime	CaO	-	0.2 – 2.5

3.1.3. Fly Ash

The fly ash used was DuraPozz supplied by Ash Resources. The chemical composition of the specific batch of fly ash, as well as the general chemical composition of DuraPozz, is presented in Table 3.3. DuraPozz conforms with Category S of SANS 50450-1 (2011) and is classified as a type F fly ash. The relative density of the fly ash was 2.8.

Table 3.3: Typical chemical composition of DuraPozz fly ash (Ash Resources, 2011).

Chemical Compound	DuraPozz	Fly ash for this research
Silicon (SiO_2)	47.0 – 55.0	54.10
Aluminium (Al_2O_3)	25.0 – 35.0	31.83
Calcium (CaO)	4.0 – 10.0	4.86
Iron (Fe_2O_3)	3.0 – 4.0	3.22
Magnesium (MgO)	1.0 – 2.5	1.23
Titanium (TiO_2)	1.0 – 2.0	1.66
Phosphorous (P_2O_5)	0.5 – 1.0	0.41
Potassium (K_2O)	0.5 – 1.0	0.77
Sodium (Na_2O)	0.2 – 0.8	0.24
Sulphur (SO_3)	0.1 – 0.5	-
Manganese (Mn_2O_3)	0.1 – 0.2	-

3.1.4. Condensed Silica Fume

The condensed silica fume used was Microfume supplied by Silicon Smelters. The chemical composition of Microfume is presented in Table 3.4. The table contains only the major chemical components of Microfume. The relative density of the condensed silica fume is 2.1.

Table 3.4: Chemical composition of Microsilica (FerroAtlantica Group, S.A., 2007)

Chemical composition (%)	
SiO_2	> 85.0
CaO	< 1.0
Al_2O_3	< 1.0
C	< 4.0

3.1.5. Super-plasticiser

Super-plasticiser, also known as high range water reducers, is a synthetic, water-soluble organic compound (Owens, 2009). It is a powerful chemical additive that is used to reduce the amount of water required in a concrete mix, or to increase the workability of the concrete mix for a given water/binder ratio. Polymeric chains with a negative charge are formed which attract the positively charged cement particles. Repulsion forces form around the particles, leading to dispersion in the cement particles. The dispersion reduces the friction between the particles which leads to an increase in workability. If the amount of water required for the mix is reduced and the water/binder ratio is kept constant, the quantity of cement can be reduced to achieve the same strength. However, if the amount of binder is kept constant but the amount of water required in the mix is reduced by the super-plasticiser, the strength will be increased. Super-plasticiser is available in liquid and powder form. The super-plasticiser used was Dynamo SP1 liquid super-plasticiser supplied by Mapei.

3.1.6. Viscosity modifying agent

Viscosity modifying agents (VMA) are used to increase the viscosity of the mix in cases where concrete washout is undesirable, e.g. underwater placement. In the case of extrusion, where high pressure is applied to the mix, viscosity modifying agents are used to prevent water being forced out of the fresh concrete. The viscosity modifying agent used in this research is Aquabeton ZA supplied by Chryso.

3.1.7. Sisal fibre

The sisal fibre was supplied by Rebtex RSA. The specific origin of the fibre is unknown, but Rebtex imports from Brazil and Africa. The fibres were received in bundles, already washed and combed. The properties of sisal fibre were discussed in Chapter 2. The fibre preparation is discussed in the following section.

3.2. Fibre preparation

The received fibre bundles were separated into smaller bundles before being cut to required lengths. A paper guillotine was used to cut the fibres. The separation of the fibre bundles caused some of the fibres to get tangled and therefore it was combed again using a nail comb. During combing, some of the fibres get entangled in the nail comb which leads to fibre loss. The cutting of the uneven edges of the fibre also leads to fibre loss. Consequently, combing and cutting lead to fibre loss of approximately 30% of the initial weight. A picture of the nail comb and the fibres lost during combing can be seen in Figure 3.2. The untreated fibres were stored in a conditioning chamber at a temperature of $23 \pm 2°C$ and a relative humidity of $65 \pm 2\%$. Two different fibre treatments, namely alkali treatment and acetylation were also performed. They are discussed in the following section.
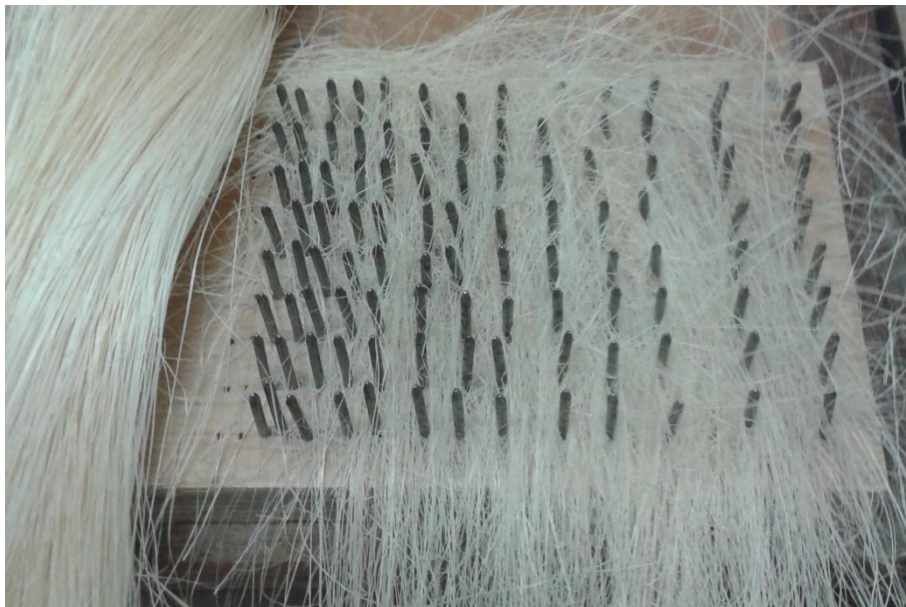

Figure 3.2: The nail comb used to separate the fibres. A combed bundle of fibres can be seen on the left.

3.2.1. Alkali treatment

Alkali treatment was performed by using 2%, 6%, 10%, 20% and 30% NaOH solutions. These concentrations were used as the highest crystallinity index reported by Mwaikambo and Ansell (1999) was for fibres treated in a 6% NaOH solution. As mentioned earlier, a higher crystallinity results in stronger, stiffer fibres.

The fibres were soaked in the different NaOH concentrations for 48 hours in a conditioning chamber, after which they were rinsed in 1% acetic acid to neutralise excessive NaOH and washed in water to remove excess acid from the fibre surface. The fibres were then spread out in the conditioning chamber and left to dry over a period of 2-3 days until constant weight was reached.

One mole of NaOH is equal to 40 grams. One molar (M) is the concentration of one mole of a chemical compound in one litre of water. Thus, one molar NaOH is equal to 40 g/l. Different authors have different ways of expressing concentration, but it is usually expressed as a percentage where 100% is equal to one molar. In this study, 100% was equal to one molar.

3.2.2. Acetylation

Acetylation was performed by using Acetic Acid and Acetic Anhydride, both at concentrations of 5% and 10%. In addition, a combination of alkali treatment and acetylation was also used. Fibres were soaked in Acetic Acid and Acetic Anhydride respectively for 1 hour. Fibres, pre-treated with 6% NaOH, were also soaked in 5% and 10% Acetic Anhydride for 1 hour. The fibres were removed from the solution and washed in water to remove excess acid from the fibre surface. The fibres were then spread out in the conditioning chamber and left to dry for a period of 2-3 days until constant weight was reached.

One mole of Acetic Anhydride is equal to 102 grams and one mole of Acetic Acid is equal to 60 grams. The concentrations were also expressed as a percentage where 100% is equal to one molar.

3.3. Specimen production

3.3.1. Mix procedure

A 50 litre pan mixer was used for all the mixes. The mixer was saturated with water and towel dried before adding the materials to prevent water loss from the mix. The dry ingredients were added first in the following order: sand, cement, fly ash, condensed silica

fume and viscosity modifying agent, if included in the specific matrix. The dry ingredients were allowed to mix for 30 seconds before the water was added to ensure thorough mixing.

After 30 seconds, a portion of the water was added to stop the dry ingredients from escaping in the form of dust. The fibres were then added after which the rest of the water and the super-plasticiser were added slowly. A small portion of the mix water was kept to rinse the measuring tube of the super-plasticiser. The fibres had to be added slowly by hand, while separating them to ensure that no fibre balling took place. If the fibres were added to quickly, the friction and interlock between the fibres caused fibre balls to form. These fibre balls are not separated during the mixing process. Adding the fibres took approximately 10-15 minutes. The mix was allowed to mix for another four minutes to allow the super-plasticiser to work effectively. The total mixing time was approximately 15-20 minutes.

3.3.2. Single fibre pull-out specimens

The single fibre pull-out specimens were cast in a mould similar to the one used by Boshoff (2007). The mould was manufactured from Perspex. The length, width and depth of the mould were 200 mm, 50 mm and 10 mm respectively. A picture of the mould can be seen in Figure 3.3. The mould consists out of three parts; the base, a frame and two bars fixed to the top. The fibre strands were secured to the frame, spaced at a distance of 10 mm between strands, and held in place by thin double sided tape. All the parts of the mould were held in place and secured by screws.

The mortar was first placed in the base up to half the depth of the mould. The frame, with the fibres secured to it, was then placed on top of the base. Thereafter, the two top bars were placed over the fibre strands on top of the base and the rest of the mould was filled with mortar. The specimen was vibrated for 60 seconds to compact and spread the mortar evenly.

After one day of curing at room temperature, the specimen was demoulded and cured in water at $24 \pm 2°$C until an age of 28 days from the date of casting. The specimen was cut into smaller samples (50x10x10 mm), with a single cast-in fibre protruding on both sides, using a diamond blade cutter. If required, the smaller samples were cut to a shorter length.
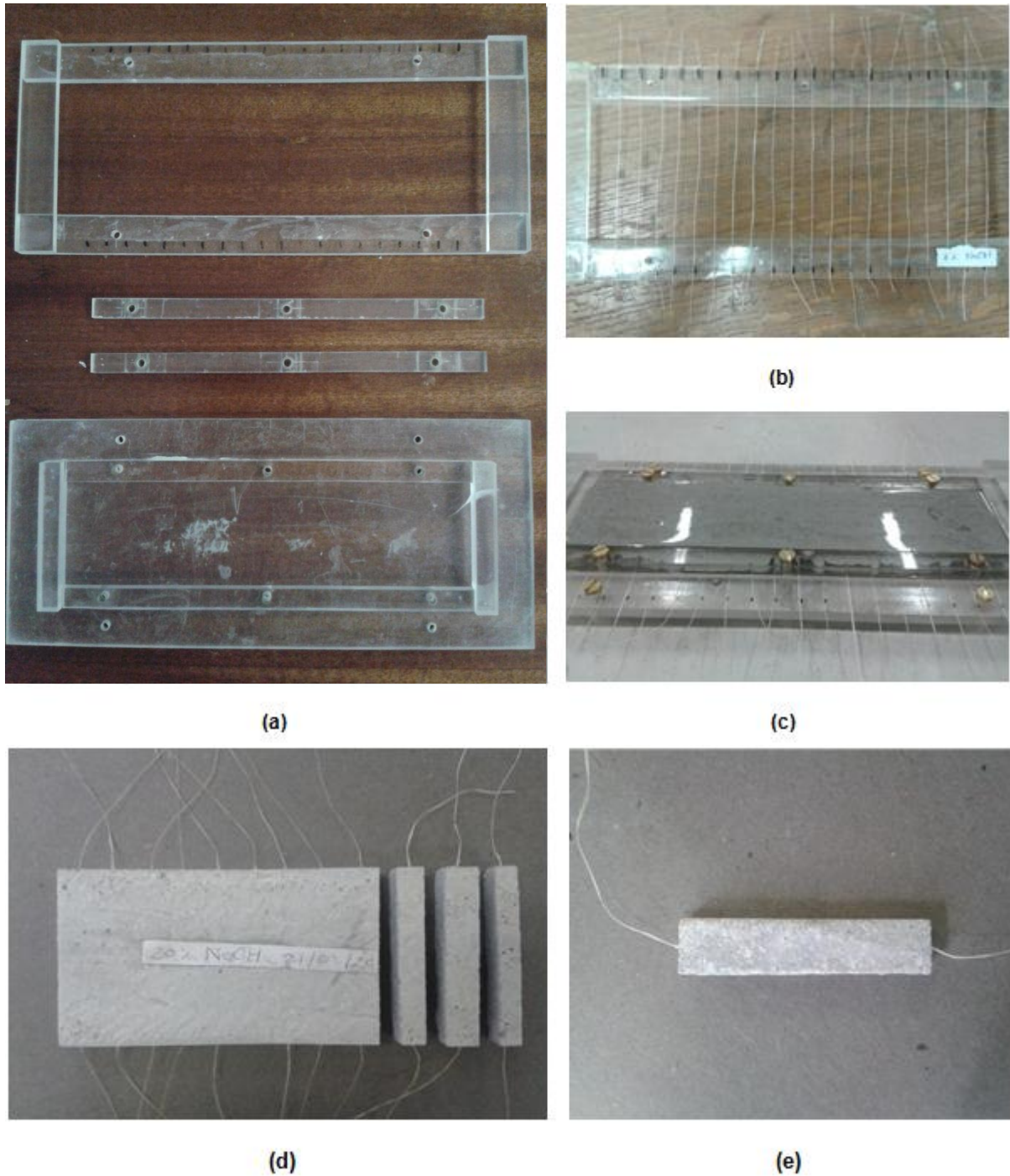
Figure 3.3: (a) The three different parts of the single fibre pull-out mould showing, from top to bottom, the frame, the two top bars and the base. (b) The fibres positioned on the frame and secured with double sided tape. (c) The complete mould filled with mortar. (d) The specimen after demoulding with a few smaller specimens cut from it. (e) One specimen cut from the larger cast specimen, showing a single fibre protruding on each side.

3.3.3. Cast specimens

Two different sets of moulds, including 600x70x15 mm beam moulds and 400x60x15 mm bone-shaped moulds, referred to as dogbones, were used for the cast specimens. The area in the middle of the dogbone where the specimen is narrower is referred to as the gauge area. The dimensions of the gauge area are 80x30x15 mm. A picture of the moulds can be seen in Figure 3.4.

After mixing, the fresh mortar was placed in the moulds and vibrated on a vibrating table for two minutes. The surface of the specimen was smoothed using a trowel. After two days of curing at room temperature, the specimens were demoulded and cured in water at $24 \pm 2°C$ until an age of 28 days from the date of casting. The 600 mm beams were cut in half to 300 mm beams to provide more specimens. A 3 mm notch was cut in the middle of the gauge area on both sides of the dogbone to ensure fracture to take place at the desired location during testing. A picture of the notch is presented in Figure 3.5. The gauge area is indicated by the red block.

(a)

(b)

Figure 3.4: Pictures of (a) beam mould and (b) dogbone mould.

34
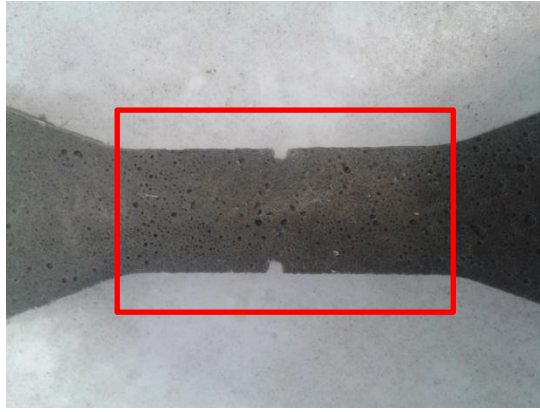
Figure 3.5: The 3 mm notch cut in the dogbone specimens.

3.3.4. Extruded specimens

An auger extruder, shown in Figure 3.6, was used to manufacture the extruded specimens. The dough like mix was fed into the loading chamber of the extruder and forced down using an air press. The size of the die, which is the point at which the mortar exits the extruder and takes shape, was 70x15 mm. PVC sheets, 600 mm in length, were placed at the tip of the die, sloping slightly downwards. The sheets were lubricated well using standard mould oil. As the mortar exited the die, it slowly progressed down the PVC sheet. When a beam of 600 mm was extruded, it was cut off using a trowel and the next sheet was placed at the tip of the die. The extrusion process is shown in Figure 3.7.

Figure 3.6: The auger extruder used to manufacture the extruded specimens.
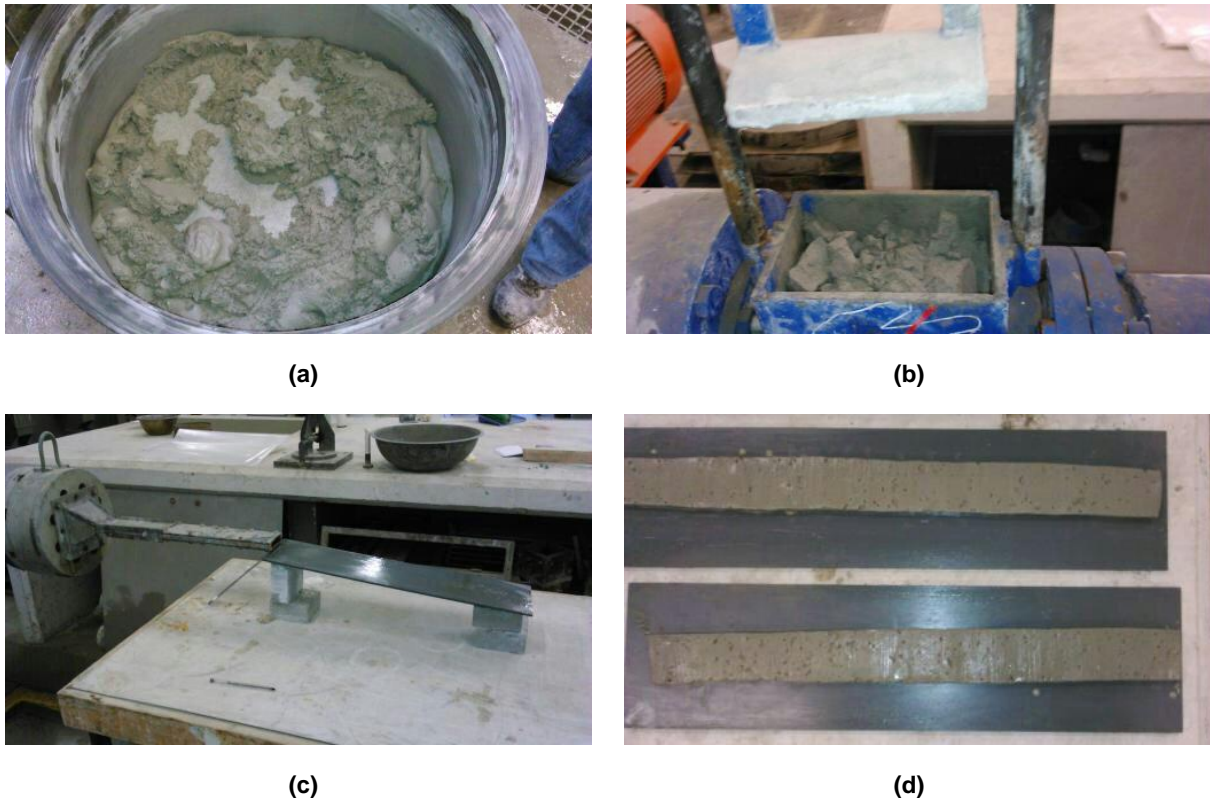
Figure 3.7: The extrusion process, showing from (a) the dough-like mix, (b) the mortar in the loading chamber of the extruder, (c) the PVC sheet at the tip of the die sloping slightly downwards and (d) two extruded beams.

The speed of the extruder motor is adjustable. At the start of extrusion it was set at a speed of 500 rpm until pressure built up and the mortar started exiting the die. The speed was then incrementally increased up to a speed of 1200 rpm. This was necessary, as the mortar became compacted inside the extruder and more pressure was required to extrude it.

After two days of curing at room temperature, the specimens were cured in water at 24 ± 2°C until an age of 28 days from the date of extrusion. The 600x70x15 mm beams were cut in half to produce the 300x70x15 mm test beams.

3.4. Ageing methods

In order to evaluate the durability of SFRCC, specimens were aged and tested at 90 days. The strength was compared to the reference specimens tested at 28 days. After 28 days of water curing at 24 ± 2°C and testing of the reference specimens, the remainder of the specimens were subjected to three different ageing conditions.

One set of specimens were placed in a hot water curing tank. The water was saturated with lime and kept at a constant temperature of 70 ± 2°C. This was done according to

ASTM C1560-03 (2009). The addition of lime makes the water alkali-based and accelerates the degradation of the sisal fibre in the matrix. Another set of specimens were subjected to alternate cycles of wetting and drying. The specimens were dried in a conditioning chamber for 4 days at $23 \pm 2°C$ and $65 \pm 2\%$ relative humidity and then saturated in water at $24 \pm 2°C$ for 3 days. One cycle was equal to 7 days. The cycle was repeated nine times until an age of 90 days from casting was reached. This ageing condition was used to simulate natural weathering. The third set of specimens was left in the curing tank at $24 \pm 2°C$ until an age of 90 days to determine whether degradation takes place under normal curing conditions.

The beams were subjected to all three ageing conditions, but the dogbones were only subjected to the hot water and normal water ageing. Not enough dogbone specimens were available to be subjected to alternate cycles of wetting and drying. All the specimens were tested at an age of 90 days from the day of casting.

3.5. Test methods

3.5.1. Moisture absorption

The moisture absorption of the fibres was measured to determine whether the chemical treatment of the fibres enhanced the hydrophobicity of the fibres. Fibre samples subjected to the different chemical treatments (Untreated, Alkali treated and Acetylated) were saturated in water for 24 hours. They were spread out on a sieve to allow excess water to drain. A 40 g sample of the saturated fibre was then dried in an oven at $50°C$ over a period of 48 hours until constant weight was reached. The amount of water absorbed was expressed as a percentage of the dry weight of the fibre specimen after it was dried in the oven.

3.5.2. Scanning Electron Microscope (SEM)

Scanning Electron Microscope (SEM) images of the fibre were taken using a LEO 1450 VP SEM. The images were used to study the effect of chemical treatment on the fibre appearance as well as the fibre structure and appearance after fibre fracture and pull-out. Images of untreated and treated fibre as well as images of the fractured and pulled-out fibres from the SFP tests were taken at magnifications of 150 and 500 times, respectively.

3.5.3. Single fibre pull-out (SFP) tests

Single fibre pull-out tests were performed to gain an understanding of the fibre-matrix interaction, the interfacial bond strength and the effect of chemical treatment on the bond strength as well as to determine the critical lengths for the fibres subjected to different treatments.

The tests were performed using a Zwick Z250 material testing machine. The bottom part of the specimen (mortar) was clamped, while the fibre was fixed with superglue to an aluminium surface attached to a Hottinger Baldwin Messtechnik (HBM) 10 N load cell. The clamp consisted of two plates which were adjustable by bolts. The two plates and the load cell were clamped in the grips of the machine. A tensile force was applied to the specimen at a constant displacement rate of 0.1 mm/s. A Linear Voltage Displacement Transducer (LVDT) was fixed across the clamps of the machine to record the displacement and thus the pull-out of the fibre. The load and displacement were logged using a HBM Spider8 data acquisition system. A picture of the test setup can be seen in Figure 3.8, showing in (a) the test specimen being clamped and the fibre glued to the flat surface attached to the load cell and in (b) a close-up of the specimen. The fibre is drawn in red for illustration purposes, as it is unclear on the photo.

(a)   **(b)**
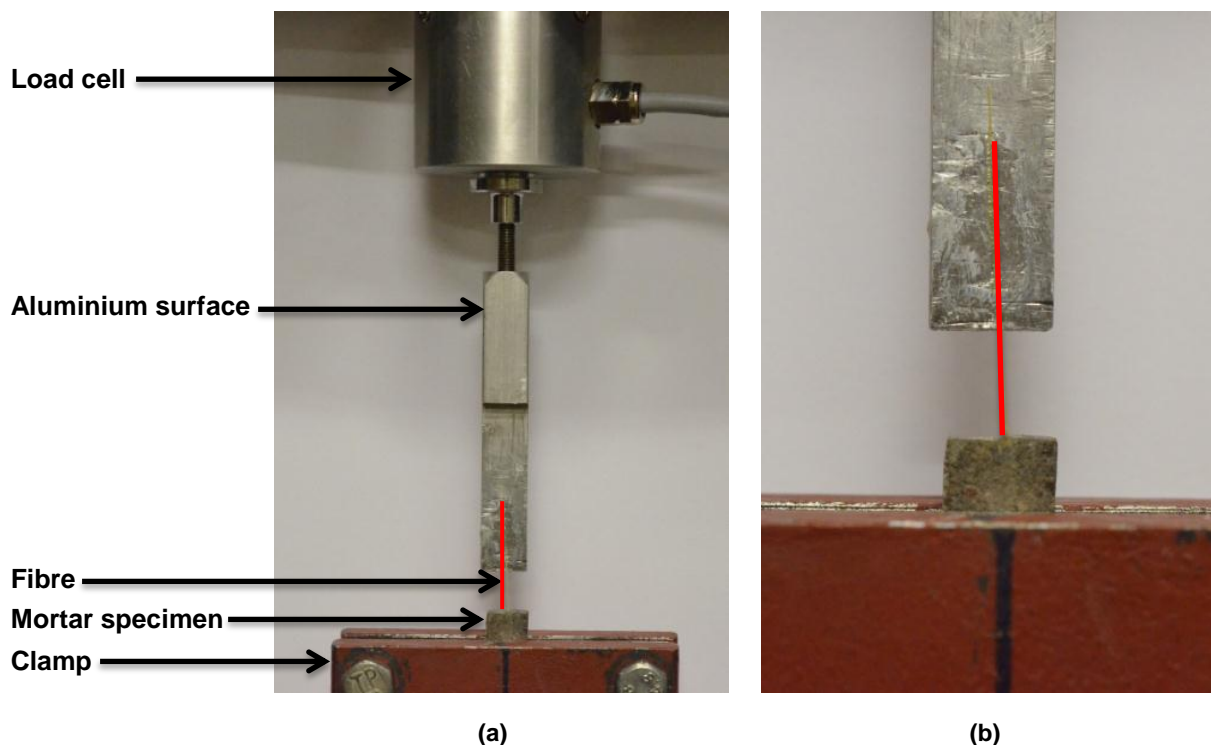
Figure 3.8: Picture of test setup for single fibre pull-out tests.

3.5.4. Compression tests

Compression tests were performed on 100x100x100 mm cubes to determine the compressive strength of the different matrices. According to SANS 5863 (1994), a standard loading rate of 120-240 kN/min should be used for 100 mm cubes. A loading rate of 180 kN/min was used. The maximum load at failure was recorded.

3.5.5. Three-point bending tests

Three-point bending tests were performed on the 300 mm beams to evaluate the flexural strength of the different matrices and to study the influence of the fibres on the post-peak (after cracking) behaviour of the specimens. The tests were also performed using the Zwick Z250. The test setup can be seen in Figure 3.9. A span of 250 mm was used. The beams were loaded at a rate of 5 mm/min. The tests were stopped after a displacement of 10 mm. In most of the series, six specimens were tested, but in some only four were tested, as some broke during demoulding.

The load and displacement was recorded and represented in graphs of flexural stress at the ultimate fibre of the beam versus the crosshead displacement of the material testing machine. The ultimate flexural stress, σ_y, is calculated as follows:

$$\boldsymbol{\sigma_y} = \frac{\boldsymbol{3PL}}{\boldsymbol{2bd^2}} \qquad\qquad (1)$$

where,

        P is the applied load in Newton (N).

        L is the support separation, in this case 250 mm.

        b is the width of the specimen, in this case 70 mm.

        d is the thickness of the specimen in mm.

Figure 3.9: Test setup for three-point bending tests.

3.5.6. Direct tensile tests

The tensile strength of the different matrices were evaluated by performing direct tensile tests on the dogbone specimens. The test setup can be seen in Figure 3.10. Two clamps, consisting out of two plates each between which the ends of the dogbones were secured by means of bolts, were fixed on the material testing machine. A HBM 20 kN load cell was fixed to the top clamp. The dogbones were positioned between the two plates of each clamp after which the top and bottom bolts were inserted through the plates and the holes of the dogbone. The bolts, as well as the rest of the screws on the clamps, were then carefully tightened. For the duration of the tightening process, the machine was set to maintain a tensile force of 10 N, by automatically adjusting the crosshead position. An extensometer was positioned over the gauge area of the dogbone to measure the crack opening. The load and crack opening were logged using a HBM Spider8 data acquisition system.

A loading rate of 1 mm/min was used. The tests were stopped after a crack opening of 3 mm was measured. In some cases the specimen cracked before the test commenced while the clamps were tightened. The tests continued, but no peak strength could be recorded. In cases like that a forth specimen was tested, if available, and the best results of the specimens tested were used.

The test data is represented in graphs of direct tensile stress versus the crack width measured by the extensometer. The direct tensile stress, σ, was calculated as follows:

$$\sigma = \frac{P}{bd} \qquad (2)$$

where,

P is the applied load in Newton (N).

b is the width of the specimen at the crack in mm.

d is the thickness of the specimen in mm.

Figure 3.10: Test setup for direct tensile tests.

3.6. Mix design

3.6.1. Initial trial mixes

The initial trial mix consisted only of water, OPC and Malmesbury sand. No fibres or additives were added to the initial mix. The workability was measured by the Flow-test according to SANS 5862-2 (2006). The water/binder ratio was equal to 0.22 to achieve a

slump-flow diameter of 500 mm. With the addition of fibres, super-plasticiser was added to maintain workability. The amount of super-plasticiser was adjusted for different volumes of fibres. The mix design is presented in Table 3.5. The amount of super-plasticiser added for 20 mm fibres, presented as a percentage of the weight of the cement, and the slump flow for different fibre volumes is presented in Table 3.6. As can be seen from Table 3.6, the slump-flows for the different mixes were not exactly equal. This was due to the sensitivity of the mix to super-plasticiser.

Table 3.5: Initial trial mix.

Constituent	RD	Weight kg/m^3
Water	1	286
Cement (OPC)	3.14	1300
Sand	2.6	780
	Total	2366

Table 3.6: Amount of super-plasticiser added for 20 mm fibres and slump flow for different fibre volumes.

Fibre volume (%)	SP (% of cement)	Slump flow (mm)
0.5	0.65	480
1	0.75	550
1.5	1	620
2	1.5	480

The effect of fibre length on workability was evaluated by using fibre lengths of 10 mm and 20 mm. It was found that the longer fibres tend to form fibre balls if they were not added slowly enough to be well dispersed while mixing. It was easier to add the shorter fibres, because the friction and interlock between the fibres was not as high as with the longer fibres.

From these trial mixes, 600x70x15 mm beams and 100x100x100 mm cubes were cast for every fibre volume and length. The specimens were tested after 7 days of curing in water to study the effect of different fibre volumes and lengths on the strength of the composite.

3.6.2. Final trial mixes

A water/binder ratio of 0.6 was used for the final trial mixes. Several matrices were developed to evaluate the effect of supplementary cementitious materials on the strength of SFRCC and the durability of the fibres. The composition and consistency of the mixes were tested by making 2 litre mixes in a 10 litre pan mixer. The workability and compact ability was

evaluated by a small slump flow test. The slump flow test was performed in accordance to the flow test described in ASTM C1437-07 (2007).

Six matrices were designed and tested prior to producing specimens. The first matrix, the control, contained only OPC as binder and no supplementary cementitious materials. Further on, FA and CSF were introduced into additional matrices to evaluate the effect of supplementary cementitious materials on the fibre-matrix interaction and -bond and the durability of the SFRCC. This was done based on what was found in previous research by Coetzee (2013). It was found, by thermo gravimetric results, that the substitution of 40% of cement with FA did not reduce the amount of $Ca(OH)_2$ and thus the alkalinity significantly, but a matrix containing 30% FA and 20% CSF as binder contained the smallest amount of $Ca(OH)_2$. CSF is however expensive in South Africa, thus less CSF and more FA was used. FA and CSF were evaluated separately in two different matrices to study their individual effect on the composite before combining them in one matrix. The proportions of the matrices are presented in Section 3.6.3.

In the cases where it is possible that not all of the FA was used during the pozzolanic reaction, it served as fine filler and created a denser matrix as mentioned previously. GGBS was not used, because in previous research by Tolêdo Filho et al., (2002) it was found that GGBS did not improve the durability of the fibres but showed strong deterioration over time.

The matrix containing only OPC as binder was used as the control matrix. After the matrix was tested in the small pan mixer, a 5 litre mix, containing 2% fibres by volume, was tested in a 25 litre pan mixer to determine the amount of super-plasticiser required to obtain the same workability as without the fibres. It was found that 1% super-plasticiser (by mass of cementitious material) was sufficient, without causing segregation of the materials.

For the other matrices the amount of water was increased or decreased with the addition of supplementary cementitious materials, but the water/binder ratio was kept constant. In the case of FA, less water was typically required, but at large amounts, where the FA also substituted some of the sand, more water was required. The addition of CSF also required more water. It was assumed that if all the mixes had the same workability prior to adding fibres, the addition of fibres would not require more super-plasticiser than the mix containing only OPC. For all the mixes, slump flows of between 145 and 155 mm were measured.

For the extruded specimens, the same water/binder ratio of 0.6 was used. Three extruded matrices were designed to evaluate and compare casting and extrusion. A mix with a higher viscosity is typically required for extrusion. A VMA was added to increase the viscosity. After the first trial mix with the control OPC mix, it was clear that the mix contained too little fines.

The mix was very stiff and brittle and was un-extrudable. After adding more SP and increasing the cement content to increase the fines content, the mix was still un-extrudable.

To overcome this issue, the fines content was increased by replacing 40% of the sand (by volume) with FA. The mixes were similar to the cast mixes, but some of the cement was replaced with supplementary cementitious materials and 40% of the sand was replaced with FA. One mix containing FA as supplementary cementitious material, one mix containing CSF as supplementary cementitious material and one mix containing a combination of FA and CSF as supplementary cementitious materials was designed to compare the extruded mixes to the cast mixes.

After trial mixes, suitable mix designs were found which extruded well. In the first mix 30% of the OPC was replaced with FA as binder. It is considered that not more than 30% FA will react as binder. In the second mix 10% of the OPC was replaced with CSF as binder. The third mix was a combination of the first two mixes, containing 20% and 10% FA and CSF respectively as binder. The mix proportions are presented in Section 3.6.3. In all the mixes 40% of the sand (by volume) was replaced with FA to aid as fine filler.

3.6.3. Proportions

The matrices used for the cast specimens were denoted C1 to C6 and the proportions are presented in Table 3.7. The matrices for the extruded specimens were denoted E1 to E3 and the proportions are presented in Table 3.8. In Table 3.8, the "Potlife" refers to the time from the end of mixing to the stage where the mix becomes too stiff to be extruded. The "extruder speed" is the speed of the extruder motor in revolutions per minute. The w/b ratio for all the matrices was equal to 0.6. In matrices C5 and C6, which is a representation of matrices E1 and E2 without the VMA, 40% of the sand (by volume) was replaced with FA. In these cases the FA was not considered as binder but rather as fine filler. The "(b)" and "(f)" in Table 3.7 refers to "binder" and "filler", respectively. Matrix C1 is the control matrix and was the same matrix used to cast the single fibre pull-out specimens.

With the addition of fibres, SP was added to enhance workability. For matrix C1, 1% SP was added for 1% of untreated fibres. However, when the same amount of SP was added for the same volume of fibres treated with NaOH, the mix was much more workable. The amount of super-plasticiser was reduced to achieve the same workability. A dosage of 0.6% SP was found to be sufficient. The same dosage was used in the remainder of the matrices which contained chemically treated fibres. For matrices C5 and C6 where FA was used as fine filler, more SP had to be added to achieve the same workability.

Table 3.7: Mix designs as used for cast specimen production.

		C1	C2 (30% FA)	C3 (10% CSF)	C4 (10% CSF, 20% FA)	C5 (30% FA (b), 40% FA (f))	C6 (10% CSF (b), 40% FA (f))
Constituent	RD	Weight (kg)					
Water	1	260	250	260	260	250	260
Cement (OPC)	3.14	433.3	291.7	390	303.3	291.7	390
Fly ash	2.8		125		86.7	811	619
Condensed silica fume	2.1			43.3	43.3		43.3
Malmesbury sand	2.6	1565.2	1592.4	1547.4	1538.7	955.5	972.7

Table 3.8: Mix designs as used for extruded specimen production.

		E1	E2	E3
Constituent	RD	Weight (kg)		
Water	1	250	260	260
Cement (OPC)	3.14	291.7	390	303.3
Fly ash	2.8	811	619	749.5
Condensed silica fume	2.1		43.3	43.3
Malmesbury sand	2.6	955.5	972.7	923.2
Super plasticiser (%)		1.75%	1.0%	1%
Viscosity modifying agent (%)		0.25%	0.22%	0.2%
Potlife (min)		90	60	100
Extruder speed (rpm)		700-900	700-900	1000-1200

3.7. Test programme

A summary of the tests performed on the respective matrices are presented in Table 3.9. In addition to the compression-, three-point bending- and direct tensile tests, single fibre pull-out tests were performed on untreated as well as alkali treated and acetylated fibres using matrix C1.

Compression tests were only performed after 28 days from the date of casting after curing in water. Three-point bending- and direct tensile tests were also performed after 28 days to establish references. Thereafter, specimens were subjected to the various ageing methods and tested in three-point bending and direct tension at an age of 90 days. Dogbones could not be manufactured by extrusion. The dogbone specimens were only subjected to extended curing in water and ageing in lime saturated hot water. Not enough specimens were available to be submitted to cycles of wetting and drying. Beam specimens from matrix E3 were not subjected to ageing in lime saturated hot water or cycles of wetting and drying, as some of the specimens broke during curing in the first 28 days.

45

Table 3.9: Summary of tests performed on respective matrices.

Specimen designation	Compression	Three-point bending	Direct tensile
C1-0.5-10-untr	X		
C1-1-10-untr	X		
C1-1.5-10-untr	X		
C1-2-10-untr	X		
C1-0.5-20-untr	X		
C1-1-20-untr	X	X	X
C1-1.5-20-untr	X		
C1-2-20-untr	X	X	X
C1-1-30-untr	X	X	X
C1-1-20-2%NaOH		X	X
C1-1-20-6%NaOH		X	X
C1-1-20-10%NaOH		X	X
C1-1-20-20%NaOH		X	X
C1-1-20-30%NaOH		X	X
C1-1-20-5%A.Acid		X	X
C1-1-20-10%A.Acid		X	X
C1-1-20-5%A.Anh		X	X
C1-1-20-10%A.Anh		X	X
C1-1-20-6%NaOH,5%A.Anh		X	X
C1-1-20-6%NaOH,10%A.Anh		X	X
C2-1-20-untr	X	X	X
C3-1-20-untr	X	X	X
C4-1-20-untr	X	X	X
C5-1-20-untr	X	X	X
C6-1-20-untr	X	X	X
E1-1-20-untr		X	
E1-2-20-untr		X	
E2-1-20-untr		X	
E3-1-20-untr		X	

CHAPTER 4

Results PART 1: Fibre and matrix properties

In this chapter the results obtained from the moisture absorption, single fibre pull-out (SFP)- and compression tests as well as images taken with the Scanning Electron Microscope (SEM) are presented and brief discussions are made. An in-depth discussion will follow in Chapter 6. The fibre properties, which were evaluated by moisture absorption, SEM images and SFP tests, are presented first. Thereafter, the results of the compression tests are presented.

4.1. Fibre properties

4.1.1. Moisture absorption

The results of the moisture absorption tests performed on the untreated and treated fibre are presented in Table 4.1. The moisture absorption for the untreated fibre was the lowest. The fibres treated with NaOH had the highest water absorption, of which 20% NaOH had the highest percentage. The fibres treated with 6% NaOH had the lowest percentage water absorption of the fibres treated with NaOH. Overall, the acetylated fibres had lower water absorption than the fibres treated with NaOH. Amongst the acetylated fibre samples, 5% Acetic Anhydride, 6% NaOH had the highest water absorption and 5% Acetic Anhydride had the lowest water absorption.

From the results it is clear that the chemical treatment does not reduce the water absorption of the fibres. For all cases of chemical treatment, the water absorption of the treated fibre samples was higher than for the untreated fibre sample.

Table 4.1: Moisture absorption of sisal fibre.

Fibre treatment	Moisture Absorption (%)
Untreated	185.7
2% NaOH	244.8
6% NaOH	236.1
10% NaOH	263.6
20% NaOH	284.6
30% NaOH	247.8
5% Acetic Acid	212.5
10% Acetic Acid	198.5
5% Acetic Anhydride	187.8
10% Acetic Anhydride	215.0
6% NaOH, 5% Acetic Anhydride	222.6
6% NaOH, 10% Acetic Anhydride	198.5

4.1.2. Surface structure and impurities

The images of the alkali treated and acetylated fibres, taken with the scanning electron microscope, are presented in this section. Figure 4.1 shows the image of an untreated fibre. Impurities on the fibre surface are encircled. These impurities are known to be mineral matter and waxy substances. In Figure 4.2 to Figure 4.6, images of fibres subjected to alkali treatment with NaOH are presented.

As the concentration of the NaOH increased, the signs of impurities on the fibre surface decreased. This is known to happpen during alkali treatment. The fibre surface roughness also increased as the ultimate fibres or fibrils are exposed. The fibres treated with 30% NaOH had almost no impurities visible on the surface. In Figure 4.5 signs of damage to the fibre wall is visible. Kabir et al., (2012) found that at high concentrations of NaOH, delignification takes place. The lignin which binds the ultimate fibres together is removed, which leads to defibrillation.

20 µm*	EHT = 7.00 kV	Signal A = SE1	Date :3 Jul 2014
	WD = 6 mm	Photo No. = 1659	Time :14:41:13
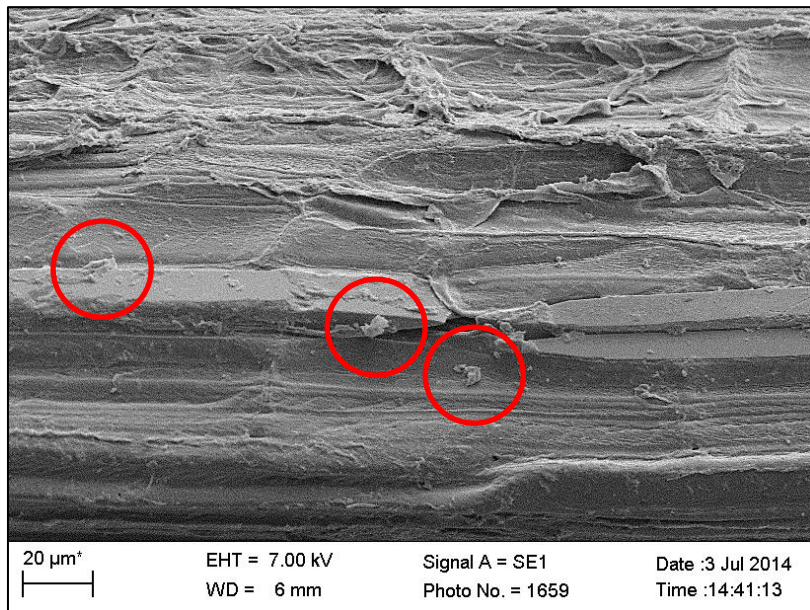
Figure 4.1: Untreated fibre.

20 µm*	EHT = 7.00 kV	Signal A = SE1	Date :3 Jul 2014
	WD = 6 mm	Photo No. = 1687	Time :16:23:22
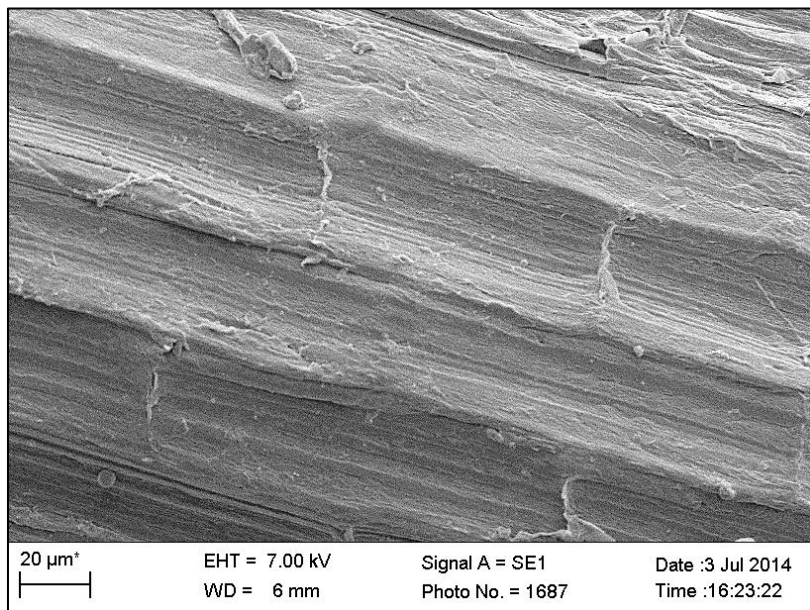
Figure 4.2: 2% NaOH treated fibre.
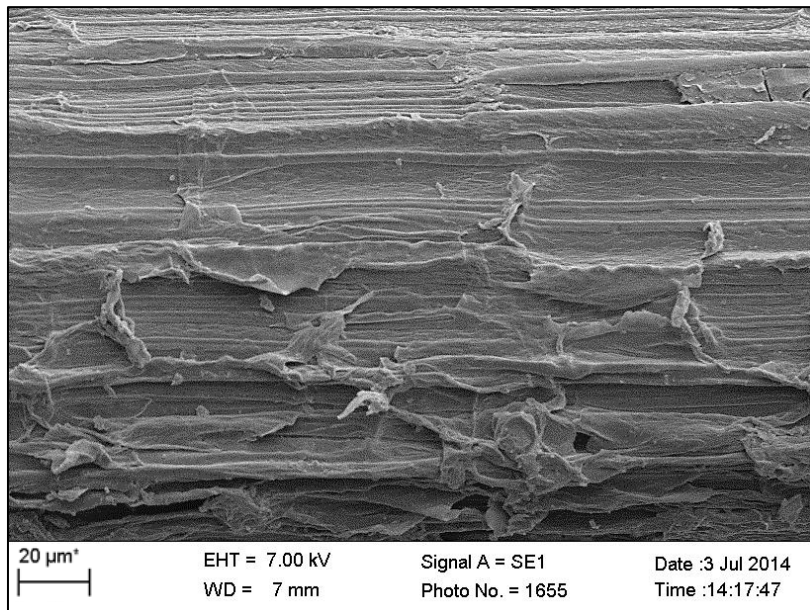
Figure 4.3: 6% NaOH treated fibre.
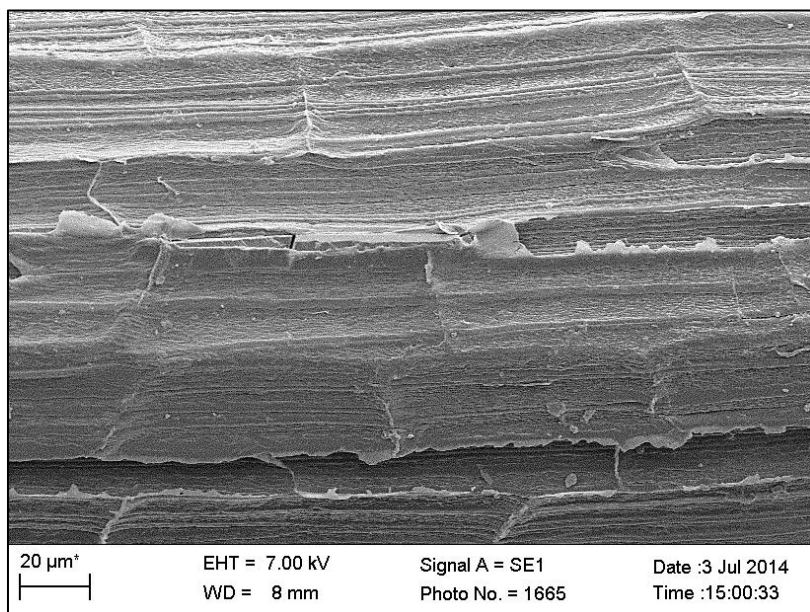
Figure 4.4: 10% NaOH treated fibre.

| 20 µm* | EHT = 7.00 kV | Signal A = SE1 | Date :3 Jul 2014 |
| | WD = 8 mm | Photo No. = 1668 | Time :15:10:00 |

Signs of damage to the fibre structure.
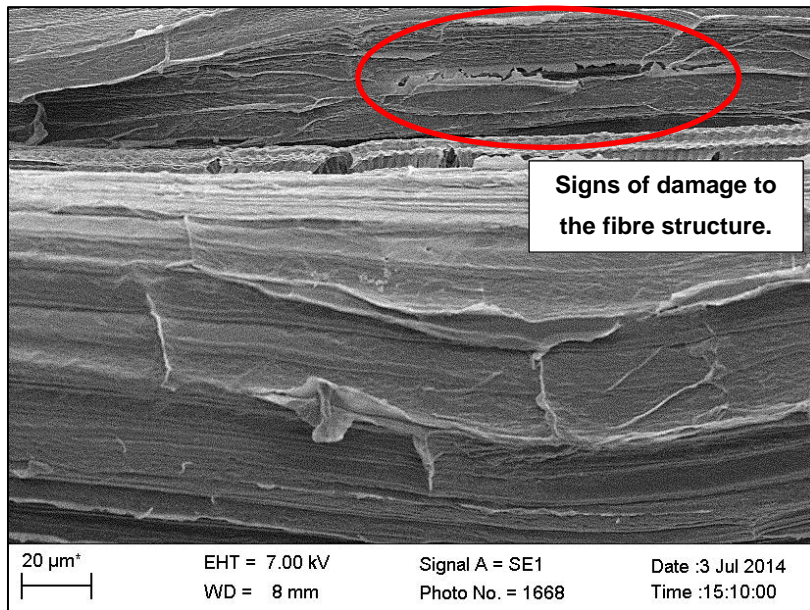
Figure 4.5: 20% NaOH treated fibre.

| 20 µm* | EHT = 7.00 kV | Signal A = SE1 | Date :3 Jul 2014 |
| | WD = 7 mm | Photo No. = 1678 | Time :15:45:50 |
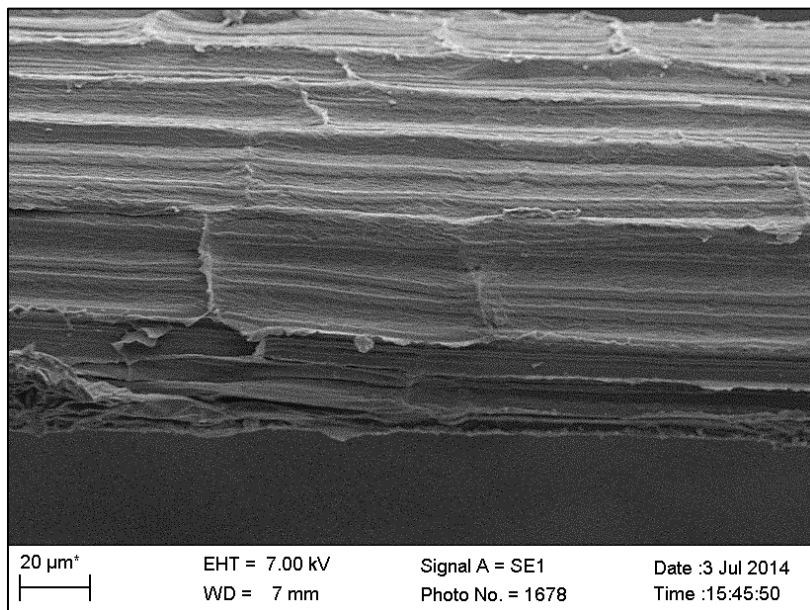
Figure 4.6: 30% NaOH treated fibre.

Figure 4.7 to Figure 4.10 presents images of fibres subjected to acetylation. In Figure 4.7 and Figure 4.8 it is clear that Acetic Acid was less effective than NaOH in removing surface impurites. When compared with the untreated fibre, there is a similarity in the fibre surfaces with regards to surface impurities. Acetic Acid is usually used as an acid catalyst to swell the fibre wall for other chemicals to ingress and modify the fibre structure. From Figure 4.9 and Figure 4.10 it is clear than Acetic Anhydride was more effective than Acetic Acid in removing

51

surface impurities. Although impurities are still visible on the surface, the surface is cleaner and smoother. It was however still less effective than NaOH.
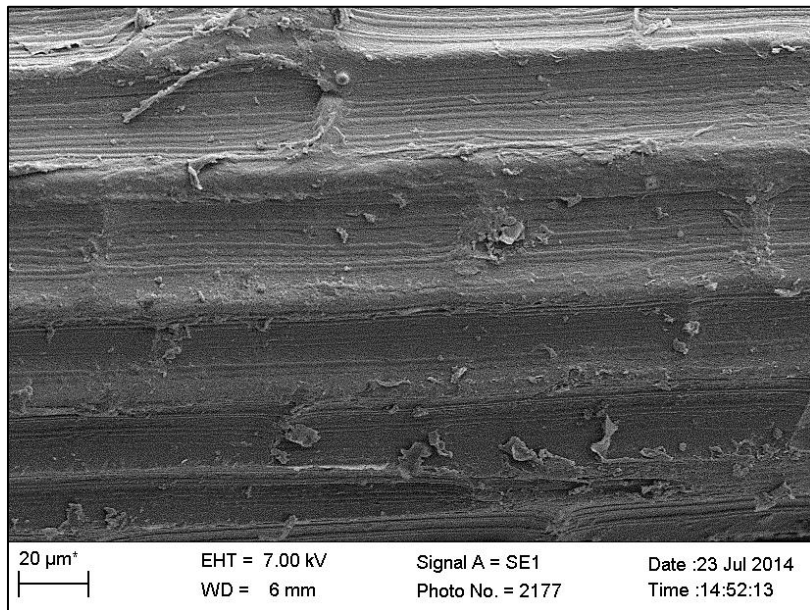
Figure 4.7: 5% Acetic Acid treated fibre.
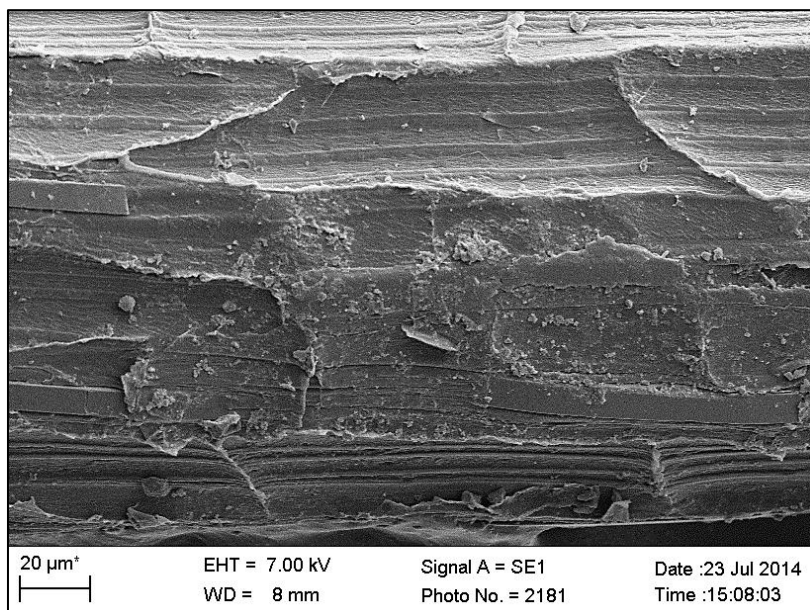
Figure 4.8: 10% Acetic Acid treated fibre.
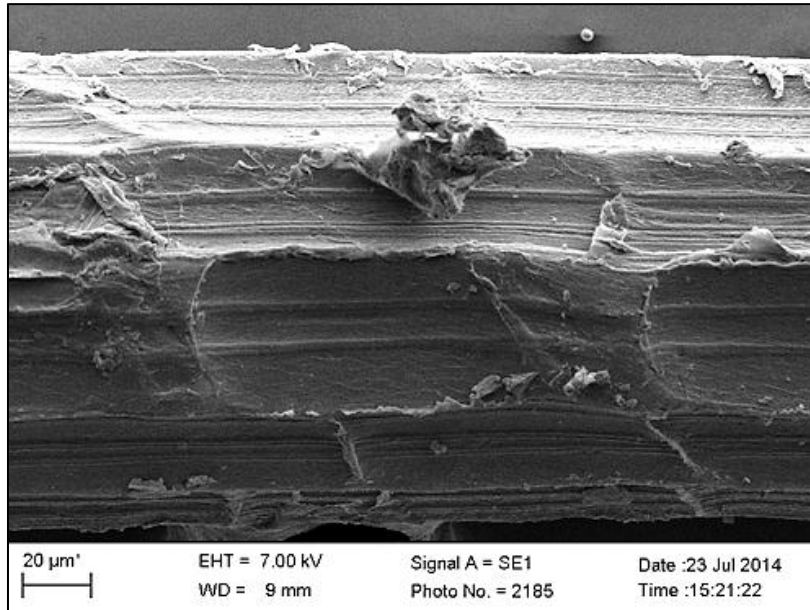
Figure 4.9: 5% Acetic Anhydride treated fibre.
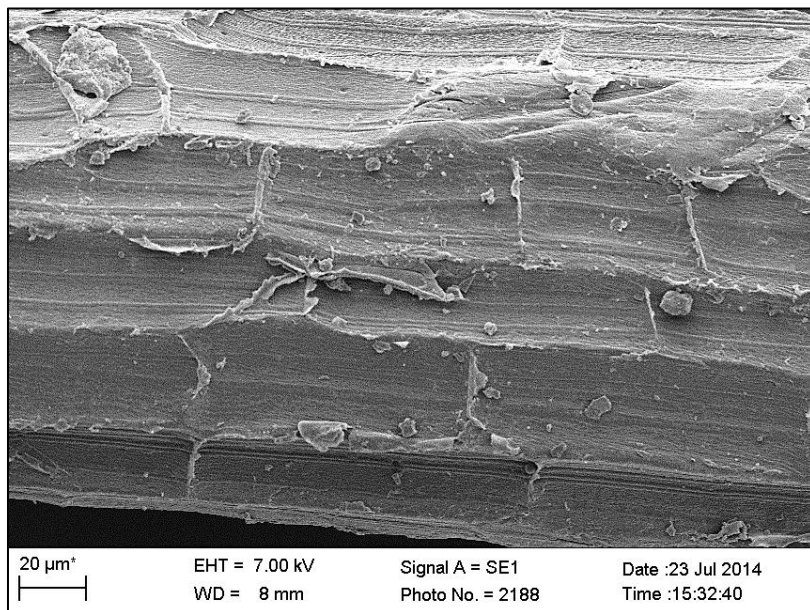
Figure 4.10: 10% Acetic Anhydride treated fibre.

Figure 4.11 and Figure 4.12 presents images of fibres where a combination of NaOH and Acetic Anhydride was used for fibre treatment. Although the fibre surface has a rough texture, especially in Figure 4.12, there are almost no impurities on the surface.

| 20 µm* | EHT = 7.00 kV | Signal A = SE1 | Date :23 Jul 2014 |
| | WD = 8 mm | Photo No. = 2192 | Time :15:48:15 |
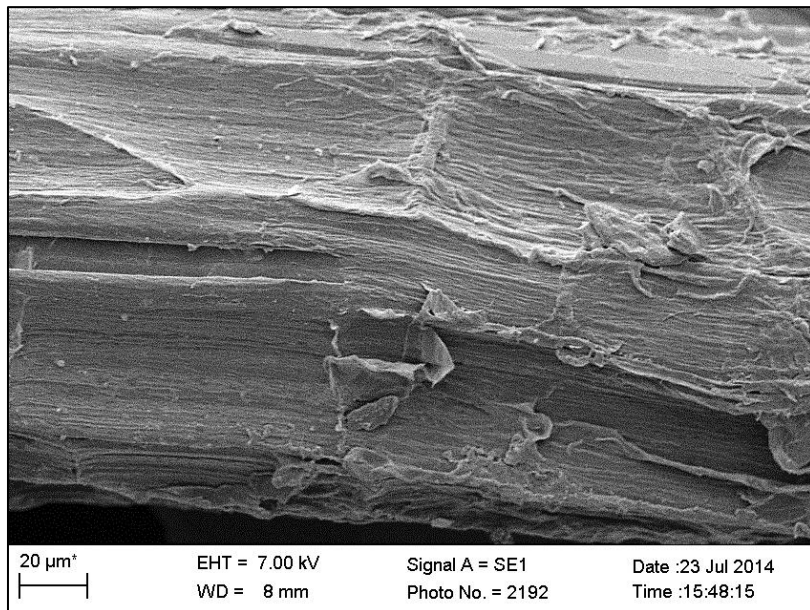
Figure 4.11: 5% Acetic Anhydride, 6% NaOH treated fibre.

| 20 µm* | EHT = 7.00 kV | Signal A = SE1 | Date :23 Jul 2014 |
| | WD = 8 mm | Photo No. = 2195 | Time :15:59:05 |
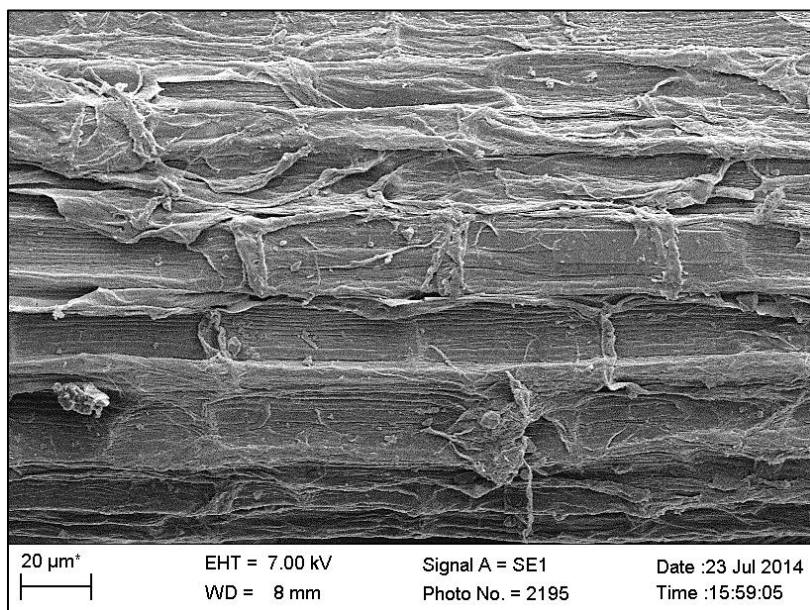
Figure 4.12: 10% Acetic Anhydride, 6% NaOH treated fibre.

54

4.1.3. Tensile strength

From experiments done by Morrissey et al., (1985), it followed that the critical length for sisal fibre was equal to 30 mm. A different matrix was used in this study and therefore the embedment depth at which the fibre would fracture was unknown. The tests were started with the maximum embedment depth of 50 mm allowed by the size of the specimen. The fibres were tested at embedment depths of 50, 40, 30, 20, 15 and 10 mm respectively, in descending order. If fibre pull-out was the prevalent failure mechanism at a certain embedment depth, the tests were not continued for shorter embedment depths. It is also worth noting that the fibres might all fracture at a shorter embedment depth, but pull-out for a longer embedment depth in the same matrix. This is due to the fibres not being uniform in thickness and strength.

Images of fibres which pulled-out during the SFP tests, taken by the SEM, are presented in Figure 4.13 and Figure 4.14. The separation of the ultimate fibres and the split in the fibre visible in Figure 4.13 indicates that the fibre was damaged by the high friction during pull-out. In Figure 4.14 signs of the mortar are still visible on the fibre surface at the point where the fibre entered the specimen, as well as through the rest of the fibre length. The smoother surface also indicates that there was less resistance during pull-out.
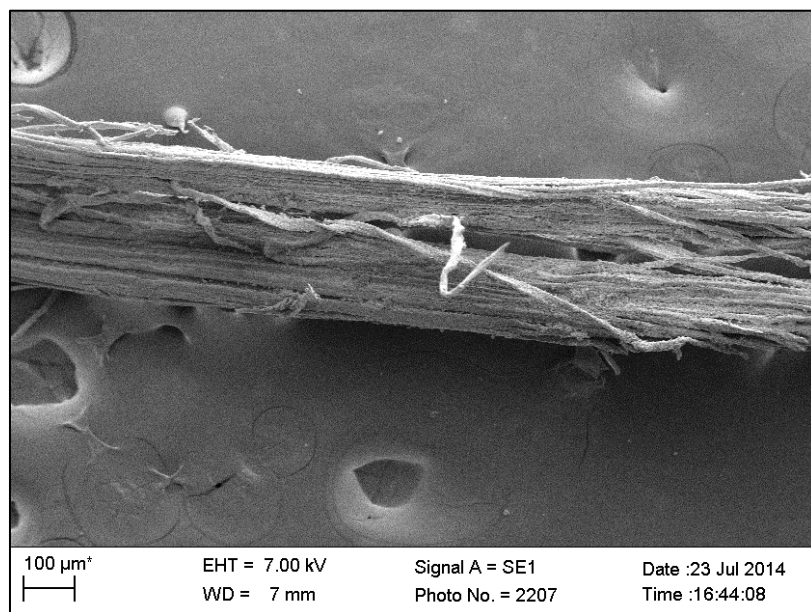
Figure 4.13: Pulled-out fibre.

100 µm*	EHT = 7.00 kV	Signal A = SE1	Date :23 Jul 2014
	WD = 7 mm	Photo No. = 2200	Time :16:20:39
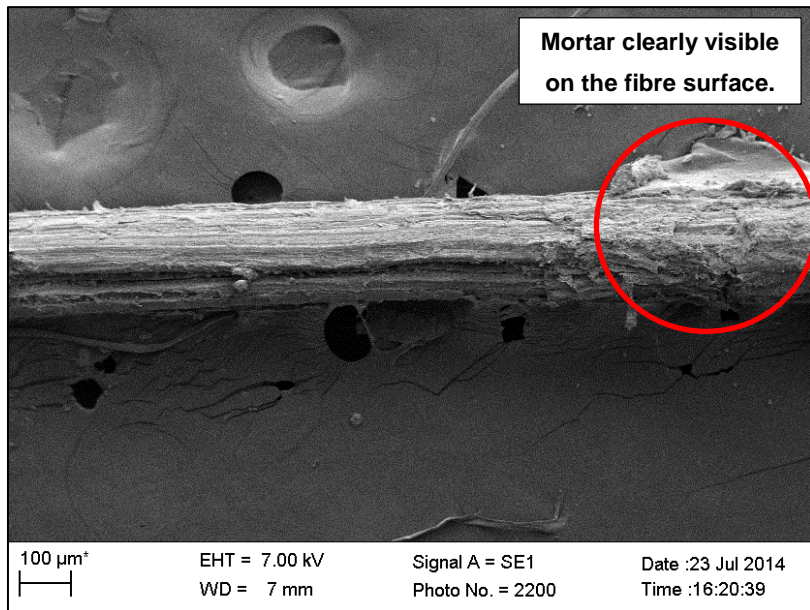
Figure 4.14: Pulled-out fibre.

Figure 4.15 and Figure 4.16 presents images of fibres which fractured during the single fibre pull-out tests. The fracture is not a clean fracture. The fracture surface is rough and the ultimate fibres are exposed and deformed.

200 µm*	EHT = 7.00 kV	Signal A = SE1	Date :23 Jul 2014
	WD = 7 mm	Photo No. = 2205	Time :16:37:13
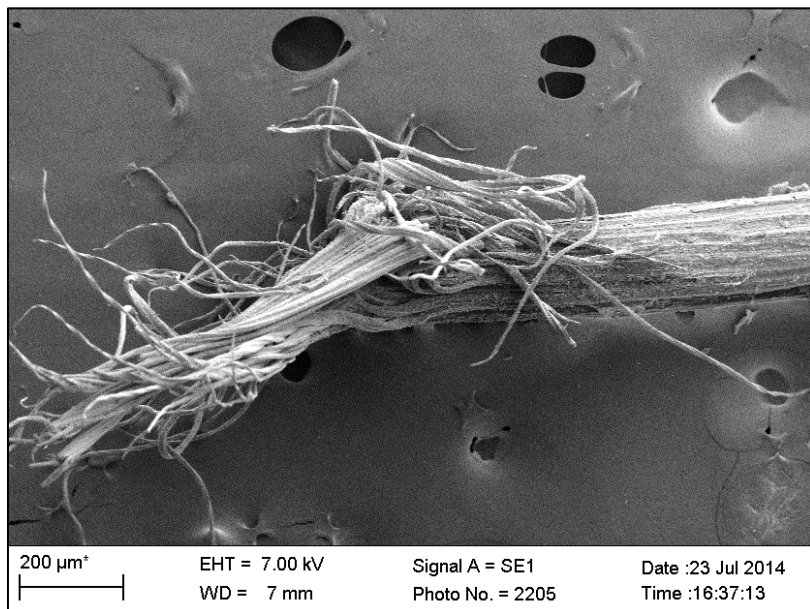
Figure 4.15: Fractured fibre.

56

| 200 μm* | EHT = 7.00 kV | Signal A = SE1 | Date :23 Jul 2014 |
| | WD = 7 mm | Photo No. = 2203 | Time :16:30:09 |
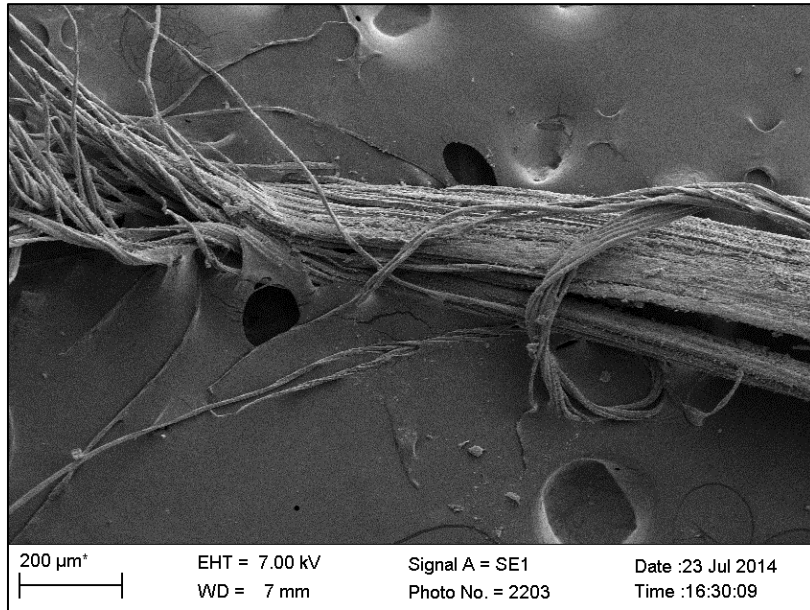
Figure 4.16: Fractured fibre.

The results of the SFP tests were recorded as graphs of pull-out force versus pull-out or displacement. These graphs, together with a table summarising all the results, are presented in Appendix A for the different treatment conditions and fibre lengths. A typical pull-out response is presented in Figure 4.17, showing fibre pull-out, as well as fracture.
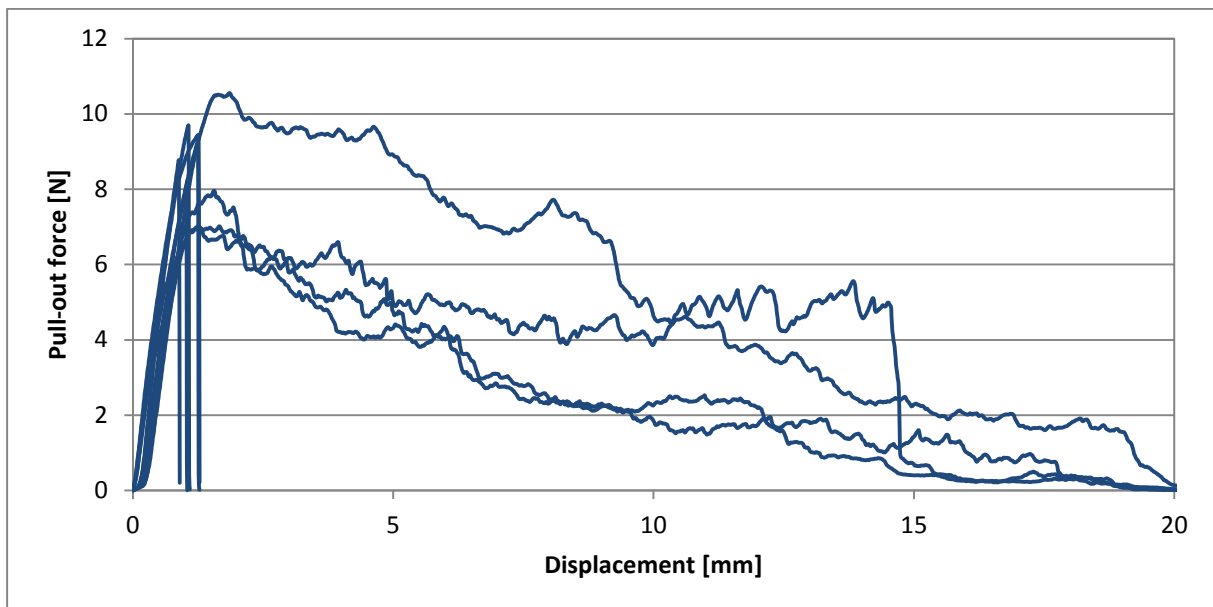
Figure 4.17: Typical single fibre pull-out response.

57

The average pull-out force (in N/mm) was calculated as the pull-out force (in N) divided by the original embedment depth. This model assumes a uniform bond shear stress over the length of the embedded part of the fibre. Graphs of the average pull-out force (in N/mm) and fracture force (in N) for the different treatment conditions are presented in Figure 4.18 to Figure 4.21. The diameters of the individual fibres were not constant and were difficult to measure, therefore the pull-out and fracture force were not expressed as an interfacial shear stress and tensile stress, respectively. The error bars indicate the minimum and maximum force for the specific series. The pull-out length, which is the embedment depth at which no fibres fractured, for the various treatment conditions is presented in Table 4.2.

Table 4.2: Pull-out length for various treatment conditions.

Fibre treatment	Pull-out Length (mm)
Untreated	15
2% NaOH	10
6% NaOH	10
10% NaOH	10
20% NaOH	15
30% NaOH	10
5% Acetic Acid	15
10% Acetic Acid	15
5% Acetic Anhydride	10
10% Acetic Anhydride	10
6% NaOH, 5% Acetic Anhydride	10
6% NaOH, 10% Acetic Anhydride	10

For the majority of the treatment conditions the critical embedment depth was equal to 10 mm except for the untreated, 20% NaOH and, 5% and 10% Acetic Acid fibres for which it was 15 mm. At 15 mm, the 10% and 30% NaOH, the 5% and 10% Acetic Anhydride and the 6% NaOH-5% Acetic Anhydride, showed fibre fracture. The 2% and 6% NaOH and 6% NaOH-10% Acetic Anhydride, showed both pull-out and fracture. For the 6% NaOH an equal amount of fibres fractured as what pulled-out, but for the 2% NaOH and the 6% NaOH-10% Acetic Anhydride, fibre pull-out was the governing failure mode at 15 mm. At 20 mm almost all the fibres fractured, except for a small number of specimens where the fibres pulled out. Fibre fracture was still the governing failure mode at 20 mm. The fibres that fractured at 15 mm were not tested for an embedment depth of 20 mm.

Only two cases of fibre fracture were recorded throughout the series of tests for a 10 mm embedment depth. This indicated that the critical fibre length was equal to 20 mm and was therefore the fibre length used in the production of the majority of the specimens for this research project. A longer fibre length would mean a greater possibility of fibre fracture which could lead to a more brittle than ductile failure mode.

As mentioned earlier in Section 2.3.1, the critical fibre length differs for cast and extruded composites. Therefore the critical fibre length determined by performing single fibre pull-out tests on a cast specimen would not be the critical fibre length to be used in extruded specimens. However, to be able to compare cast and extruded specimens, the same fibre length was used for both processes.

In Figure 4.18 the average pull-out force for the alkali treated fibres are presented. The 2%, 6% and 10% NaOH fibres had higher resistance to pull-out than the untreated fibres, while the 20% and 30% NaOH fibres had lower resistance than the untreated fibres. The 2% NaOH fibres had the highest resistance to pull-out, while the 20% NaOH fibres had the lowest resistance to pull-out. The 10% NaOH fibres had the most variability in its results. The untreated and 20% NaOH fibres pulled out at an embedment depth of 15 mm, while the other alkali treated fibres pulled out at 10 mm and had a combination of pull-out and fracture at 15 mm. The increased resistance of the 2%, 6% and 10% NaOH fibres at a shorter embedment depth indicates an improved bond between the fibre and the matrix.
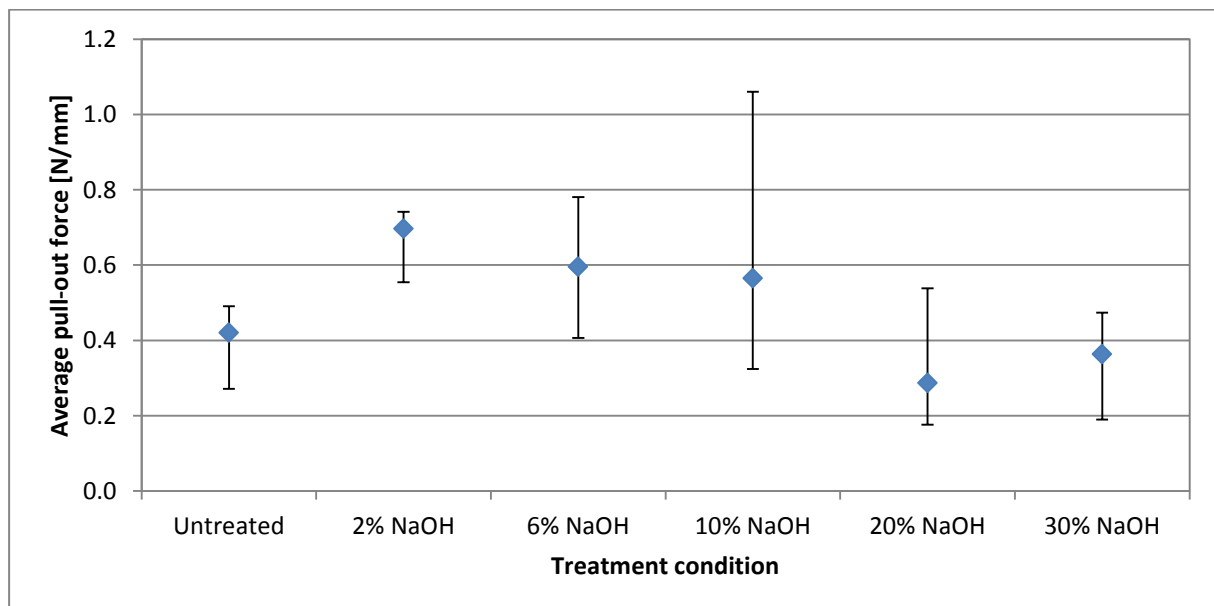
Figure 4.18: Average pull-out force for alkali treated fibres.

The average pull-out force for the acetylated fibres is presented in Figure 4.19. The resistance of the 5% and 10% Acetic Acid fibres to pull-out was much lower than the untreated and other acetylated fibres. The fibres treated with Acetic Acid pulled out at embedment depths of 15 mm and 20 mm and also fractured at 20 mm, while the fibres treated with Acetic Anhydride pulled out at 10 mm and fractured at 15 mm. A number of fibres pre-treated with 6% NaOH and then with 10% Acetic Anhydride pulled out at 15 mm, but at a higher force than the Acetic Acid specimens, indicating that the 6% NaOH-10% Acetic Anhydride had the highest resistance to pull-out. The higher average pull-out force and the shorter embedment depth at which they pulled out, indicates a stronger bond between the fibres and the matrix for the fibres treated with Acetic Anhydride than for the fibres treated with Acetic Acid. The fibres treated with 6% NaOH-10% Acetic Anhydride pulled out at 15 mm while all the other fibres treated with Acetic Anhydride pulled out at 10 mm.

In comparison, the fibres treated with 2% NaOH had the highest resistance to pull-out of all the fibres, followed by fibres treated with 6% NaOH. The fibres pre-treated with 6% NaOH and then with 5% and 10% Acetic Anhydride had higher resistance to pull-out than the fibres treated with only Acetic Anhydride, but lower resistance than the fibres treated with only 6% NaOH. Acetic anhydride improved the bond strength of the untreated fibre, but reduced the bond strength of the 6% NaOH treated fibre.
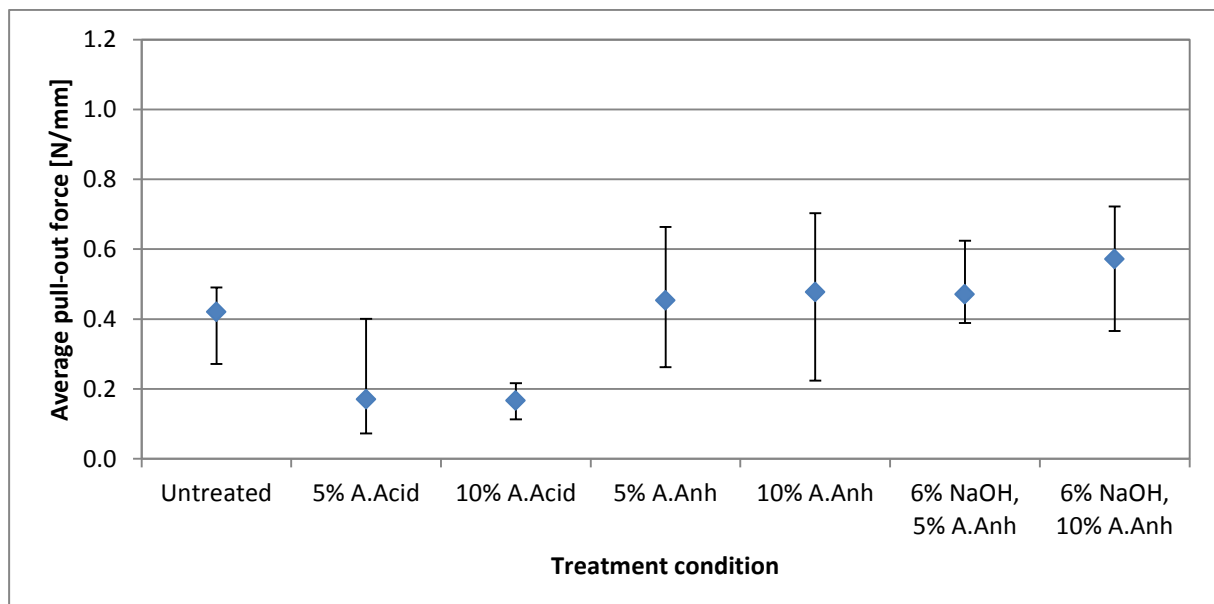
Figure 4.19: Average pull-out force for acetylated fibres.

60

The average fracture force for the alkali treated fibres is presented in Figure 4.20. The average force increased for the 2% NaOH fibres compared to the untreated fibres. The fracture force decreases linearly as the NaOH concentration increases from 2% to 30%. Only the 2% and 6% NaOH fibres had higher resistance to fracture than the untreated fibres. This confirms that at higher concentrations of NaOH the fibre cells are damaged and the strength is reduced.
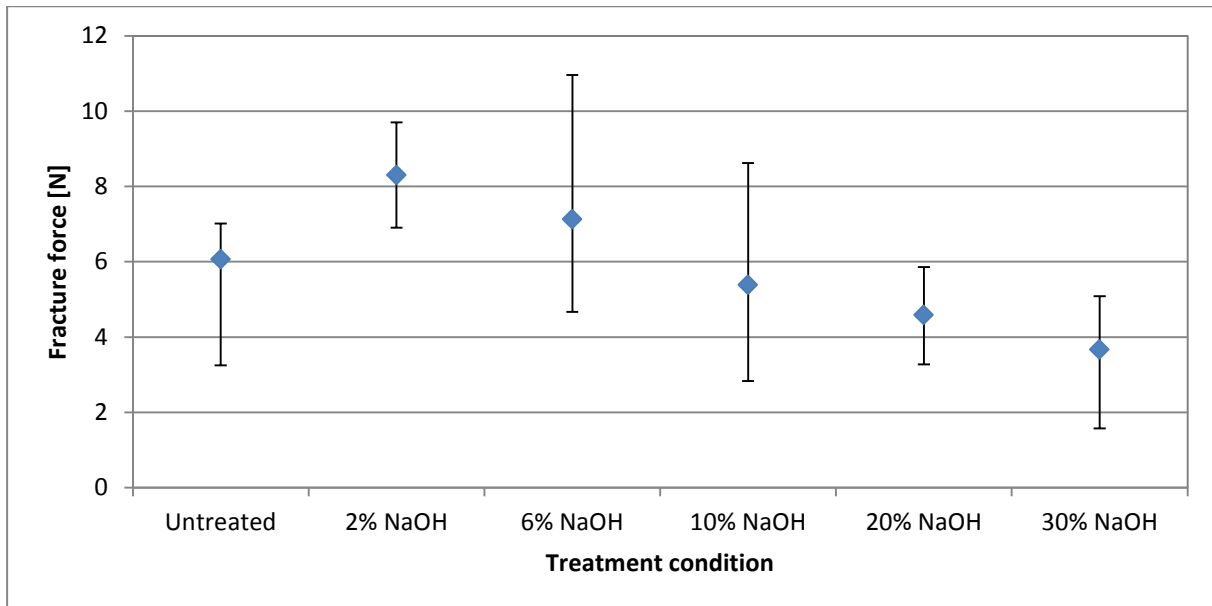
Figure 4.20: Average fracture force for alkali treated fibres.

The average fracture force for the acetylated fibres is presented in Figure 4.21. The strength of the Acetic Acid and Acetic Anhydride treated fibres were similar, however when comparing the corresponding concentrations, the fibres treated with Acetic Anhydride had slightly higher strength than the fibres treated with Acetic Acid. Only the fibres pre-treated with 6% NaOH before treatment with Acetic Anhydride had higher strength than the untreated fibres. The fibres pretreated with 6% NaOH and then with 10% Acetic Anhydride had the highest strength.

In comparison, the fibres treated with 2% NaOH had the highest strength followed by 6% NaOH, 6% NaOH-10% Acetic Anhydride and 6% NaOH-5% Acetic Anhydride in order of decreasing strength. Only these fibres had higher strength than the untreated fibres. In both cases where the untreated and 6% NaOH treated fibre were treated with Acetic Anhydride, the strength of the fibres decreased.
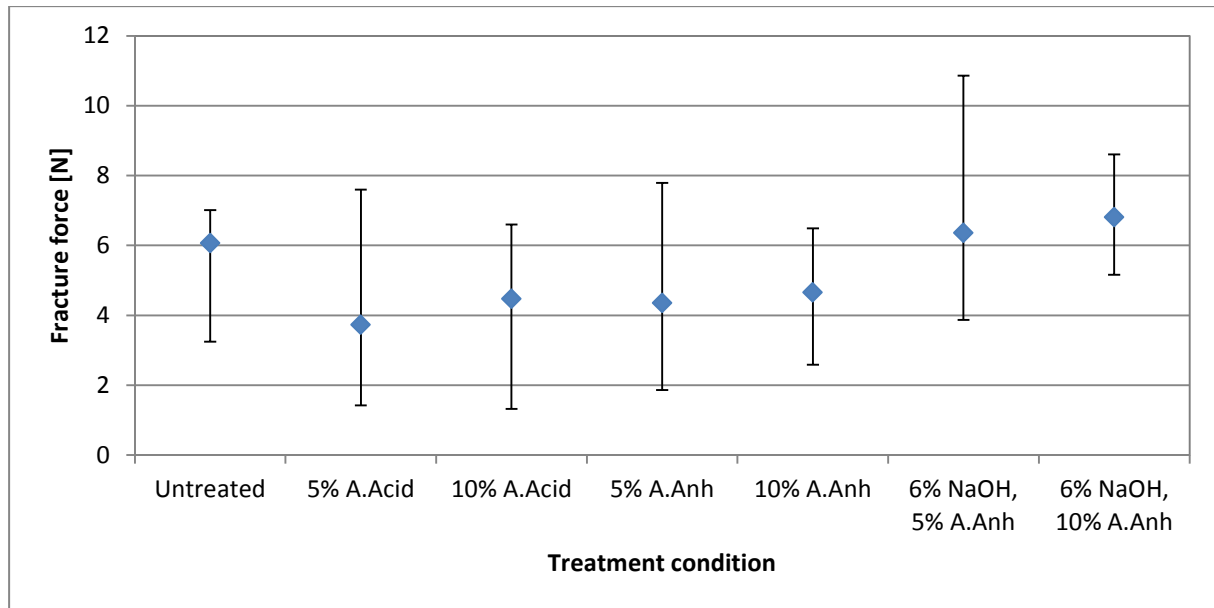
Figure 4.21: Average fracture force for acetylated fibres.

The results show that the fibre-matrix bond can be improved and the fibre strength can increase by chemical treatment. The type of treatment is important, as some treatments are more effective than others. The concentration is also important, as higher concentrations may be detrimental to the fibre strength. Low concentrations of 2% and 6% NaOH were more effective than higher concentrations of NaOH, while Acetic Anhydride was more effective than Acetic Acid.

4.2. Compression tests

Compression tests were not performed on all the mixes, because the same matrix (C1) was used for most of the mixes. They were performed for matrix C1 with different fibre volumes of 0.5, 1.0, 1.5 and 2.0% for lengths of 10 mm and 20 mm and also at a fibre volume of 1% for a length of 30 mm. In addition, it was performed for the different matrices C2 to C6 (containing supplementary cementitious materials) with a fibre volume and length of 1% and 20 mm, respectively. A summary of the results of the compressive strength tests is presented in Table 4.3 and graphs are presented in Figure 4.22 to Figure 4.25.

A graph of compressive strength versus fibre volume is presented in Figure 4.22 and a graph of compressive strength versus density in Figure 4.23. The compressive strength decreased as the fibre volume increased. This is in agreement with what was found by Coetzee (2013). For the 20 mm fibre, the compressive strength for a volume fraction of 2.0% was higher than for a volume fraction 1.5%. This is due to better compaction during vibration. This was also

confirmed by the higher average density of the cubes containing 2.0% fibre compared to the cubes containing 1.5% fibre. In Figure 4.23 it is evident that the compressive strength is directly proportional to the density. In all cases, the matrix with 20 mm fibre had a higher strength than the matrix with 10 mm fibre. The matrix with longer fibre had better compaction than the matrix with shorter fibre.

Table 4.3: Compressive strength test results.

Matrix	Fibre Volume (%)	Fibre Length (mm)	Compressive Strength (MPa)		Average Density (kg/m^3)
			Average	Standard Deviation	
C1 (OPC)	0.5	10	27.5	0.2082	2026
	1.0	10	27.0	0.5454	1993
	1.5	10	19.3	0.2769	1839
	2.0	10	11.5	0.2332	1766
C1 (OPC)	0.5	20	31.3	0.4773	2057
	1.0	20	28.3	0.6057	1991
	1.5	20	21.3	0.295	1859
	2.0	20	25.9	0.4858	1923
C1 (OPC)	1.0	30	2.4	0.1033	1788
C2 (30% FA)	1.0	20	6.4	0.7937	1800
C3 (10% CSF)	1.0	20	30.9	1.5726	1903
C4 (10% CSF, 20% FA)	1.0	20	11.2	0.8626	1870
C5 (70% FA)	1.0	20	1.6	0.0125	1910
C6 (10% CSF, 40% FA)	1.0	20	24.5	1.1937	2028

In matrices C2, C4 and C5, where some of the OPC was replaced with FA, the compressive strength was significantly lower. The cubes of matrices C2 and C5 crushed completely during the tests and upon investigation it was found that the matrix was soft, as if the cement did not hydrate properly. For matrix C3, where 10% of the OPC was replaced with CSF, the compressive strength was higher than for C1 with the same fibre volume and length, but when more of the OPC was replaced with FA, as in matrix C4, the strength reduced considerably. The strength even decreased when 40% of the sand (by volume) was replaced with FA, as in matrix C6. From Figure 4.25 it can be seen that the matrix with 30 mm fibre had almost no strength. The average density of the cubes was also much lower than for the cubes with 10 mm and 20 mm fibre at the same fibre volume.
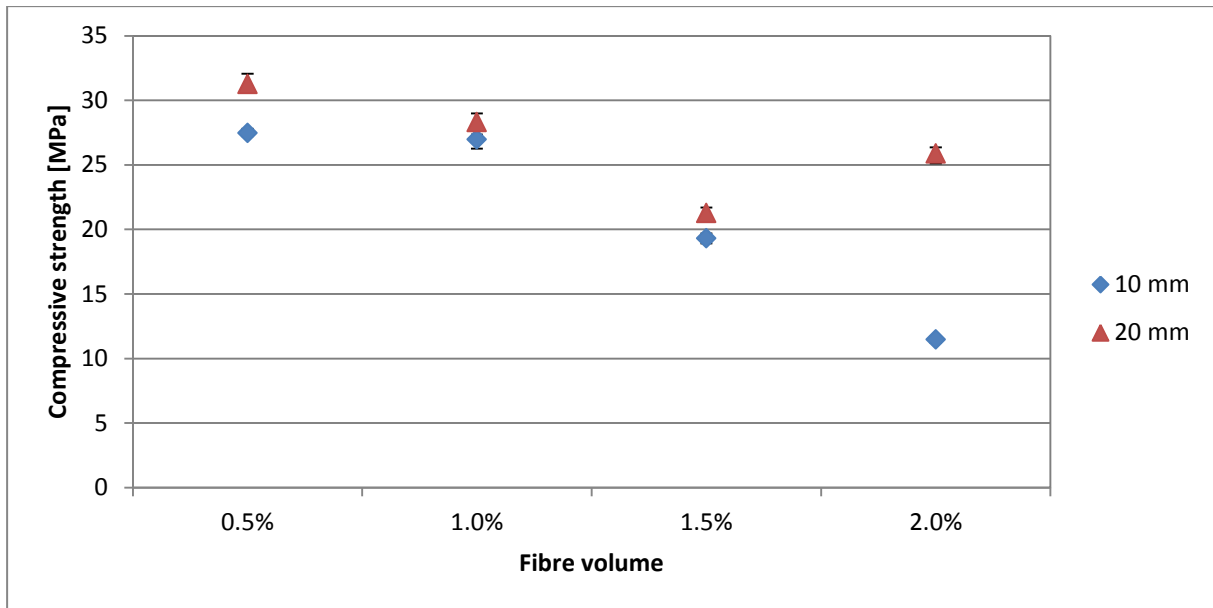
Figure 4.22: Compressive strength of matrix C1 with 10 mm and 20 mm fibre respectively.
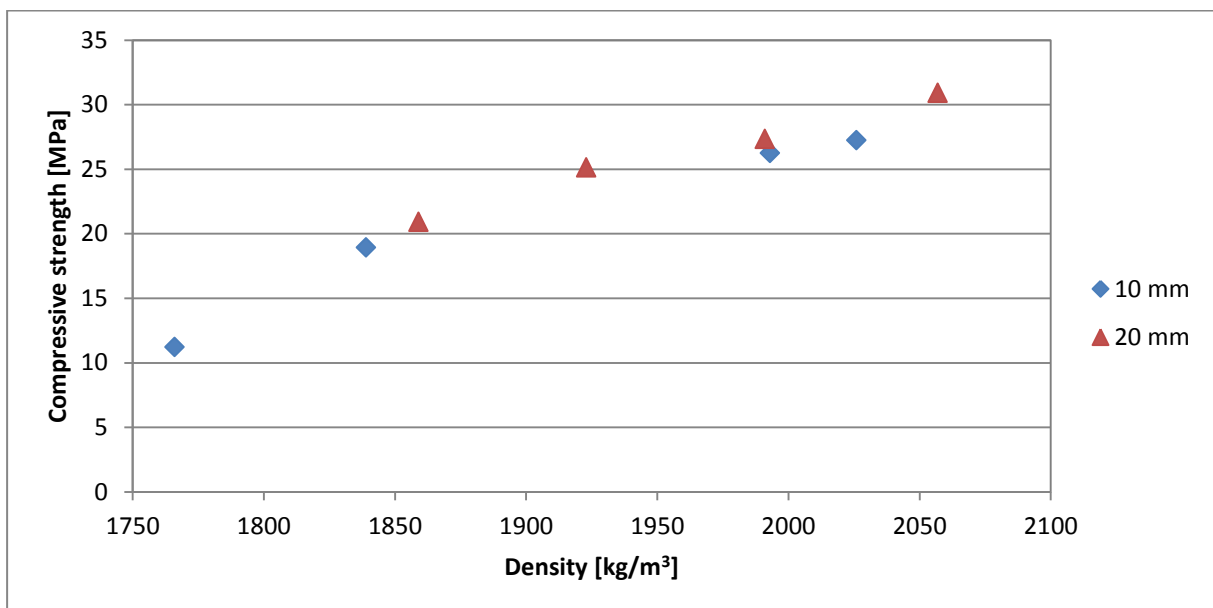
Figure 4.23: Compressive strength versus cube density for matrix C1 with 10 mm and 20 mm fibre respectively.

64
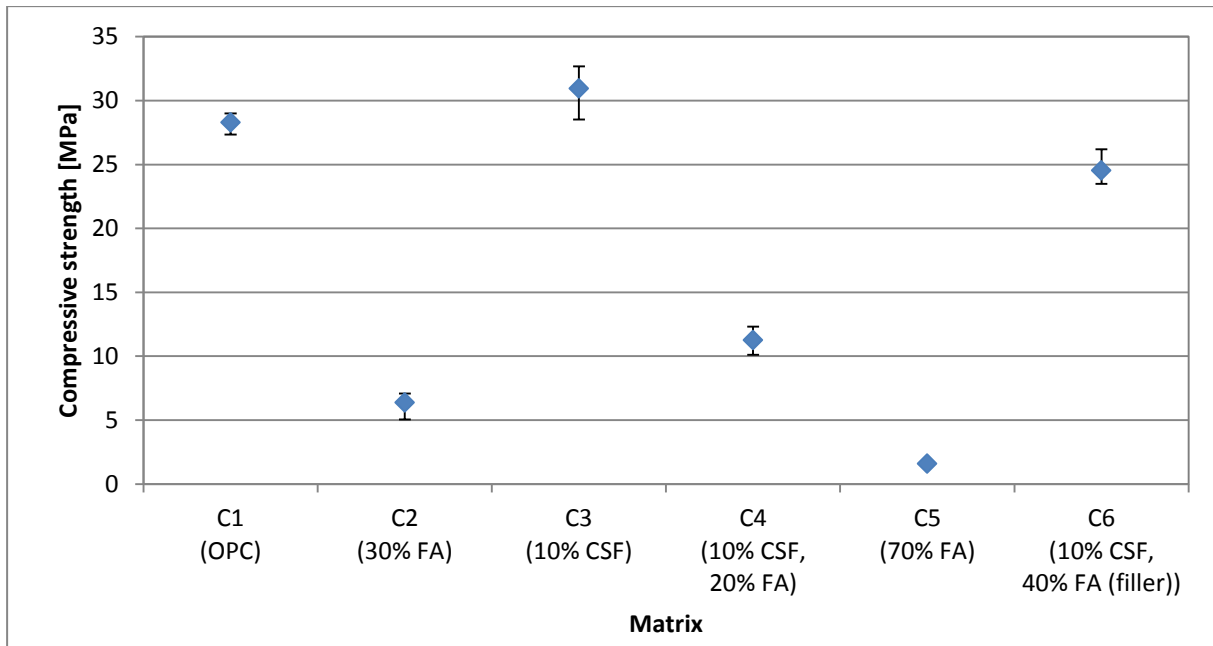
Figure 4.24: Compressive strength of different matrices with 1% 20 mm fibre.
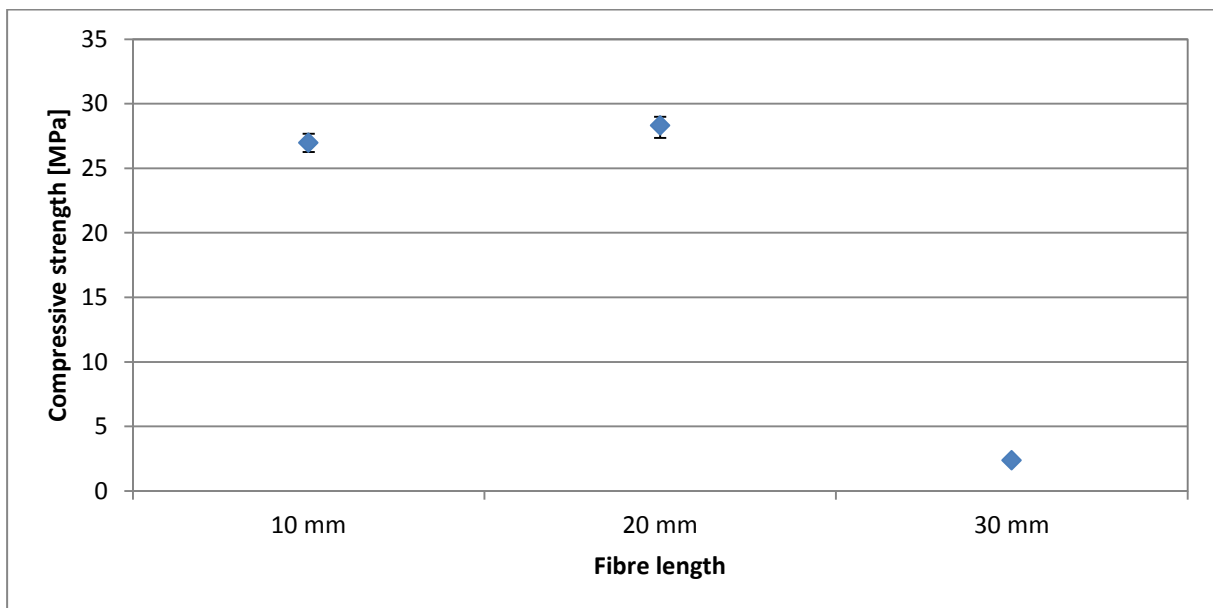
Figure 4.25: Compressive strength of matrix C1 with different lengths at 1% fibre volume.

65

CHAPTER 5

Results PART 2: Durability

The durability of natural sisal fibre reinforced cement-based composites was evaluated by comparing the strength of the specimens tested at an age of 90 days after ageing to the strength of the reference specimens tested at 28 days. The results obtained from the three-point bending- and direct tensile tests are presented in this chapter. Brief discussions are made, but an in-depth discussion will follow in Chapter 6.

5.1. Three-point bending tests

The results of the specimens tested in the three-point bending test setup are presented in this section. A table summarising all the results is presented in Appendix B. A typical graph for a series of specimens is presented in Figure 5.1. The stress increases up to the point where the specimen cracks which is at the peak of the graph. Thereafter a sudden decrease in stress is noted. It is at this stage that the fibres interlock with the matrix and start acting in tension. This is called the post-peak behavior. In some cases a slight increase in stress was noted after the decrease, as the fibres anchored themselves in the matrix, but as they started pulling out the stress decreased again. In other cases where the interlock was not sufficient, the stress did not increase after the sudden decrease. The tests were stopped after a displacement of 10 mm was measured. The deviation in the loading phase, seen at approximately 2 MPa, is due to the rotation mechanism of the crosshead pushing into position. This does not influence the accuracy of the results.

The results of the reference specimens are presented first. Both the peak- and post-peak strength is presented for the reference specimens tested at an age of 28 days. For the aged specimens tested on 90 days, only the post-peak strength is presented. The ageing was performed in order to evaluate the degradation of the fibres which can be studied best by evaluating the post-peak behaviour.

66
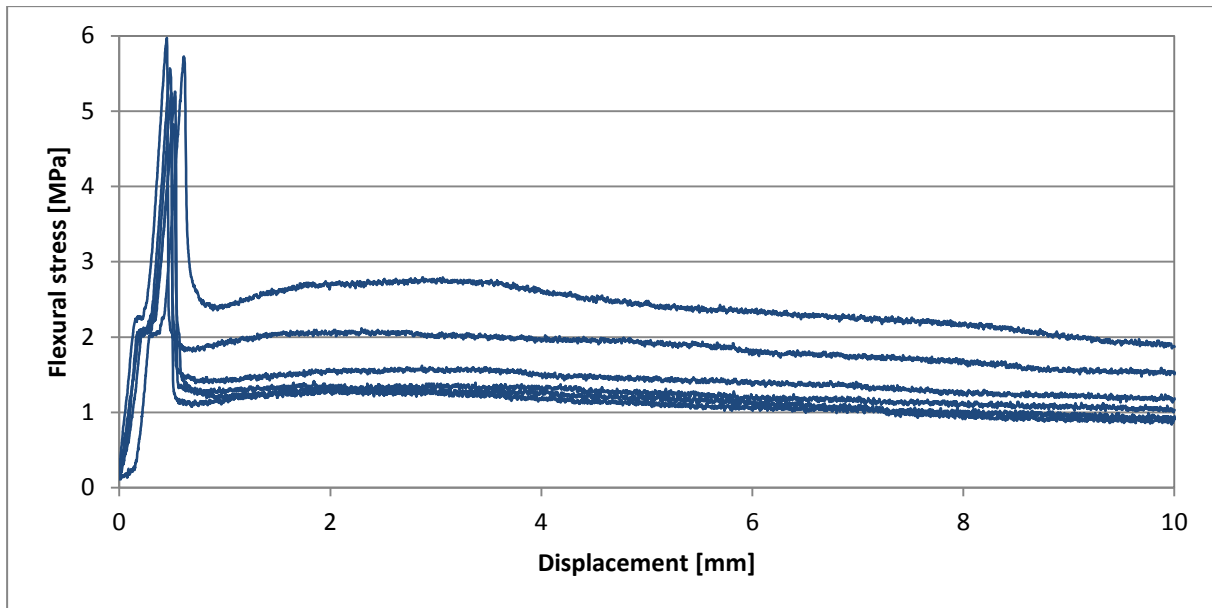
Figure 5.1: Typical graph for a series of specimens tested in three-point bending.

5.1.1. Reference specimens

A series of specimens were tested at 28 days to establish references. The graphs of the tests for all the different series of specimens tested at 28 days are presented in Appendix B. A summary of the results are represented in Figure 5.2 to Figure 5.6. The graphs show the average peak and post-peak flexural stress for a series of specimens for different fibre volumes and lengths as well as different fibre treatment conditions and specimens with different matrices. The post-peak flexural stress gives a clear indication of the influence of the fibres.

The average peak stress was calculated from the individual peak stress for each specimen in a series. The average post-peak stress for an individual specimen was calculated as an average over a displacement of 2 mm from 0.5 mm from the limit of proportionality (LOP), which is at the peak of the graph. The error bars indicate the maximum and minimum values recorded in that series.

Figure 5.2 presents the results of matrix C1 reinforced with fibres with a length of 20 mm at volumes of 1% and 2%, respectively. At a fibre volume of 2% the peak stress was lower, but the post-peak stress was higher. The increase in post-peak stress was typically expected, as there are more fibres to distribute and carry the load at a higher fibre volume.

67
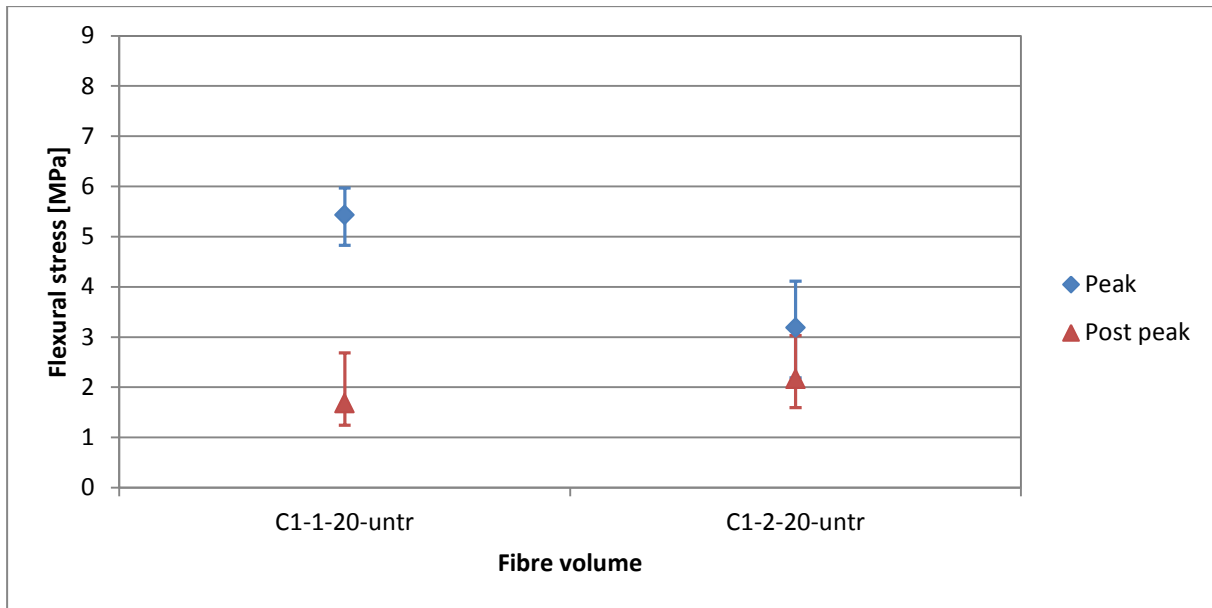
Figure 5.2: Average peak and post-peak flexural strength for matrix C1-1-20-untr and C1-2-20-untr respectively.

In Figure 5.3 a trend of decreasing peak strength can be observed for the specimens reinforced with alkali treated fibres. The trend is however not constant as was expected e.g. a trend of constant decreasing strength for an increasing NaOH concentration. An increased strength was recorded for the 2%, 6% and 10% NaOH specimens with regards to the untreated specimens. The specimens reinforced with 6% NaOH fibre had the highest strength. The 20% and 30% NaOH specimens had a lower strength than the untreated specimens. The specimens reinforced with 20% NaOH fibre had the lowest peak strength. For the post-peak stress the same trend can be observed. The 10% NaOH specimens had the highest post-peak strength and the 30% NaOH specimens had the lowest post-peak strength.

In Figure 5.4 a general trend of increasing peak and post-peak strength can be observed. The strength of the Acetic Acid specimens was slightly lower than for the untreated specimens, but the 10% Acetic Acid had a higher strength than the 5% Acetic Acid. The Acetic Anhydride specimens had a lower peak strength but higher post-peak strength than the untreated specimens, with the 10% Acetic Anhydride also having a higher strength than the 5% Acetic Anhydride. The Acetic Anhydride specimens pre-treated with 6% NaOH had the highest peak and post-peak strength. The 10% Acetic Anhydride pre-treated with 6% NaOH had the highest post-peak strength when compared with the untreated, alkali treated and acetylated specimens.

68
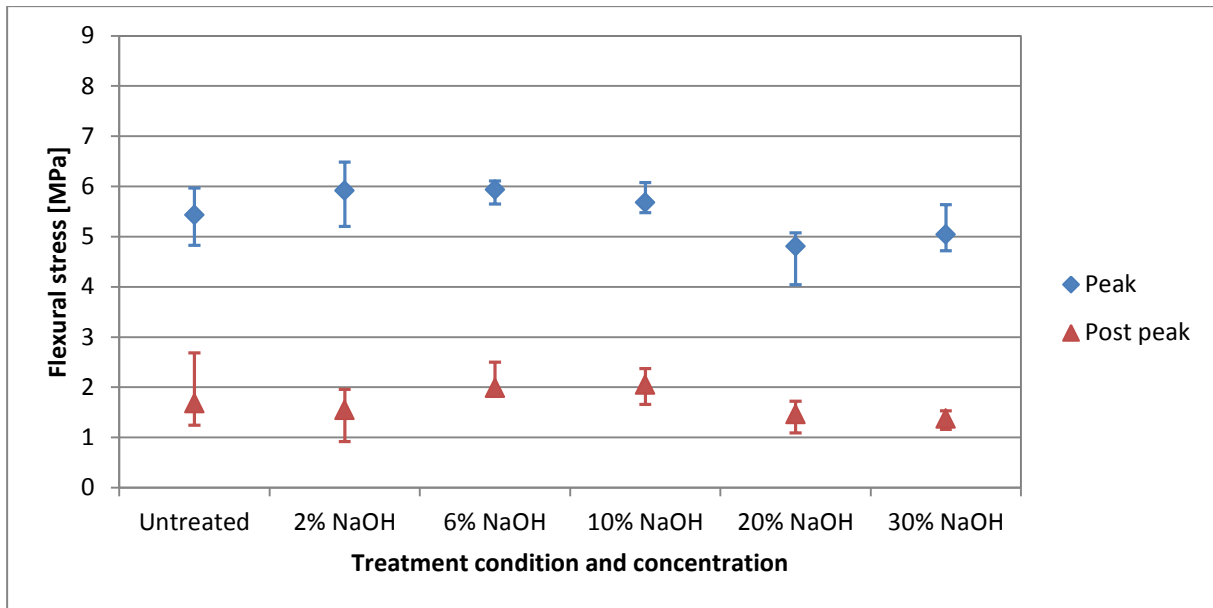
Figure 5.3: Average peak and post-peak flexural strength for matrix C1-1-20 with untreated and alkali treated fibres.
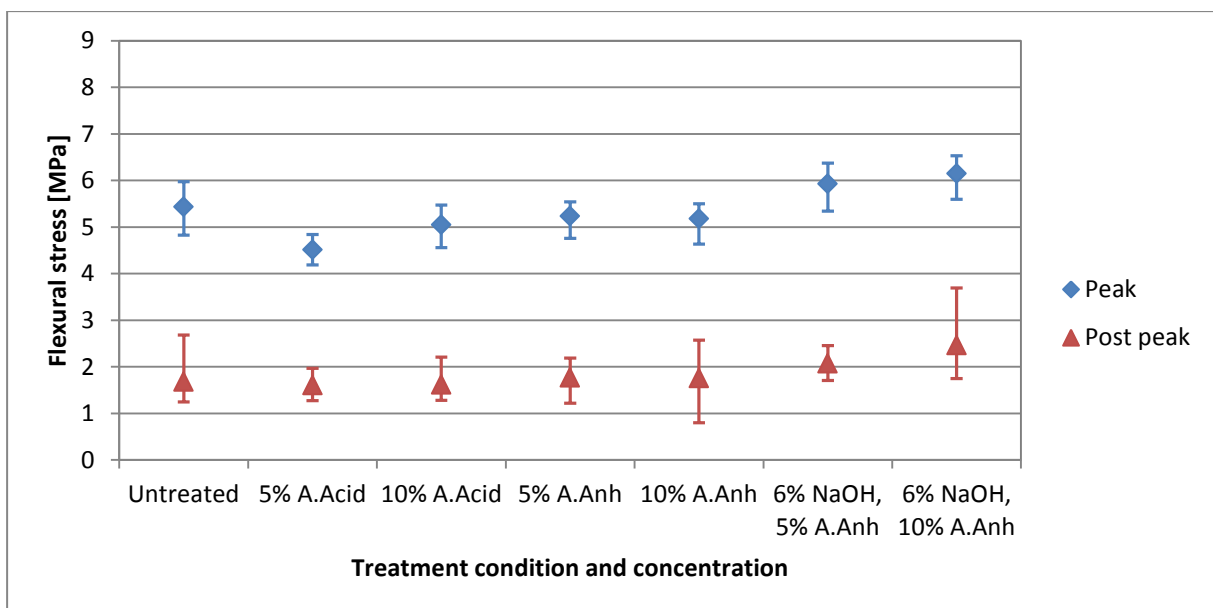
Figure 5.4: Average peak and post-peak flexural strength for matrix C1-1-20 with untreated and acetylated fibres.

Figure 5.5 presents the results of different matrices reinforced with 1% fibre cut to a length of 20 mm. Matrices C2, C4 and C5 have relatively low peak strengths. The specimens were brittle and soft as was the case with the specimens tested in compression. These were matrices where a fraction of the OPC was replaced with FA, 30% in matrix C2 and C5 and 20% in matrix C4. In addition to the replacement of cement with FA in matrices C4 and C5, 10% of the cement was replaced with CSF in matrix C4 and 40% of the sand (by volume)

was replaced with FA in matrix C5. The slightly higher strength of matrix C4, in comparison to matrices C2 and C5, is attributed to the lower percentage cement replacement with FA, but also the addition of CSF. The lower strength of matrix C4 in comparison to matrix C3 is attributed to the FA in matrix C4. Matrices C3 and C6 had the highest post-peak strength of all the alternative matrices. In both these matrices, 10% of the OPC was replaced with CSF and in matrix C6, 40% of the sand (by volume) was replaced with FA. The higher peak strength of matrix C6 compared to C3 can be attributed to a denser matrix (average density of cubes in Section 4.2) which also led to a better fibre-paste interface and increased post-peak strength. It is also possible that a fraction of the FA reacted as binder.
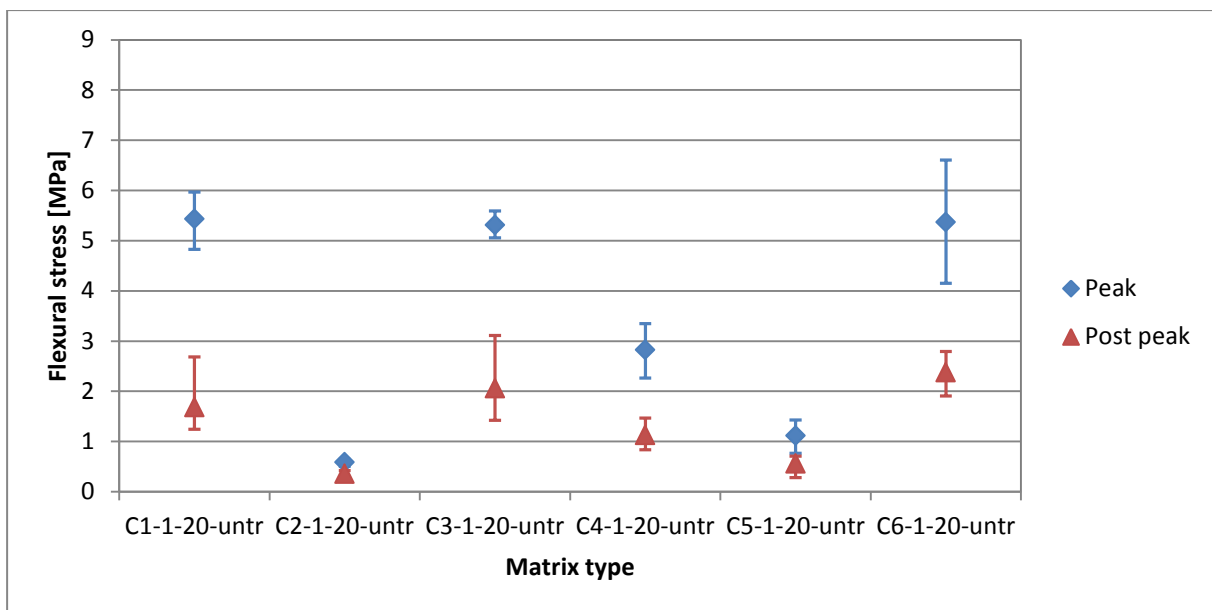
Figure 5.5: Average peak and post-peak flexural strength for matrices C1 to C6 with 1%, 20 mm untreated fibres

In Figure 5.6 it is evident that the peak strength decreased as the fibre length increased. The decrease for matrix C1-1-30 is more severe. The decrease in strength can be attributed to better compaction achieved when shorter fibres are used compared to longer fibres. The post-peak strength increased from a fibre length of 10 mm to 20 mm but decreased from 20 mm to 30 mm. The post-peak strength was the lowest for the 10 mm fibre.
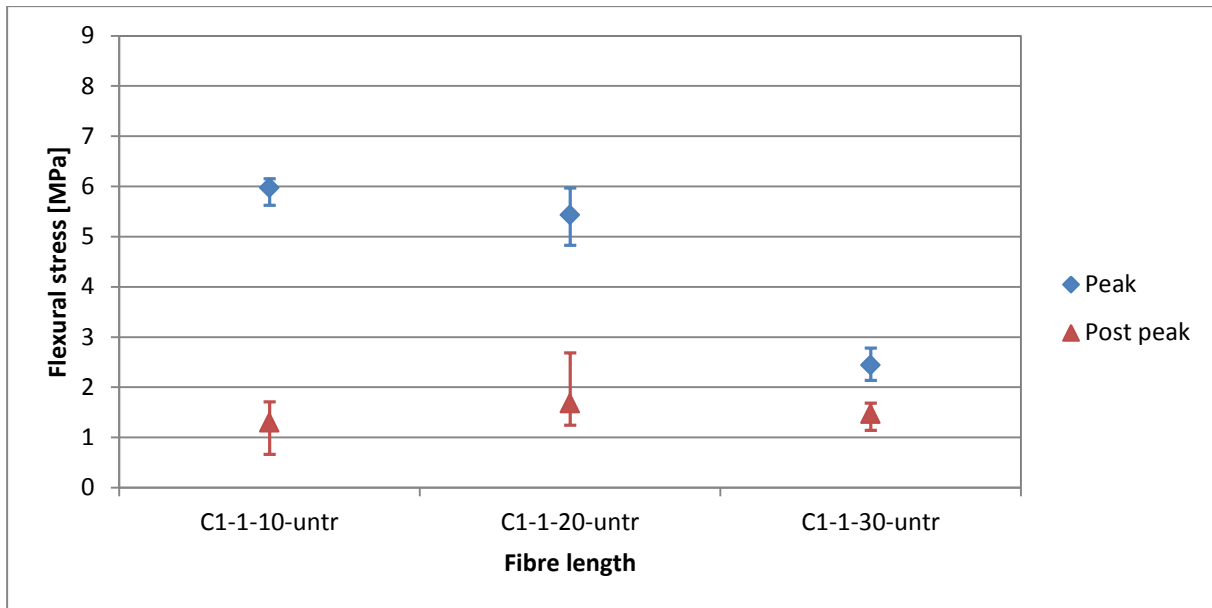
Figure 5.6: Average peak and post-peak flexural strength for OPC matrix with fibre lengths of 10 mm, 20 mm and 30 mm.

In Figure 5.7 a similar trend can be observed for the extruded specimens with comparison to the cast specimens. The results of the cast matrices C5 and C6 are represented for comparison purposes. The matrices containing FA as supplementary cementitious material had a lower strength when compared to the matrices containing CSF or a combination of FA and CSF. Matrix E1-1-20, which was the same as matrix C5-1-20 used for the cast specimens, had the lowest strength of the extruded specimens. Both the peak- and post-peak strength was approximately two times greater for matrix E1 compared to matrix C5. Matrix E2-1-20 also had higher strength than the similar cast matrix C6-1-20. The post-peak strength was however slightly lower for the extruded specimen than for the cast specimen. The peak- and post-peak strength of matrix E3-1-20 was higher than for matrix E1-1-20, but lower than for matrix E2-1-20. The replacement of 20% of cement with FA is responsible for the decrease in strength compared to matrix E2. Although only 20% of cement was replaced with FA in matrix E3 compared to 30% in matrix E1, the increased strength compared to matrix E1 is attributed to the addition of CSF.

Pictures of the extruded specimens can be seen in Figure 5.8 and Figure 5.9. The edges of the specimens containing FA delaminated. The matrix swelled slightly in the water and cracked along the edges. The same phenomenon was observed for matrices C2 and C5.

71
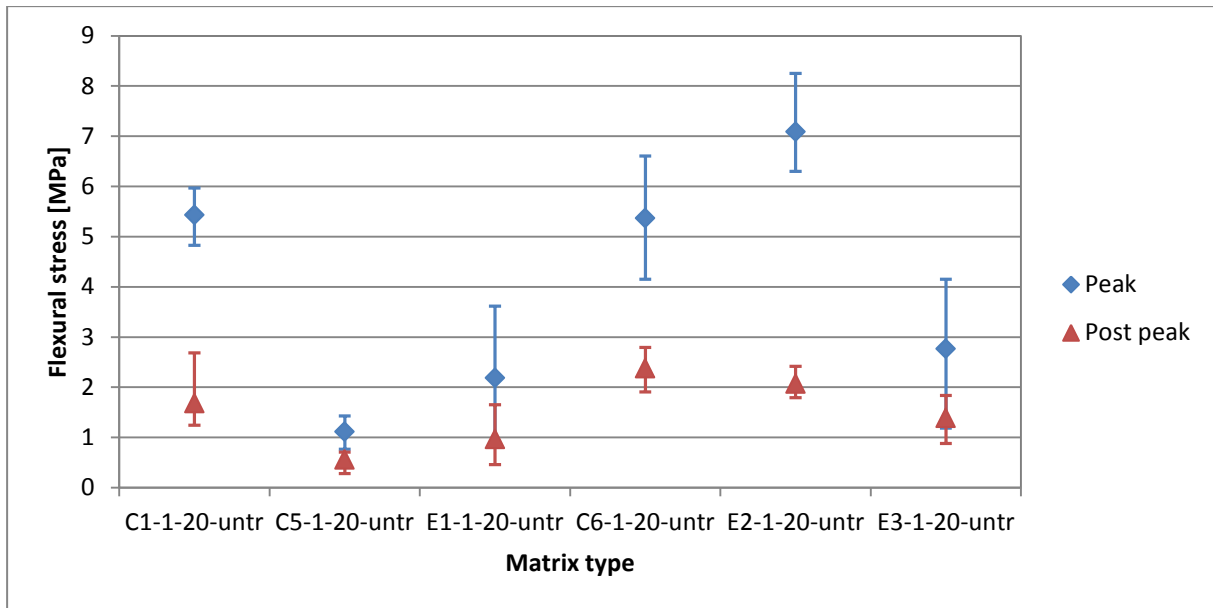
Figure 5.7: Average peak and post-peak flexural strength for cast specimens C1-1-20 versus extruded specimens.
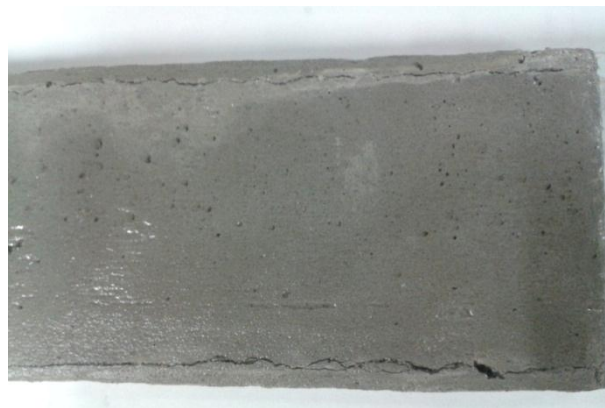
Figure 5.8: Extruded specimen E1-1-20-untr.

Figure 5.9: Extruded specimen E3-1-20-untr.

72

5.1.2. 90 Day water cured aged specimens

The results of the average post-peak flexural stress at 90 days for the specimens subjected to extended curing in water are presented in Figure 5.10 to Figure 5.14. From Figure 5.10 it can be seen that the specimens with 2% untreated fibre had increased strength at 90 days whereas the specimens with 1% untreated fibre had decreased strength.
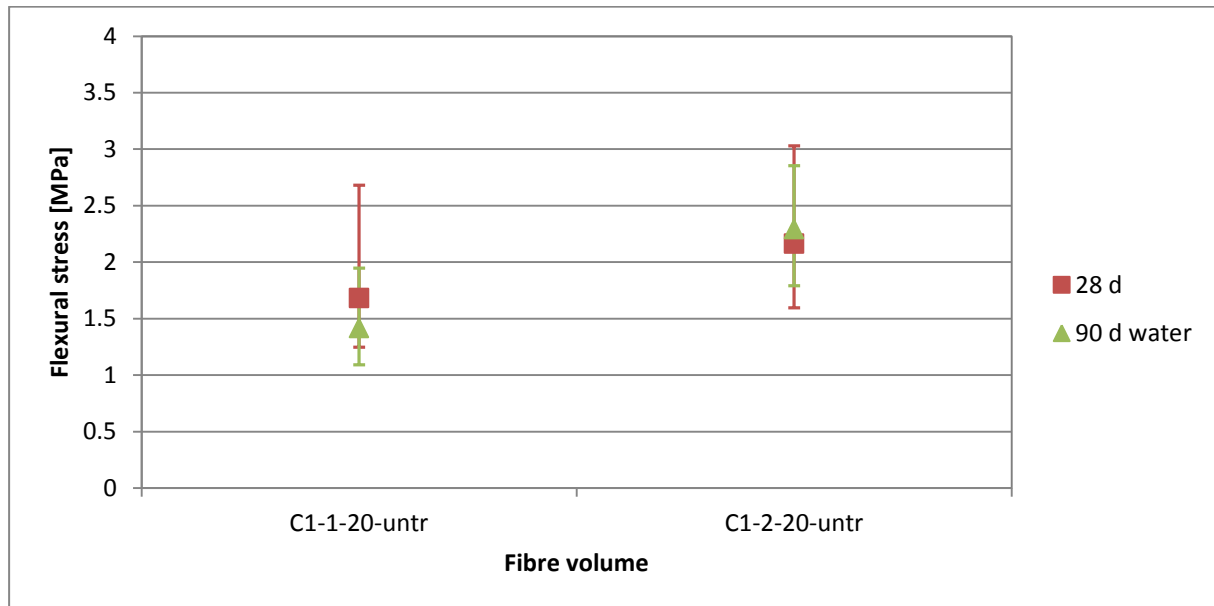
Figure 5.10: Average post-peak flexural strength for matrix C1-2-20-untr and C1-1-20-untr subjected to ageing in water.

For the alkali treated fibres shown in Figure 5.11, it can be seen that the strength increased slightly for the 2% and 30% NaOH specimens. For all the other specimens, the strength decreased. The decrease was the least for 20% NaOH. For the 10% NaOH, the decrease in strength was more than for the untreated reference specimen, but the strength was still higher.

For the acetylated fibres shown in Figure 5.12, a similar trend of increasing post-peak flexural strength can be observed at both 28 days and 90 days of curing in water. For the 6% NaOH-5% Acetic Anhydride, the stress was however higher at 90 days than at 28 days. This may be considered as an outlier, but the result is not disregarded. The 6% NaOH-10% Acetic Anhydride had the largest decrease in strength, but it still had the highest strength (not taking account of 6% NaOH-5% Acetic Anhydride) after ageing, even when compared to the alkali treated fibre specimens.
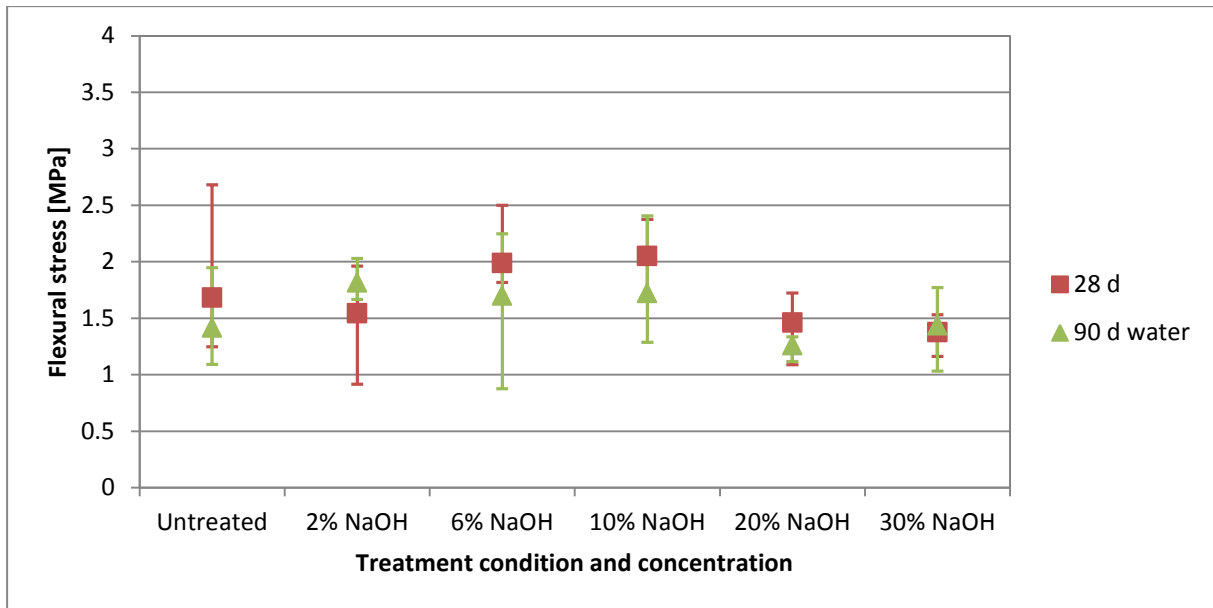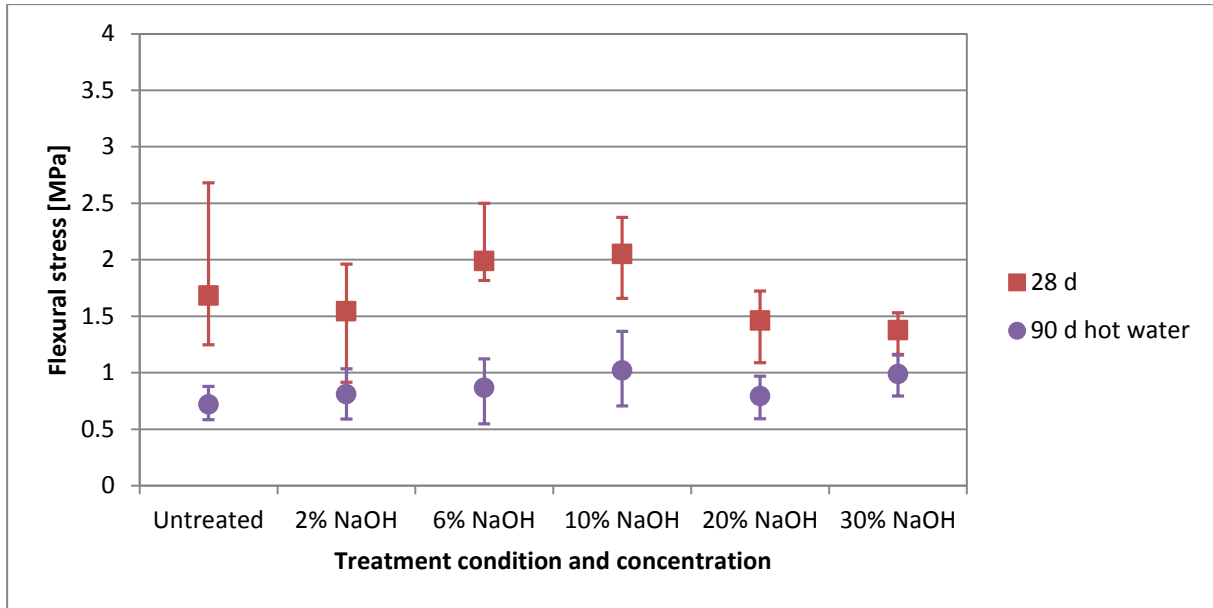
Figure 5.11: Average post-peak flexural strength for matrix C1-1-20 with untreated and alkali treated fibres subjected to ageing in water.
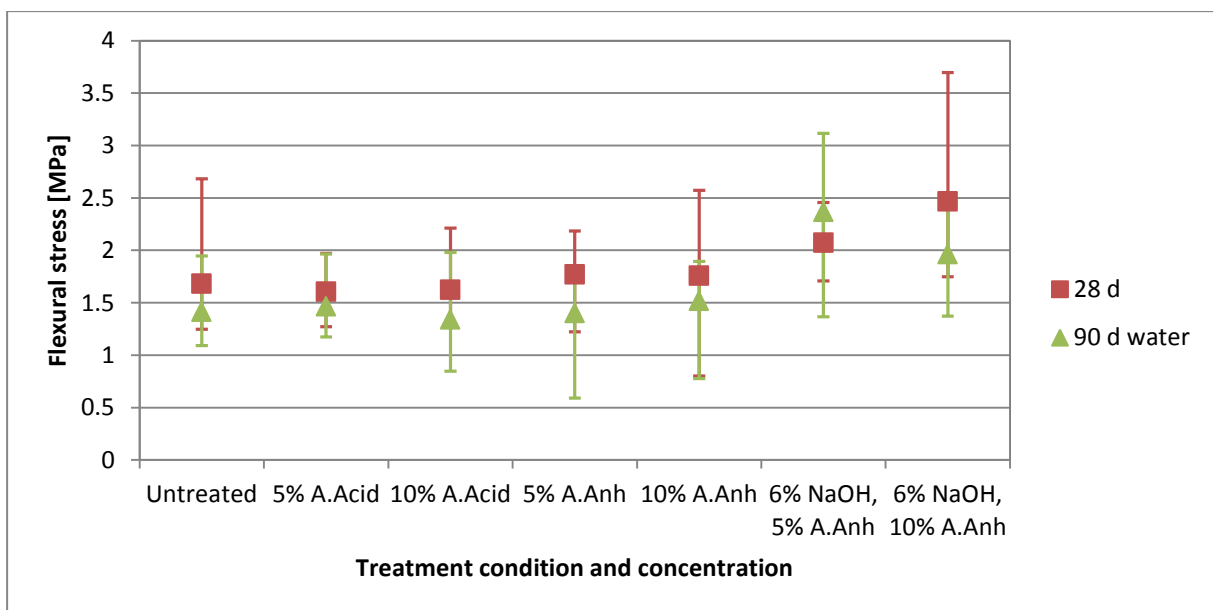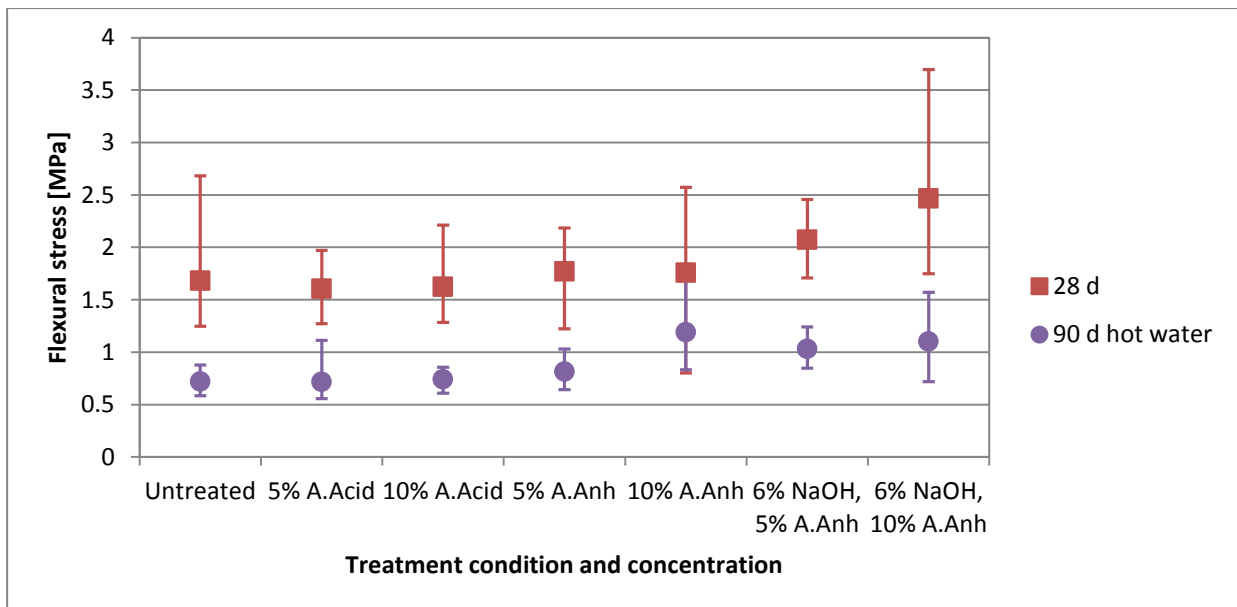

Figure 5.12: Average post-peak flexural strength for matrix C1-1-20 with untreated and acetylated fibres subjected to ageing in water.

For the different matrices with untreated fibre in Figure 5.13, matrix C2 and C5 had increased strength after 90 days. In both matrices 30% of the cement was replaced with FA, but in C5 40% of the sand was also replaced with FA. The increase in post-peak strength is attributed to the continuous reaction of FA with $Ca(OH)_2$. The higher increase of matrix C3 indicates that the fibre-matrix bond was better than for C5. Matrices C1, C3, C4 and C6 had decreased

74

strength. Matrix C4 had the lowest percentage decrease, while matrices C3 and C6 both had decreases larger than the control matrix C1.
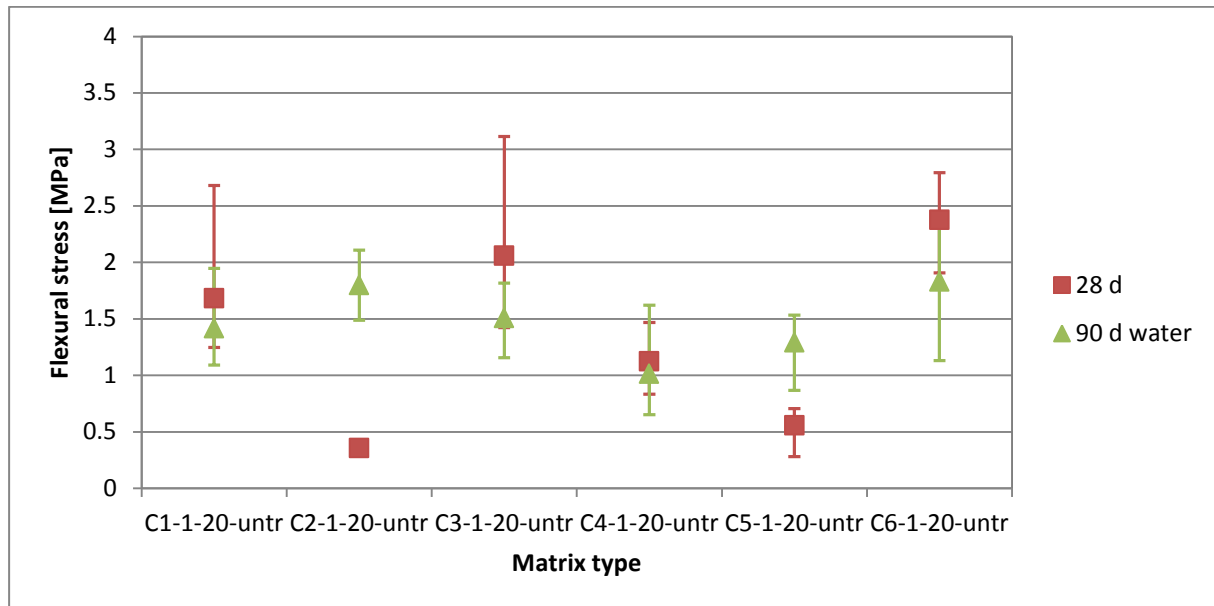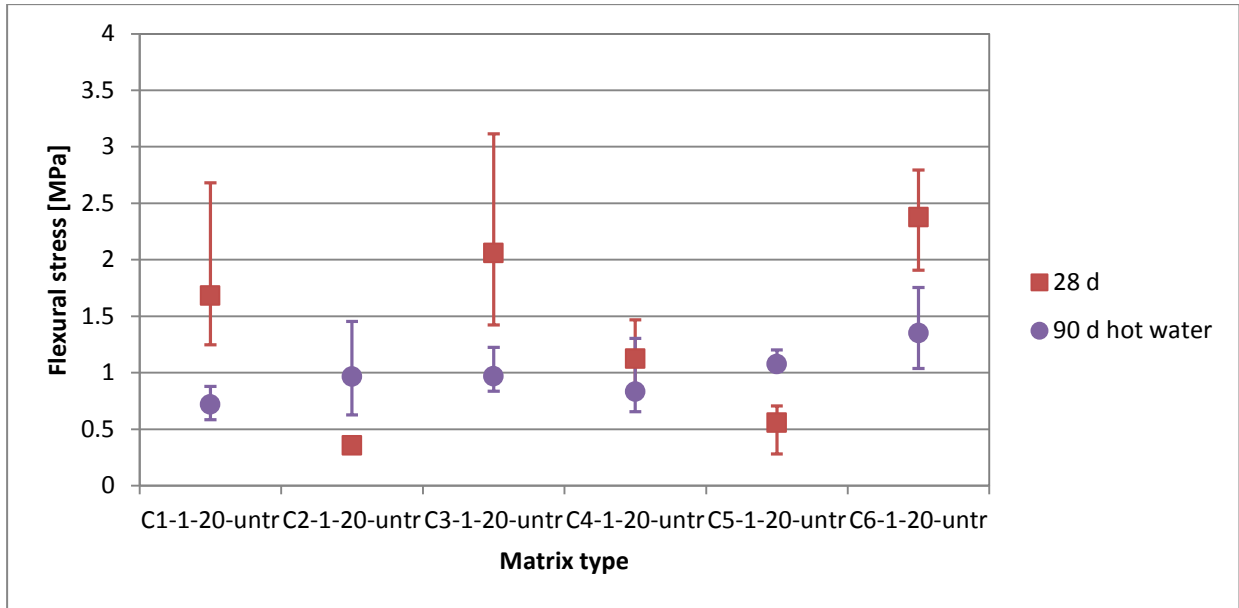

Figure 5.13: Average post-peak flexural strength for matrices C1 to C6 with 1%, 20 mm untreated fibres, subjected to ageing in water.

For matrix C1 with different fibre lengths shown in Figure 5.14, the specimens with the 30 mm fibre had a smaller percentage decrease than the specimens with 20 mm fibre. The latter still had higher strength than the former after 90 days.

The post-peak strength of the extruded specimens is presented in Figure 5.15. Matrices E1 and E3 had increased strength after 90 days, while matrix E2 had decreased strength. Matrices E1 and E2 are the same matrices as matrices C5 and C6, respectively. The results are similar for the cast specimens. Matrix E1, which contained 30% FA as supplementary cementitious material had increased strength after ageing, while matrix E2, which contained 10% CSF as supplementary cementitious material, had decreased strength after ageing. Matrix E3, containing FA and CSF as supplementary cementitious materials, had a slight increase in strength. The increase was however lower than for matrix E1.
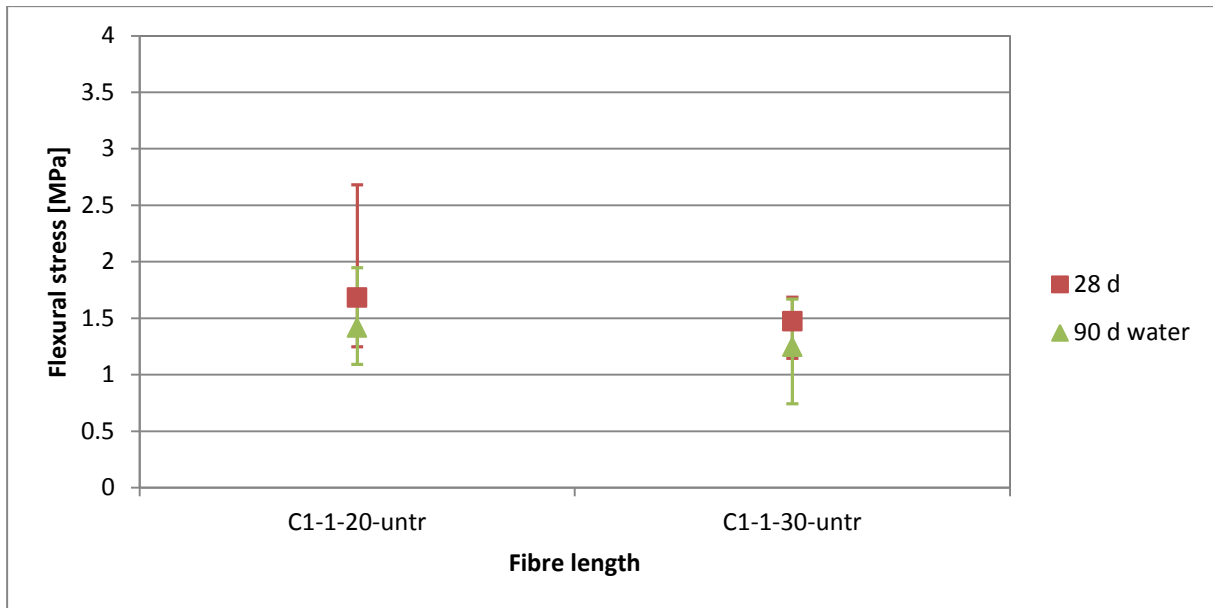
Figure 5.14: Average post-peak flexural strength for OPC matrix with fibre lengths of 20 mm and 30 mm subjected to ageing in water.
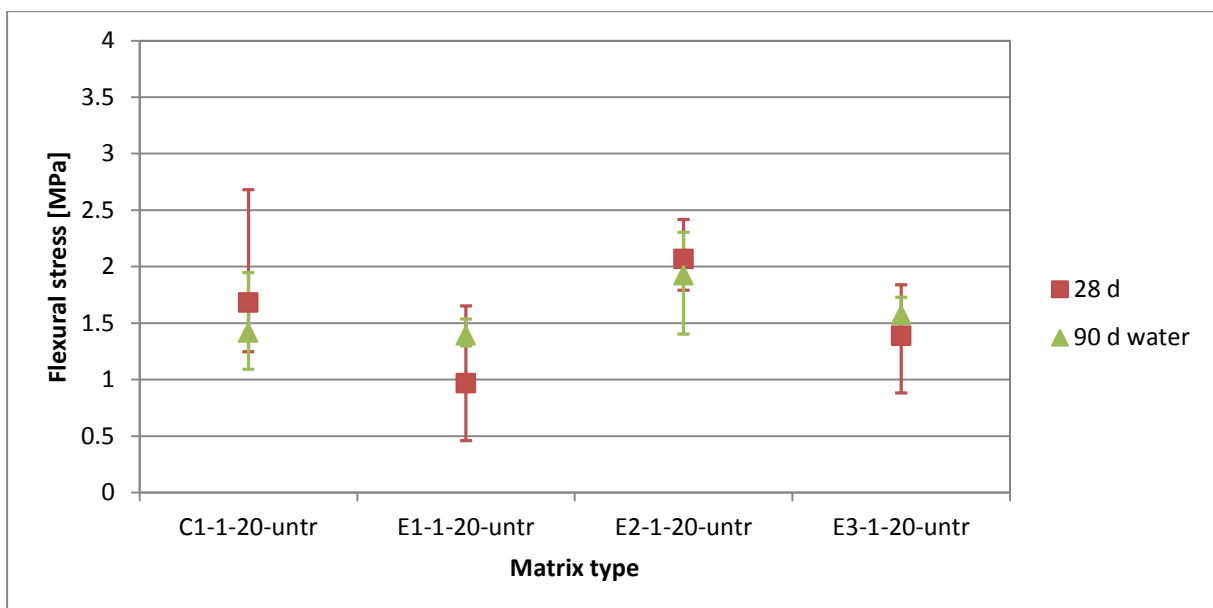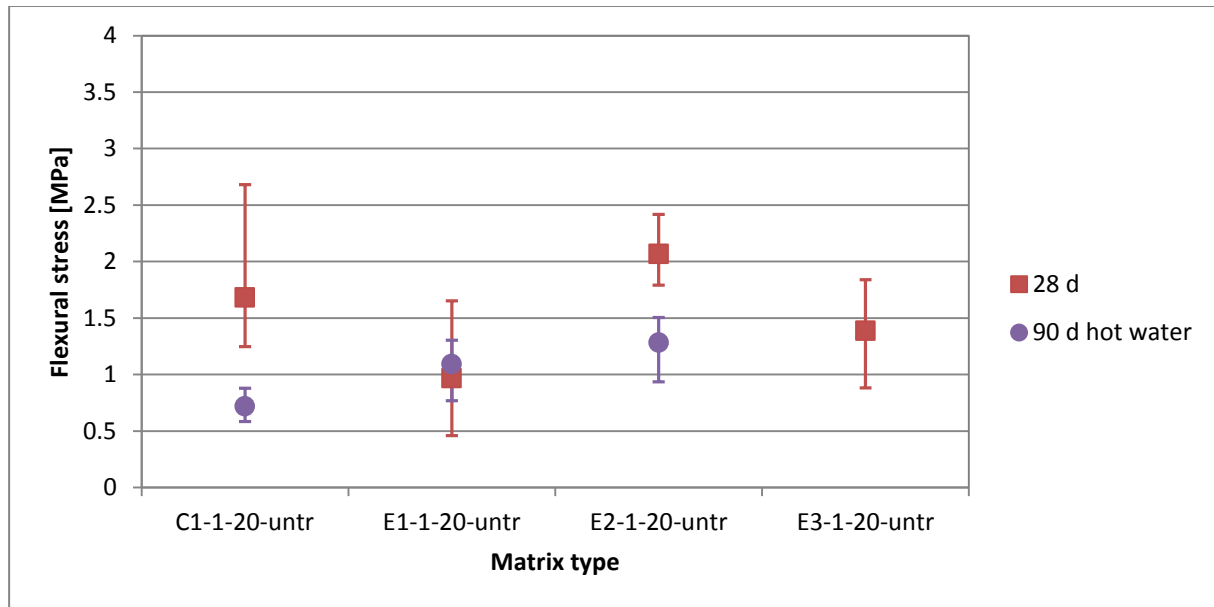

Figure 5.15: Average post-peak flexural strength for cast specimens C1-1-20 versus extruded specimens subjected to ageing in water.

5.1.3. 90 Day hot water accelerated aged specimens

The results of the average post-peak flexural sttress at 90 days for the specimens subjected to hot water ageing are presented in Figure 5.16 to Figure 5.20. For all the specimens the post-peak flexural stress was considerably lower after ageing in hot water, except for matrices C2, C5 and E1. In Figure 5.16, a similar trend can be observed at both ages. The

specimens with a higher fibre volume had higher strength. Both matrices had a similar percentage decrease in strength.
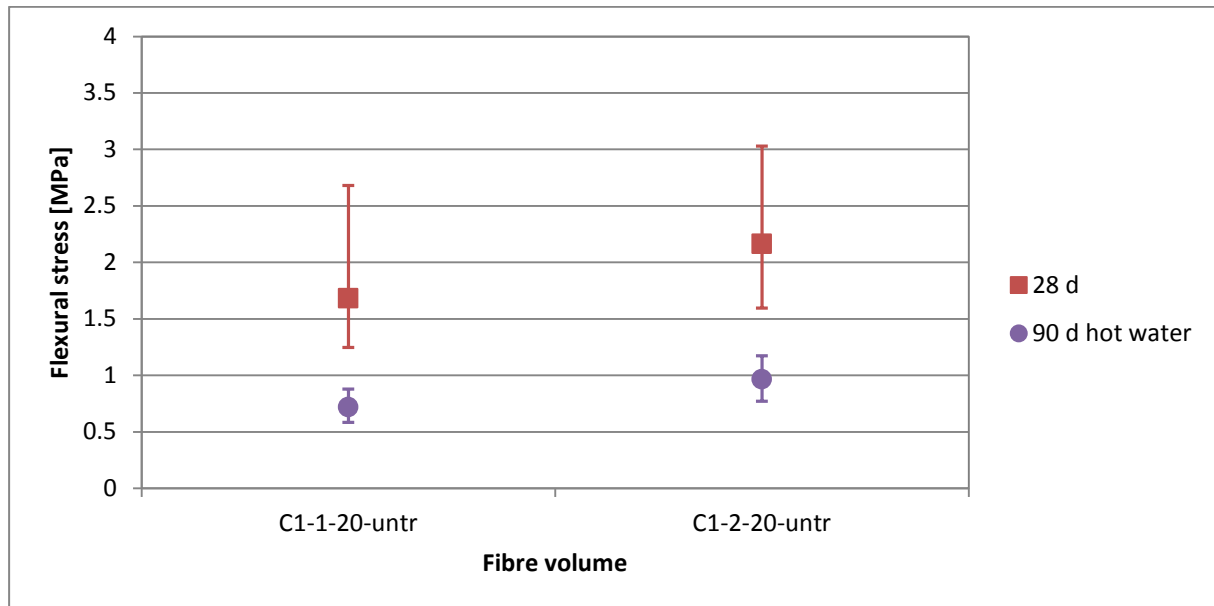
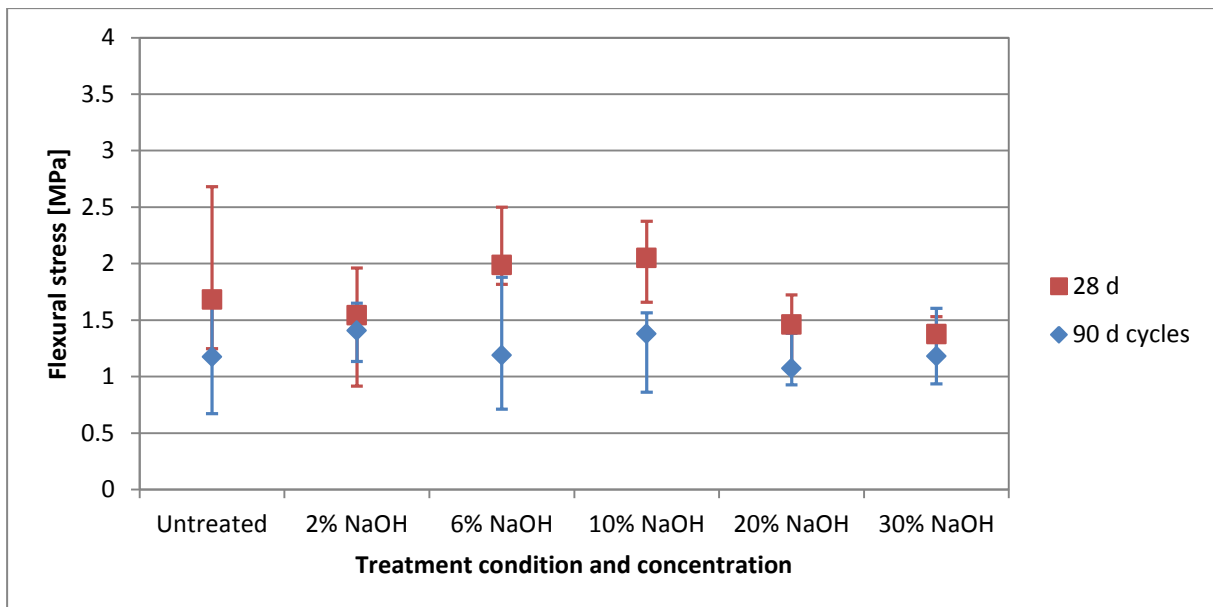**Figure 5.16: Average post-peak flexural strength for matrix C1-2-20-untr and C1-1-20-untr subjected to ageing in hot water.**

The specimens with alkali treated fibres had a similar trend at both 28 days and 90 days. All the alkali treated fibre specimens had higher post-peak strength after ageing than the matrix with untreated fibre. Of the treated fibre specimens, the 10% NaOH had the highest strength after ageing while the 20% NaOH had the lowest strength.

In Figure 5.18 the specimens with acetylated fibres also had a similar trend at both ages. It is evident that the specimens with the fibre pre-treated with 6% NaOH and then with Acetic Anhydride had lower strengths than expected when looking at the trend. The specimens with 10% Acetic Anhydride fibres had the highest strength, while the 6% NaOH-10% Acetic Anhydride had the second highest strength. The specimens with 6% NaOH-5% Acetic Anhydride had just slightly lower strength than the 6% NaOH-10% Acetic Anhydride specimens, but higher strength than the 5% Acetic Anhydride specimens. All the acetylated fibre specimens had higher strength than the untreated fibre specimens after ageing.

Figure 5.17: Average post-peak flexural strength for matrix C1-1-20 with untreated and alkali treated fibres subjected to ageing in hot water.

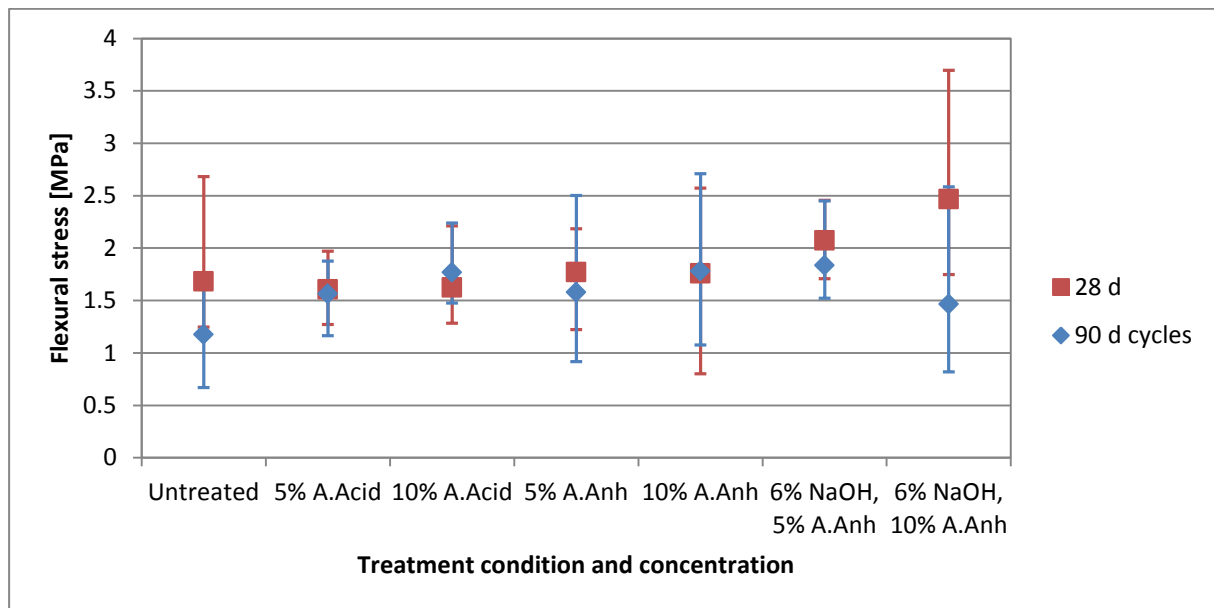**Figure 5.18: Average post-peak flexural strength for matrix C1-1-20 with untreated and acetylated fibres subjected to ageing in hot water.**

In Figure 5.19 the trend was similar as for ageing in water. Matrices C2 and C5 had increased strength after 90 days, while matrix C4 had the lowest reduction in strength. Matrix C6 had the highest strength of all specimens tested at 90 days after ageing in hot water. All the matrices C2 to C6 had higher strength than matrix C1.
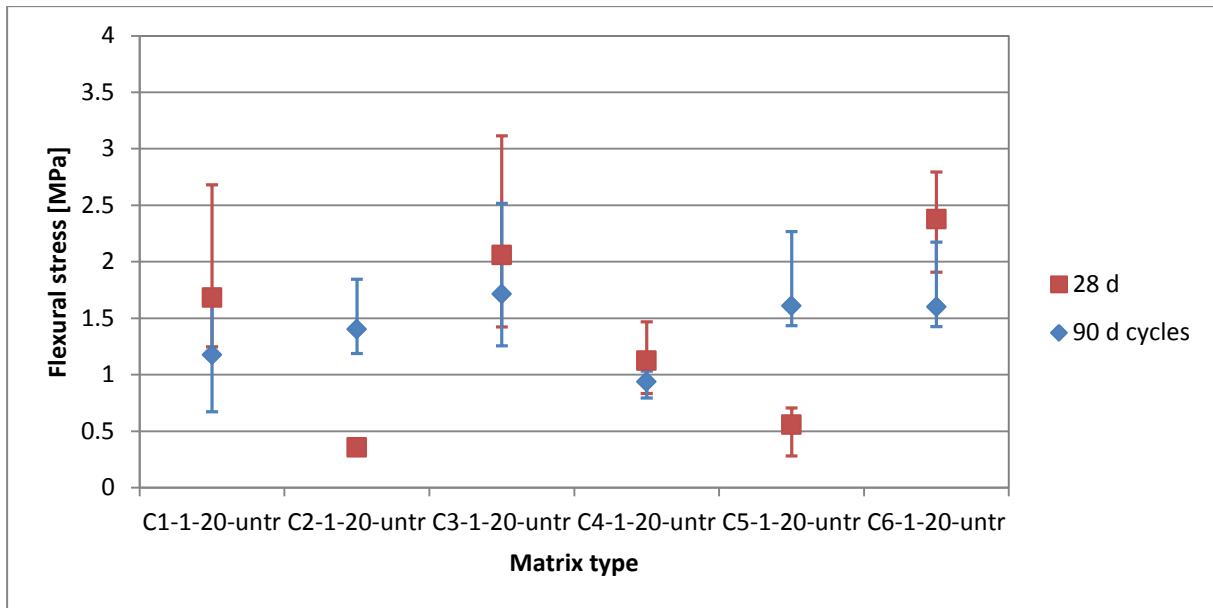
Figure 5.19: Average post-peak flexural strength for matrices C1 to C6 with 1%, 20 mm untreated fibres, subjected to ageing in hot water.

For matrix C1 with different fibre lengths shown in Figure 5.20, the specimens with the 30 mm fibre had a smaller percentage decrease than the specimens with 20 mm fibre. The latter still had higher strength than the former at 90 days.
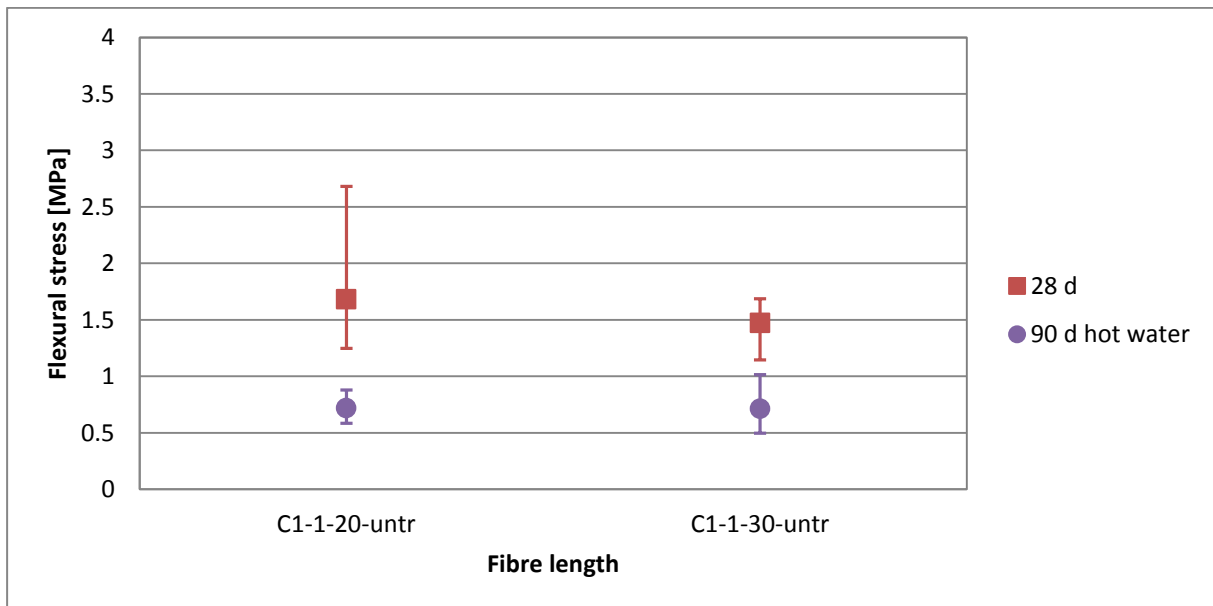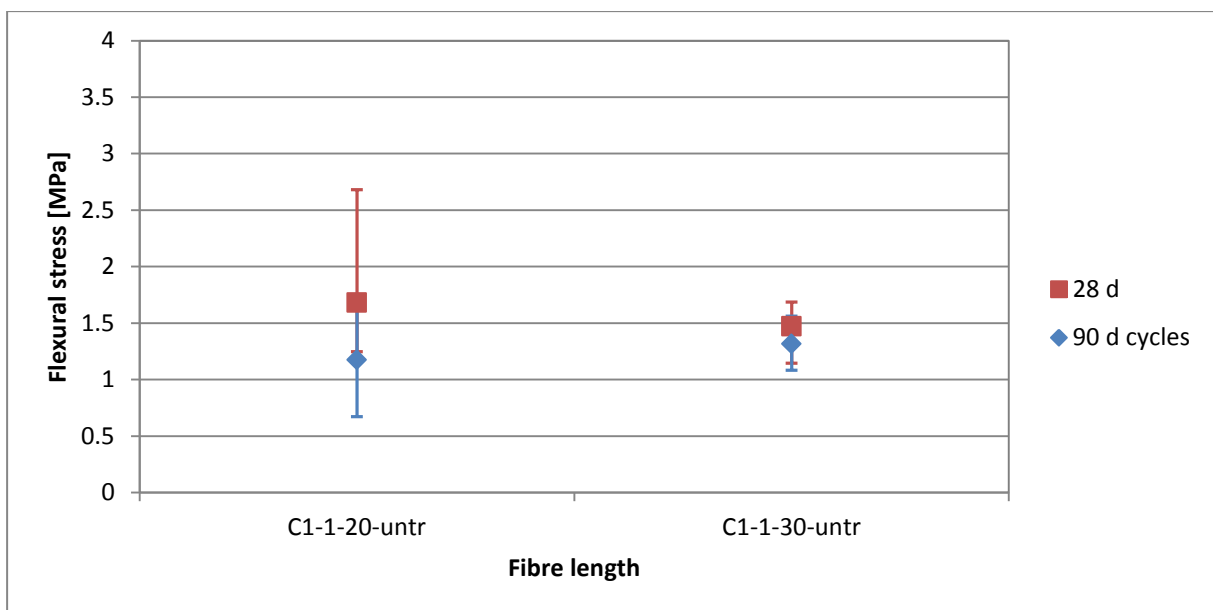

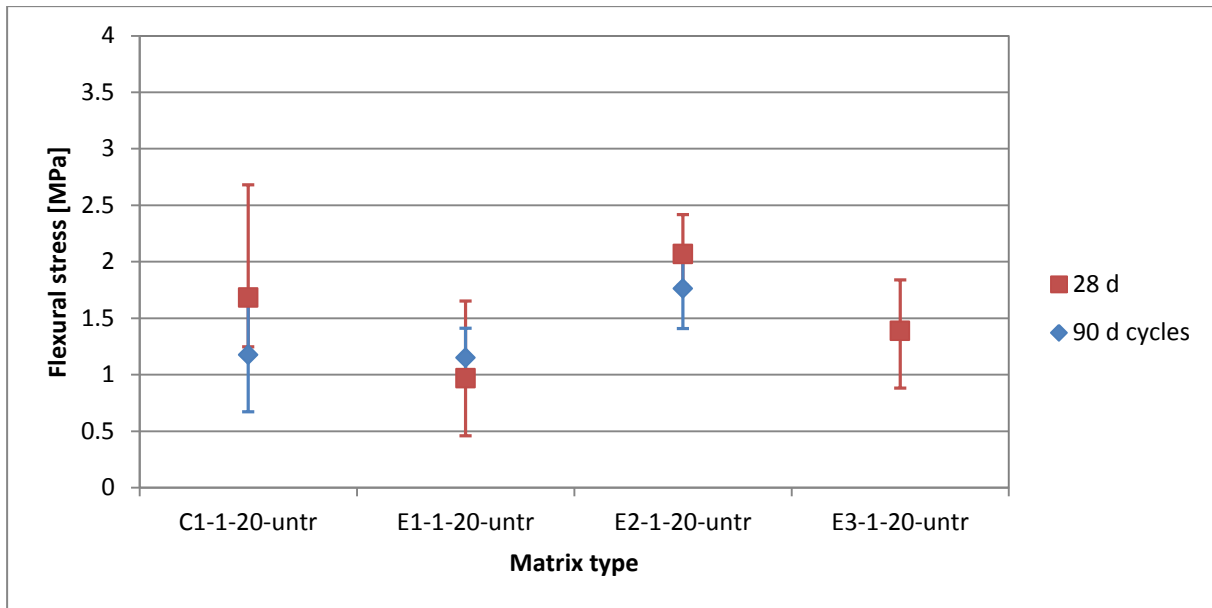**Figure 5.20: Average post-peak flexural strength for OPC matrix with fibre lengths of 20 mm and 30 mm subjected to ageing in hot water.**

In Figure 5.21 the trend is similar for ageing in hot water than for normal ageing in water. Matrix E1 had a slight increase in strength, while matrix E2 had a decrease in strength. Matrix E2 still had the highest strength after ageing. Due to a shortage of specimens, matrix E3 was not aged in hot water.

Figure 5.21: Average post-peak flexural strength for cast specimens C1-1-20 versus extruded specimens subjected to ageing in hot water.

5.1.4. 90 Day wet/dry cycle aged specimens

The results of the average post-peak flexural stress at 90 days for the specimens subjected to alternate cycles of wetting and drying are presented in Figure 5.22 to Figure 5.26. The results were quite variable as indicated by the error bars. In Figure 5.22, matrix C1 with 2% fibre only had a slight decrease in strength, while matrix C1 with 1% fibre had a larger decrease in strength.

For the alkali treated fibre specimens presented in Figure 5.23, the trend was similar at both ages and also similar to the 90 day water cured test results. The specimens containing 2% NaOH treated fibres had the highest strength after ageing and the smallest reduction in strength. The 2% NaOH specimens also had the highest strength in the case of the normal water ageing. All the specimens, except for 20% NaOH, had higher strength than the untreated fibre specimens. The 6% NaOH specimens had the highest decrease in strength.
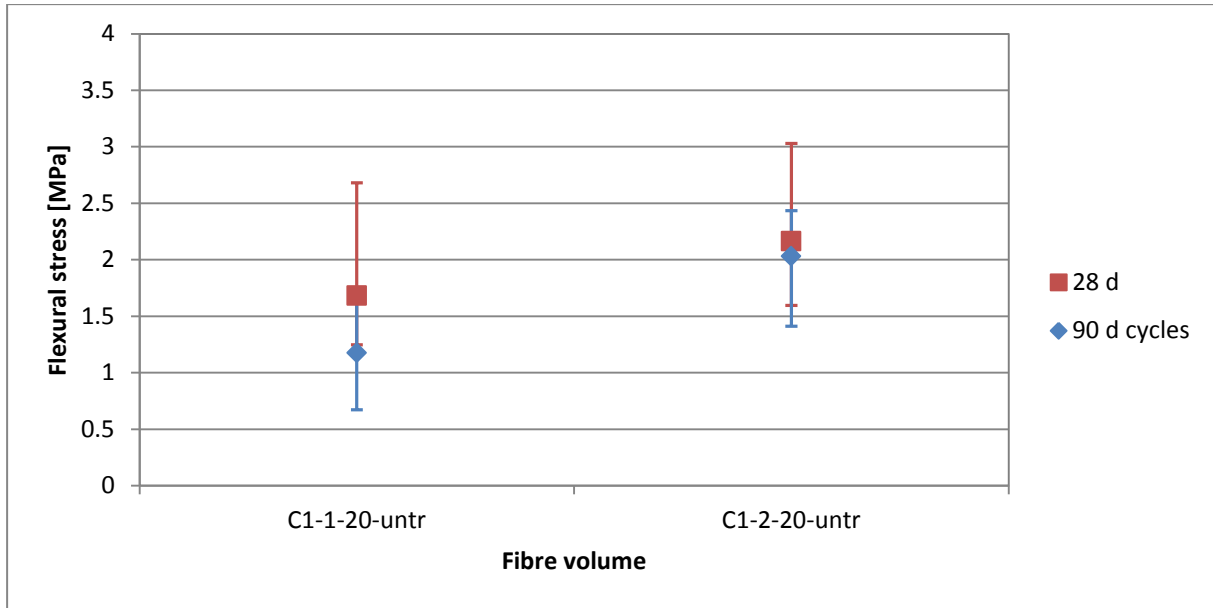
Figure 5.22: Average post-peak flexural strength for matrix C1-2-20-untr and C1-1-20-untr subjected to wet/dry cycle ageing.

Figure 5.23: Average post-peak flexural strength for matrix C1-1-20 with untreated and alkali treated fibres subjected to wet/dry cycle ageing.

No clear trend can be observed for the acetylated fibre specimens presented in Figure 5.24. The 10% Acetic Acid and 10% Acetic Anhydride specimens both had a slight increase in strength. The 6% NaOH-5% Acetic Anhydride specimens had the highest strength and 10% Acetic Anhydride had the second highest strength. The 5% Acetic Acid specimens had the smallest decrease in strength, while 6% NaOH-10% Acetic Anhydride had the largest

decrease in strength. It however still had higher strength than the untreated fibre specimens. Overall, the acetylated fibre specimens had the highest strength after wet/dry cycle ageing.

Figure 5.24: Average post-peak flexural strength for matrix C1-1-20 with untreated and acetylated fibres subjected to wet/dry cycle ageing.

For the different cast specimens C1 to C6 in Figure 5.25, Matrix C2 and C5, in which 30% of cement was replaced with FA, had increased strength. This was also the case with ageing in water and lime saturated hot water. Matrix C4, in which 20% and 10% of cement was replaced with FA and CSF, respectively, had the lowest decrease in strength, while matrix C6 had the highest decrease in strength. Matrix C3 also had decreased strength, but it had the highest strength after ageing followed by matrix C5 and matrix C6. In both matrices C3 and C6, 10% of cement was replaced with CSF, but in matrix C6, 40% of the sand was also replaced with FA.

In Figure 5.26, matrix C1 with 30 mm fibre had the highest strength after ageing and the lowest reduction in strength. For the extruded specimens, presented in Figure 5.27, matrix E1, containing FA as part of the binder, had increased strength. Matrix E2, containing CSF as part of the binder, had decreased strength, but it had the highest strength after ageing. The decrease was lower than for matrix C1. This agrees with the results from the normal water and lime saturated hot water ageing. Due to a shortage of specimens, matrix E3 was not subjected to cycles of wetting and drying.

Figure 5.25: Average post-peak flexural strength for matrices C1 to C6 with 1%, 20 mm untreated fibres, subjected to wet/dry cycle ageing.

Figure 5.26: Average post-peak flexural strength for OPC matrix with fibre lengths of 20 mm and 30 mm subjected to wet/dry cycle ageing.

Figure 5.27: Average post-peak flexural strength for cast specimen C1-1-20 versus extruded specimens subjected to wet/dry cycle ageing.

5.2. Direct tensile tests

The results of the specimens tested in direct tension are presented in this section. A table summarising all the results is presented in Appendix C. A typical graph for a series of specimens is presented in Figure 5.28. From the graph it is clear that the stress increases up to the point where the specimen cracks which is at the peak of the graph. Thereafter the stress decreases rapidly. It is at this point that the fibres start acting in tension and it is called the post-peak behavior. In some cases a slight increase in stress is noted, as in Figure 5.28, as the fibres interlock with the matrix, but as they start pulling out the stress decreases again. The tests were stopped after a crack width of 3 mm was measured.

5.2.1. Reference specimens

A series of dogbone specimens were tested in direct tension at 28 days to establish references. The graphs of the tests for all the different series of specimens tested at 28 days are presented in Appendix C. A summary of the results is represented in this section in Figure 5.29 to Figure 5.33. The graphs show the average peak and post-peak direct tensile stress for a series of specimens for different fibre volumes and lengths as well as the different fibre treatment conditions and specimens manufactured from the different matrices. The post-peak tensile stress gives a clear indication of the influence of the fibres.
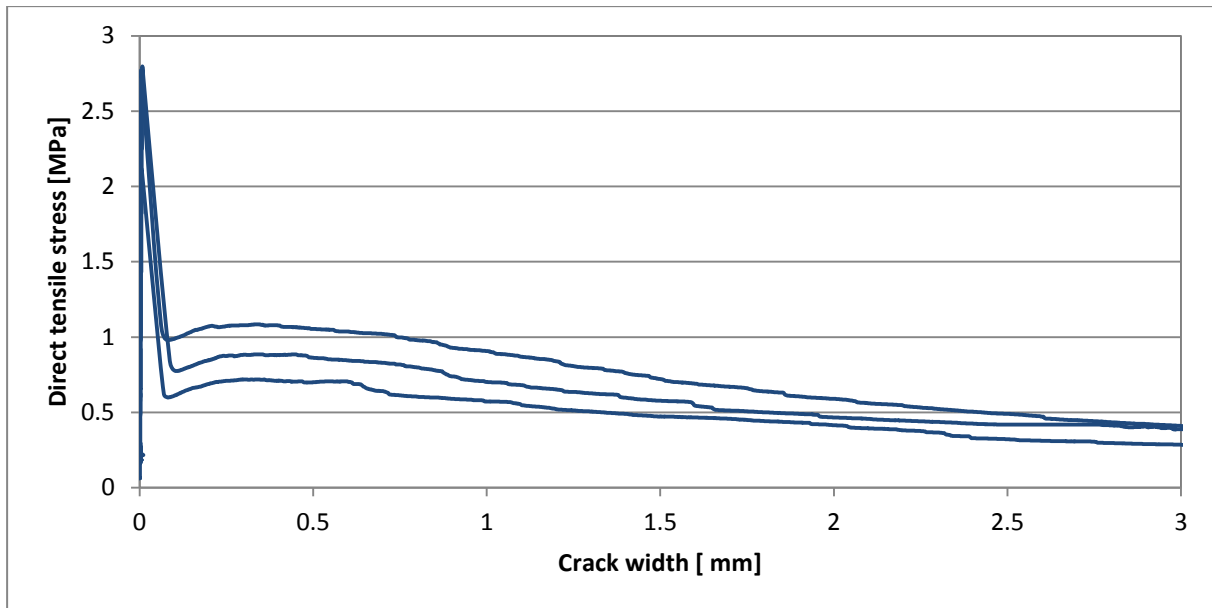
Figure 5.28: Typical graph for a series of specimens tested in direct tension.

To calculate the average peak stress, the individual peak stress for each specimen in a series was read from the data. The average post-peak stress was calculated as an average from 0.15 mm of the limit of proportionality (LOP) over a displacement of 0.3 mm. The error bars indicate the maximum and minimum values recorded in each series.

In Figure 5.29 it can be seen that matrix C1-2-20-untr had lower peak strength but higher post-peak strength than matrix C1-1-20. These results are in agreement with the results from the compression and three-point bending tests. The increase in post-peak strength is due to the higher fibre volume which allows more fibres to bridge the crack and resist the tensile force. The maximum tensile stress recorded for the series C1-2-20-untr was almost double than that recorded for the series C1-1-20-untr. The minimum however, was lower. The series C1-2-20-untr had more variability in its results.

From Figure 5.30, it can be seen that the peak strength for all the specimens reinforced with alkali treated fibres was significantly lower compared to untreated fibres. For the 2%, 6%, and 10% NaOH specimens, the peak strength was similar, but from 10% to 30% NaOH an almost linear decrease is noted. The post-peak strength for all the specimens is similar, with an almost linear trend of slightly decreasing strength, except for 20% NaOH which is lower than expected. In the single fibre pull-out tests, the 20% NaOH fibres did however pull out at a longer embedment depth than the other alkali treated fibres. These results confirm that the 20% NaOH fibres had a lower bond strength than the other alkali treated fibres. The higher post-peak strength of the 2% NaOH specimens compared to the untreated specimens shows

85

increased bond strength, which is due to the removal of impurities such as fats, waxes and mineral matter from the fibre surface.
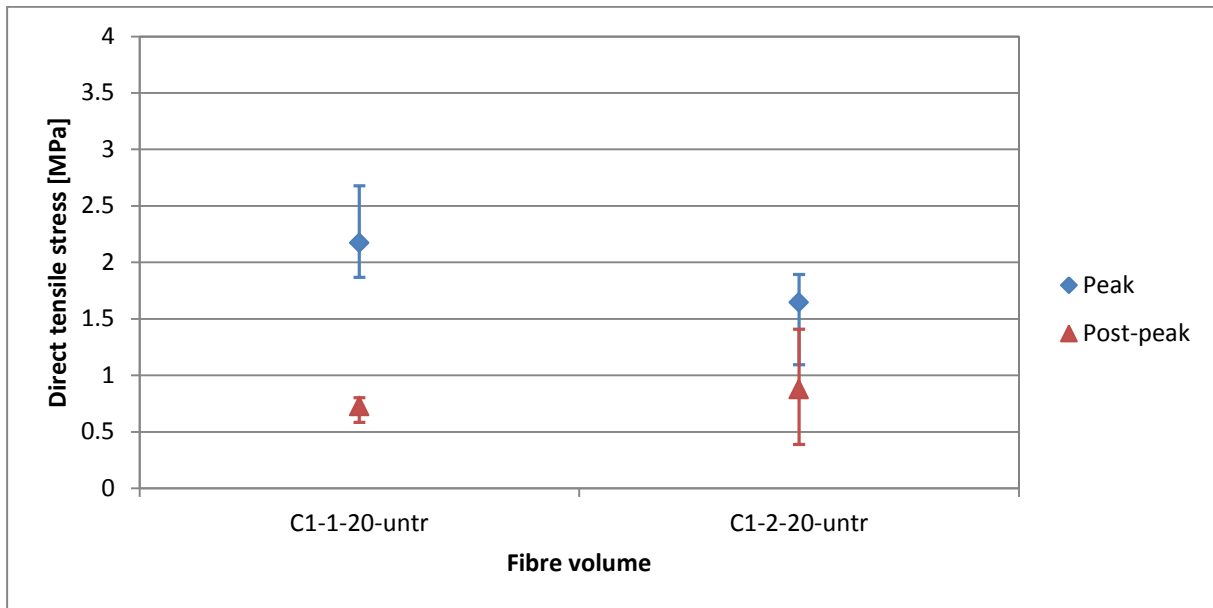
Figure 5.29: Average peak and post-peak tensile strength for matrix C1-1-20-untr and C1-2-20-untr respectively.
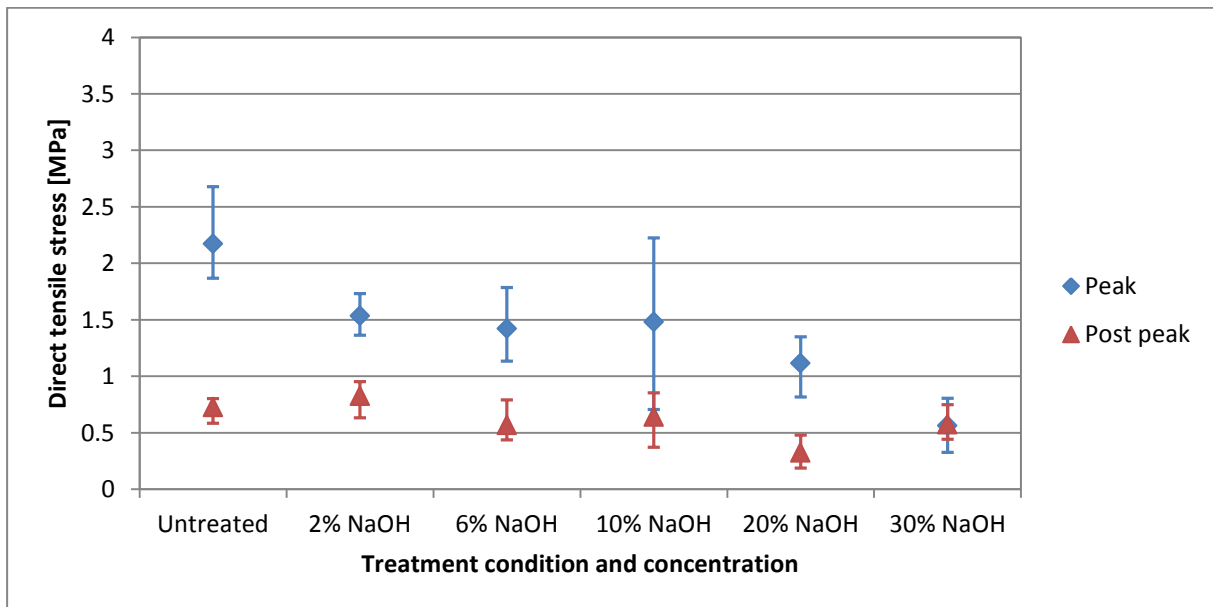
Figure 5.30: Average peak and post-peak tensile strength for matrix C1-1-20 with untreated and alkali treated fibres.

For the acetylated fibre specimens, a trend of a slight decrease in peak strength and increase in post-peak strength can be observed in Figure 5.31. The specimens containing fibre pretreated with 6% NaOH followed by 5% and 10% Acetic Anhydride respectively, had the highest post-peak strength, also higher than the untreated fibre specimens. The strength is however not higher than the specimens containing 2% NaOH treated fibre. The post-peak strength of the 10% Acetic Anhydride specimens is lower than expected and falls outside the linear trend. A high variability was noted in the peak strength. This can be due to the sensitivity of the specimens.
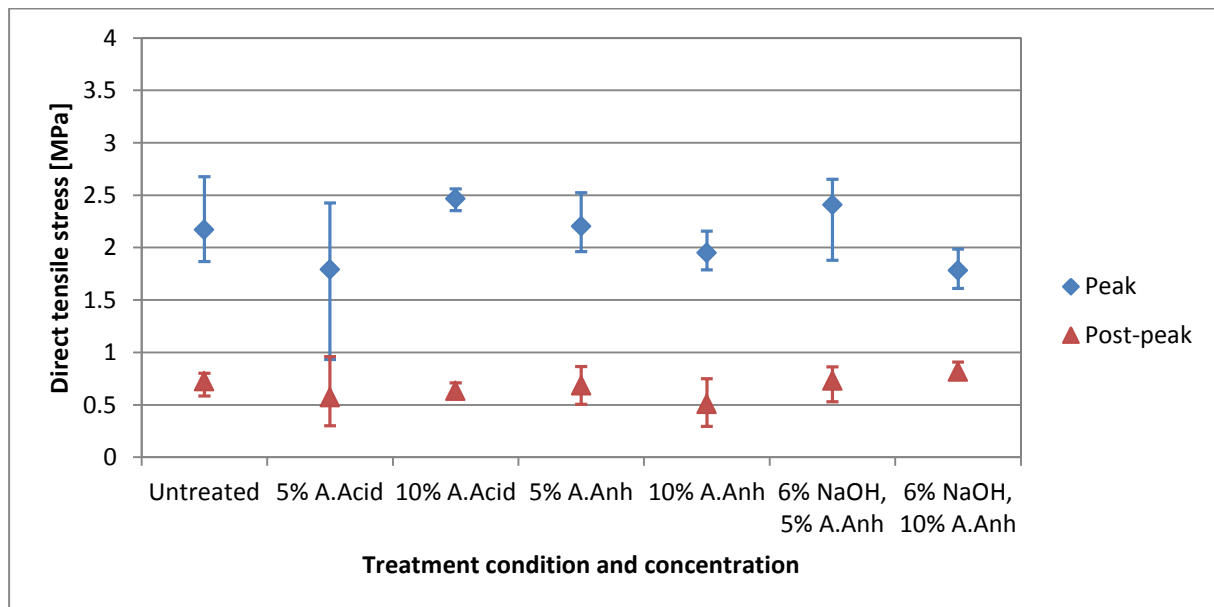
Figure 5.31: Average peak and post-peak tensile strength for matrix C1-1-20 with untreated and acetylated fibres.

In Figure 5.32, the post-peak tensile strength of the matrices C2 to C6 is lower than for matrix C1. This indicates that the bond strength between the fibre and matrix decreased with the use of supplementary cementitious materials. The matrices C2, C4 and C5, where a fraction of the OPC was replaced by FA, had very low peak strength and also the lowest post-peak strength. This was also seen in the three-point bending tests. Matrix C3 had just slightly lower peak strength than matrix C1. The peak stress of matrix C5 was very low. The matrix had very low strength and no definite peak could be observed from the graphs. The peak and post-peak strength is similar for this matrix. Matrix C6 had the highest peak strength of all the matrices and also the highest post-peak strength of all the alternative matrices C2 to C6. This indicates that the replacement of sand with FA leads to improved compaction and fibre-matrix bond, but it is also possible that a fraction of the FA reacted as binder, leading to higher strength.
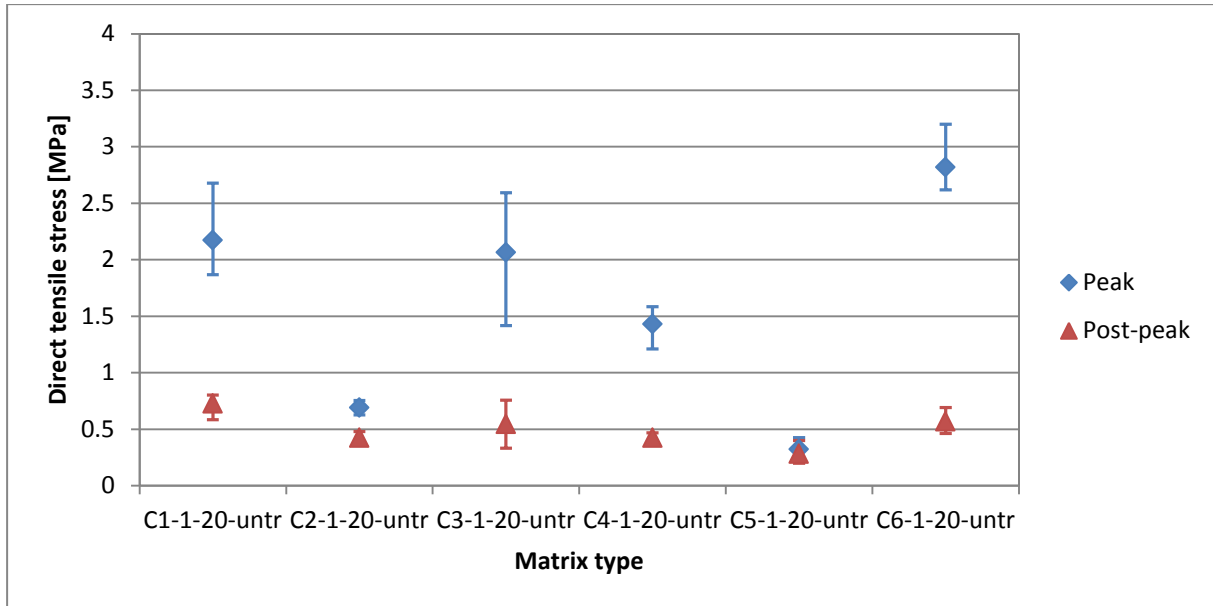
Figure 5.32: Average peak and post-peak tensile strength for matrices C1 to C6 with 1%, 20 mm untreated fibres.

In Figure 5.33, the peak and post-peak strength for the matrix with 30 mm fibre is lower than for the matrix with 20 mm fibre. A longer fibre length at the same fibre volume leads to less individual fibres present in the matrix to bridge the crack and carry the load. It is also a possibility that at 30 mm some of the fibres fractured, leading to lower post-peak strength. The peak stress of matrix C1-1-30 is very low. This can also be seen in the compression and three-point bending test results. The results indicate that at a fibre volume of 1.0%, 20 mm is a much more effective length.
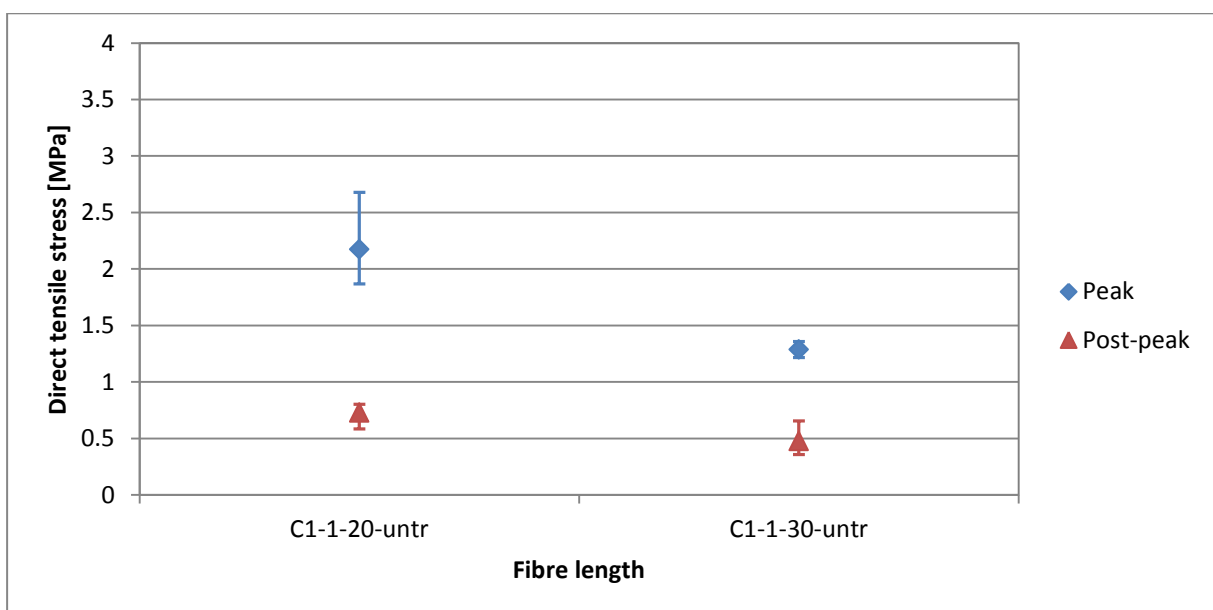
Figure 5.33: Average peak and post-peak strength for OPC matrix with fibre lengths of 20 mm and 30 mm.

88

5.2.2. 90 Day water cured aged specimens

The results of the average post-peak tensile strength at 90 days for the specimens subjected to ageing in water are presented in Figure 5.34 to Figure 5.37.

For the alkali treated fibre specimens the trend is similar at both 28 days and 90 days of water curing. The trend was also similar for the alkali treated fibre specimens tested in three-point bending. Of the alkali treated specimens, the specimens with 6% NaOH fibre had the lowest decrease in strength, while specimens with 30% NaOH had the highest decrease. All the alkali treated fibre specimens had a lower decrease than the specimen containing untreated fibre. The 2% NaOH specimens had the highest strength among the alkali treated fibre specimens at 90 days after ageing in water, while the 20% NaOH specimens had the lowest strength.

For the acetylated fibre specimens presented in Figure 5.35, 5% and 10% Acetic Acid had the smallest decrease in strength. The specimens with 5% Acetic Anhydride had the largest decrease in strength, while 10% Acetic Anhydride had increased strength. The 28 day strength of the 10% Acetic Anhydride specimens is however much lower than expected. The specimens with 6% NaOH-5% Acetic Anhydride and 6% NaOH-10% Acetic Anhydride had a similar decrease in strength. The 6% NaOH-10% Acetic Anhydride had the highest post-peak strength of all the specimens, also when compared to the alkali treated fibre specimens.
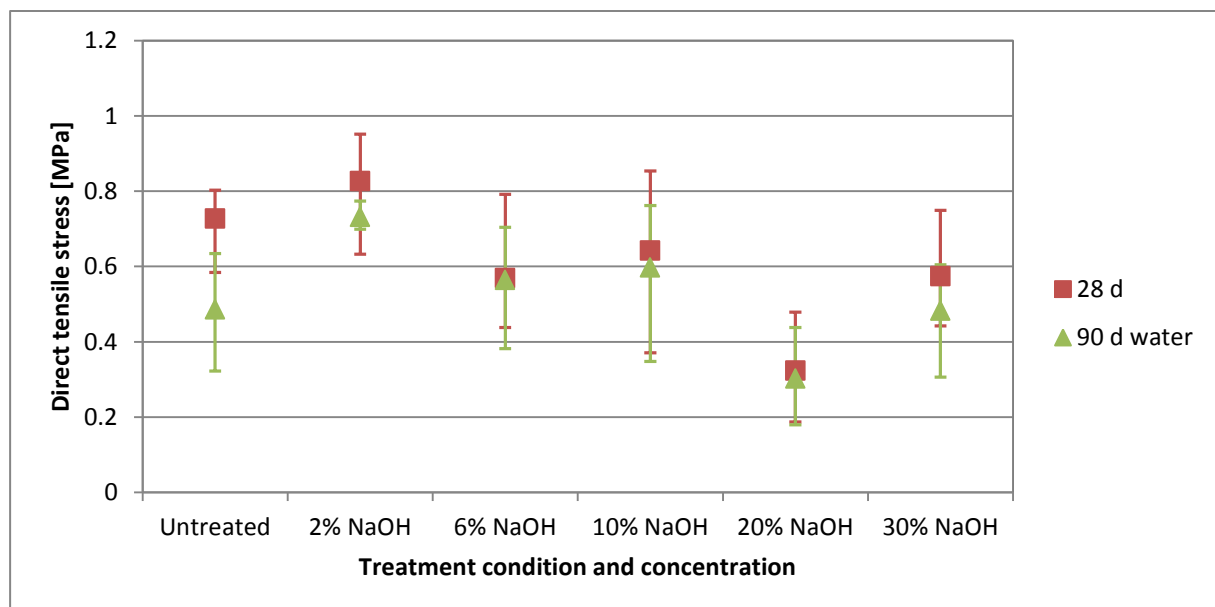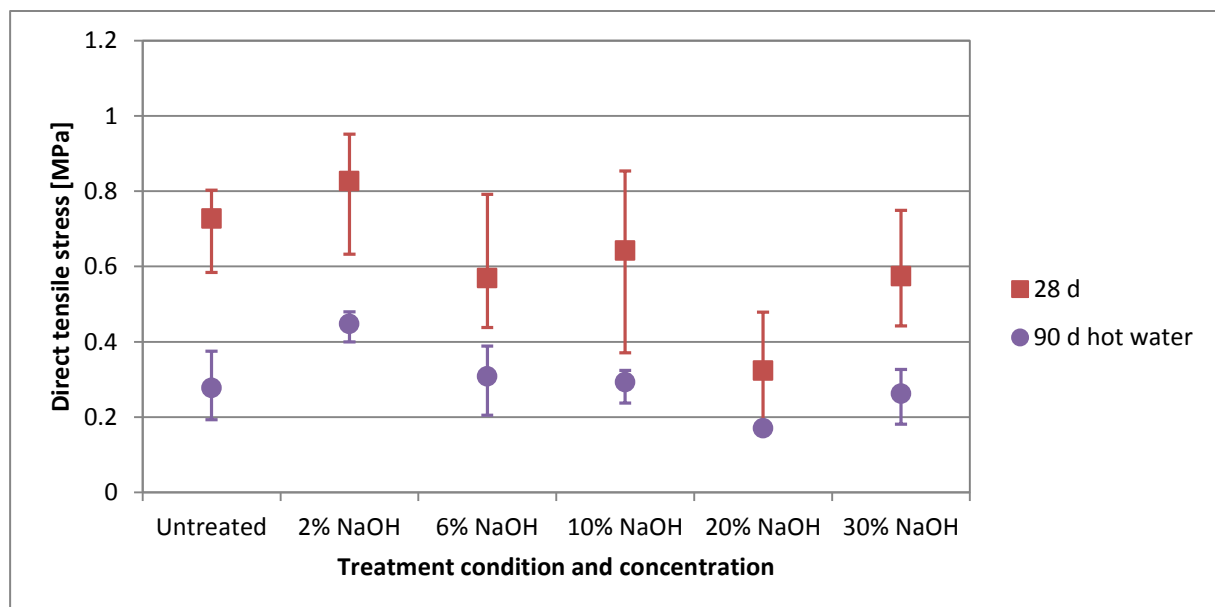

Figure 5.34: Average post-peak tensile strength for matrix C1-1-20 with untreated and alkali treated fibres subjected to ageing in water.
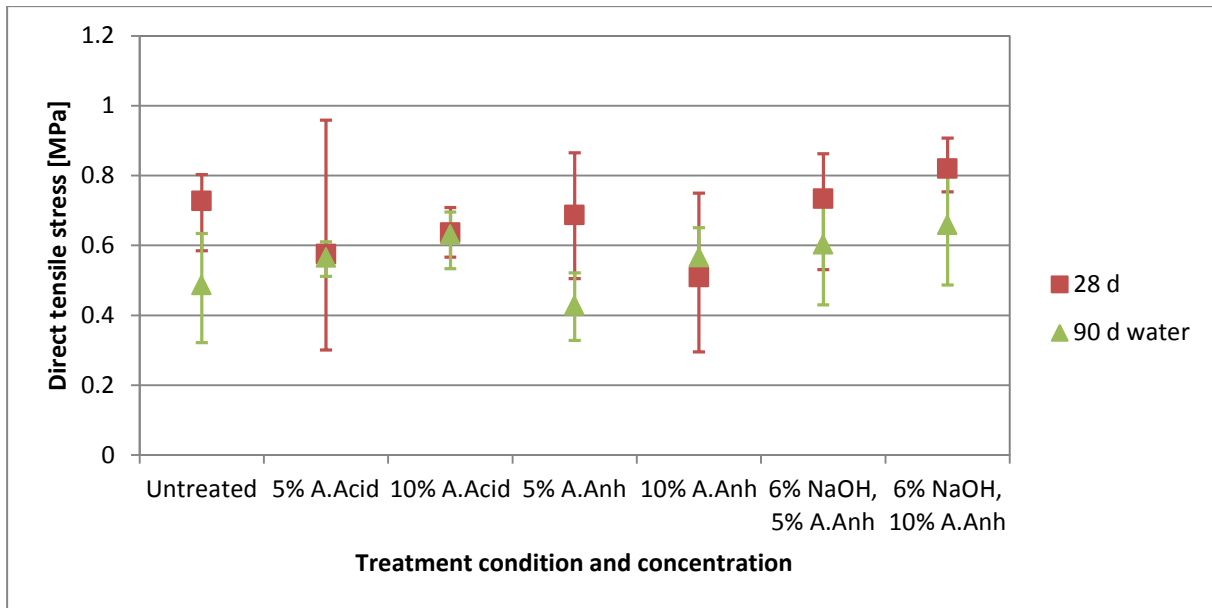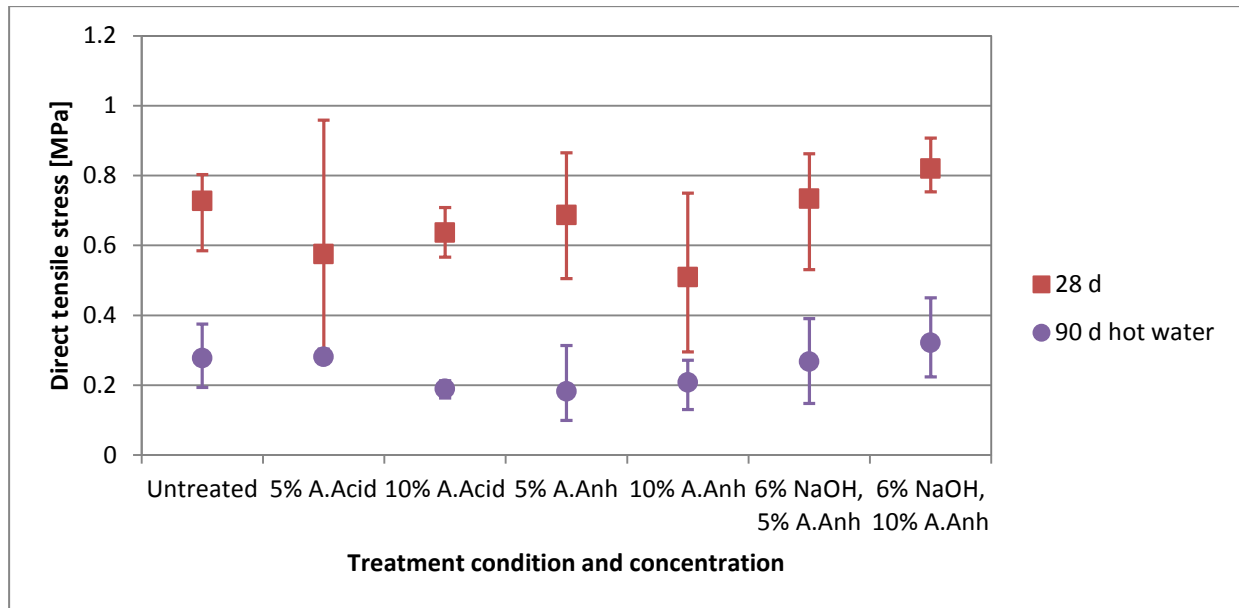
Figure 5.35: Average post-peak tensile strength for matrix C1-1-20 with untreated and acetylated fibres subjected to ageing in water.

For the different matrices C2 to C6 with untreated fibres, presented in Figure 5.36, the degradation was less severe than for matrix C1. The results do not agree with the results from the three-point bending tests under the same conditions. Matrices C5 and C6, which contained 40% FA as filler, were the only matrices that had increased strength after ageing. Matrix C5, which contained FA as supplementary cementitious material, had the largest increase in strength, while matrix C6, which contained 10% CSF as supplementary cementitious material, had less of an increase. Matrix C6 had the highest strength of all the untreated fibre specimens after ageing. When comparing matrices C3, C4 and C6 which contained the same amount of CSF but different amounts of FA, matrix C6 had increased strength, while matrix C4 had the lowest decrease in strength and matrix C3 which contained no FA had the largest decrease in strength. This is attributed to the FA. It was expected that matrix C2 would also have increased strength as was the case with the three-point bending tests.

For matrix C1 with 20 mm and 30 mm fibre respectively, the specimens with the 20 mm fibre had higher post-peak strength than the specimens with 30 mm fibre at both ages as can be seen from Figure 5.37. The trend is similar for both 28 and 90 days. The decrease in strength was however lower for the specimens with 30 mm fibre.
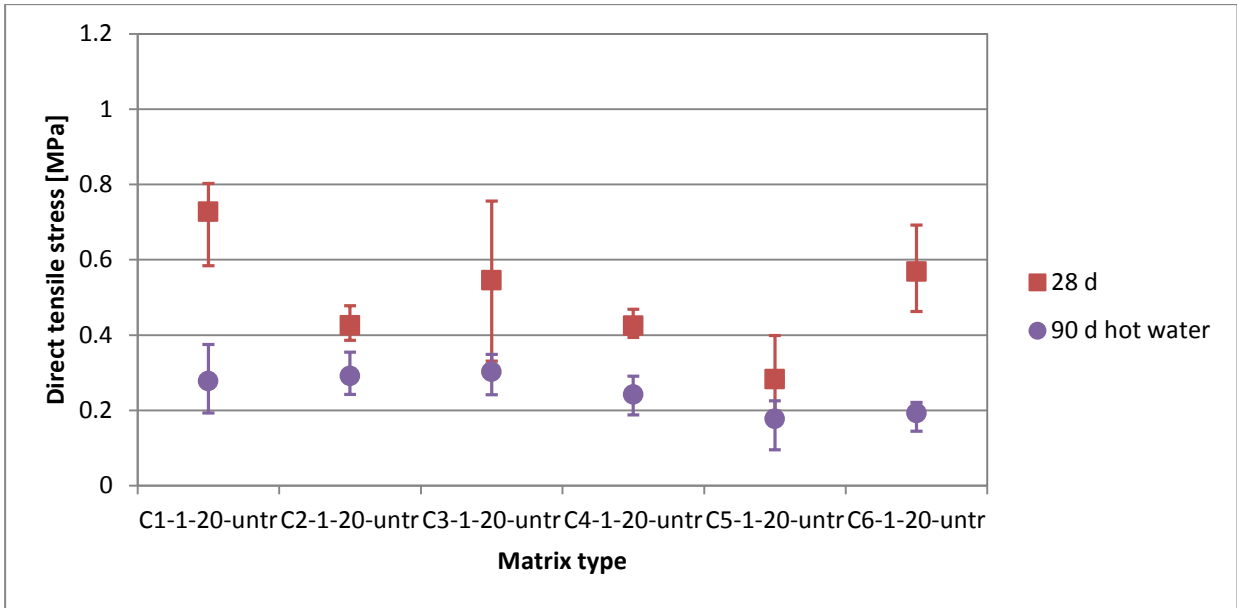
90
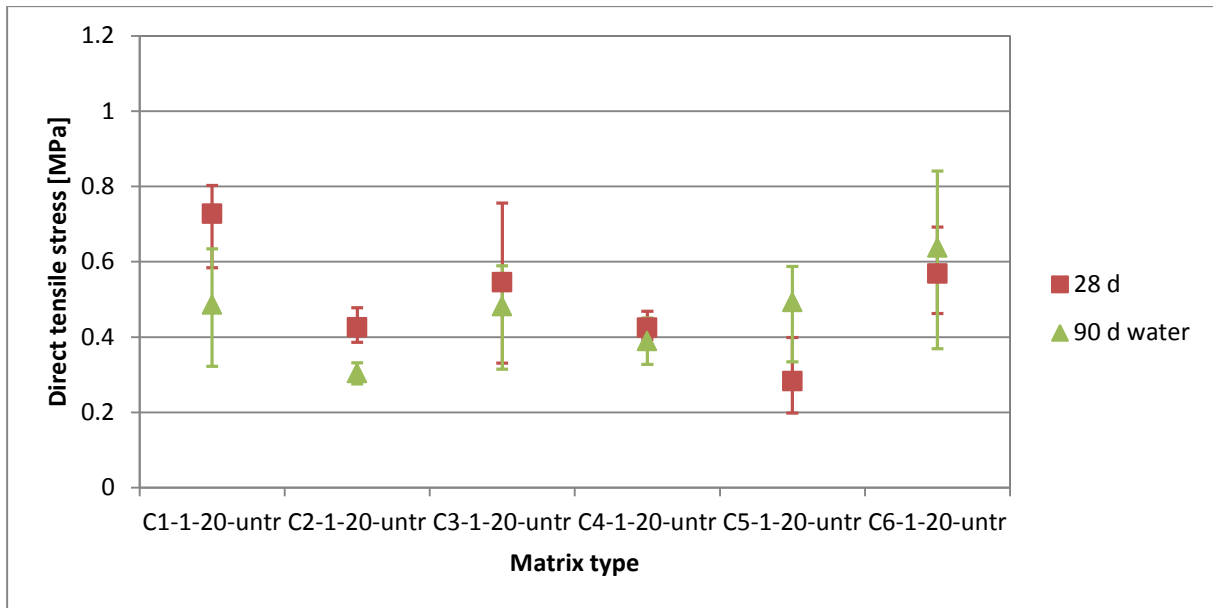
Figure 5.36: Average post-peak tensile strength for matrices C1 to C6 with 1%, 20 mm untreated fibres, subjected to ageing in water.
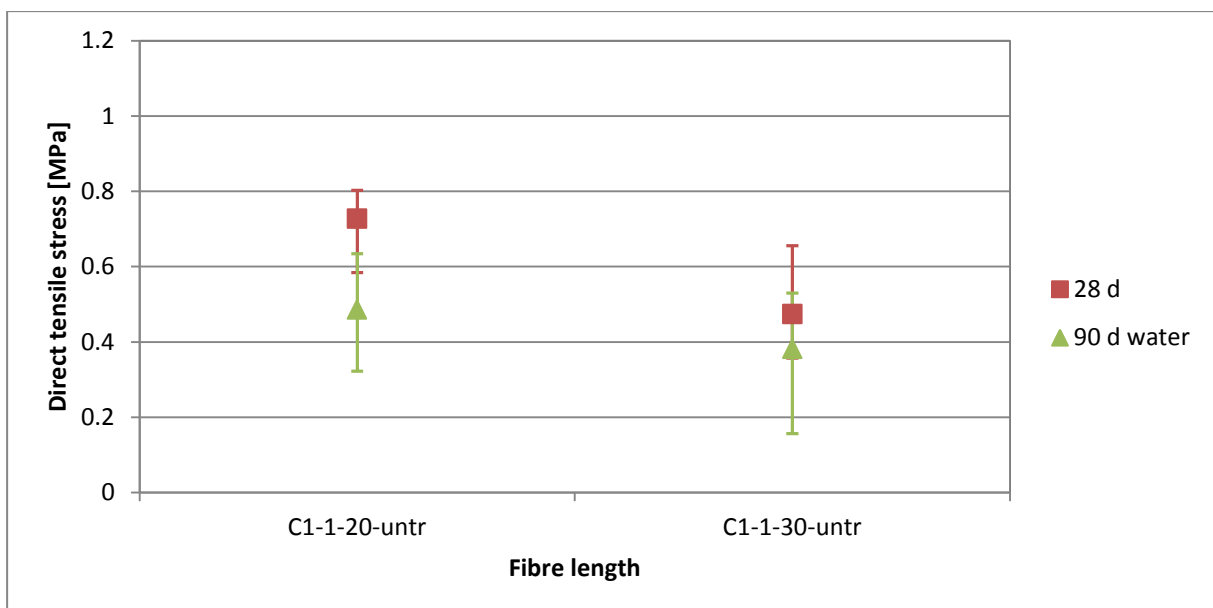
Figure 5.37: Average post-peak strength for OPC matrix with fibre lengths of 20 mm and 30 mm, subjected to ageing in water.

Overall, matrix C1 with 6% NaOH-10% Acetic Anhydride treated fibre had the highest strength after ageing. Matrix C1 with 20% NaOH treated fibre had the lowest strength after ageing. Matrix C1 with 5% Acetic Anhydride treated fibres had the largest decrease in strength while matrix C5 with untreated fibre had the highest increase in strength.

5.2.3. 90 Day hot water accelerated aged specimens

The results of the average post-peak tensile strength at 90 days for the specimens subjected to ageing in lime saturated hot water are presented in Figure 5.38 to Figure 5.41. From the error bars it can be seen that the results for the specimens subjected to hot water ageing are much less variable. The average post-peak strength was significantly lower for the hot water aged specimens than the 28 day water cured specimens.

In Figure 5.38 a similar trend can be seen as for the ageing in water. The specimens with 10% NaOH treated fibre had the largest decrease in strength, while 2% NaOH had the lowest decrease. The 2% NaOH specimens had the highest strength after ageing while the 20% NaOH specimens had the lowest strength after ageing. Only the specimens with 20% and 30% NaOH treated fibre had lower strength than the untreated fibre specimens after ageing. The decrease in strength for all the specimens was however lower than for the untreated fibre specimens.

From Figure 5.39 it follows that the specimens with 5% Acetic Acid treated fibres had the lowest decrease in strength, while the specimens with 5% Acetic Anhydride treated fibres had the highest decrease in strength. Only the 5% Acetic Acid and 6%NaOH-10% Acetic Anhydride treated fibre specimens had higher strength than the untreated fibre specimen. The 6%NaOH, 10% Acetic Anhydride specimens had the highest strength.

Figure 5.38: Average post-peak tensile strength for matrix C1-1-20 with untreated and alkali treated fibres subjected to ageing in hot water.

Figure 5.39: Average post-peak tensile strength for matrix C1-1-20 with untreated and acetylated fibres subjected to ageing in hot water.

In Figure 5.40, matrix C2 had the lowest decrease in strength after ageing in hot water, followed by matrix C5. Matrix C6 had the largest decrease in strength. Matrix C3 had the highest strength after ageing, followed by matrix C2 and C1. A similar phenomenon can be seen as for the ageing in water. The specimens containing FA as supplementary cementitious material had less of a decrease in strength than the specimens containing CSF or than matrix C1. When comparing matrices C2 and C5, which both contained 30% FA as supplementary cementitious material, matrix C5 which also contained FA as filler had a larger decrease in strength. This is also the case with matrix C3 and C6. In matrix C4, which also contained 20% FA in addition to the 10% CSF as in matrix C3, the decrease in strength was slightly lower than for matrix C3. This indicates that the fibre-matrix bond improves over time as the FA continues to react with the $Ca(OH)_2$ produced by the hydration of cement.

For Matrix C1 with fibre different fibre lengths of 20 mm and 30 mm, shown in Figure 5.41, the trend is similar as for ageing in water. The matrix with 30 mm fibre had a smaller decrease in strength, but the matrix with 20 mm fibre still had higher strength.

Overall, matrix C1 with 2% NaOH treated fibres had the highest average post-peak tensile strength after ageing in hot water, while the matrix with 20% NaOH treated fibre had the lowest strength. Specimens with 6% NaOH-10% Acetic Anhydride fibre had the second highest post-peak tensile strength. Matrix C2 with untreated fibre had the lowest decrease in strength while matrix C1 with 5% Acetic Anhydride treated fibre had the largest decrease.

93

Figure 5.40: Average post-peak tensile strength for matrices C1 to C6 with 1%, 20 mm untreated fibres, subjected to ageing in hot water.
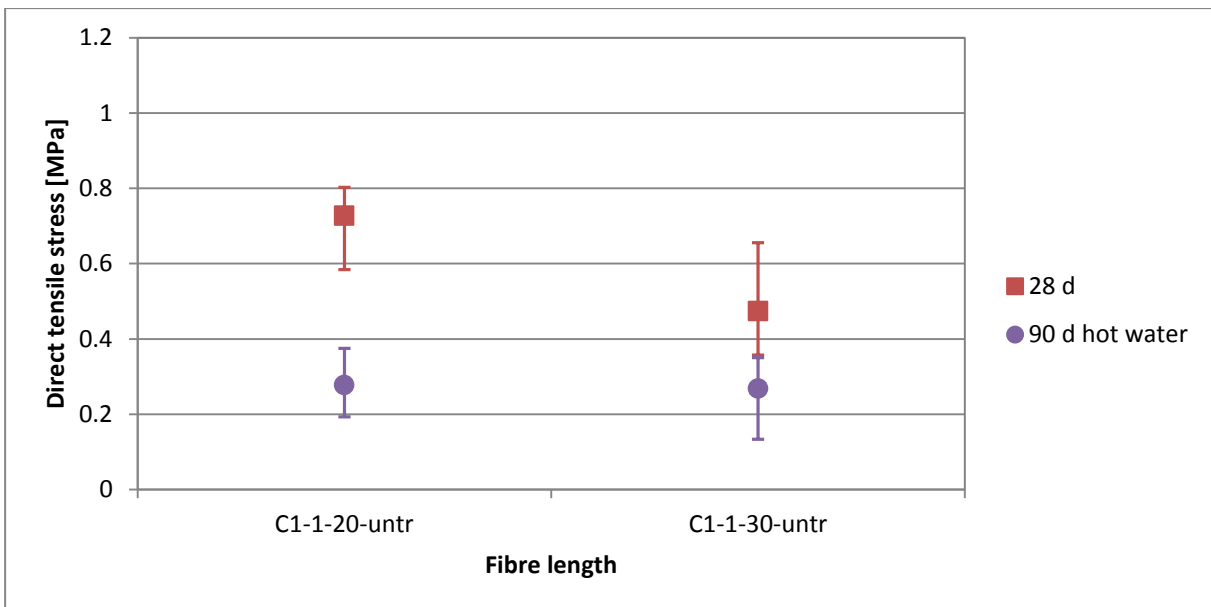
Figure 5.41: Average post-peak strength for OPC matrix with fibre lengths of 20 mm and 30 mm, subjected to ageing in hot water.

CHAPTER 6

Discussion of results

6.1. Influence of fibres on matrix strength

From the 28-day compression test results it was evident that the compressive strength decreased as the fibre volume increased. Similar results were also found by Coetzee (2013). The addition of fibres has an adverse effect on the compaction of the mortar and the density decreased, leading to lower compressive strengths. The low compressive strength of the matrix with 30 mm fibres was possibly due to retarded hydration in the first two days after casting. When the specimens were demoulded and placed in water for curing, water entering the matrix increased the water/binder ratio, leading to a lower strength.

From the three-point bending tests and direct tensile tests, it can also be seen that the peak strength (at first crack) decreased with an increase in fibre volume. As the fibre length increased, the peak flexural strength of the matrix also decreased. The strength is similar for a fibre length of 10 mm and 20 mm at a volume of 1%, but at a length of 30 mm the strength decreased considerably. This was also the case in the compression tests. At a fibre volume of 1%, the post-peak strength was the highest for a fibre length of 20 mm. The post-peak strength was slightly lower for a fibre length of 30 mm, but the lowest at a length of 10 mm. The 10 mm fibres had low bond strength between the fibre and matrix due to a shorter length, while the matrix with the 30 mm fibre had low bond strength due to the poor compaction and low strength of the matrix. The matrix with 20 mm fibre had the best combination of compaction and embedment depth to carry and transfer loads from the mortar to the fibre.

6.2. Chemical treatment

6.2.1. Fibre properties

From the single fibre pull-out (SFP) tests it followed that at low concentrations of NaOH the fibre strength increased, but at higher concentrations the fibre strength decreased. At NaOH concentrations of 2%, 6% and 10%, the fibres had higher average pull-out strength than for the untreated fibre and at NaOH concentrations of 2% and 6% the strength of the fibres at fracture also increased. The fibre-matrix bond was also improved through alkali treatment. Although the strength of the fibres was higher, they fractured at a shorter embedment depth than the untreated fibre. The bond was improved through the removal of fats, waxes and mineral matter from the fibre surface. This was confirmed by the Scanning Electron Microscope (SEM) images.

At concentrations of 20% and 30% NaOH the average pull-out- as well as fracture force was lower than the untreated fibre. In Figure 4.5, damage to the wall of a fibre treated with 20% NaOH is encircled. The damage and strength loss confirmed the phenomenon of delignification which is known to take place at high alkalinity. The fibre structure and morphology is modified by the NaOH. At higher concentrations too much of the hemi-cellulose and lignin is removed, which results in a loss of strength and rigidity of the fibre. The physical appearance of the fibres also changed from being more rigid and stiff to being softer. The fibres treated with higher concentrations of NaOH also tend to clog more during mixing.

The fibres pre-treated with 6% NaOH and then with 5% and 10% Acetic Anhydride respectively had the highest strength of all the acetylated fibres. The strength was also higher than for the untreated fibre, but it was lower than the 2% and 6% NaOH treated fibres. Pre-treatment with NaOH was more effective in removing surface impurities. This is confirmed by the higher average pull-out force of the 6% NaOH-5% Acetic Anhydride compared to the 5% Acetic Anhydride and also of the 6% NaOH-10% Acetic Anhydride compared to the 10% Acetic Anhydride. Acetic Anhydride did improve the fibre-matrix bond.

The fibres treated with Acetic Acid and Acetic Anhydride (without pre-treatment) had reduced strength when compared to the untreated fibres. The fibres treated with 5% and 10% Acetic Acid pulled out at 15 mm for both concentrations, while the other acetylated fibres mostly fractured at 15 mm. The pull-out force at 15 mm was however low, indicating that the fibre-matrix bond was relatively weak. In the SEM images of the fibres treated by acetylation, it was clear that the acetic acid treatment did not remove the impurities from the fibre surface. The fibres pre-treated with NaOH however had a cleaner surface.

From the SFP results, it is however evident that change in the fibre structure took place during acetylation as the strength of all the fibres reduced in all cases. The fibres only treated with acetic acid or acetic anhydride had lower strength than the untreated fibre, while the fibres pre-treated with 6% NaOH and then with acetic anhydride had lower strength than the fibres only treated with 6% NaOH.

6.2.2. Durability

The durability of sisal fibre reinforced cement-based composites (SFRCC) was evaluated by comparing the average post-peak strength of the specimens subjected to ageing to the 28 day post-peak strength. It was found that the post-peak strength was lower for almost all of the specimens except for a few exceptions.

Ageing in lime saturated hot water was the most severe ageing condition and the results also indicated less variability than the other ageing methods. After ageing in lime saturated hot water the specimens with fibre treated at low concentrations of 2%, 6% and 10% NaOH had a higher average post-peak strength than the untreated fibre specimens in both the three-point bending and direct tensile tests. The specimens with fibre treated with 20% and 30% NaOH had higher strength than the untreated fibre specimens in the three-point bending tests, but lower strength in the direct tensile tests. At concentrations of 2% and 10% NaOH, the post-peak strength was higher than for the untreated fibre specimens at all ages under all ageing conditions. Higher concentrations of 20% and 30% NaOH were detrimental to the fibre strength as indicated by the post-peak strength at 28 days and 90 days for almost all ageing conditions.

For the acetylated fibre specimens, the majority also showed less of a decrease in average post-peak strength compared to the untreated fibre specimens. After ageing in lime saturated hot water, all the specimens, except for the 5% Acetic Acid, subjected to three-point bending tests had a higher average post-peak strength than the untreated fibre specimens. For the specimens subjected to direct tensile tests, only the 5% Acetic Acid and 6% NaOH-10% Acetic Anhydride had a strength equal to or higher than the untreated fibre specimens after ageing in lime saturated hot water. For the specimens tested in three-point bending, the specimens with fibre treated with 10% Acetic Anhydride had the highest strength followed by 6%NaOH-10% Acetic Anhydride. For the specimens tested in direct tension, 6% NaOH-10% Acetic Anhydride had the highest strength after ageing in lime saturated hot water.

The combination of alkali treatment and acetylation proved to be the best treatment condition. At 28 days, for matrix C1, the highest strength was recorded for specimens where

97

a combination of the treatments was used. At 90 days strengths in excess of that of the untreated fibre specimens were achieved for all ageing conditions.

6.3. Supplementary cementitious materials

An interesting trend was noted in the matrices where a fraction of the ordinary Portland cement (OPC) was replaced by supplementary cementitious materials. When 10% of the OPC was replaced with condensed silica fume (CSF) the strength was higher than for the OPC matrix at 28 days, but when 30% of the OPC was replaced with fly ash (FA) the strength was considerably lower than expected. The addition of FA delays strength development as it only starts reacting once the hydration of cement produces $Ca(OH)_2$. The low strength can also be due to retarded hydration in the first two days after casting. When the specimens were demoulded and put in water for curing, water entering the matrix increased the water/binder ratio, leading to a lower strength. In the specimens where 40% of the sand was replaced with FA, the strength was higher than for the corresponding specimens in which none of the sand was replaced with FA. This indicates that although the FA was added as binder, a fraction of it might have reacted as binder. In the specimens where a portion of the OPC was replaced by a combination of FA and CSF, the strength was still lower than for the OPC matrix and the 10% CSF matrix, but higher than for the 30% FA matrix.

In the cast matrices where FA was used to replace 30% of the OPC, an increase in post-peak strength was recorded under all ageing conditions for the specimens tested in three-point bending. All the matrices containing CSF or a combination of CSF and FA had decreased strength after ageing with respect to the 28 day post-peak strength. Matrices C3 and C6, where 10% of the OPC was replaced with CSF, as well as 40% of the sand replaced with FA in matrix C6, had the highest decreases in strength. Matrix C4, containing a combination of FA and CSF had less of a decrease, but the lowest strength under all conditions after ageing. All the matrices, except C4 (under water and wet/dry cycle ageing) and C5 (under water ageing), had higher post-peak strength than the control matrix C1 after ageing under all conditions.

6.4. Cast versus Extrusion

At an age of 28 days, the extruded matrices had higher peak strength than their corresponding cast matrices. Matrices E1 and C5 were the same matrix and matrices E2 and C6 were the same matrix. After ageing, matrix E1 only had higher peak strength than matrix

C5 under normal water ageing. After lime saturated hot water ageing and wet/dry cycles, matrix C5 had a higher peak strength. Matrix E2 had lower peak strength than matrix C6 under all ageing conditions. Matrix E1 had lower strength than matrix C1 at all ages and curing conditions, except for 90 days of ageing in hot water. Matrix E2 had a higher strength than matrix C1 at all ages and curing conditions.

The same phenomenon as for the cast matrices containing FA and CSF was also true for the extruded matrices. Matrix E1, where 30% of the OPC was replaced with FA, had increased post-peak strength under all ageing conditions. The post-peak strength was also similar for the corresponding cast matrix C5, except for the specimens subjected to wet/dry cycle ageing, for which the cast specimen had higher strength. Matrix E2, where 10% of the OPC was replaced with CSF, had decreased strength under all ageing conditions, but still had the highest post-peak strength for the extruded matrices under all conditions. The post-peak strength of matrices E2 and C6 was similar after ageing in hot water, but under the other ageing conditions matrix E2 had a higher strength. Although matrix E3, where 20% and 10% of the OPC was replaced with FA and CSF respectively, was only subjected to ageing in water, an increase in peak and post-peak strength was recorded after ageing. At 28 days, matrix E3 had a higher peak and post-peak strength than matrix E1, but lower than matrix E2. After ageing, matrix E3 had higher post-peak strength than matrix E1 but lower post-peak strength than matrix E2. It also had the lowest peak strength after ageing.

.

CHAPTER 7

Conclusions and Recommendations

7.1. Conclusions

The main objective of this investigation was to determine the properties and evaluate the durability of sisal fibre reinforced cement-based composites (SFRCC). The use of chemical treatment to improve the fibre-matrix bond and durability, as well as the use of supplementary cementitious materials to improve durability was investigated. Casting and extrusion were also compared as two different manufacturing processes. The following conclusions can be made from experimental work performed in this research project:

7.1.1. Fibre volume and length

- The addition of sisal fibre to a cement-based matrix reduces the compressive strength of the matrix considerably.
- As the fibre volume increases, the compressive strength and peak flexural strength decrease.
- At the same fibre volume, the compressive strength for matrices with 20 mm fibre was higher than for 10 mm fibre. At a fibre length of 30 mm the strength was considerably lower.
- The process of adding the fibres to the matrix during mixing is time consuming. If the fibres are not separated properly by hand and added slowly enough, the fibres tend to clog and fibre balls form within the mix. As the fibre length increases, the clogging becomes worse.

7.1.2. Chemical treatment

- Chemical treatment of sisal fibre improved the fibre-matrix interaction in a cement-based matrix.

- From the single fibre pull-out (SFP) tests it was evident that at low concentrations of 2%, 6% and 10% NaOH the fibre strength increased and the fibre-matrix bond was improved. Higher concentrations of 20% and 30% NaOH caused damage to the fibre structure.

- Acetylation of sisal fibre with Acetic Acid and Acetic Anhydride at concentrations of 5% and 10% damaged the fibre and the strength decreased considerably. However, when it was pre-treated with NaOH, the strength was slightly higher than for the untreated fibre.

- From the SEM analysis it was evident that the fibre surface became cleaner and smoother with an increase in NaOH concentration, but at higher concentrations fibre damage was visible.

- Chemical treatment also improved the post-peak strength of the specimens in the majority of the specimens under all ageing conditions. At low concentrations of NaOH, the post-peak strength of the specimens was improved, but at higher concentrations the strength decreased. Similar results were found in a study by Kabir et al., (2012). Mwaikambo & Ansell (1999) also found that there are optimum concentrations of NaOH at which the best results are found. In this study, 2%, 6% and 10% NaOH were found to be the optimum concentrations under which the best results were found in terms of post-peak strength.

- The use of Acetic Acid and Acetic Anhydride to treat fibres proved to be less effective in improving the durability of SFRCC. The combination of NaOH and Acetic Anhydride treatment however proved to be more effective. A significant decrease in strength was recorded for these specimens after ageing in hot water, which is ascribed to the pre-treatment with NaOH. However, under wet/dry cycle ageing, the specimens with acetylated fibres were more durable. Mwaikambo & Ansell (1999) stated that the dimensional stability of sisal fibre is improved through acetylation. Thus, under wet/dry cycle ageing, the acetylated fibres were more stable than the alkali treated fibres, leading to the increased durability.

7.1.3. Supplementary cementitious materials

- The use of FA as supplementary cementitious material led to remarkably low strength at an early age of 28 days, while the use of CSF led to higher strength. After ageing, all specimens containing FA, whether cast or extruded, had increased peak and post-peak strength, while specimens containing CSF or a combination of CSF and FA had decreased strength.

- The use of supplementary cementitious materials does improve the durability of SFRCC, but the optimum combination between FA and CSF needs to be found. The highest strength was recorded for matrix C6 where CSF was used as binder and FA was used as fine filler. The inclusion of FA leads to a denser matrix which resulted in a better fibre-matrix bond. It is also possible that a fraction of the FA reacted with $Ca(OH)_2$, leading to an increase in strength The highest percentage decreases in strength was however recorded for these matrices.

- The matrices which contained 10% CSF as binder and 40% FA as fine filler had the highest strength after ageing in hot water. Ageing in hot water was the most aggressive ageing environment.

7.2. Recommendations

Useful results and information regarding SFRCC were obtained from this investigation. More investigation on SFRCC is however required to be able to improve the durability. The results from the tests were quite variable in some cases. Some questions regarding the rate of degradation and the time allowed for degradation still exists. The effectiveness of chemical treatment of fibres and the use of alternative matrices on the durability of SSFRC after periods extending 90 days are also uncertain. The following recommendations can be made with regards to the experimental work:

- When working with such sensitive materials and specimens, strict quality control methods should be in place. Although the laboratory environment is controlled, some factors such as the temperature under which the specimens were allowed to set before demoulding and curing in water have to be considered.

- More samples can be tested per series to improve the reliability of the results.

- The fibre diameter should be measured to improve the results of the SFP tests. The pull-out and fracture can be presented as interfacial shear- and tensile stresses, respectively. Better comparisons can then be made between the different fibre treatments and embedment depths.

- Ageing in lime saturated hot water is very effective in terms of degrading the specimens. Ageing by wet/dry cycles is also effective in terms of evaluating the stability of the fibre in the matrix during ageing. These ageing methods are recommended for future studies. It is also recommended that specimens subjected to ageing in lime saturated hot water be tested in more regular intervals as described in ASTM C1560-03 (2009) to determine whether and when the degradation stabilises.

Both chemical treatment of fibres and the use of supplementary cementitious materials improved the durability of SFRCC at an age of 90 days after being subjected to different ageing environments. The following recommendations can be made with regards to chemical treatment and supplementary cementitious materials:

- The combination of alkali treatment and acetylation can be studied in more detail, meaning a broader range of concentrations, to determine the most effective combination.
- The combination of chemical treatment and supplementary cementitious materials can be investigated. This might have the best results in terms of durability. More combinations of FA and CSF can also be tested. At high volumes of FA, the mix tends to become very sticky. This should be avoided as it is not practically workable.

The following recommendations can be made with regards to the specimen production:

- The extrusion process is challenging and time consuming. The results did not differ significantly from the cast specimens. More time can be spent to manufacture different sets of cast specimens than on extrusion.
- The "dogbone" moulds should not be used for specimens with a high water/binder ratio. The specimens are very sensitive and tend to break while inserting them in the clamps before the test. At lower water/binder ratios this should however not be a problem.

References

Agopyan, V., Savastano Jr, H., John, V. & Cincotto, M., 2005. Development on vegetable fibre-cement based materials in Sao Paulo, Brazil: an overview. *Cement and Concrete Composites*, 27, pp.527-36.

Aldea, C., Marikunte, S. & Shah, S., 1998. *Extruded Fiber Reinforced Cement Pressure Pipe*. Illinois: Elsevier Science Ltd. National Science Foundation for Science and Technology of Advanced Cement-Based Materials.

Anderson, J. & Bausch, C., 2006. *Climate Change and Natural Disasters: Scientific evidence of a possible relation between recent natural disasters and climate change*. Brussels: European Parliament.

Ash Resources, 2011. *Ash Resources Fly ash products*. [Online] Available at: www.ash.co.za/upload/file/DuraPozz.pdf [Accessed 23 January 2014].

ASTM International, 2007. *Standard Test Method for Flow of Hydraulic Cement Mortar*. Pennsylvania: ASTM International.

ASTM International, 2009. *Standard Test Method for Hot Water Accelerated Aging of Glass-Fiber Reinforced Cement-Based Composites*. Pennsylvania: ASTM International.

Awwad, E. et al., 2012. *Studies on fiber-reinforced concrete using industrial hemp fibers*. Elsevier Ltd.

Bentur, A. & Mindess, S., 2007. *Fibre Reinforced Cementitious Composites*. 2nd ed. New York: Taylor and Francis.

Boshoff, W., 2007. *Time-Dependant Behaviour of Engineered Cement-Based Composites*. PhD Thesis. University of Stellenbosch.

Boshoff, W., 2010. *Development of a cement-based mix for the press forming of window frames*. Institution of Structural Engineering.

Boshoff, W., 2013. *Personal discussion: Mix design for extruded concrete*.

Coetzee, G., 2013. *The mechanical and volumetric behaviour of sisal fibre reinforced concrete blocks*. MEng Thesis. Stellenbosch University.

Cooke, T., 2002. *Formation of Films on Hatschek Machines*. Building Materials and Technology Pty Ltd.

De Koker, D., 2004. *Manufacturing Processes for Engineered Cement-Based Composite Material Products*. MSc Thesis. Stellenbosch: Stellenbosch University.

Elsaid, A., Dawood, M. & Seracino, R.B.C., 2011. *Mechanical properties of kenaf fiber reinforced concrete*. Elsevier Ltd.

FerroAtlantica Group, S.A., 2007. [Online] Available at: http://www.ferroatlantica.es/index.php/en/productos-ss/silica-fume [Accessed 23 January 2014].

Goodier, R., 2013. *Engineering for Change*. [Online] Available at: https://www.engineeringforchange.org/news/2013/01/04/alex_odundos_sisal_twine_manufacturing_machines.html [Accessed 15 January 2014].

Hill, R. & Bowen, P., 1996. *Sustainable construction: principles and a framework for attainment*. Construction Management and Economics.

Kabir, M., Wang, H., Lau, K. & Cardona, F., 2012. *Chemical treatments on plant-based natural fibre reinforced polymer composites: An overview*. Elsevier.

Kalia, S., Kaith, B. & Kaur, I., 2009. *Pretreatments of Natural Fibers and their Application as Reinforcing Material in Polymer Composite - A Review*. Wiley InterScience.

Kicinska-Jakubowska, A., Bogacz, E. & Zimniewska, M., 2012. *Review of Natural Fibers*. Poznan: Institute of Natural Fibres.

Kirby, R., 1963. *Vegetable Fires: Botany, Cultivation and Utilization*. 1st ed. New York: Interscience Publishers Inc.

Le Troëdec, M., Peyratout, C., Smith, A. & Chotard, T., 2009. *Influence of various chemical treatments on the interactions between hemp fibres and a lime matrix*. ScienceDirect.

Li, X., Tabil, L. & Panigraphi, S., 2007. Chemical Treatments of Natural Fiber for Use in Natural Fiber-Reinforced Composites: A Review. *J Polym Environ*, 15, pp.25-33.

Martins, M., Kiyohara, P. & Joekes, I., 2004. *Scanning Electron Microscopy Study of Raw and Chemically Modified Sisal Fibers*. Brazil: Wiley InterScience.

Mater, J., 1998. *Application of extrusion for manufacture of short fiber reinforced cementitious composite*. Journal of Materials in Civil Engineering.

Mehta, P. & Gjorv, O., 1982. *Properties of portland cement concrete containing fly ash and condensed silica-fume*. Pergamon Press Ltd.

Mohan, T. & Kanny, K., 2012. *Chemical treatment of sisal fiber using alkali and clay method*. Elsevier Ltd.

Mohanty, A.K., Misra, M. & Drzal, L.T., 2005. *Natural fibers, biopolymers and biocomposites*. Taylor and Francis.

Morrissey, F., Coutts, R. & Grossman, P., 1985. Bond between cellulose fibres and cement. *The International Journal of Cement Composites and Lightweight Concrete*, 7(2), pp.73-80.

Mwaikambo, L. & Ansell, M., 1999. *The effect of chemical treatment on the properties of hemp, sisal, jute and kapok for composite reinforcement*. Bath: Wiley University of Bath.

Owens, G., 2009. *Fulton's concrete technology*. 9th ed. Midrand, South Africa: Cement & Concrete Institute.

Owens, G., 2012. *Fundamentals of concrete*. 2nd ed. Midrand: Cement and Concrete Institute.

Pacheco-Torgal, F. & Jalali, S., 2010. *Cementitious building materials reinforced with vegetable fibres: A review*. Guimaraes: Construction and Building Materials University of Minho.

Pal, S., Mukherjee, A. & Pathak, S., 2003. *Investigation of hydraulic activity of ground granulated blast furnace slag in concrete*. Elsevier Science Ltd.

Peled, A. & Shah, S., 2003. Processing effects in Cementitious Composites: Extrusion and Casting. *Journal of Materials in Civil Engineering*, 15(2), pp.192-99.

Rieger, C. & van Mier, J., 2010. *Pullout of microfibers from hardened cement paste*. London: Taylor and Francis Group.

SANS, 1994. *SANS 5844: Particle and relative densities of aggregates*. Pretoria: Standards South Africa SANS.

SANS, 1994. *SANS 5845: Bulk densities and voids content of aggregates*. Pretoria: Standards South Africa SANS.

SANS, 1994. *SANS 5863: Concrete tests - Compressive strength of hardened concrete*. Pretoria: Standards South Africa SANS.

SANS, 2000. *SANS 50197-1: Cement Part 1: Composition, specifications and conformity criteria for common cements.* Pretoria: Standards South Africa SANs.

SANS, 2002. *SANS 201: Sieve analysis, fines content and dust content of aggregates*. Pretoria: Standards South Africa SANS.

SANS, 2006. *SANS 5862-2: Concrete tests - Consistence of freshly mixed concrete - Flow test.* Pretoria: Standards South Africa SANS.

SANS, 2006. *SANS 685: Fibre-cement sheets (flat and profiled).* Pretoria: Standards South Africa SANS.

SANS, 2011. *SANS 50450-1: Fly ash for concrete - Part 1: Definition, specifications and conformity criteria.* Pretoria: Standards South Africa SANS.

Satyanarayana, K., Guimaraes, J. & Wypych, F., 2007. *Studies on lignocellulosic fibers of Brazil. Part I: Source, production, morphology, properties and applications.* Elsevier Ltd.

Savastano, H., Warden, P. & Coutts, R., 2003. *Potential of alternative fibre cements as building materials for developing areas.* Elsevier Science Ltd.

Sedan, D., Pagnoux, C.S.A. & Chotard, T., 2007. *Mechanical properties of hemp fibre reinforced cement: Influence of the fibre/matrix interaction*. ScienceDirect.

Silva, F., Toledo Filho, R., Melo Filho, J. & Fairbairn, E., 2009. *Physical and mechanical properties of durable sisal fiber-cement composites*. Science Direct.

Simkins, V., Alderson, A., Davies, P. & Alderson, K., 2005. *Single fibre pullout tests on auxetic polymeric fibres*. Journal of Materials Science.

Singh, S., Shukla, A. & Brown, R., 2004. *Pullout behavior of polypropylene fibers from cementitious matrix*. Cement and Concrete Research.

Spence, R. & Mulligan, H., 1995. *Sustainable Development and the Construction Industry*. Elsevier Science Ltd.

TED Blog, 2012. *Born to innovate: Fellows Friday with Alex Odira Odundo*. [Online] Available at: http://blog.ted.com/2012/03/23/born-to-innovate-fellows-friday-with-alex-odira-odundo/ [Accessed 15 January 2014].

Tolêdo Filho, R., Ghavami, K., England, G. & Scrivener, K., 2002. *Development of vegetable fibre-mortar composites of improved durability*. Elsevier Science Ltd.

Tolêdo Filho, R., Joseph, K., Ghavami, K. & England, G., 1999. *The use of sisal fibre as reinforcement in cement based composites*. Revista Brasileira de Engenharia Agrícola e Ambiental.

Tolêdo Filho, R., Scrivener, K., England, G. & Ghavami, K., 2000. *Durability of alkali-sensitive sisal and coconut fibres in cement.* Elsevier Science Ltd.

U.S. Environmental Protection Agency, 2014. *Green Engineering.* [Online] Available at: www.epa.gov/oppt/greenengineering/ [Accessed 10 June 2014].

Visser, C., 2007. *Mechanical and Structural Characterisation of Extrusion Moulded SHCC.* MSc Thesis. Stellenbosch: Stellenbosch University.

World Commision on Environment and Development, 1987. *Our Common Future.* Oxford: Oxford University Press.

Yang, G. et al., 1996. *Relation of modification and tensile properties of sisal fibre.* Acta Scientiarum Naturalium Universitatis Sunyatseni.

Appendix A – Single fibre pull-out test results

Table A1 presents the results of the single fibre pull-out (SFP) tests performed at 28 days. The average pull-out (PO) and fracture (FR) forces for each fibre treatment at different embedment depths are presented. If both PO and FR occurred for the same fibre treatment at the same embedment depth, the value in red indicates the failure mode which was the least dominant.

Table A1: Average pull-out and fracture forces for different fibre treatments at different embedment depths.

Length (mm)	Average force (N)											
	Untreated		2% NaOH		6% NaOH		10% NaOH		20% NaOH		30% NaOH	
	PO	FR	PO	FR	PO	FR	PO	FR	PO	FR	PO	FR
10	-	-	6.966	-	5.960	-	5.650	-	-	-	3.631	-
15	6.306	-	7.102	7.387	6.670	5.760	-	4.430	4.310	-	-	3.887
20	-	5.580	8.131	9.033	6.918	8.497	-	6.180	-	4.589	-	3.403
25	9.447	6.409	-	-	-	-	-	-	-	-	-	-

Length (mm)	Average force (N)											
	5% A.Acid		10% A.Acid		5% A.Anh		10% A.Anh		5% A.Anh, 6% NaOH		10% A.Anh, 6% NaOH	
	PO	FR	PO	FR	PO	FR	PO	FR	PO	FR	PO	FR
10	-	-	-	-	4.538	-	4.775	-	4.712	-	5.712	-
15	2.559	-	2.493	-	-	4.355	-	4.656	-	6.360	6.381	7.201
20	3.664	3.730	4.167	4.468	-	-	-	-	-	-	-	6.288
25	-	-	-	-	-	-	-	-	-	-	-	-

A summary of the single fibre pull-out results are presented in Table A2. The average PO force for each fibre treatment was calculated as an average force per length in N/mm. This was done by dividing the average PO force (in N), at the length at which no fibres fractured for that specific treatment, by the length at which no fibres fractured. The average FR force for each fibre treatment was calculated as the average force (in N) of all the fibres that fractured for that specific treatment, regardless of the embedment depth.

Table A2: Calculated average pull-out and fracture forces for different fibre treatments.

Fibre Treatment	Average pull-out force (N/mm)	Average fracture force (N)
Untreated	0.420	6.064
2% NaOH	0.697	8.301
6% NaOH	0.596	7.129
10% NaOH	0.565	5.385
20% NaOH	0.287	4.589
30% NaOH	0.363	3.667
5% Acetic Acid	0.171	3.730
10% Acetic Acid	0.166	4.468
5% Acetic Anhydride	0.454	4.355
10% Acetic Anhydride	0.478	4.656
6% NaOH, 5% Acetic Anhydride	0.471	6.360
6% NaOH, 10% Acetic Anhydride	0.571	6.810

The pull-out responses for all the different fibre treatments and embedment depths are presented in Figure A7.2.1 to Figure A7.2.30.

1. Untreated
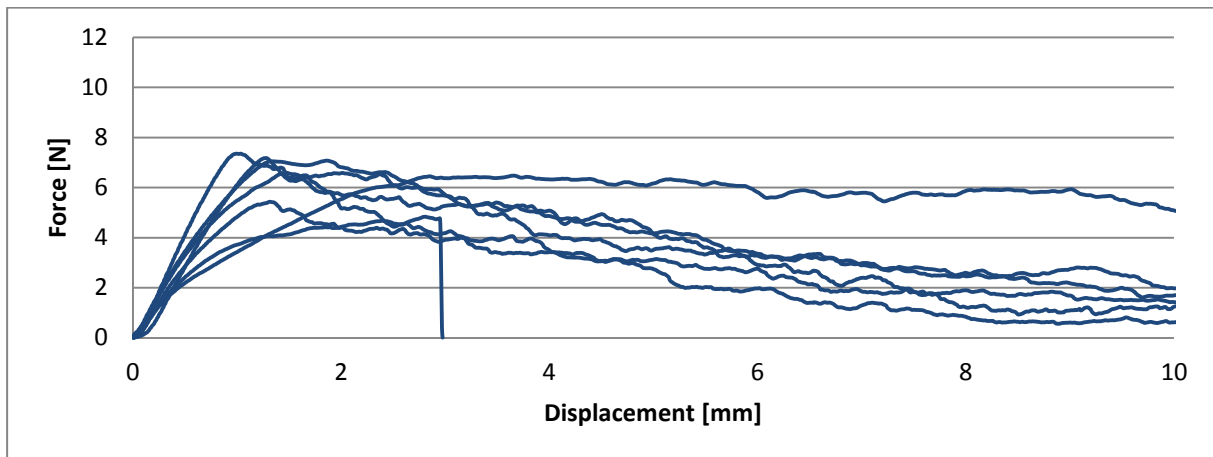
Figure A7.2.1: Pull-out response of 15 mm untreated fibre.
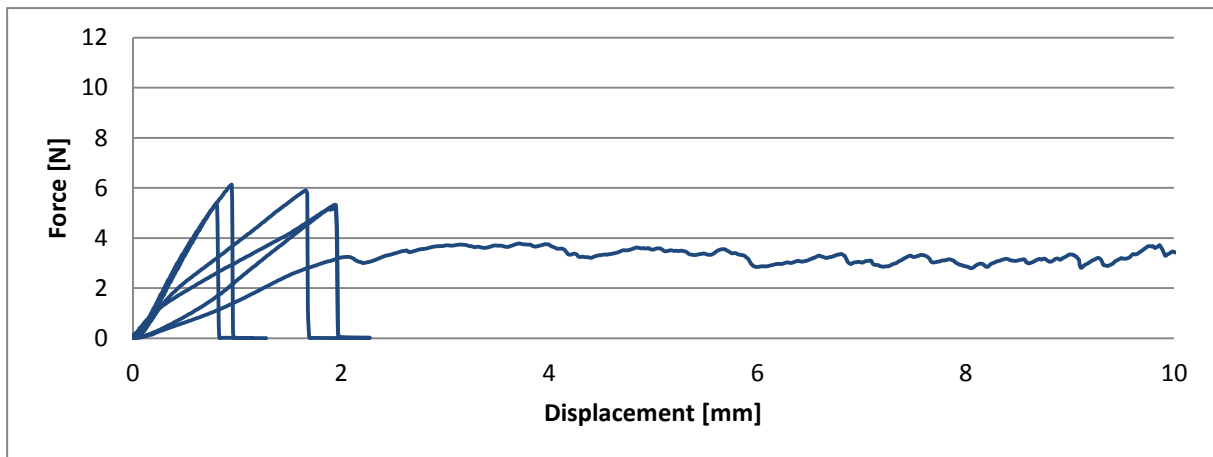
Figure A7.2.2: Pull-out response of 20 mm untreated fibre.
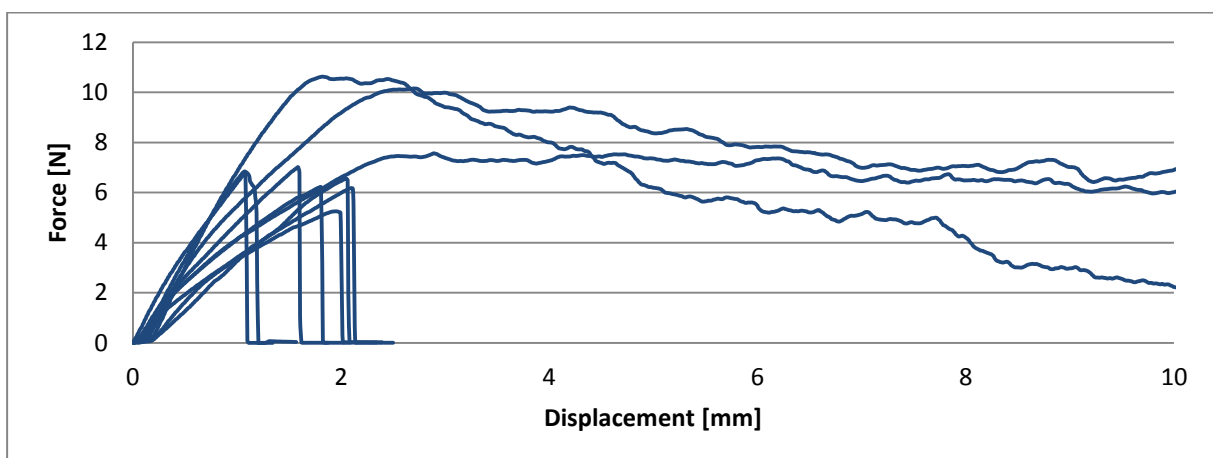
Figure A7.2.3: Pull-out response of 25 mm untreated fibre.

2. 2% NaOH
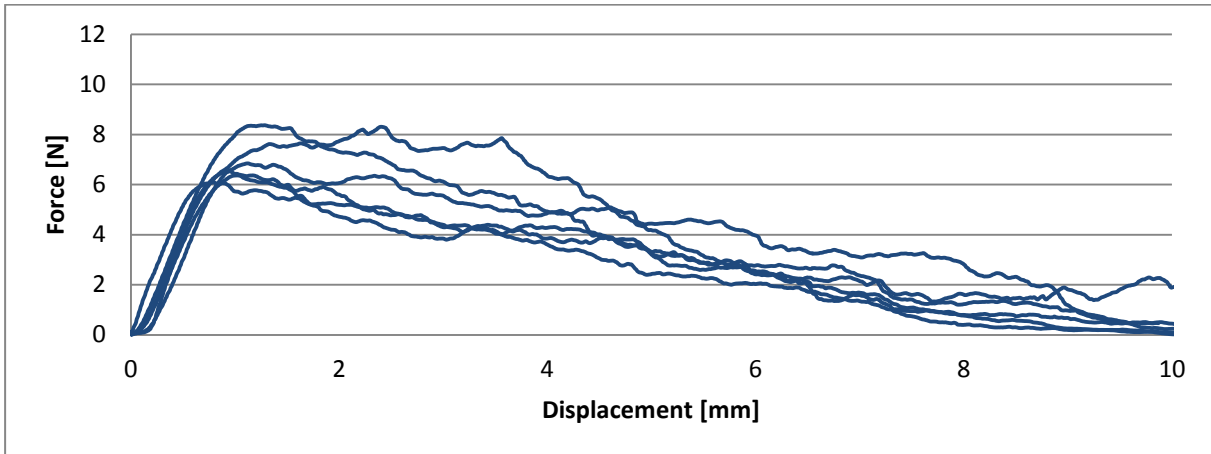
Figure A7.2.4: Pull-out response of 10 mm 2% NaOH treated fibre.
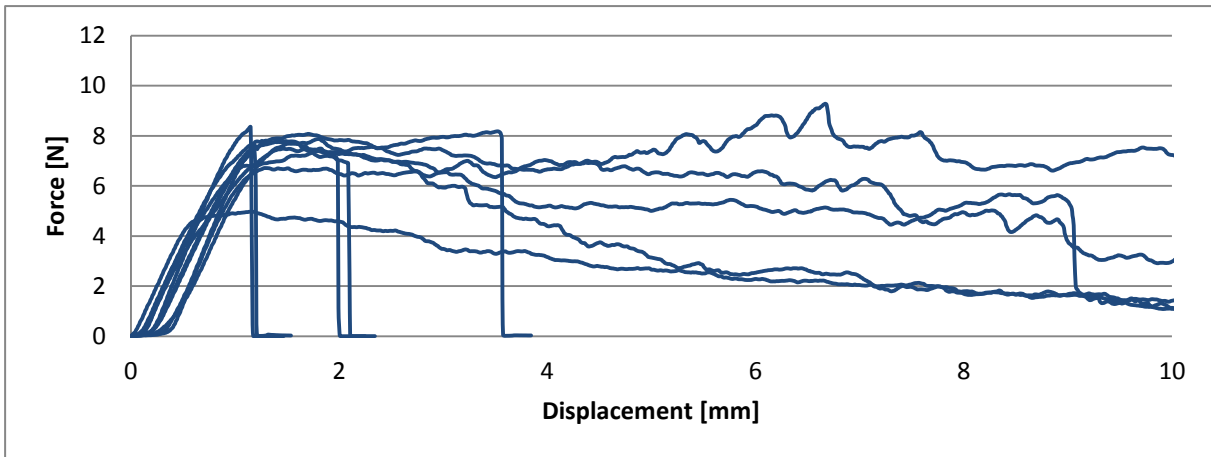
Figure A7.2.5: Pull-out response of 15 mm 2% NaOH treated fibre.
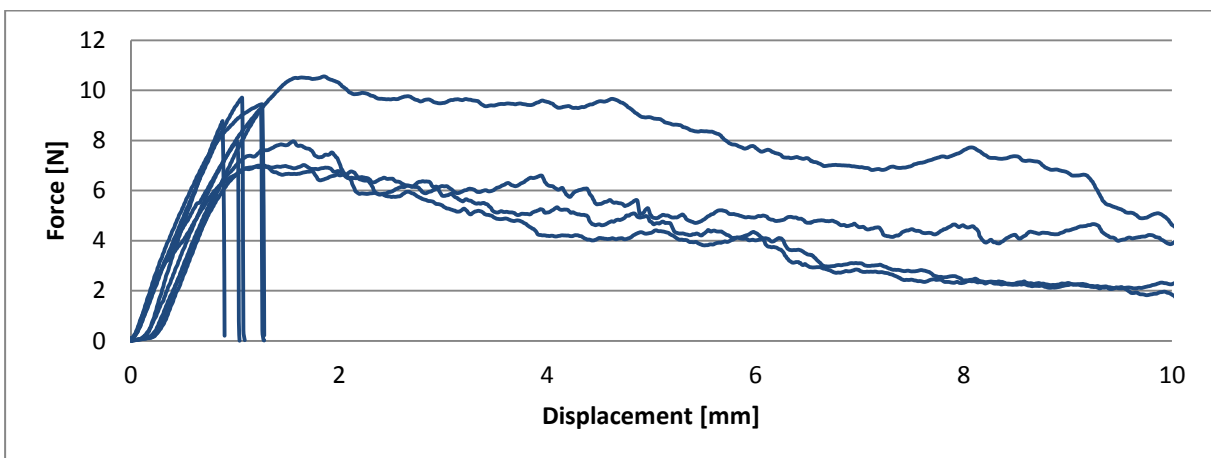
Figure A7.2.6: Pull-out response of 20 mm 2% NaOH treated fibre.

112
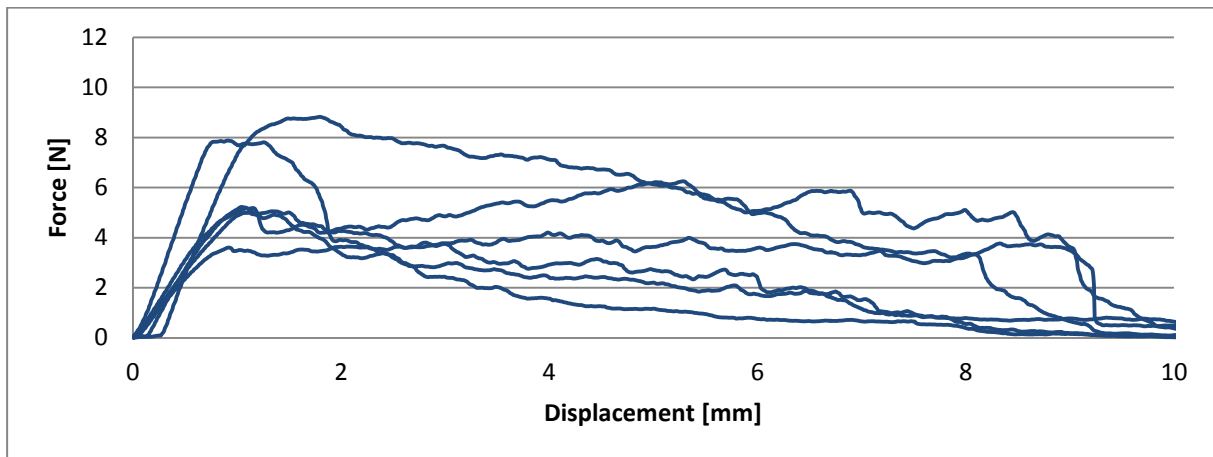
3. 6% NaOH

Figure A7.2.7: Pull-out response of 10 mm 6% NaOH treated fibre.
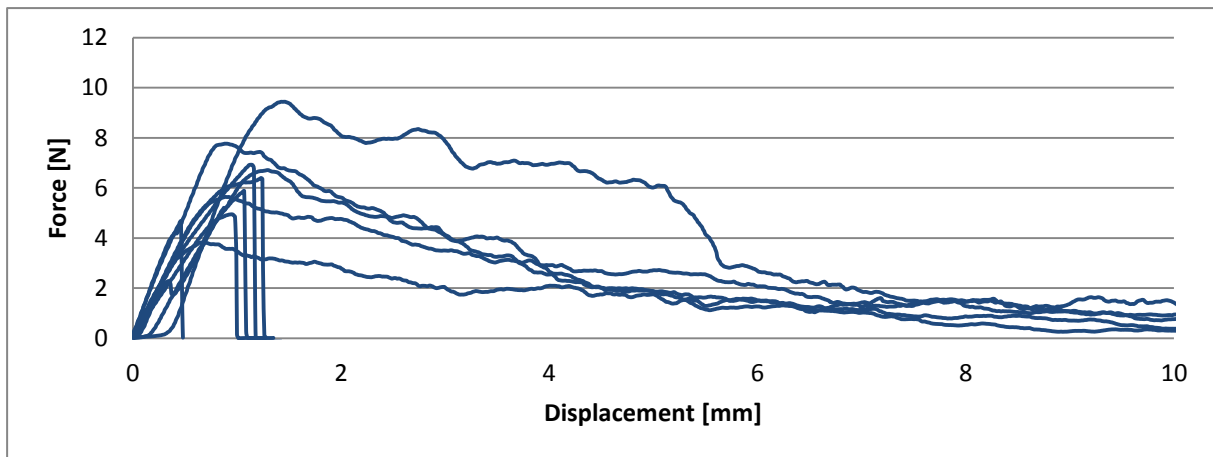
Figure A7.2.8: Pull-out response of 15 mm 6% NaOH treated fibre.
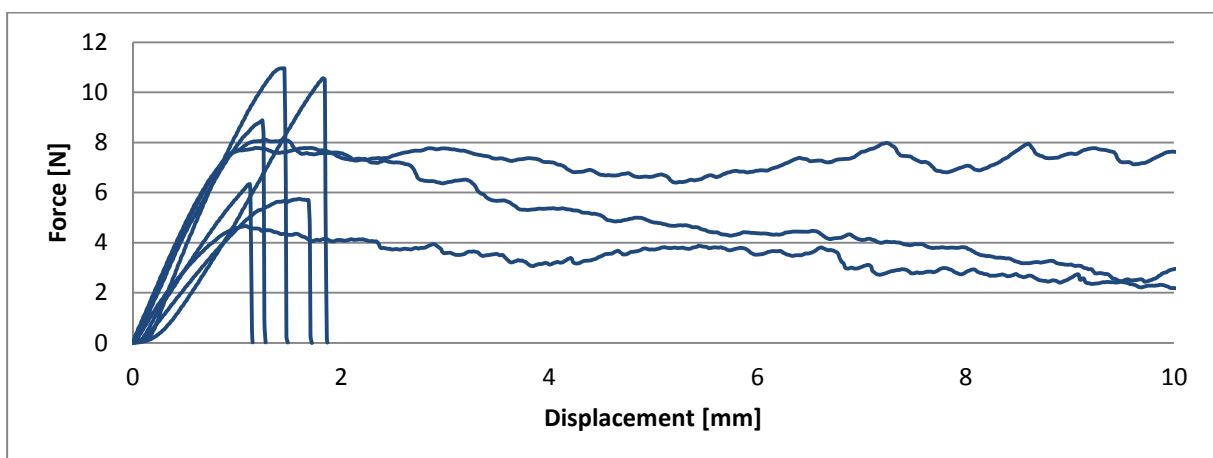
Figure A7.2.9: Pull-out response of 20 mm 6% NaOH treated fibre.

113
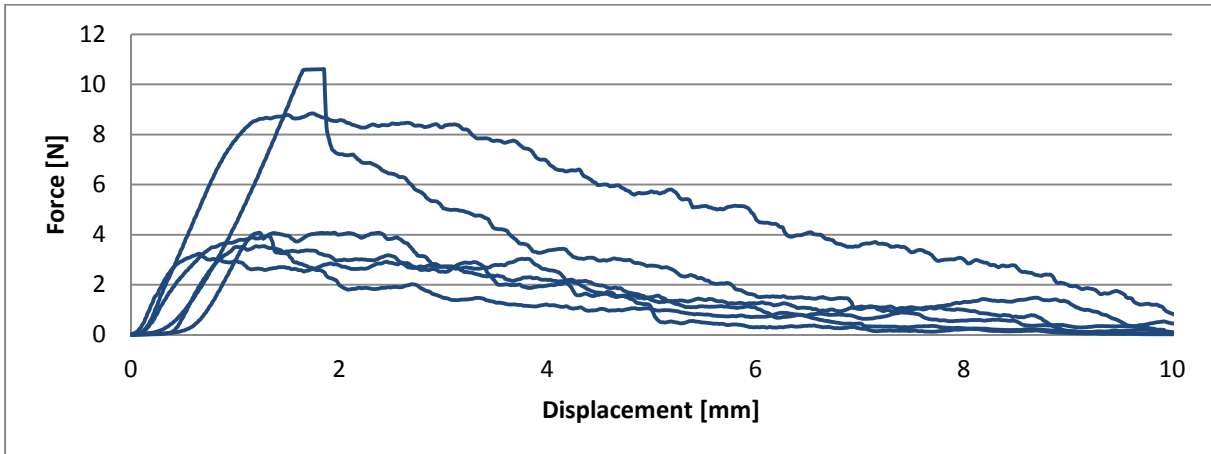
4. 10% NaOH

Figure A7.2.10: Pull-out response of 10 mm 10% NaOH treated fibre.
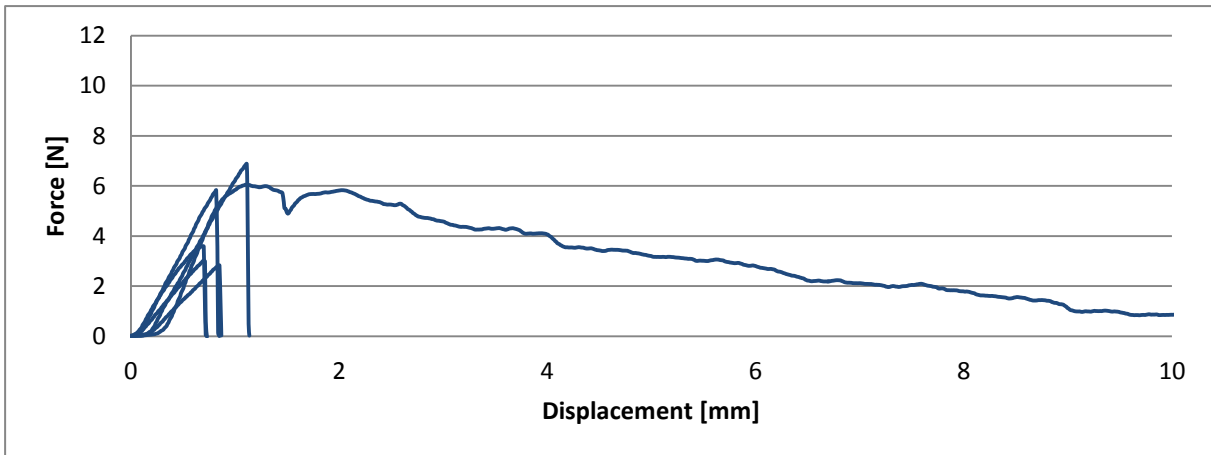
Figure A7.2.11: Pull-out response of 15 mm 10% NaOH treated fibre.
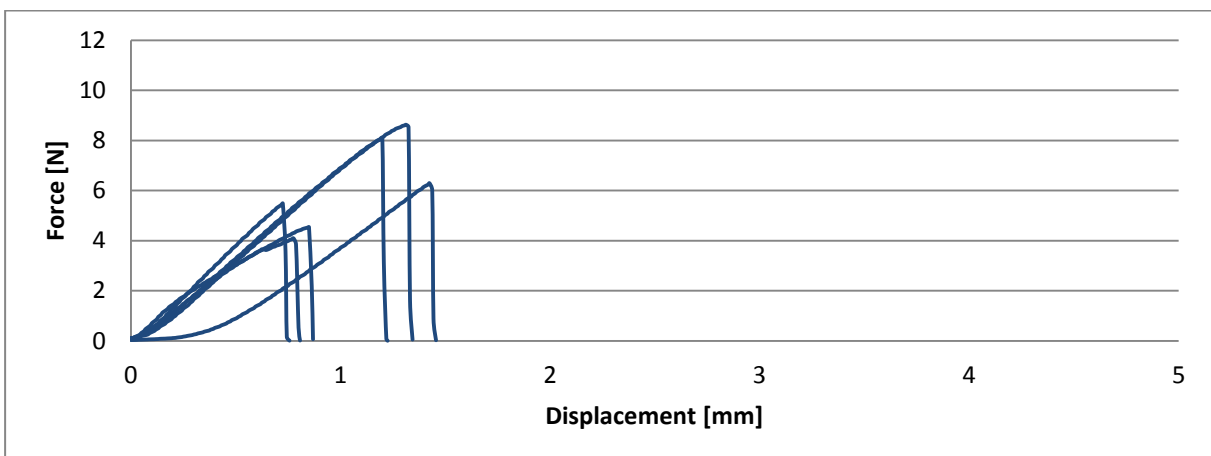
Figure A7.2.12: Pull-out response of 20 mm 10% NaOH treated fibre.

114
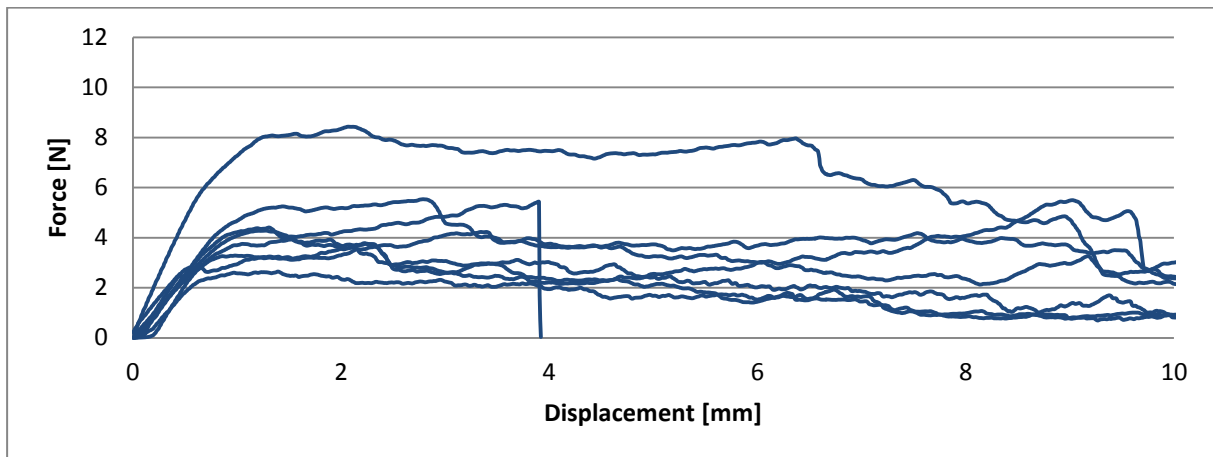
5. 20% NaOH

Figure A7.2.13: Pull-out response of 15 mm 20% NaOH treated fibre.
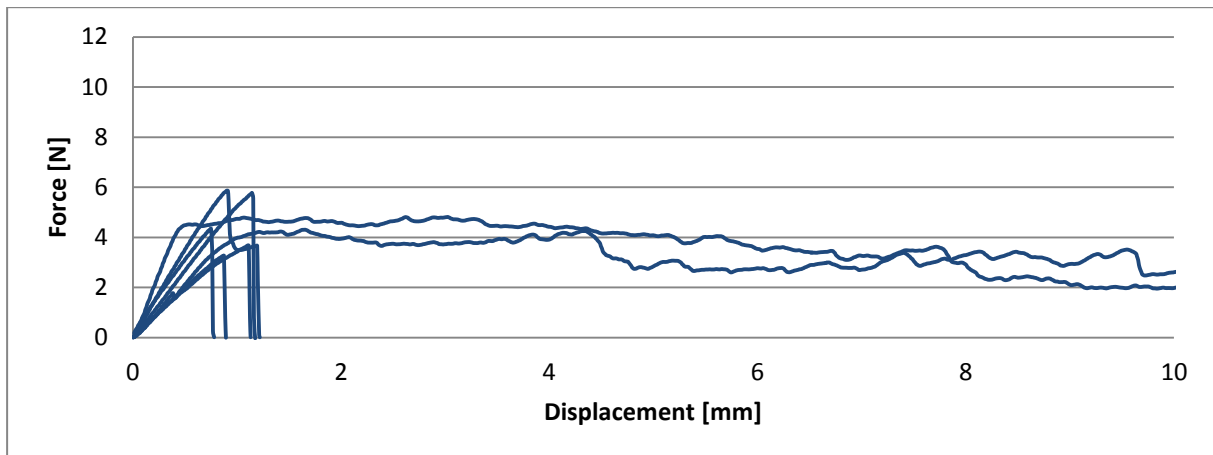
Figure A7.2.14: Pull-out response of 20 mm 20% NaOH treated fibre.

6. 30% NaOH
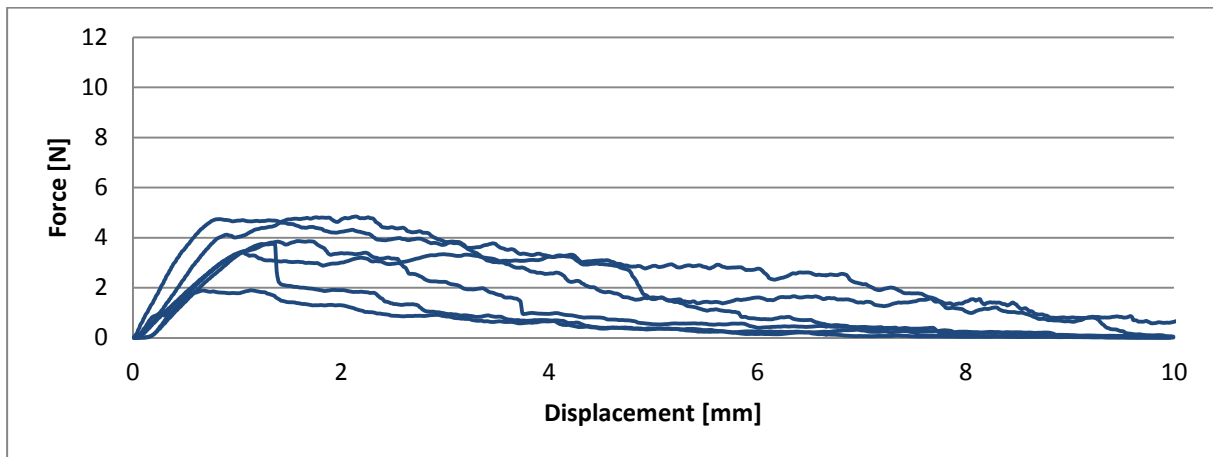
Figure A7.2.15: Pull-out response of 10 mm 30% NaOH treated fibre.
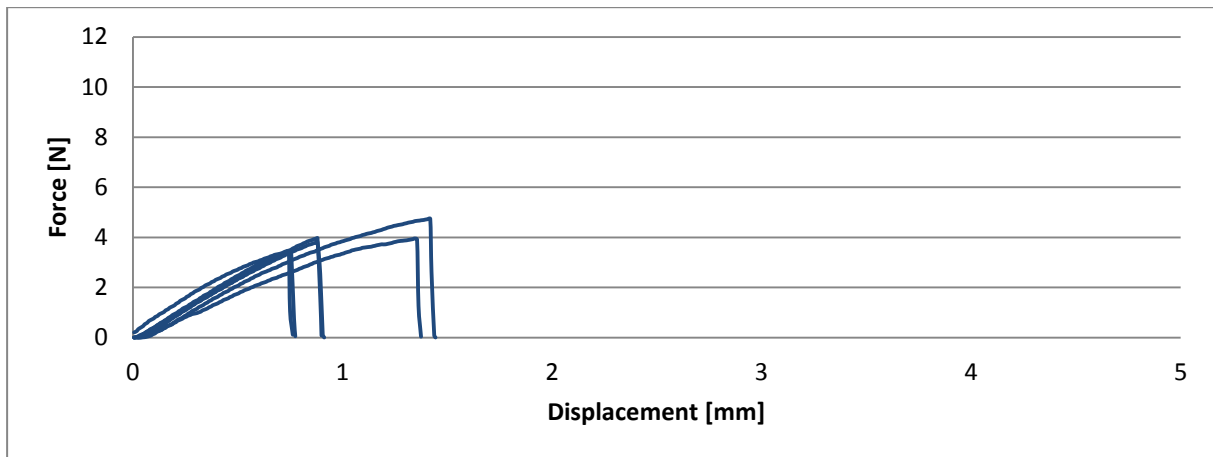
Figure A7.2.16: Pull-out response of 15 mm 30% NaOH treated fibre.
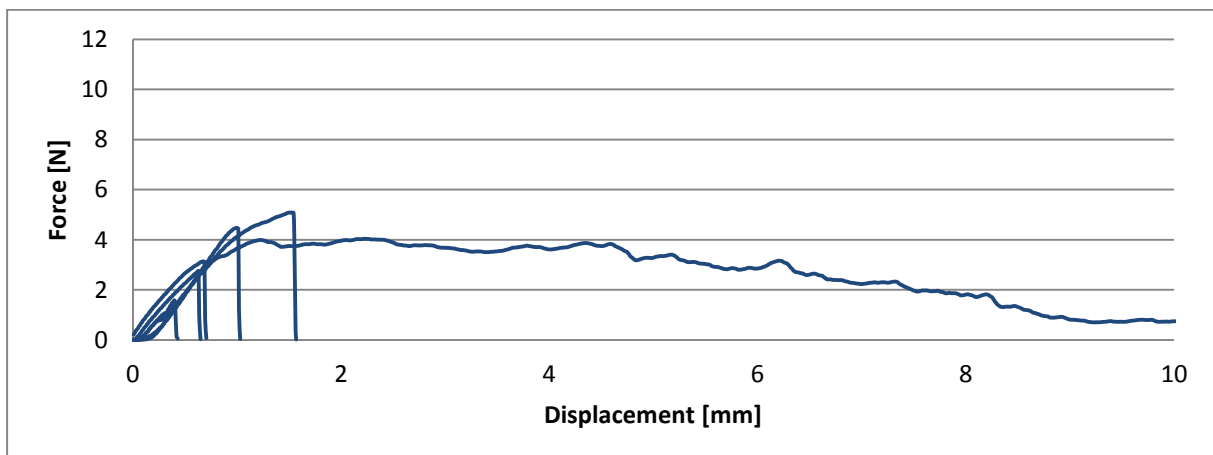
Figure A7.2.17: Pull-out response of 20 mm 30% NaOH treated fibre.

7. 5% Acetic Acid
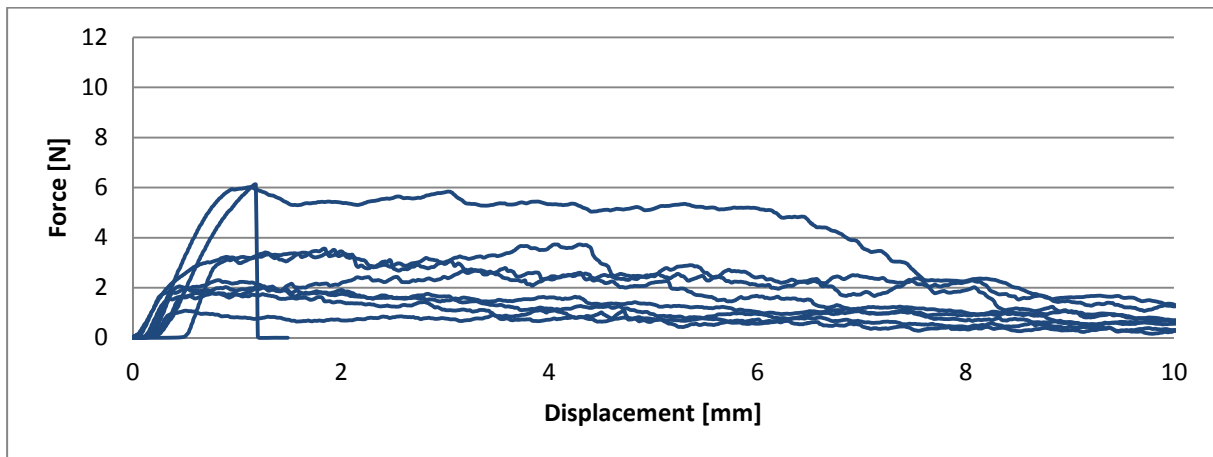
Figure A7.2.18: Pull-out response of 15 mm 5% Acetic Acid treated fibre.
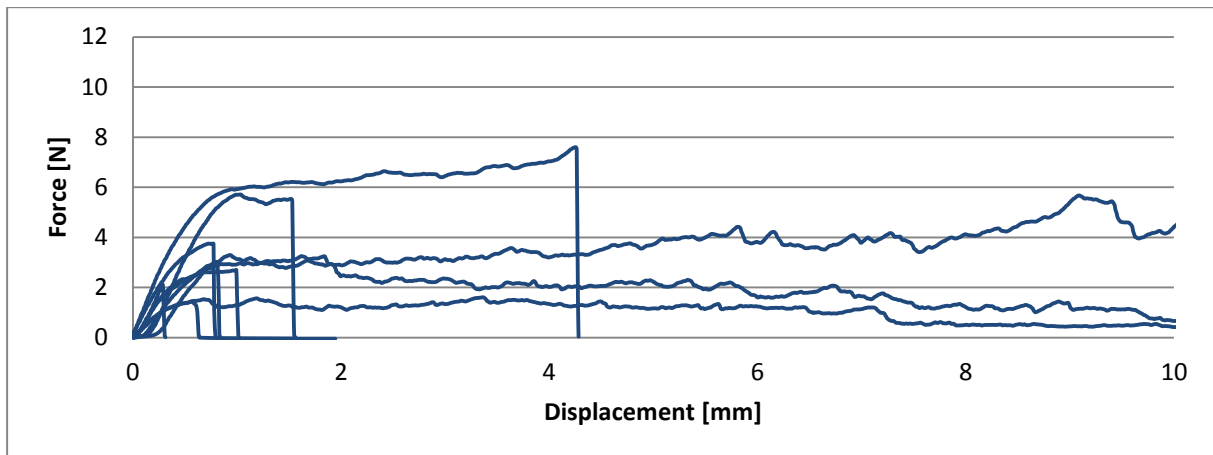
Figure A7.2.19: Pull-out response of 20 mm 5% Acetic Acid treated fibre.

117
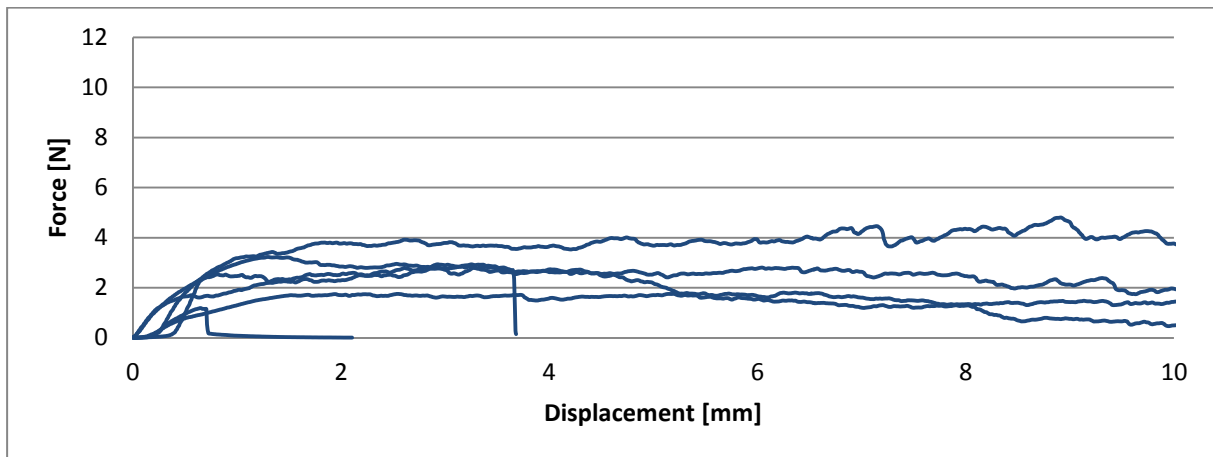
8. 10% Acetic Acid

Figure A7.2.20: Pull-out response of 15 mm 10% Acetic Acid treated fibre.
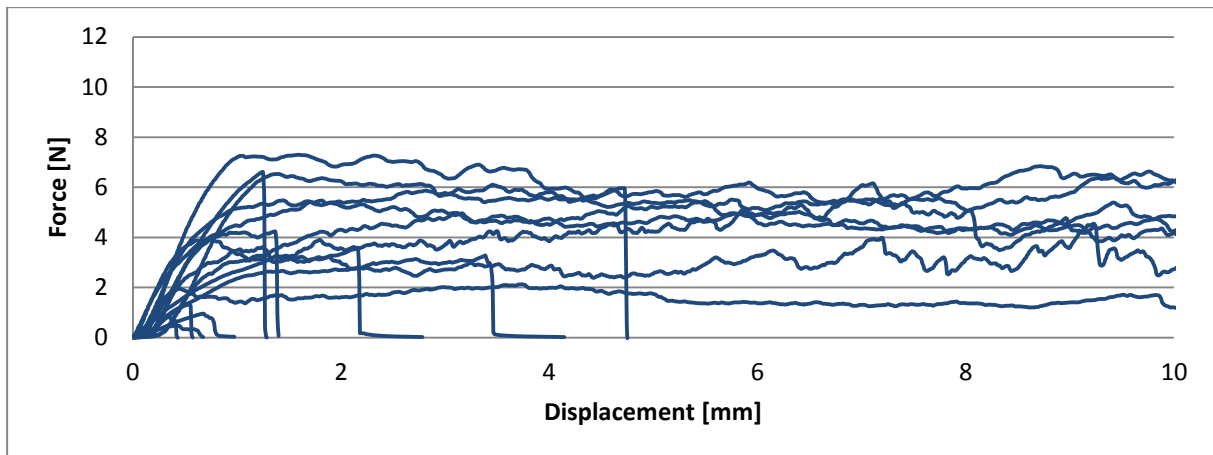
Figure A7.2.21: Pull-out response of 20 mm 10% Acetic Acid treated fibre.

118

9. 5% Acetic Anhydride
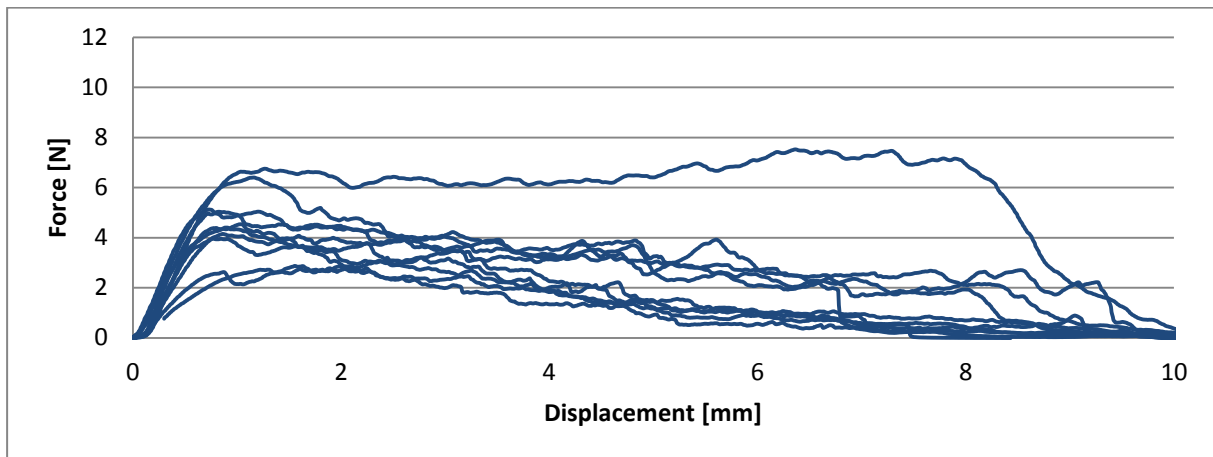
Figure A7.2.22: Pull-out response of 10 mm 5% Acetic Anhydride treated fibre.
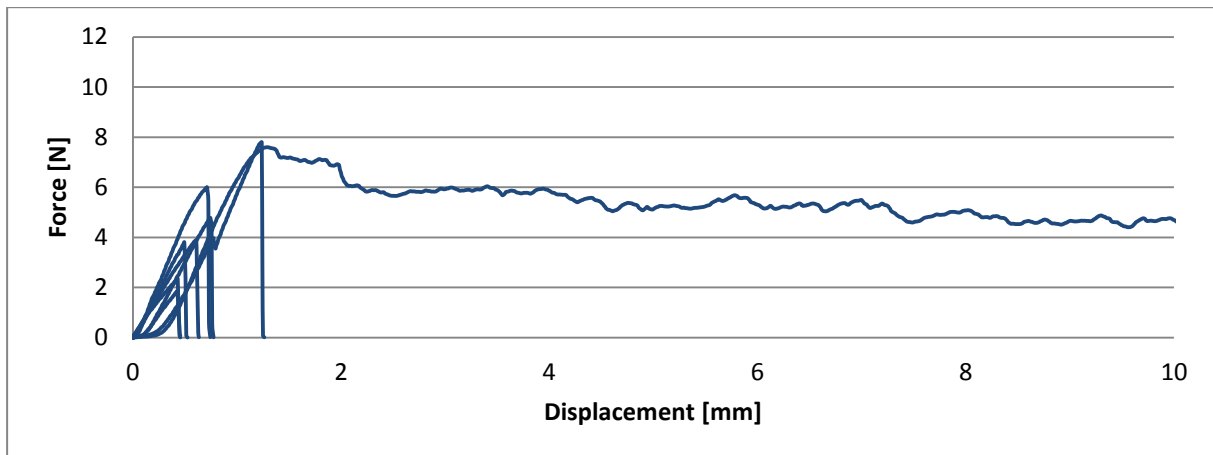
Figure A7.2.23: Pull-out response of 15 mm 5% Acetic Anhydride treated fibre.

10. 10% Acetic Anhydride
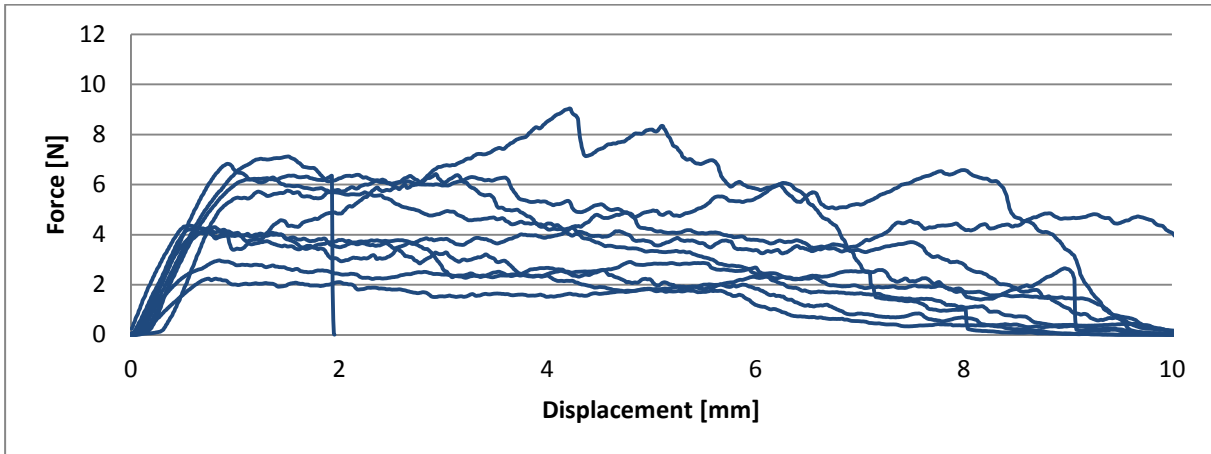
Figure A7.2.24: Pull-out response of 10 mm 10% Acetic Anhydride treated fibre.
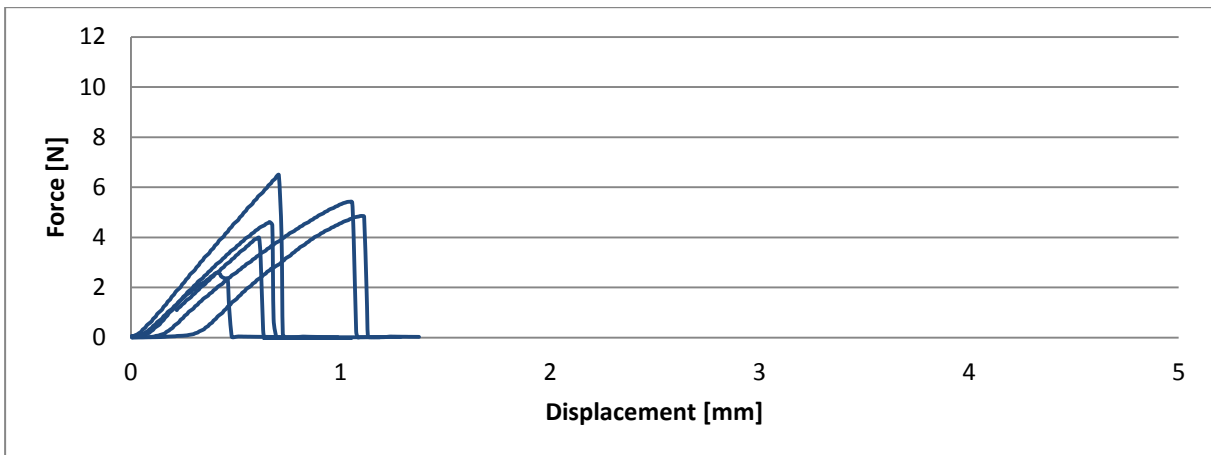
Figure A7.2.25: Pull-out response of 15 mm 10% Acetic Anhydride treated fibre.

120

11. 6% NaOH-5% Acetic Anhydride
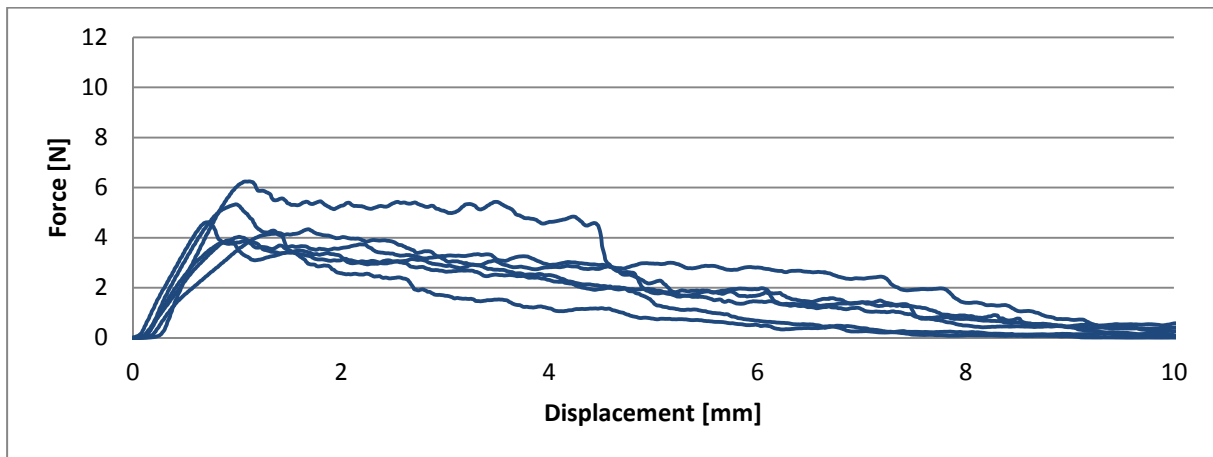
Figure A7.2.26: Pull-out response of 10 mm 6% NaOH-5% Acetic Anhydride treated fibre.
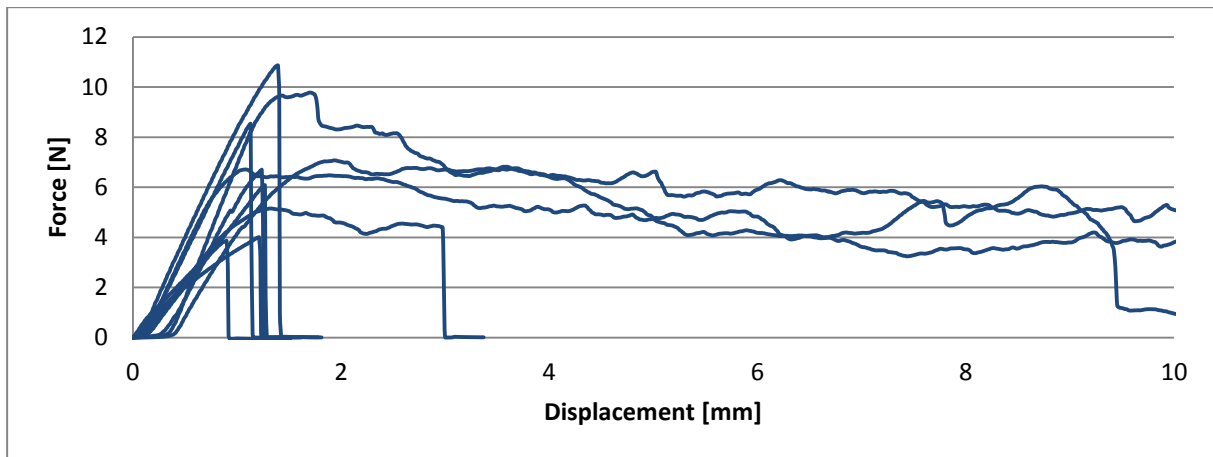
Figure A7.2.27: Pull-out response of 15 mm 6% NaOH-5% Acetic Anhydride treated fibre.

121

12. 6% NaOH-10% Acetic Anhydride
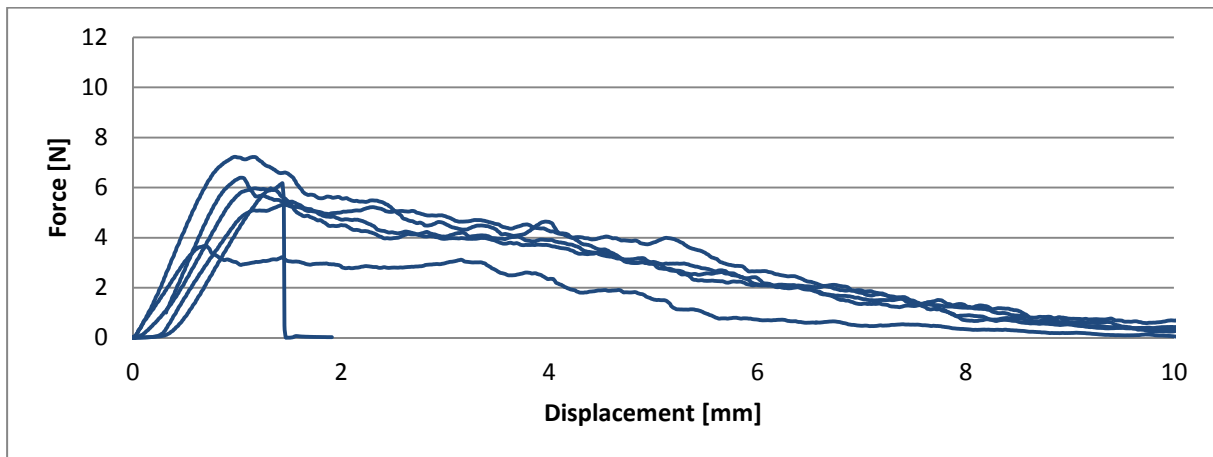
Figure A7.2.28: Pull-out response of 10 mm 6% NaOH-10% Acetic Anhydride treated fibre.
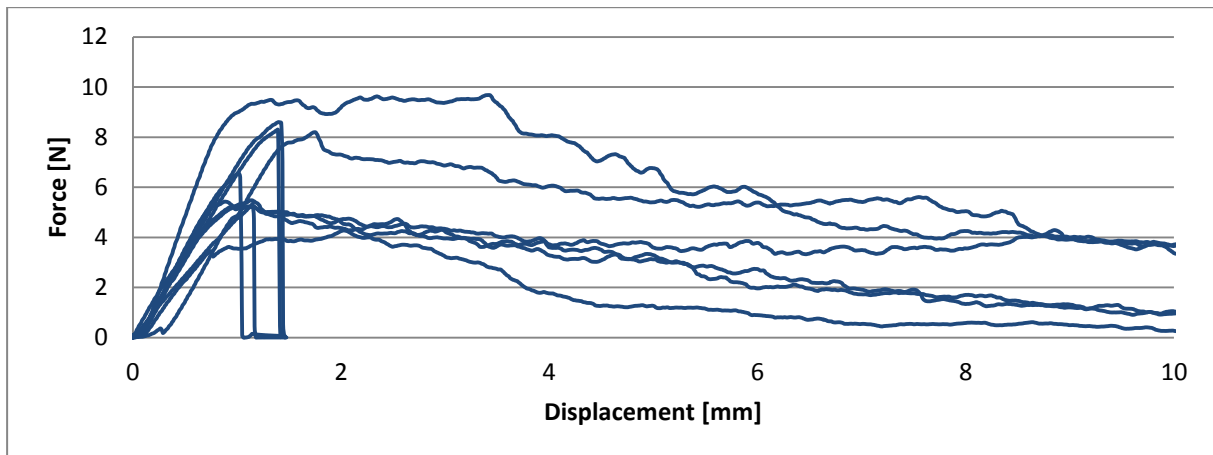
Figure A7.2.29: Pull-out response of 15 mm 6% NaOH-10% Acetic Anhydride treated fibre.
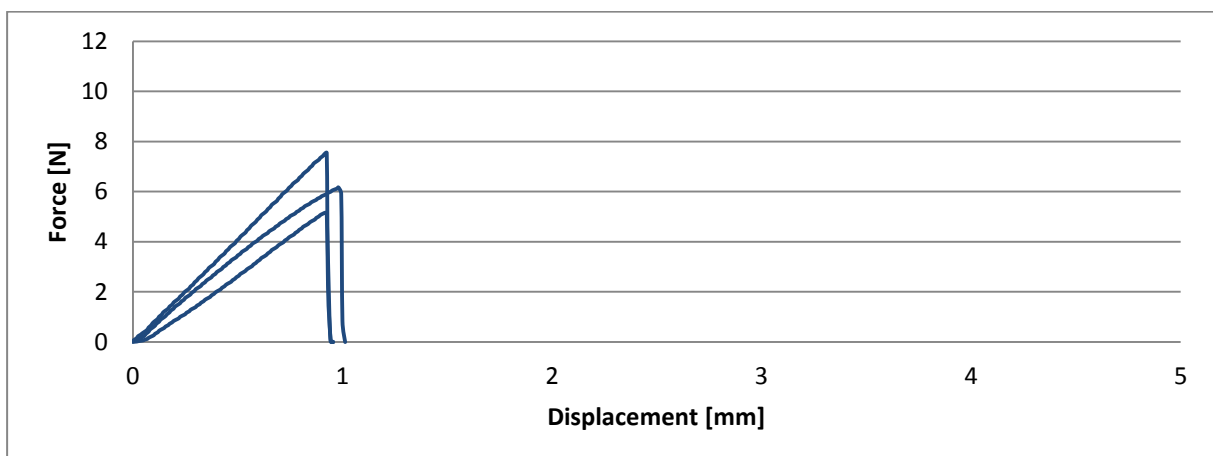
Figure A7.2.30: Pull-out response of 20 mm 6% NaOH-10% Acetic Anhydride treated fibre.

Appendix B – Three-point bending test results

1. Summary of results of three-point bending tests

Table B1 presents the results of all the three-point bending tests performed. Only the post-peak strength is provided, as it gives a clear indication on the strength of the fibres after treatment and ageing. The percentage increase or decrease calculated for each ageing regime indicates the increase or decrease in strength with regards to the corresponding 28 day reference.

Table B1: Average post-peak stress and percentage increase or decrease for specimens subjected to different ageing regimes and tested in three-point bending at an age of 90 days.

Matrix, Fibre volume, Length	Treatment	Post peak						
		28 days	90 days water		90 days hot water		90 days wet/dry	
		Avg	Avg	% inc/dec	Avg	% inc/dec	Avg	% inc/dec
C1-2-20	Untreated	2.16	2.29	5.90	0.97	-55.37	2.03	-6.20
C1-1-20	Untreated	1.68	1.41	-15.92	0.72	-57.25	1.17	-30.20
C1-1-20	2% NaOH	1.54	1.81	17.56	0.81	-47.60	1.41	-8.85
C1-1-20	6% NaOH	1.99	1.70	-14.61	0.87	-56.41	1.19	-40.30
C1-1-20	10% NaOH	2.05	1.72	-16.03	1.02	-50.32	1.38	-32.72
C1-1-20	20% NaOH	1.46	1.26	-13.68	0.79	-45.81	1.07	-26.64
C1-1-20	30% NaOH	1.38	1.44	4.21	0.99	-28.36	1.18	-14.21
C1-1-20	5% A.Acid	1.61	1.46	-8.80	0.72	-55.26	1.56	-2.65
C1-1-20	10% A.Acid	1.62	1.34	-17.49	0.74	-54.36	1.77	8.85
C1-1-20	5% A.Anh	1.77	1.40	-20.97	0.81	-54.02	1.58	-10.84
C1-1-20	10% A.Anh	1.76	1.52	-13.79	1.19	-32.30	1.78	1.23
C1-1-20	6% NaOH, 5% A.Anh	2.07	2.37	14.06	1.03	-50.21	1.84	-11.54
C1-1-20	6% NaOH, 10% A.Anh	2.47	1.96	-20.49	1.10	-55.32	1.47	-40.58
C2-1-20	Untreated	0.36	1.80	404.80	0.97	171.19	1.40	294.11
C3-1-20	Untreated	2.06	1.51	-26.89	0.97	-53.03	1.71	-16.87
C4-1-20	Untreated	1.12	1.01	-9.87	0.83	-26.00	0.94	-16.70
C5-1-20	Untreated	0.56	1.29	131.26	1.08	92.94	1.61	188.11
C6-1-20	Untreated	2.38	1.83	-22.95	1.35	-43.15	1.60	-32.71
E1-1-20	Untreated	0.97	1.39	43.75	1.09	13.00	1.15	18.87
E1-2-20	Untreated	0.27						
E2-1-20	Untreated	2.07	1.92	-7.01	1.28	-37.99	1.76	-14.71
E3-1-20	Untreated	1.39	1.57	13.15				
C1-1-30	Untreated	1.47	1.25	-15.47	0.71	-51.65	1.32	-10.54

2. Results of three-point bending tests performed at 28 days

The results of the three-point bending tests performed on all the different series of specimens at 28 days are presented in this section in **Figure B0.1** to Figure B0.23.
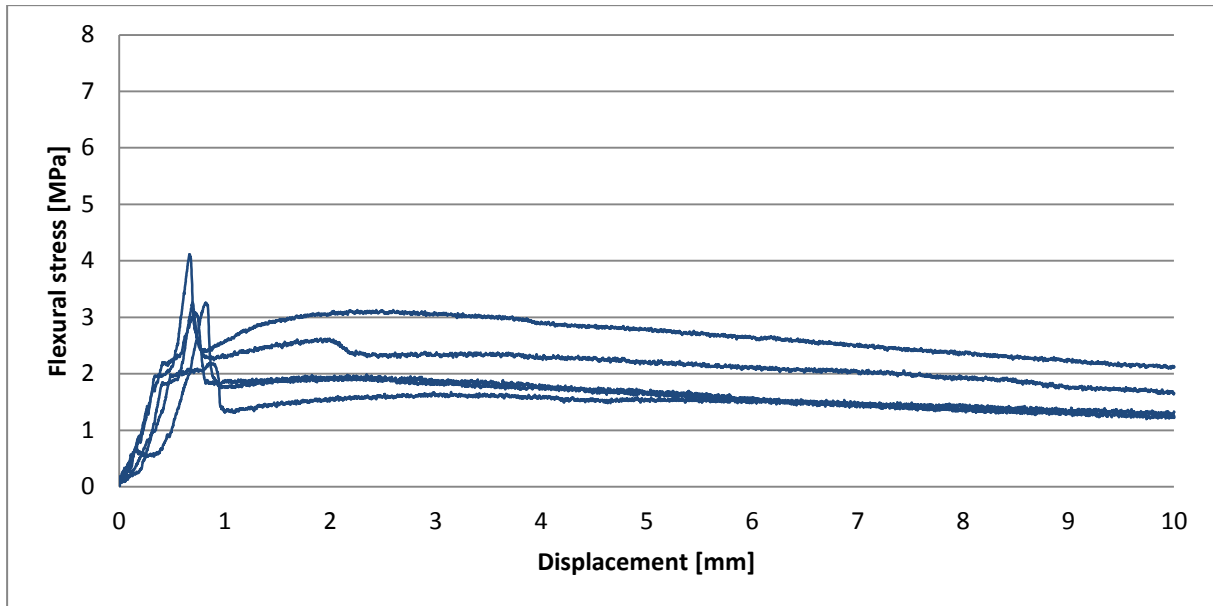
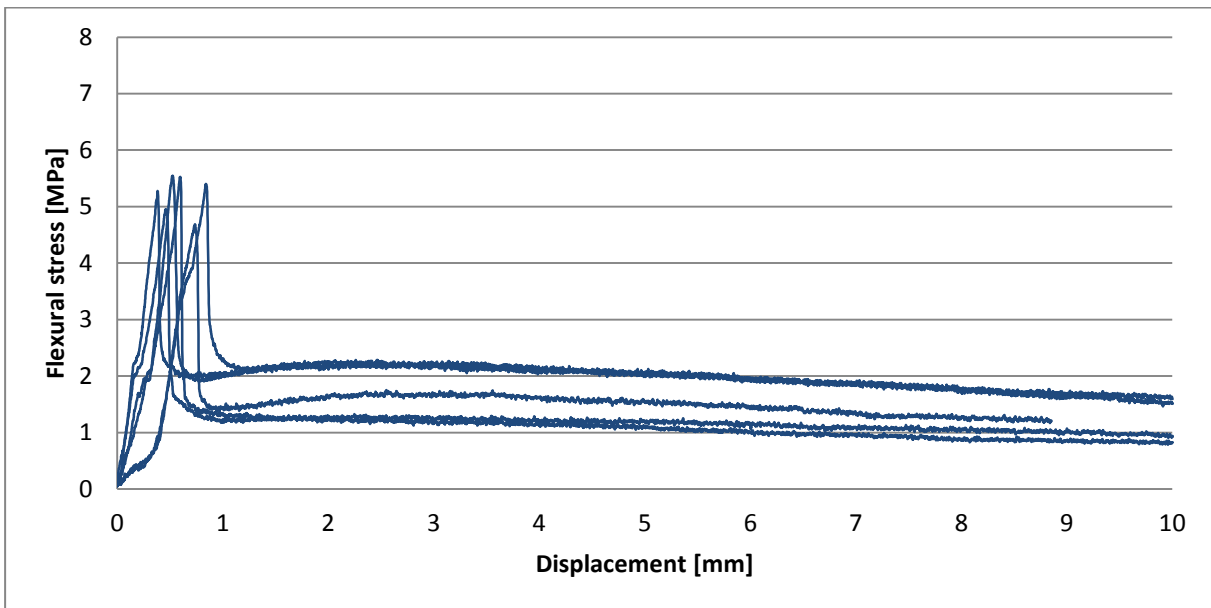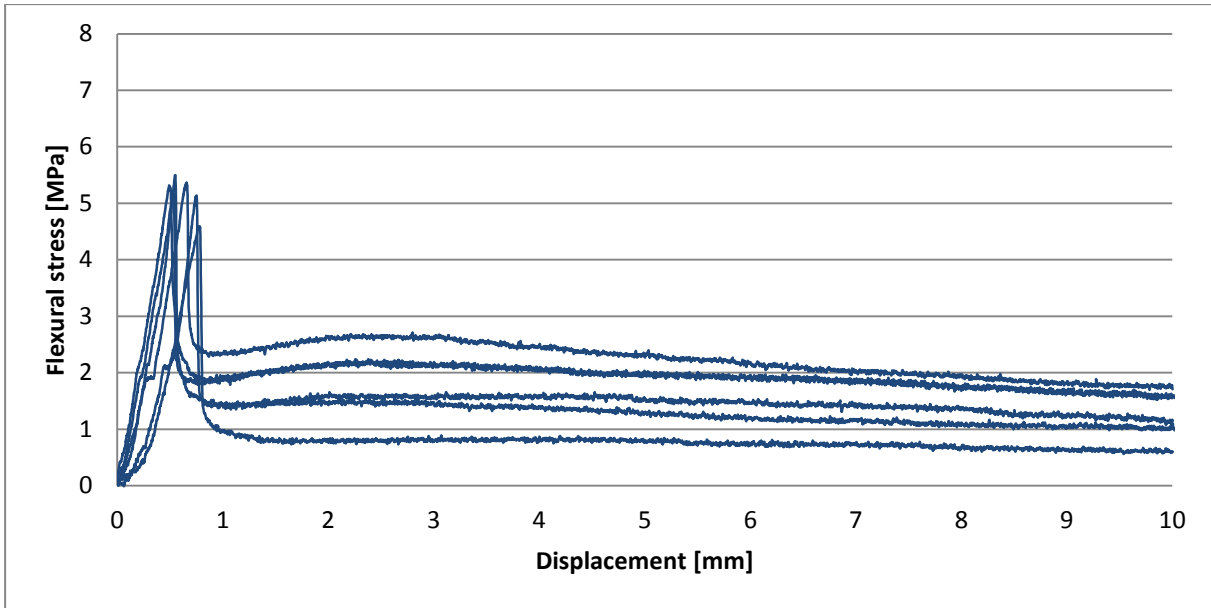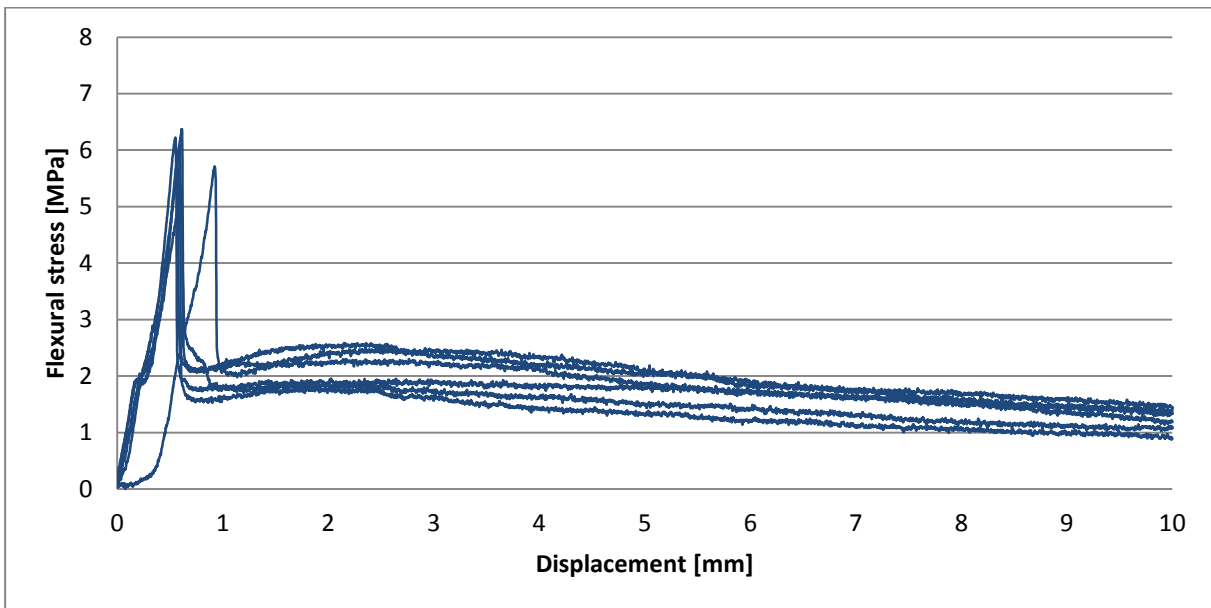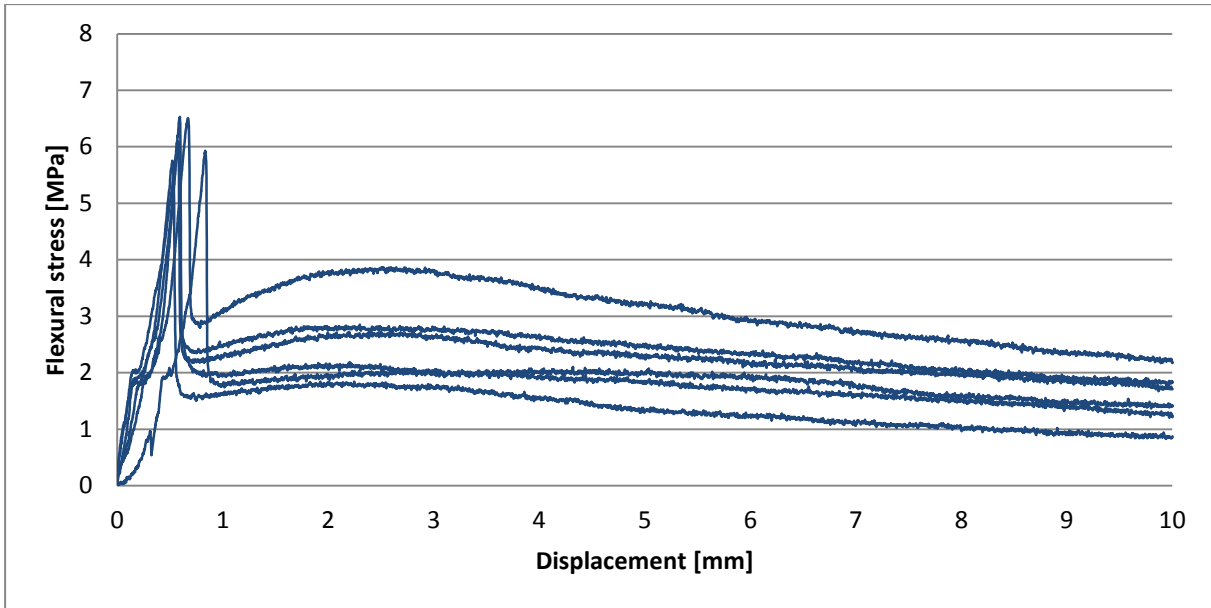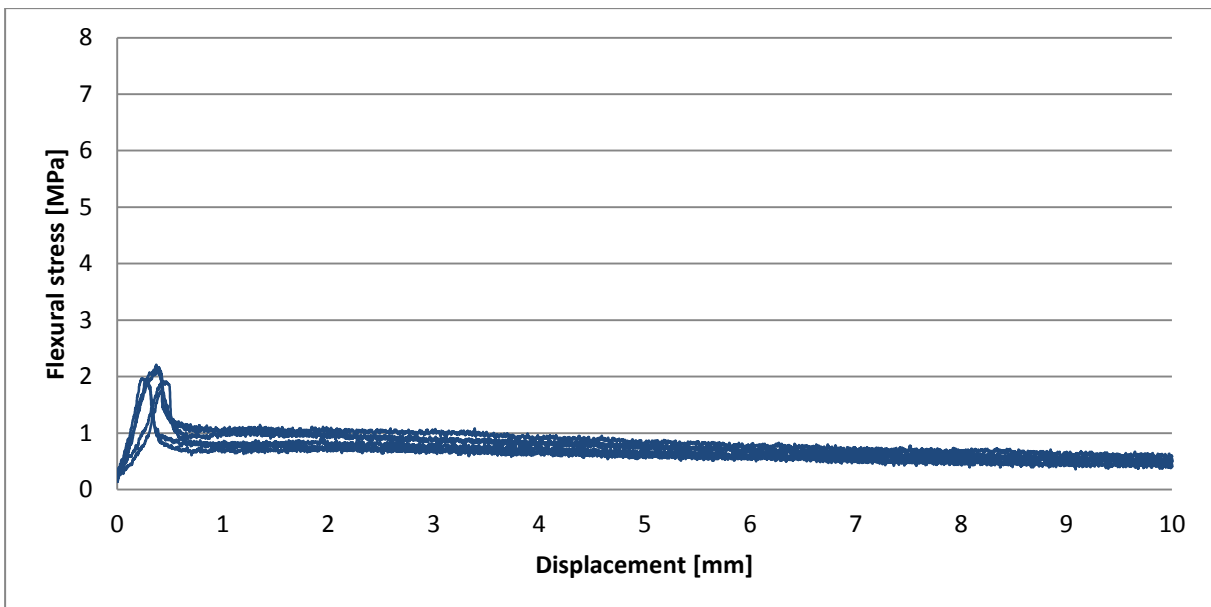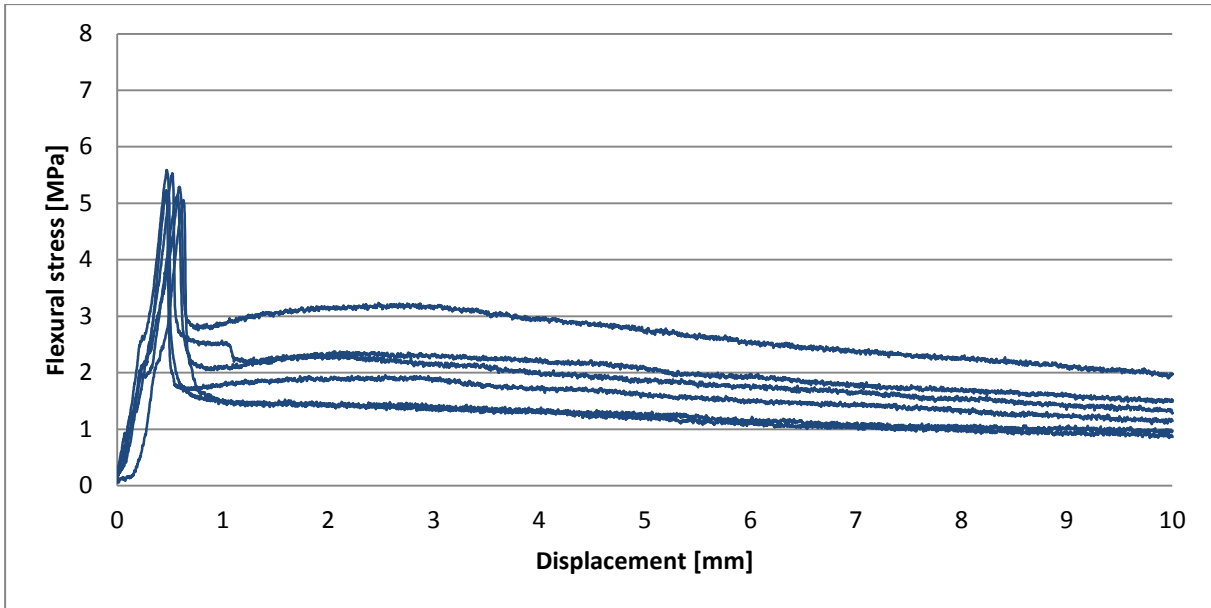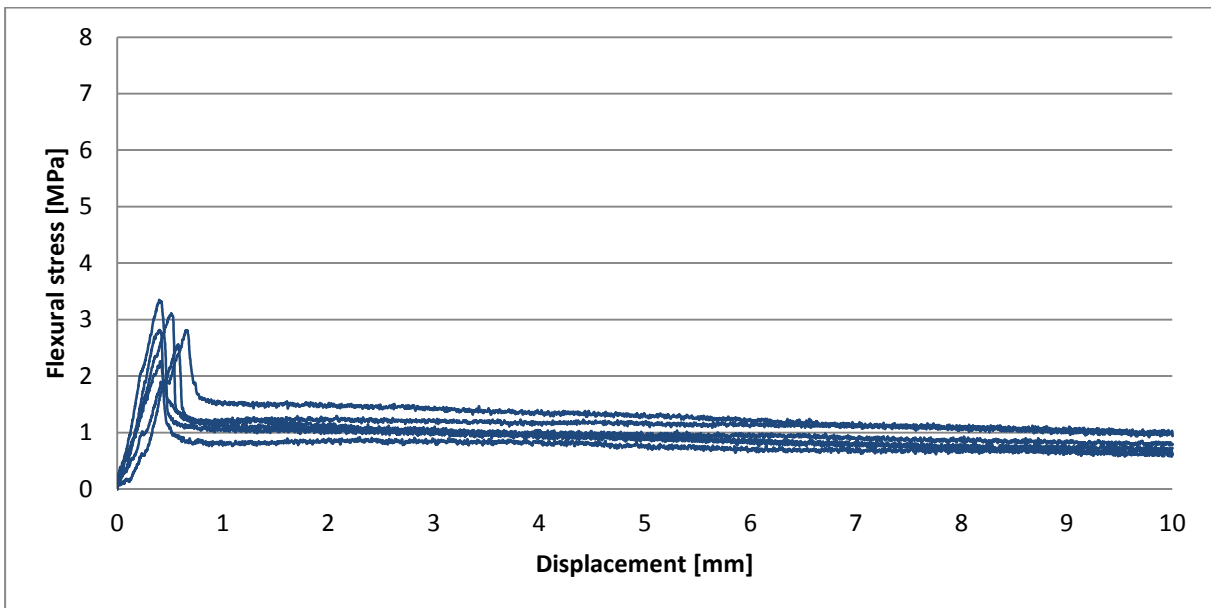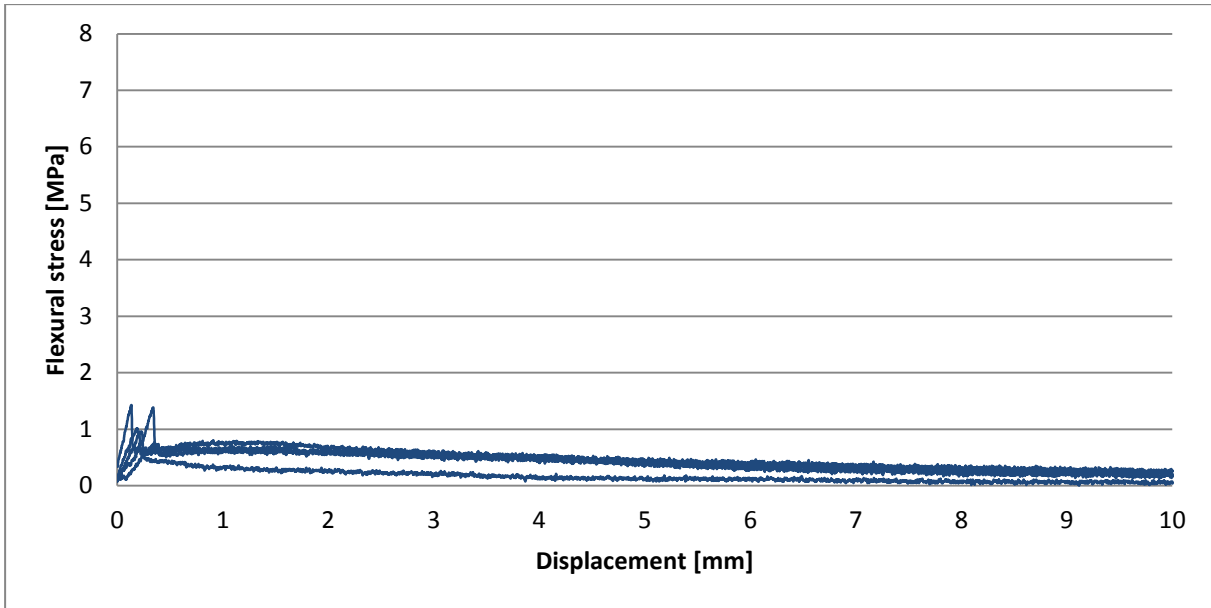**Figure B0.1: Ultimate flexural stress of matrix C1, 2%, 20mm, untreated fibre.**
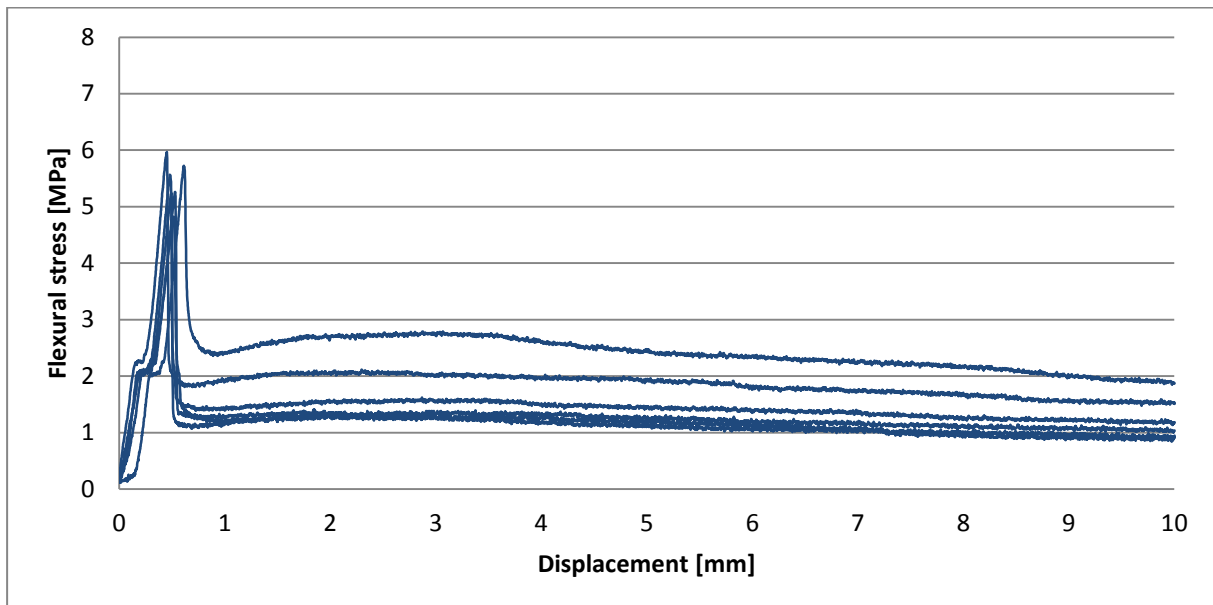
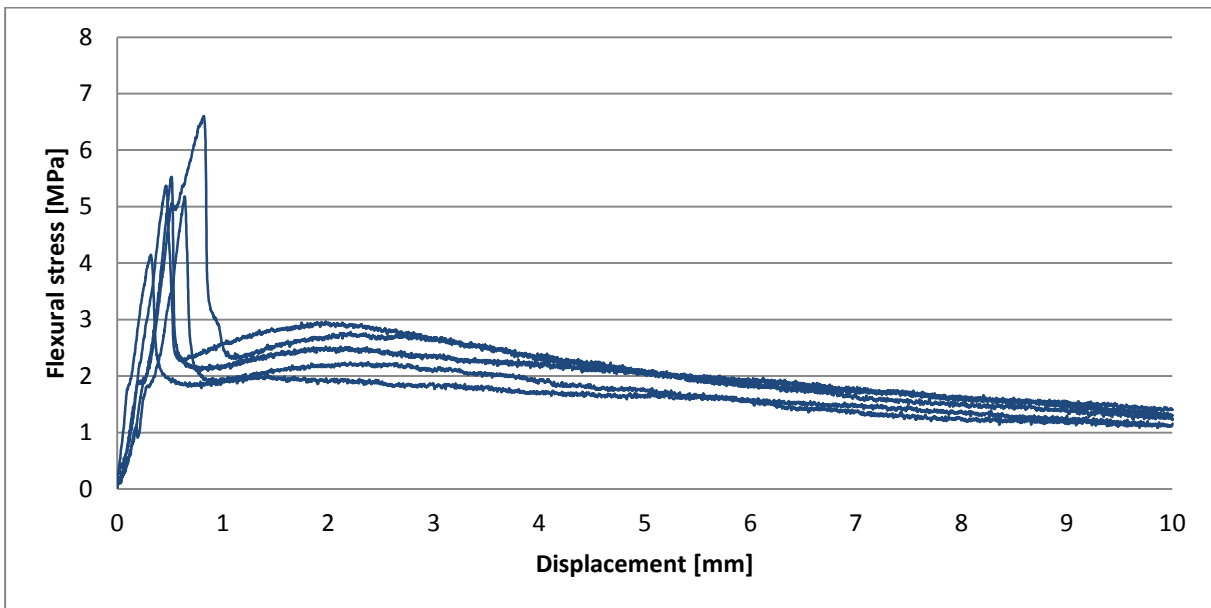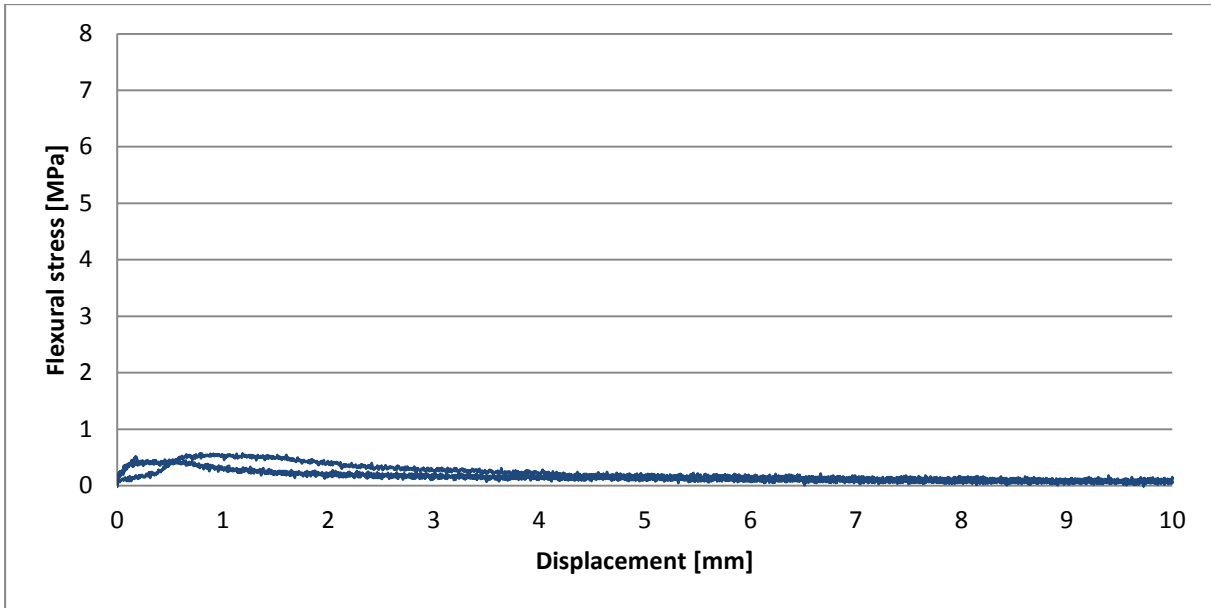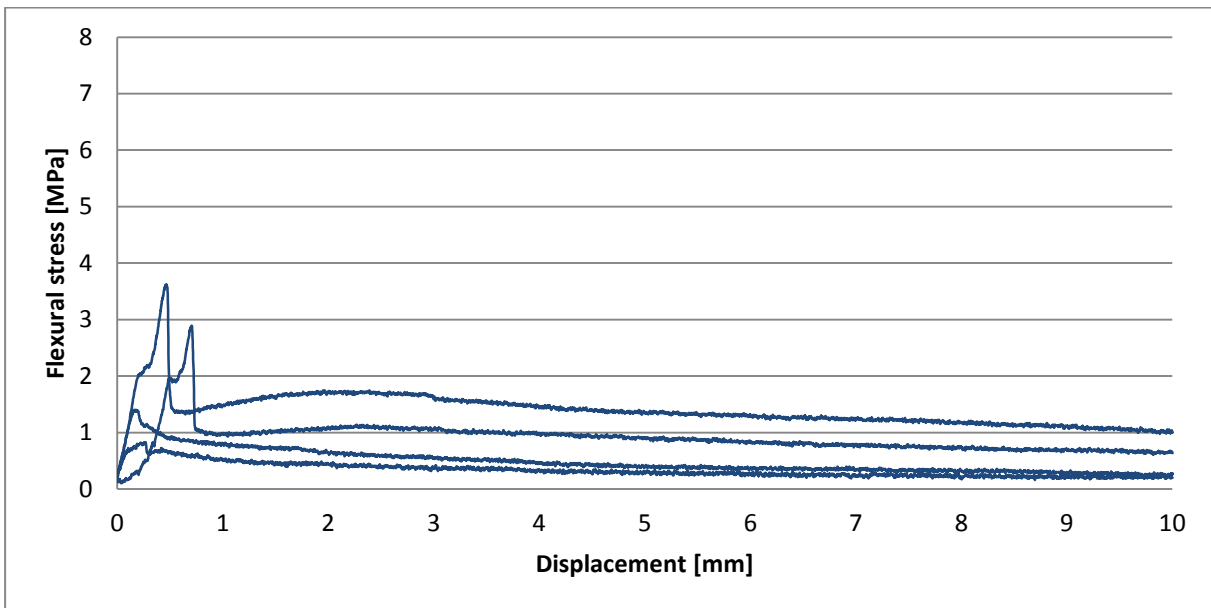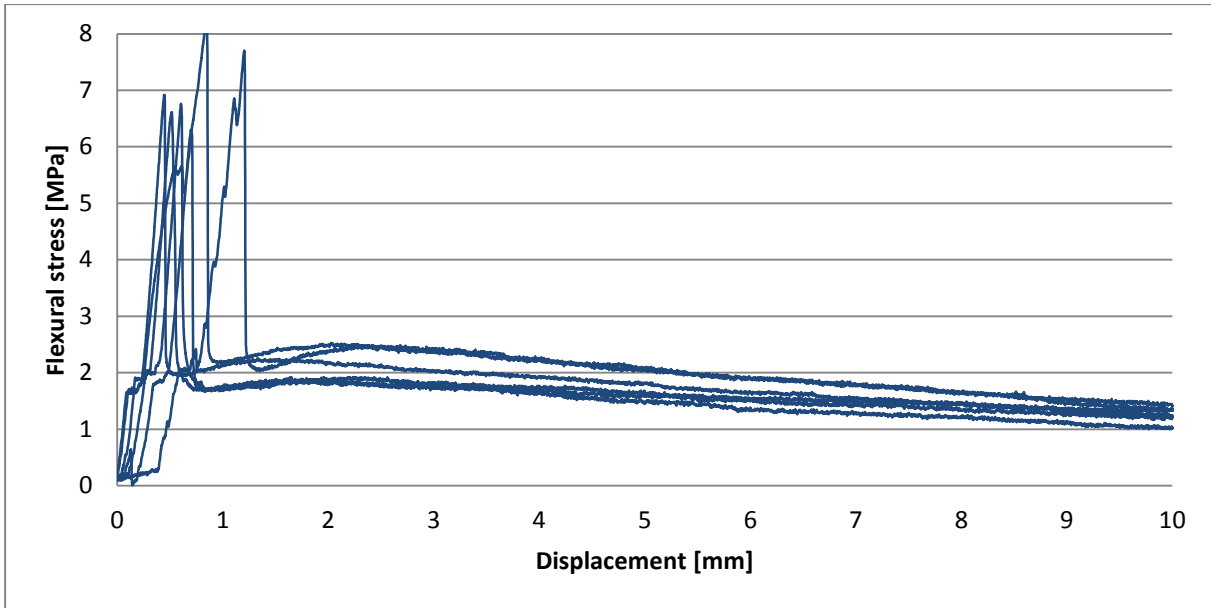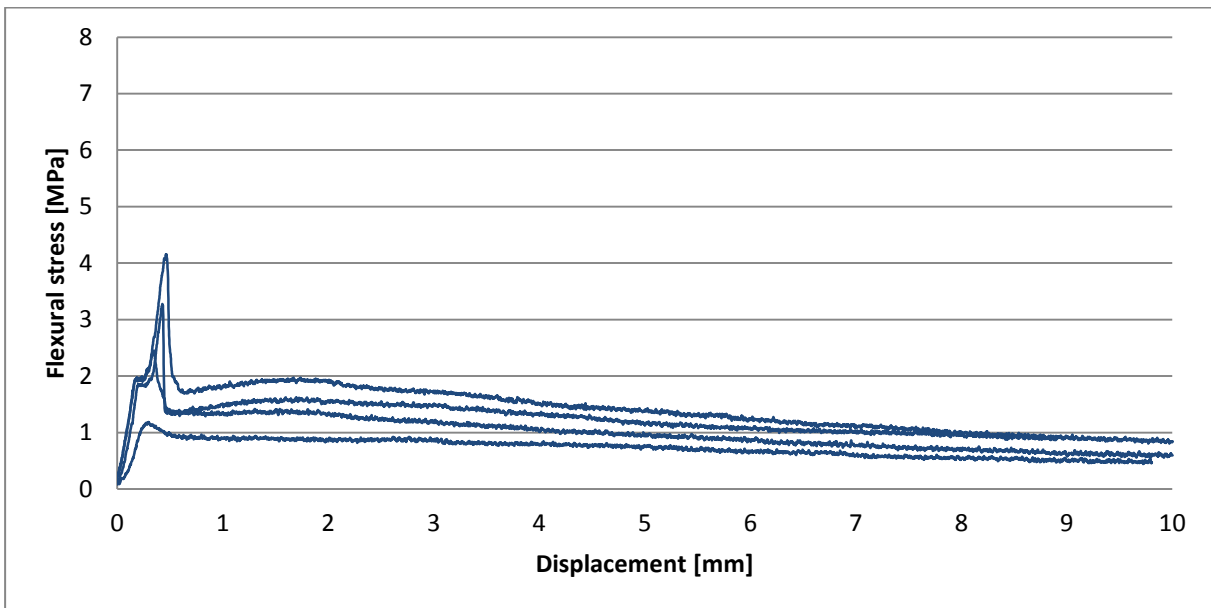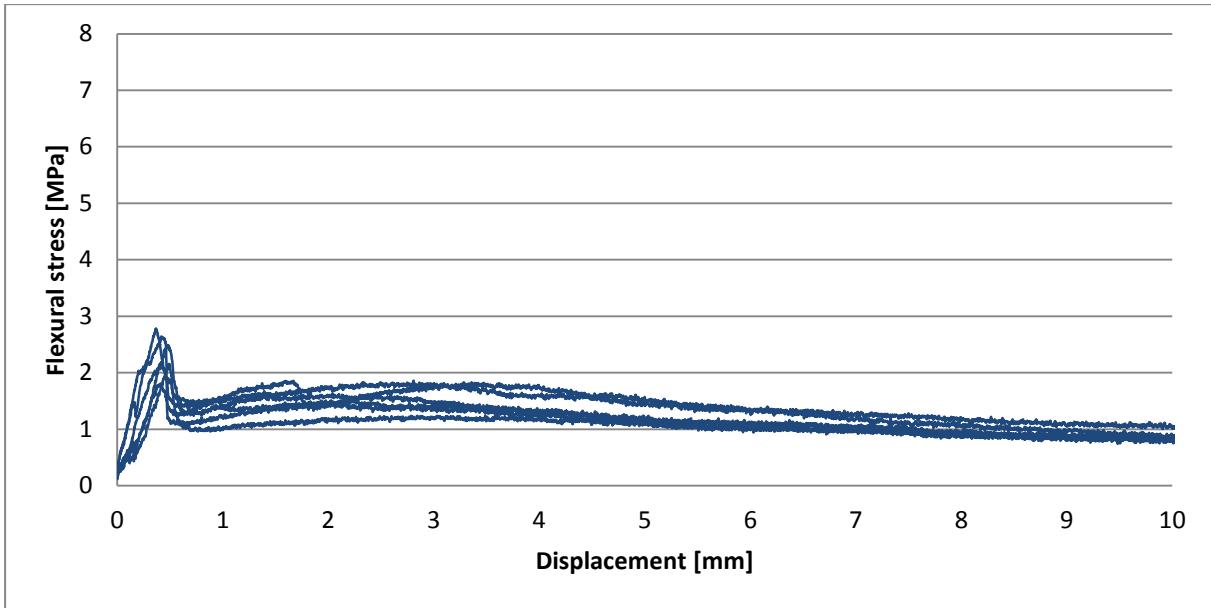**Figure B0.2: Ultimate flexural stress of matrix C1, 1%, 20mm, untreated fibre.**
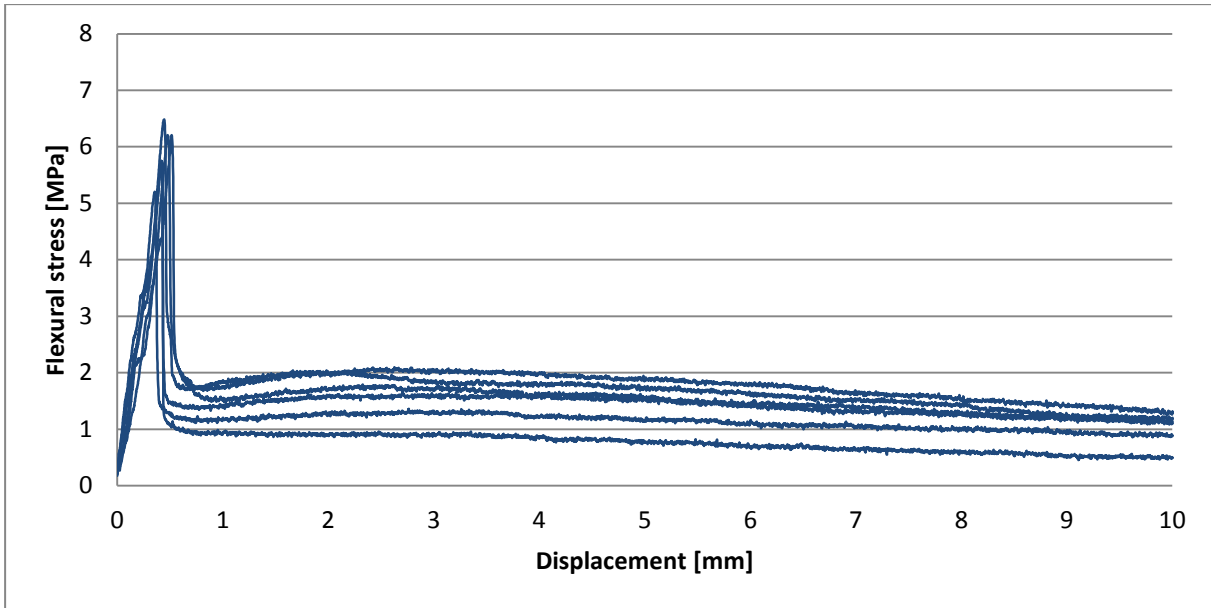
Figure B0.3: Ultimate flexural stress of matrix C1, 1%, 20mm, 2% NaOH treated fibre.
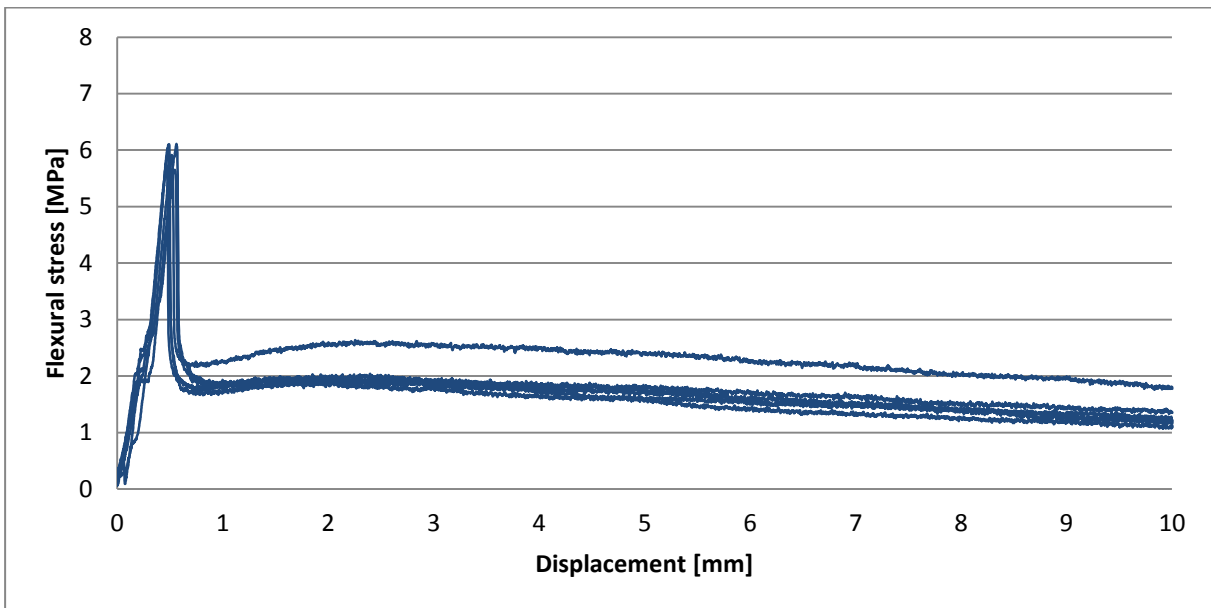
Figure B0.4: Ultimate flexural stress of matrix C1, 1%, 20mm, 6% NaOH treated fibre.
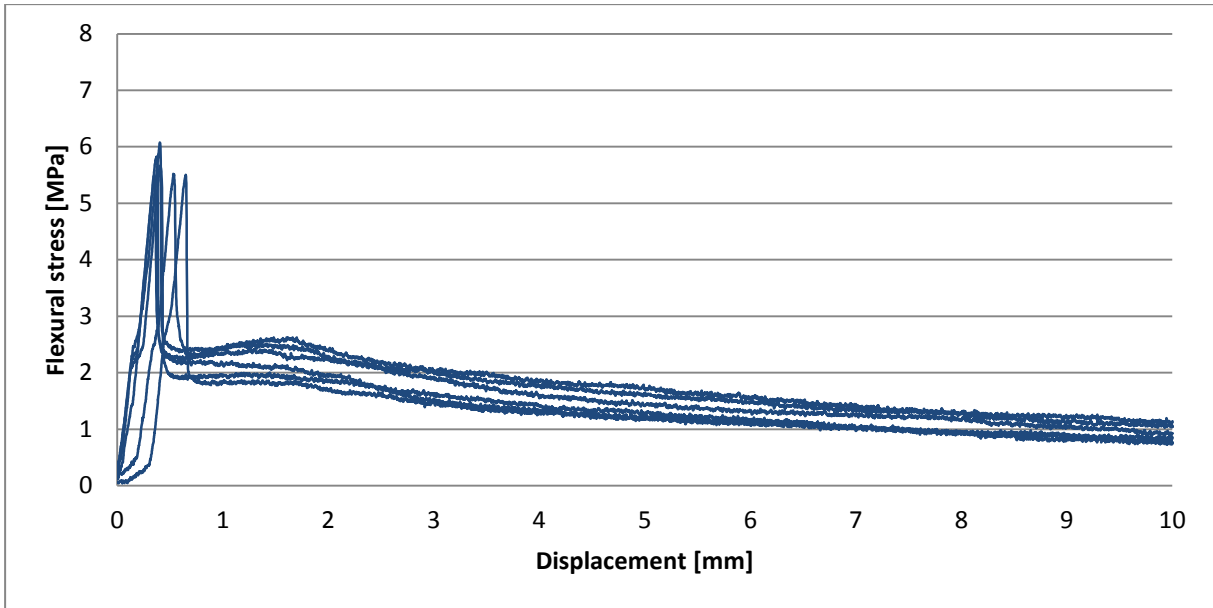
Figure B0.5: Ultimate flexural stress of matrix C1, 1%, 20mm, 10% NaOH treated fibre.
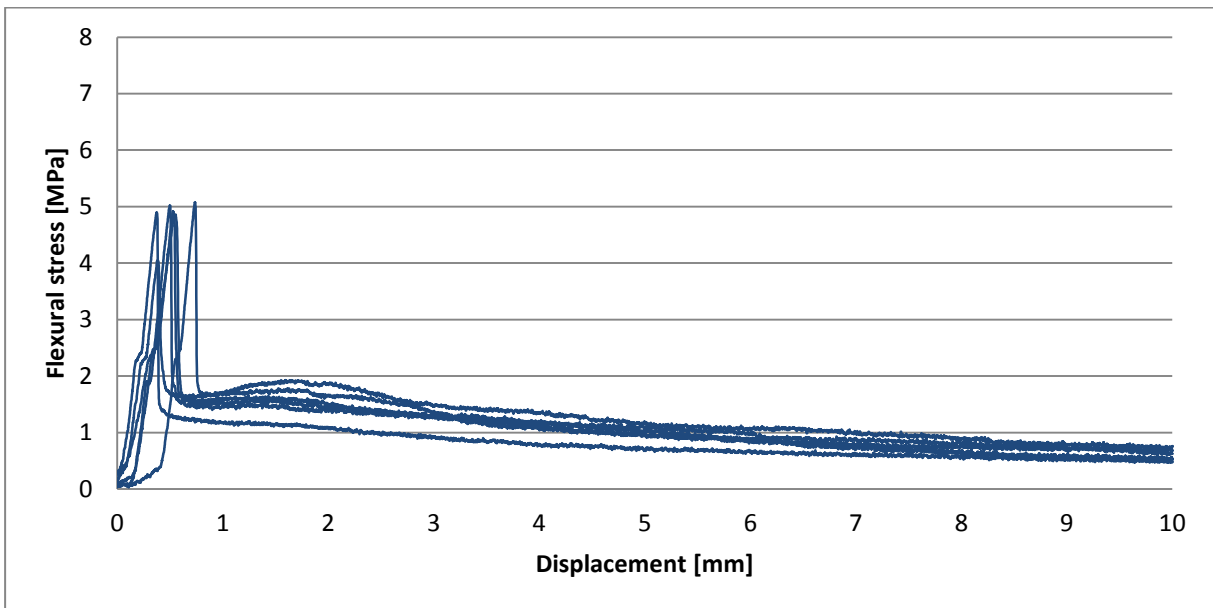
Figure B0.6: Ultimate flexural stress of matrix C1, 1%, 20mm, 20% NaOH treated fibre.
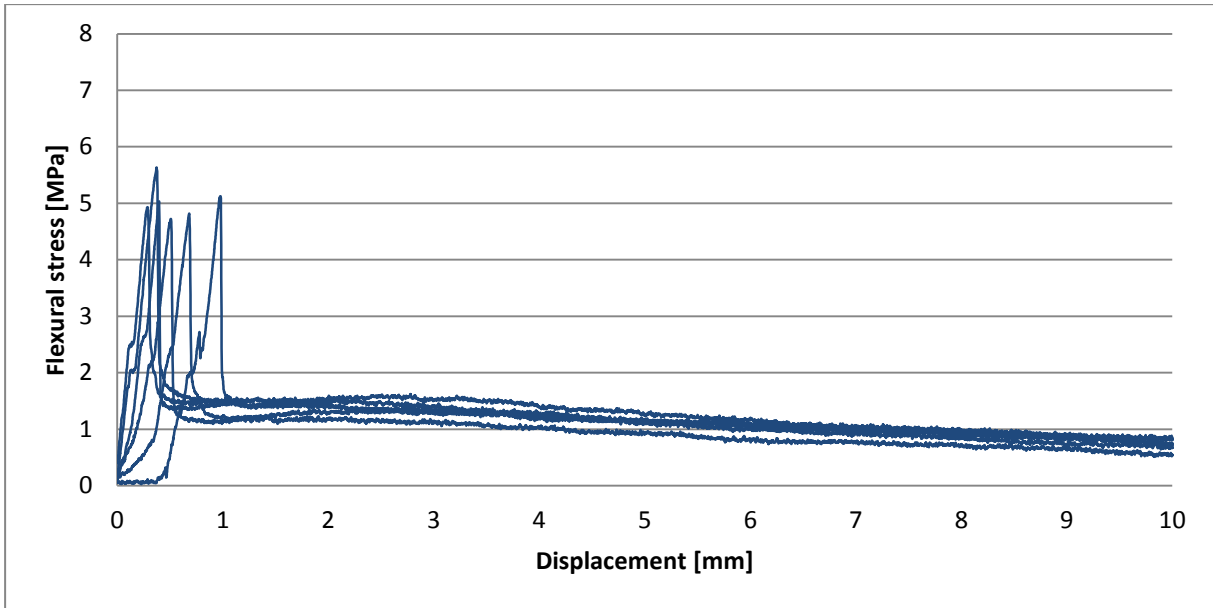
Figure B0.7: Ultimate flexural stress of matrix C1, 1%, 20mm, 30% NaOH treated fibre.
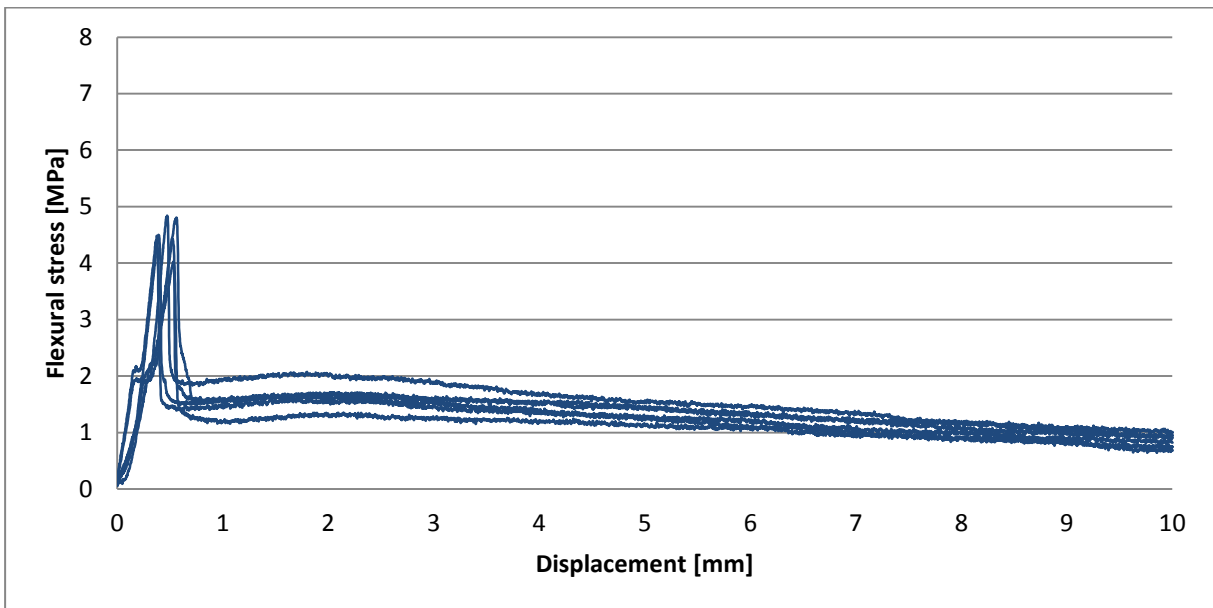
Figure B0.8: Ultimate flexural stress of matrix C1, 1%, 20mm, 5% Acetic Acid treated fibre.

127
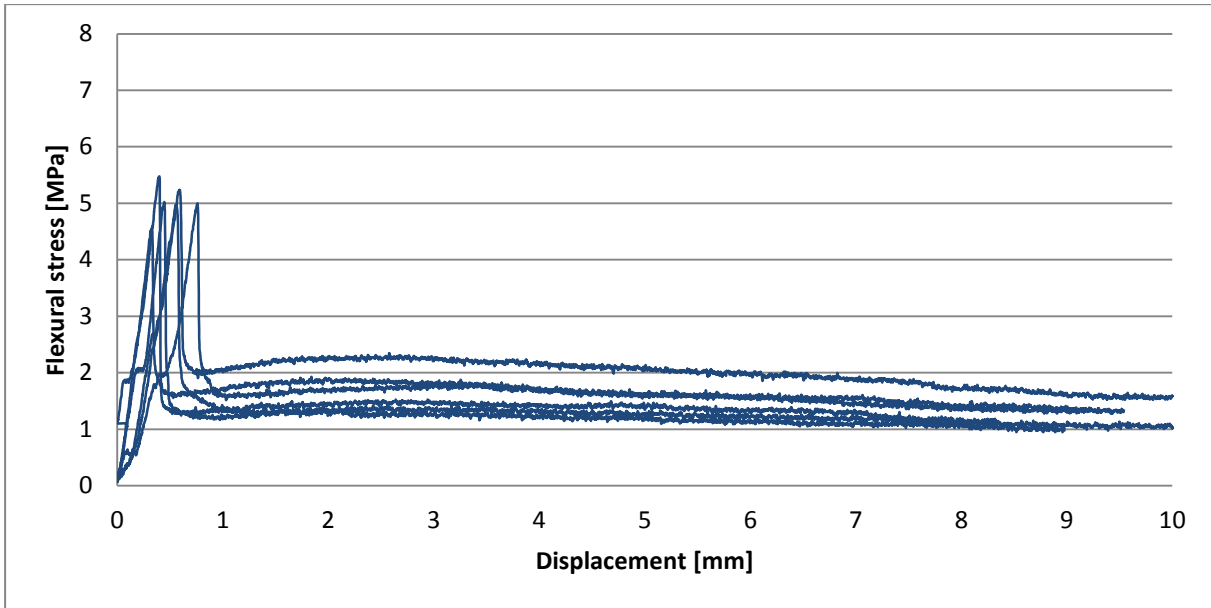
Figure B0.9: Ultimate flexural stress of matrix C1, 1%, 20mm, 10% Acetic Acid treated fibre.

Figure B0.10: Ultimate flexural stress of matrix C1, 1%, 20mm, 5% Acetic Anhydride treated fibre.

Figure B0.11: Ultimate flexural stress of matrix C1, 1%, 20mm, 10% Acetic Anhydride treated fibre.

Figure B0.12: Ultimate flexural stress of matrix C1, 1%, 20mm, 6% NaOH-5% Acetic Anhydride treated fibre.

Figure B0.13: Ultimate flexural stress of matrix C1, 1%, 20mm, 6% NaOH-10% Acetic Anhydride treated fibre.

Figure B0.14: Ultimate flexural stress of matrix C2, 1%, 20mm, untreated fibre.

130

Figure B0.15: Ultimate flexural stress of matrix C3, 1%, 20mm, untreated fibre.

Figure B0.16: Ultimate flexural stress of matrix C4, 1%, 20mm, untreated fibre.

Figure B0.17: Ultimate flexural stress of matrix C5, 1%, 20mm, untreated fibre.

Figure B0.18: Ultimate flexural stress of matrix C6, 1%, 20mm, untreated fibre.

Figure B0.19: Ultimate flexural stress of matrix E1, 2%, 20mm, untreated fibre.

Figure B0.20: Ultimate flexural stress of matrix E1, 1%, 20mm, untreated fibre.

133

Figure B0.21: Ultimate flexural stress of matrix E2, 1%, 20mm, untreated fibre.

Figure B0.22: Ultimate flexural stress of matrix E3, 1%, 20mm, untreated fibre.

Figure B0.23: Ultimate flexural stress of matrix C1, 1%, 30mm, untreated fibre.

Appendix C – Direct tensile test results

1. Summary of results of direct tensile tests

Table C1 presents the results of all the direct tensile tests performed. Only the post-peak strength is provided, as it gives a clear indication on the strength of the fibres after treatment and ageing. The percentage increase or decrease calculated for each ageing regime indicates the increase or decrease in strength with regards to the corresponding 28 day reference.

Table C1: Average post-peak stress and percentage increase or decrease for specimens subjected to different ageing regimes and tested in direct tension at an age of 90 days.

Matrix, Fibre volume, Length	Treatment	Post peak				
		28 days	90 days water		90 days hot water	
		Avg	Avg	% inc/dec	Avg	% inc/dec
C1-2-20	Untreated	0.88				
C1-1-20	Untreated	0.73	0.49	-33.22	0.28	-61.90
C1-1-20	2% NaOH	0.83	0.73	-11.50	0.45	-45.84
C1-1-20	6% NaOH	0.57	0.56	-0.89	0.31	-45.90
C1-1-20	10% NaOH	0.64	0.60	-7.09	0.29	-54.45
C1-1-20	20% NaOH	0.32	0.30	-6.63	0.17	-47.17
C1-1-20	30% NaOH	0.57	0.48	-15.90	0.26	-54.31
C1-1-20	5% A.Acid	0.57	0.57	-1.60	0.28	-51.15
C1-1-20	10% A.Acid	0.64	0.63	-0.80	0.19	-70.21
C1-1-20	5% A.Anh	0.69	0.43	-37.70	0.18	-73.48
C1-1-20	10% A.Anh	0.51	0.57	11.05	0.21	-59.20
C1-1-20	6% NaOH, 5% A.Anh	0.73	0.60	-17.86	0.27	-63.51
C1-1-20	6% NaOH, 10% A.Anh	0.82	0.66	-19.67	0.32	-60.81
C2-1-20	Untreated	0.43	0.30	-28.55	0.29	-31.45
C3-1-20	Untreated	0.55	0.48	-11.75	0.30	-44.65
C4-1-20	Untreated	0.42	0.39	-8.36	0.24	-43.04
C5-1-20	Untreated	0.29	0.49	69.73	0.18	-38.93
C6-1-20	Untreated	0.57	0.64	12.10	0.19	-66.10
C1-1-30	Untreated	0.47	0.38	-19.47	0.27	-43.37

2. Results of direct tensile tests performed at 28 days

The results of the direct tensile tests performed on all the different series of specimens at 28 days are presented in this section in **Figure C0.1** to **Figure C0.19**.
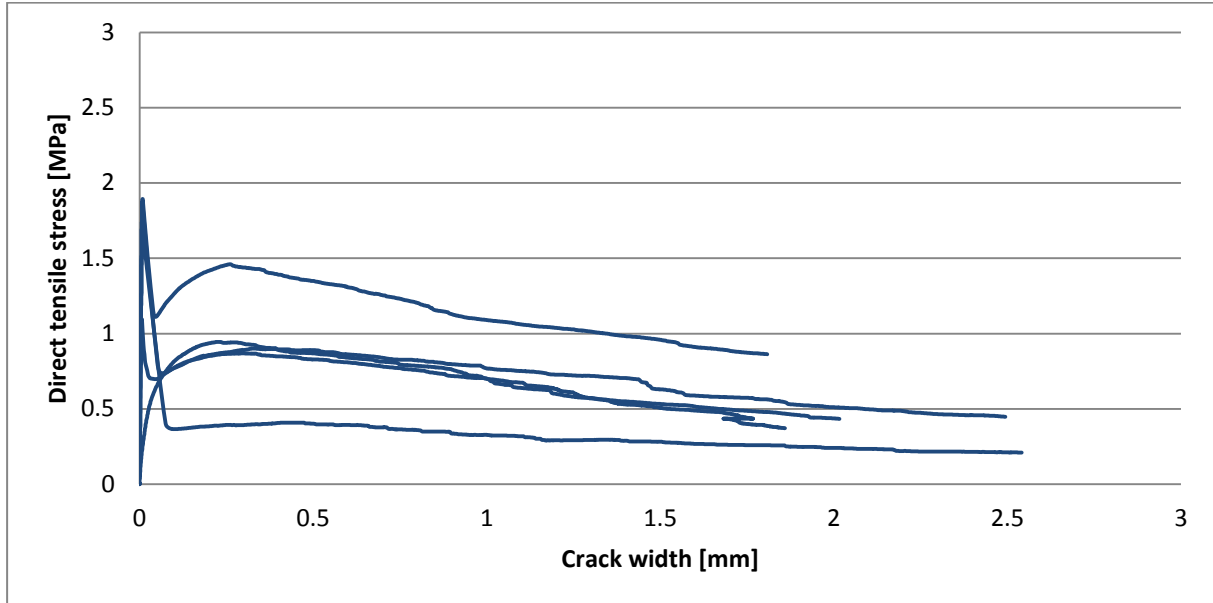
Figure C0.1: Direct tensile stress of matrix C1, 2%, 20mm, untreated fibre.
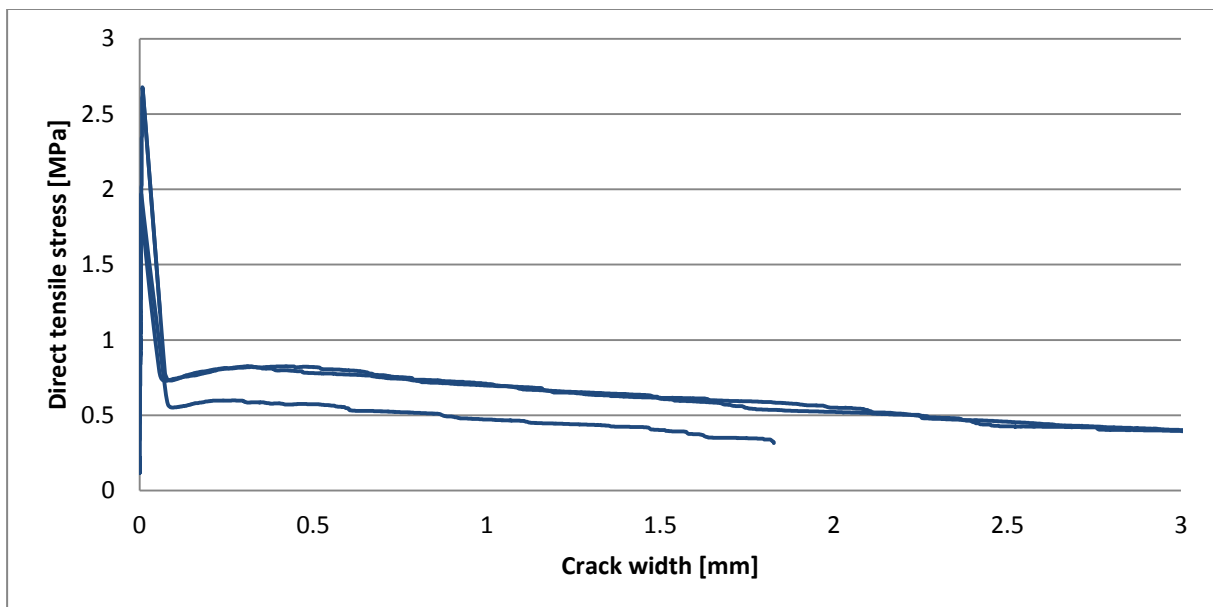
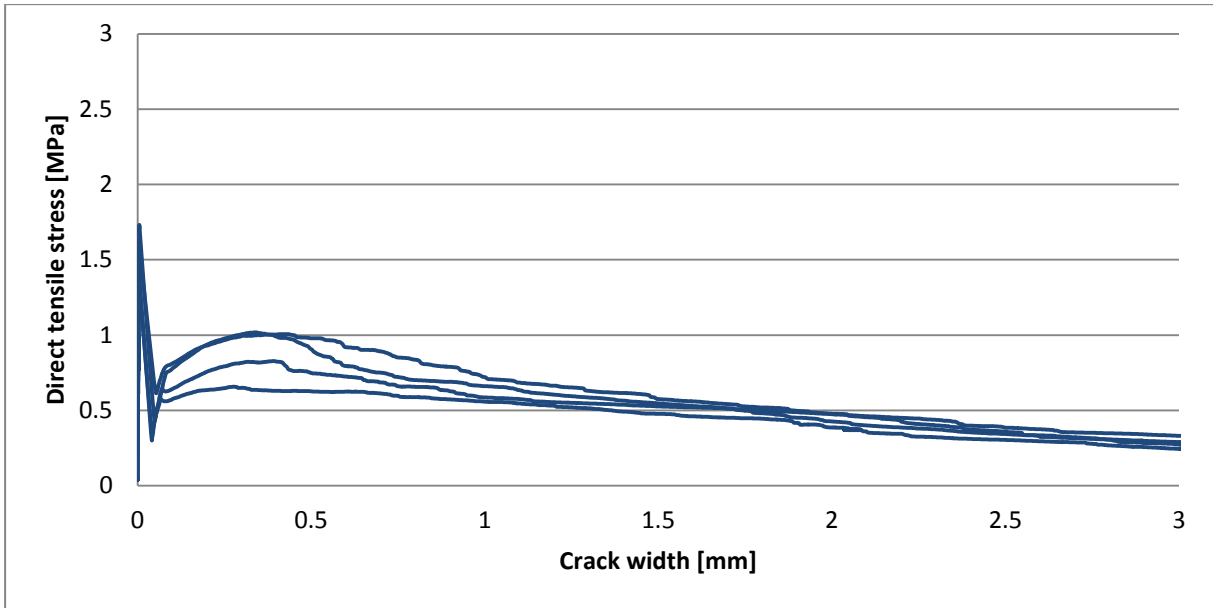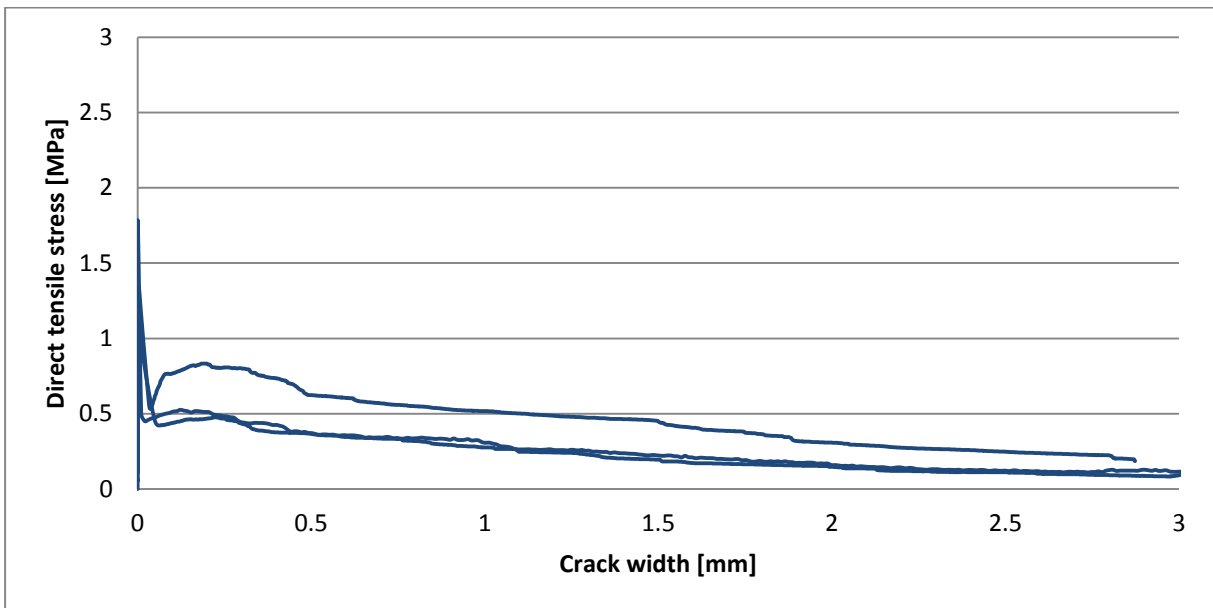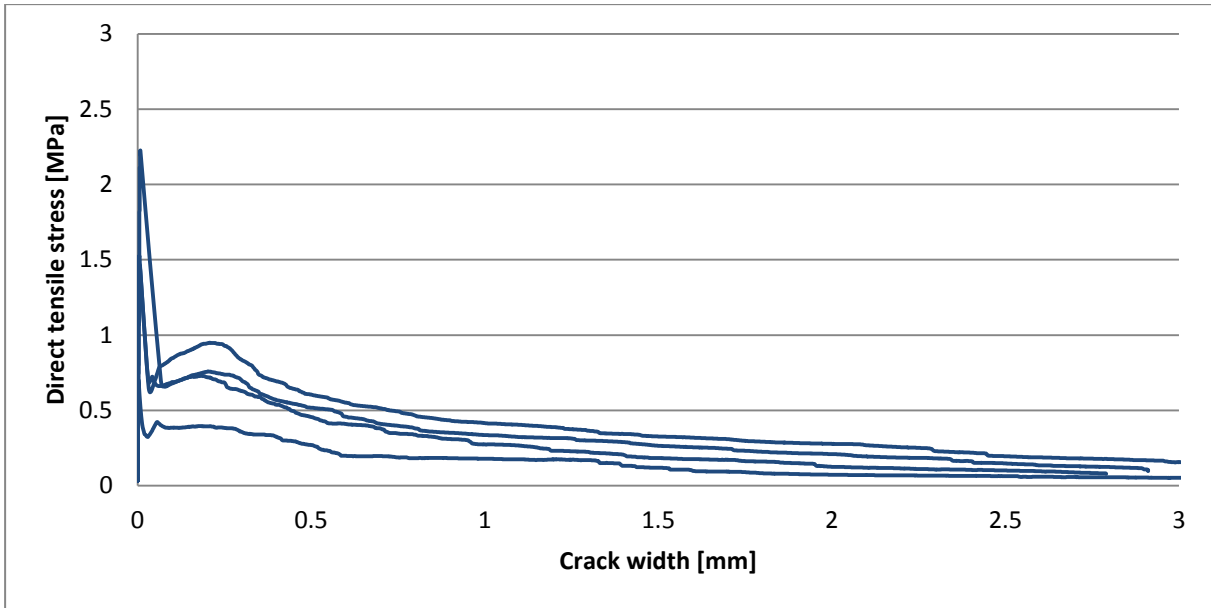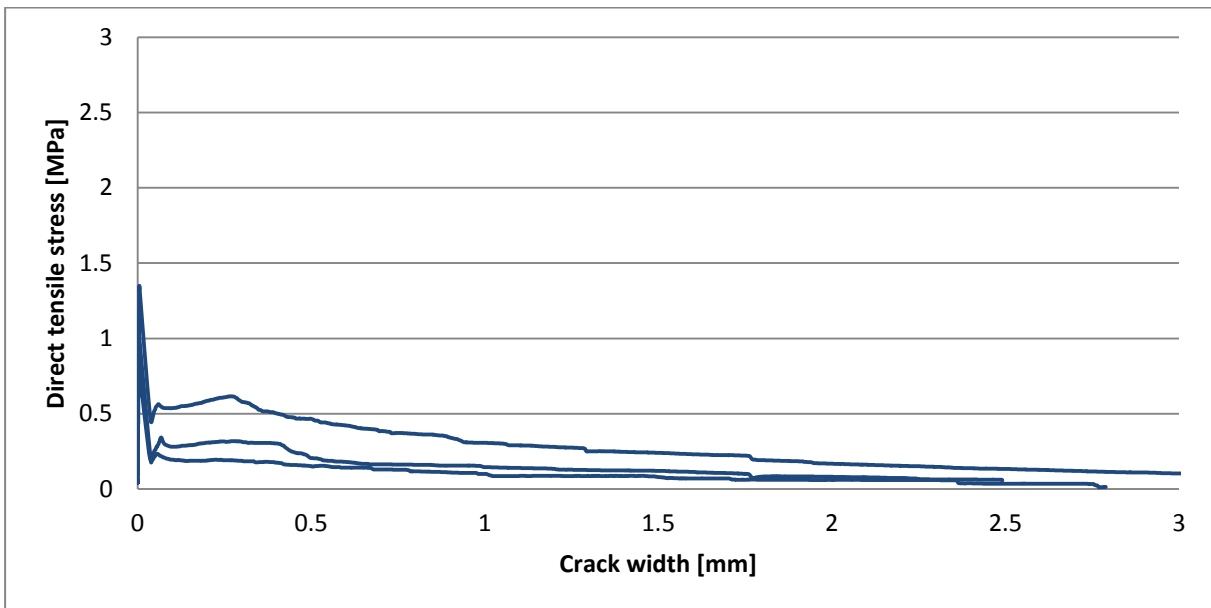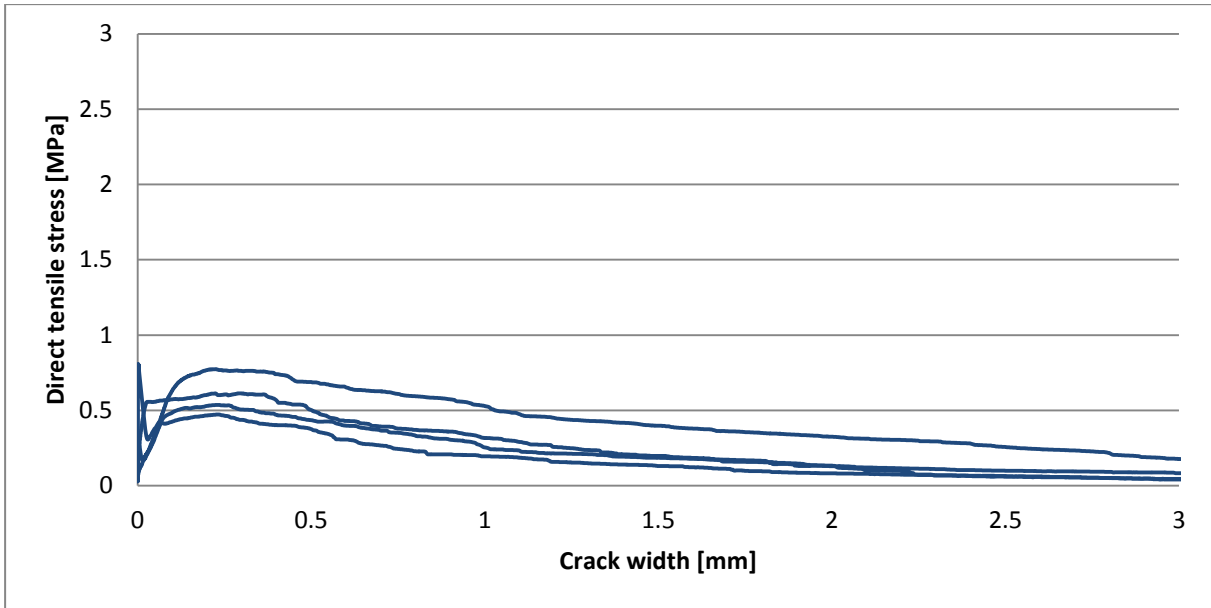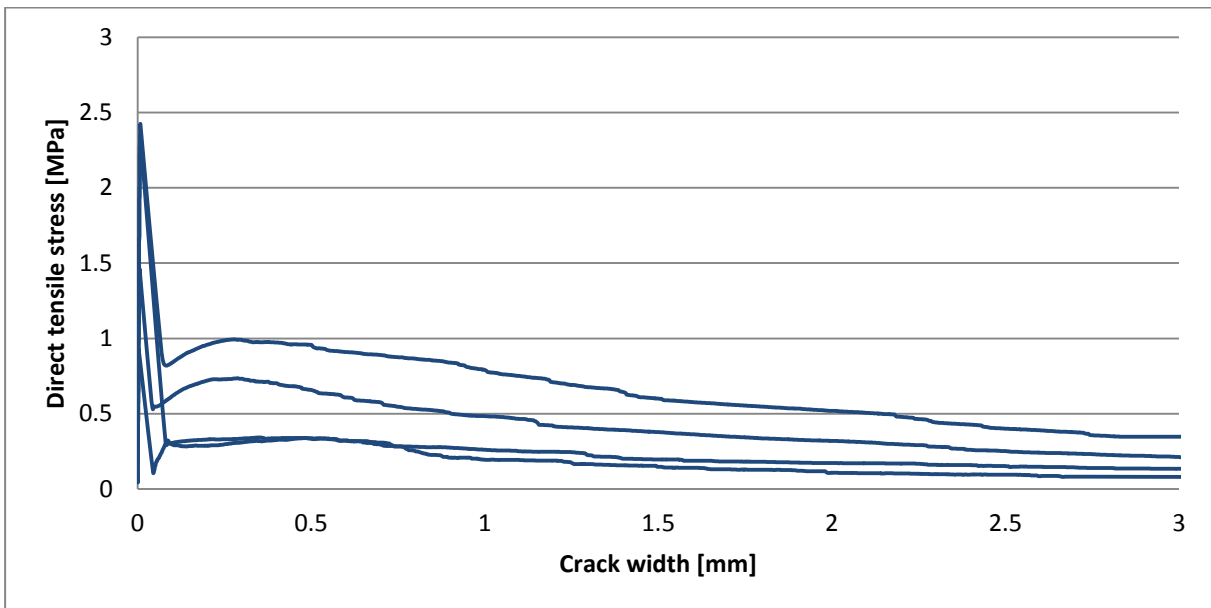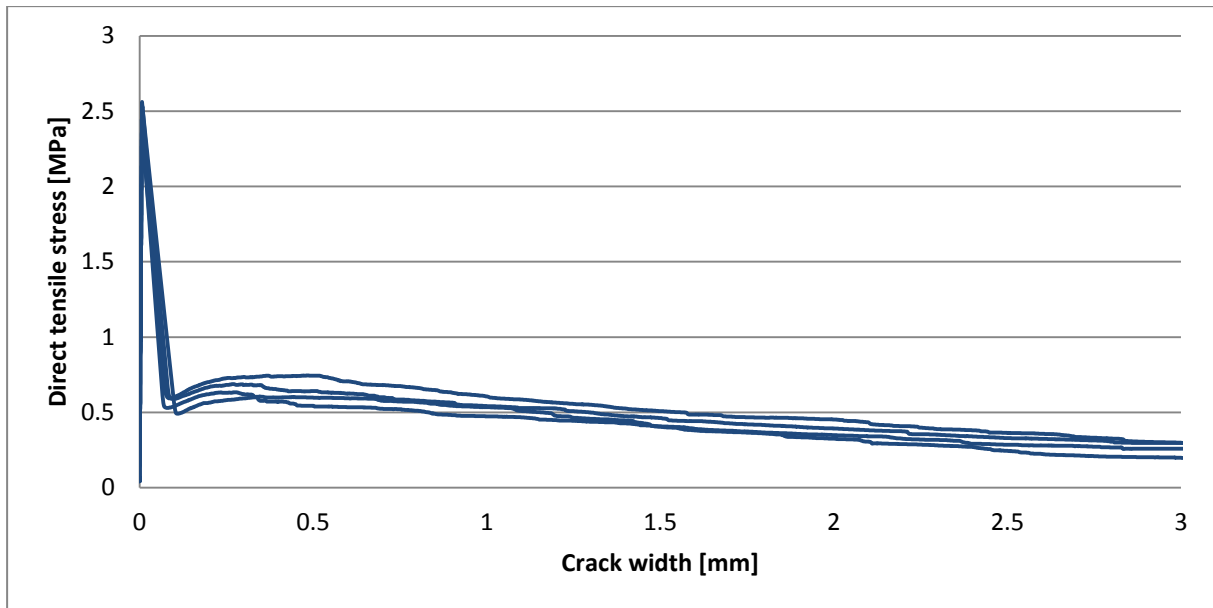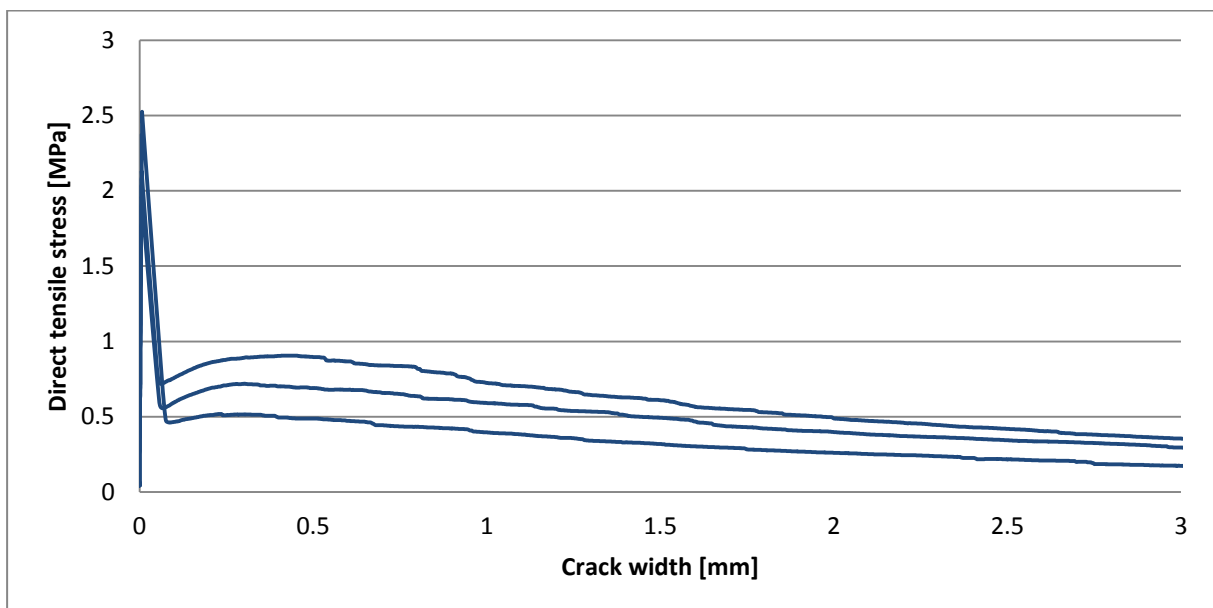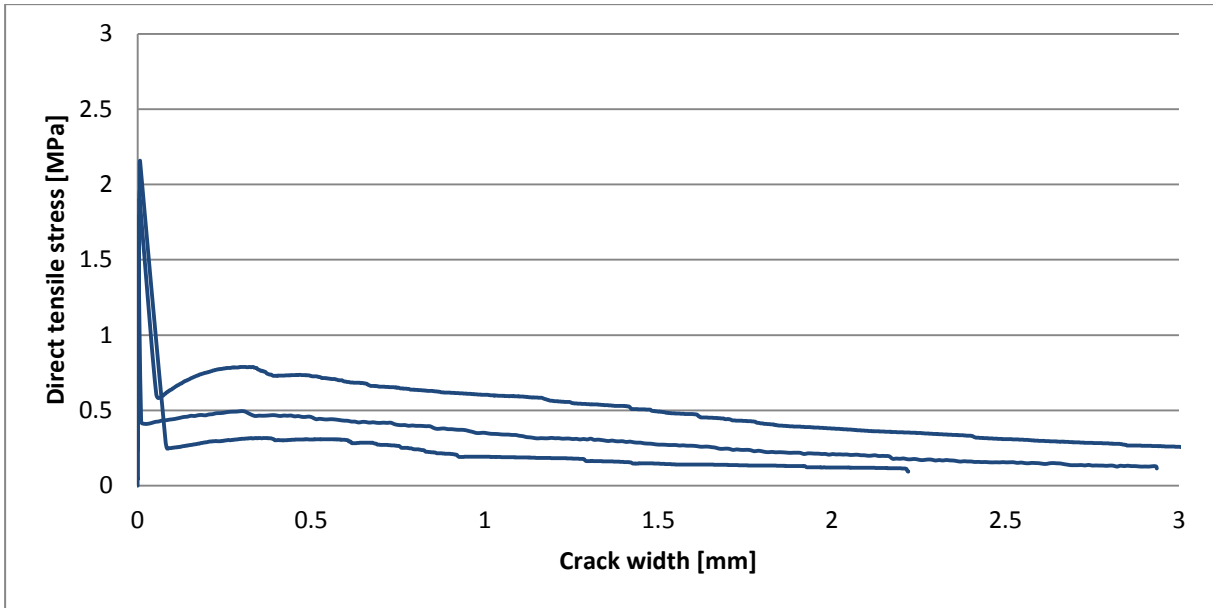**Figure C0.2: Direct tensile stress of matrix C1, 1%, 20mm, untreated fibre.**

137

Figure C0.3: Direct tensile stress of matrix C1, 1%, 20mm, 2% NaOH treated fibre.

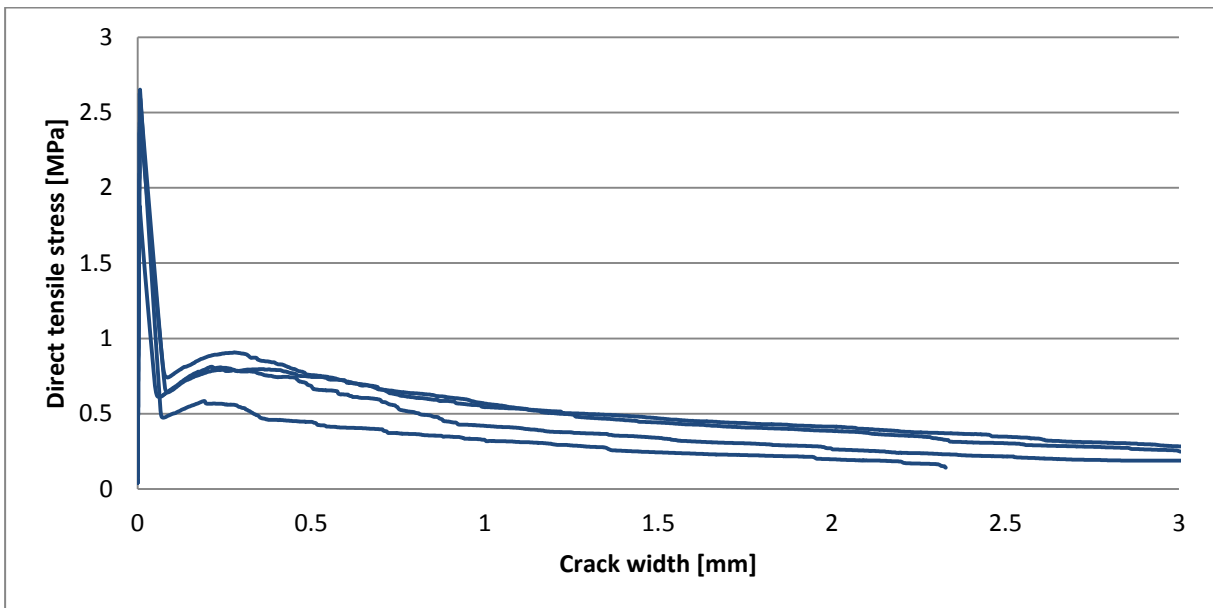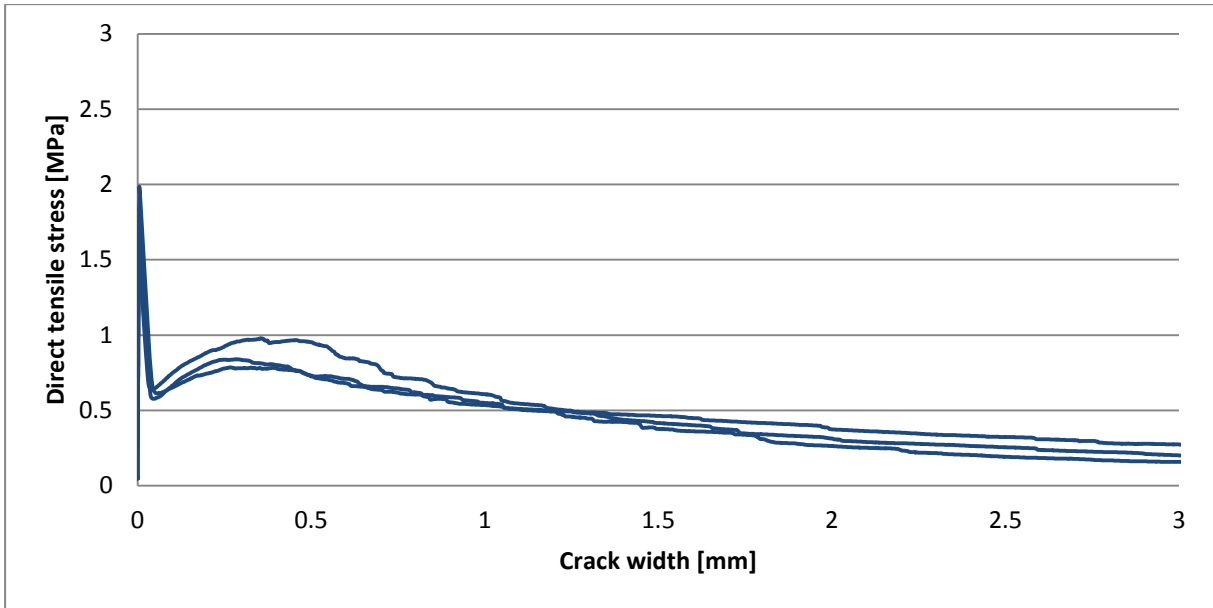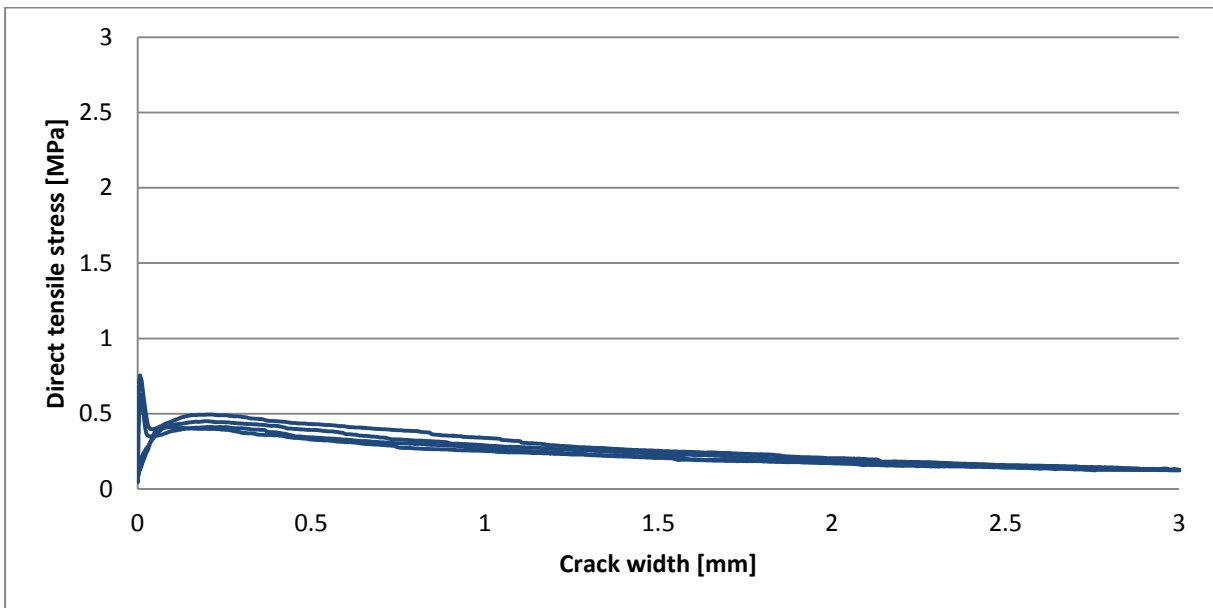**Figure C0.4: Direct tensile stress of matrix C1, 1%, 20mm, 6% NaOH treated fibre.**

Figure C0.5: Direct tensile stress of matrix C1, 1%, 20mm, 10% NaOH treated fibre.

Figure C0.6: Direct tensile stress of matrix C1, 1%, 20mm, 20% NaOH treated fibre.

139

Figure C0.7: Direct tensile stress of matrix C1, 1%, 20mm, 30% NaOH treated fibre.

Figure C0.8: Direct tensile stress of matrix C1, 1%, 20mm, 5% Acetic Acid treated fibre.

Figure C0.9: Direct tensile stress of matrix C1, 1%, 20mm, 10% Acetic Acid treated fibre.

Figure C0.10: Direct tensile stress of matrix C1, 1%, 20mm, 5% Acetic Anhydride treated fibre.

Figure C0.11: Direct tensile stress of matrix C1, 1%, 20mm, 10% Acetic Anhydride treated fibre.

Figure C0.12: Direct tensile stress of matrix C1, 1%, 20mm, 6% NaOH-5% Acetic Anhydride treated fibre.
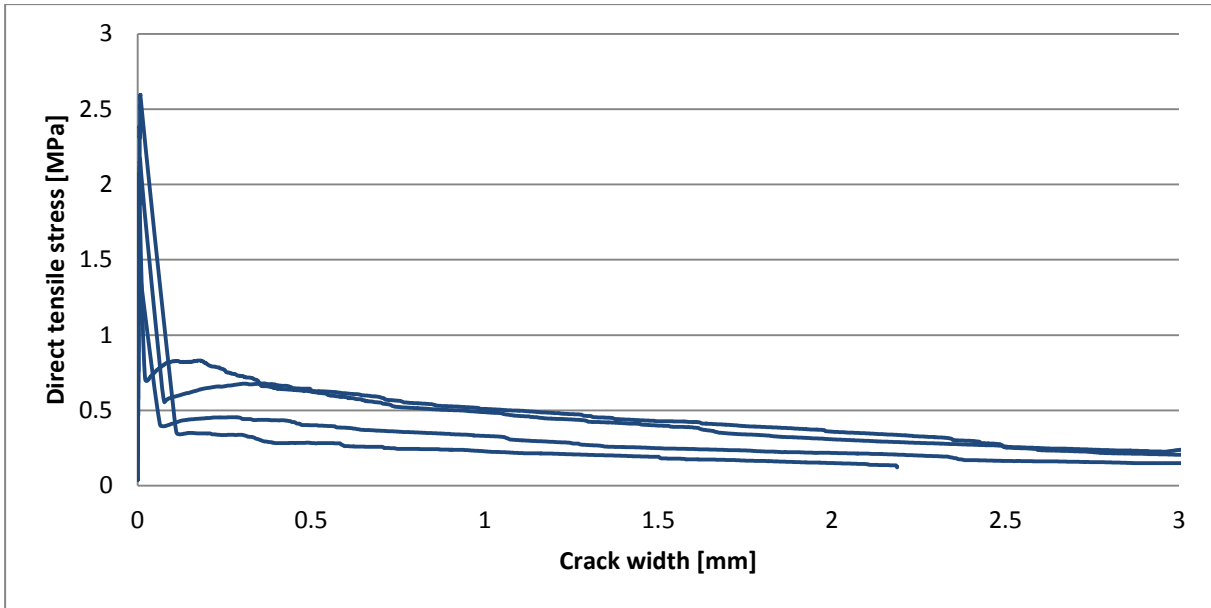
Figure C0.13: Direct tensile stress of matrix C1, 1%, 20mm, 6% NaOH-10% Acetic Anhydride treated fibre.

Figure C0.14: Direct tensile stress of matrix C2, 1%, 20mm, untreated fibre.

143

Figure C0.15: Direct tensile stress of matrix C3, 1%, 20mm, untreated fibre.
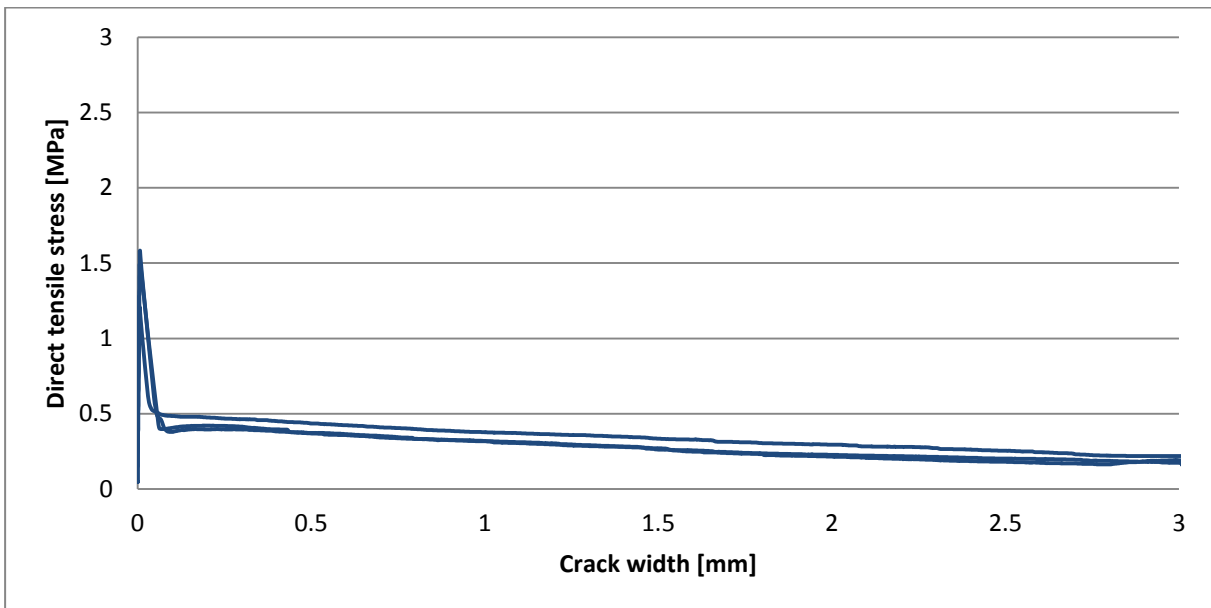
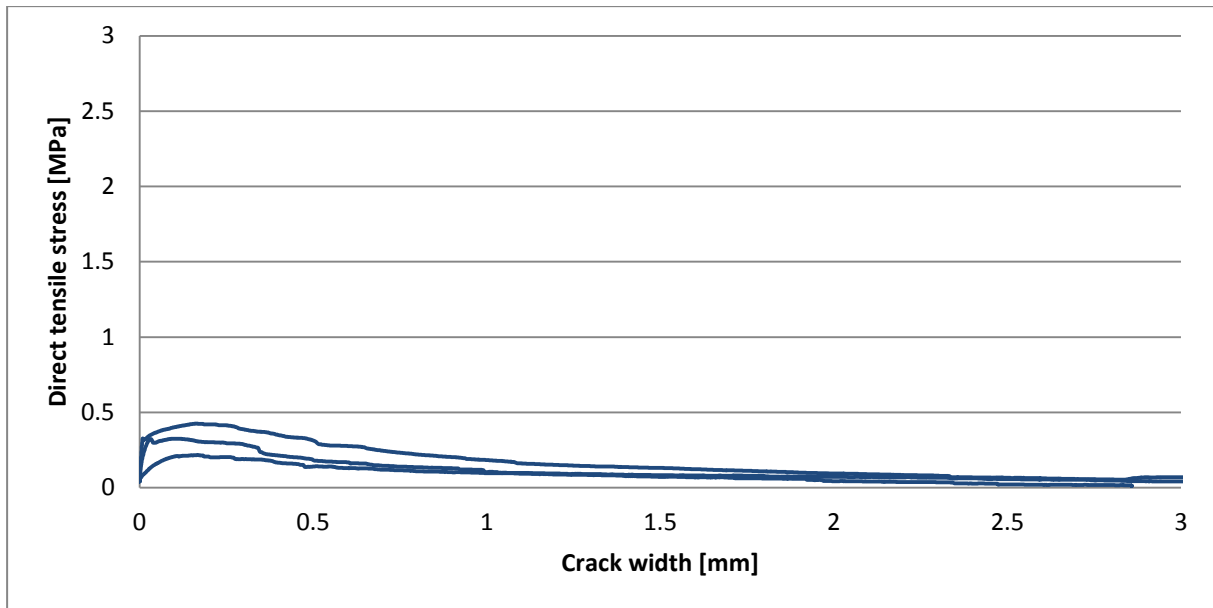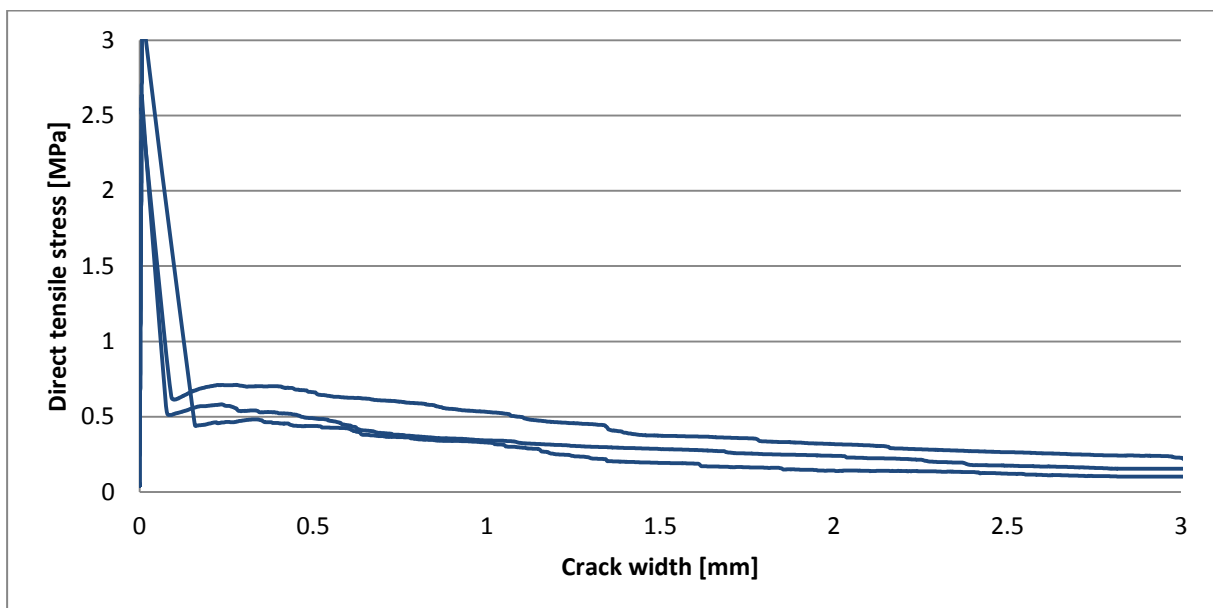**Figure C0.16: Direct tensile stress of matrix C4, 1%, 20mm, untreated fibre.**

144

Figure C0.17: Direct tensile stress of matrix C5, 1%, 20mm, untreated fibre.

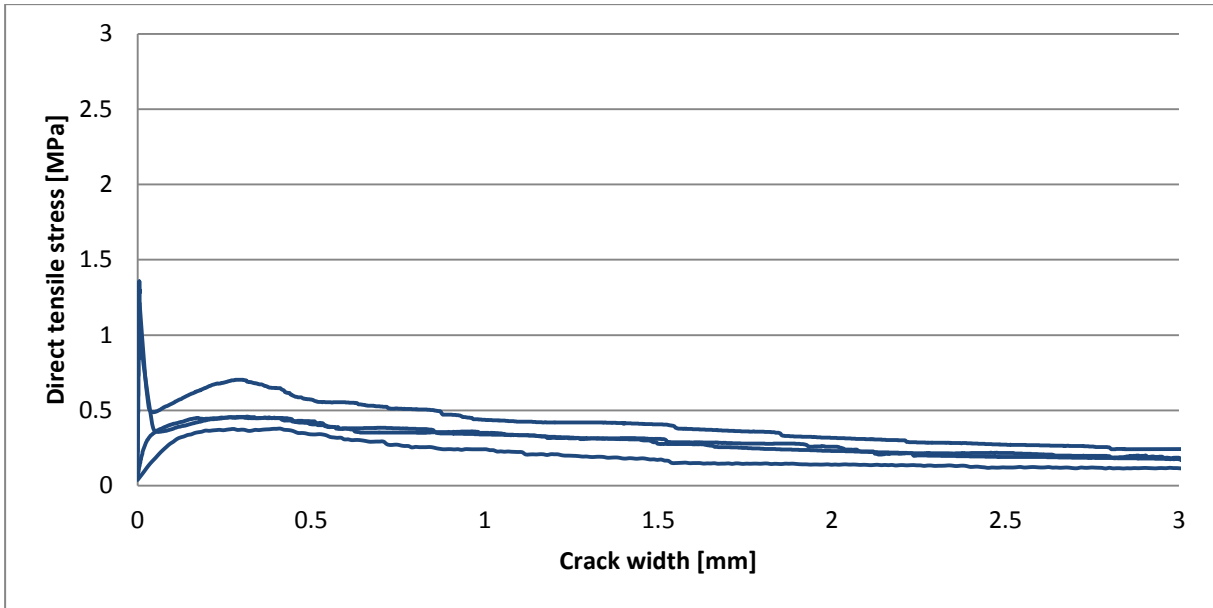**Figure C0.18: Direct tensile stress of matrix C6, 1%, 20mm, untreated fibre.**

145

Figure C0.19: Direct tensile stress of matrix C1, 1%, 30mm, untreated fibre.